ISBN 978-82-326-4062-1 (printed ver.)
ISBN 978-82-326-4063-8 (electronic ver.)
ISSN 1503-8181

Doctoral theses at NTNU, 2019:233

Amin Moazami

CLIMATE ROBUST BUILDINGS: TOWARDS BUILDINGS WITH A ROBUST ENERGY PERFORMANCE UNDER CLIMATE CHANGE

Amin Moazami

Doctoral thesis

NTNU
Norwegian University of Science and Technology
Thesis for the Degree of
Philosophiae Doctor
Faculty of Engineering
Department of Civil and Environmental
Engineering

Doctoral theses at NTNU, 2019:233

NTNU

NTNU
Norwegian University of
Science and Technology

NTNU
Norwegian University of
Science and Technology

Amin Moazami

CLIMATE ROBUST BUILDINGS: TOWARDS BUILDINGS WITH A ROBUST ENERGY PERFORMANCE UNDER CLIMATE CHANGE

Thesis for the Degree of Philosophiae Doctor

Trondheim, August 2019

Norwegian University of Science and Technology
Faculty of Engineering
Department of Civil and Environmental Engineering

NTNU
Norwegian University of
Science and Technology

NTNU
Norwegian University of Science and Technology

Thesis for the Degree of Philosophiae Doctor

Faculty of Engineering
Department of Civil and Environmental Engineering

© Amin Moazami

ISBN 978-82-326-4062-1 (printed ver.)
ISBN 978-82-326-4063-8 (electronic ver.)
ISSN 1503-8181

Doctoral theses at NTNU, 2019:233

Printed by NTNU Grafisk senter

THESIS FOR DEGREE OF DOCTOR OF PHILOSOPHY

Climate robust buildings: Towards buildings with a robust energy performance under climate change

AMIN MOAZAMI

Department of Civil and Environmental Engineering
NTNU NORWEGIAN UNIVERSITY OF SCIENCE AND TECHNOLOGY
Trondheim, Norway 2019

Abstract

Building performance simulation (BPS) is a powerful tool allowing building designers to estimate the behavior of buildings and assess the impacts of their design decisions on their performance. BPS requires large number of input variables, of which some can be predicted during design phase with reasonable certainty such as thermal properties of materials and building dimensions, and some are difficult to be predicted, such as climate and occupancy.

Climate as an input variable in BPS is the main theme of this PhD work. Climate conditions are key input variables for BPS, but traditionally and for simplification, a typical climate condition is used to represent the most likely condition that a building will experience. Such approach results for the final designs to be sensitive to variation of climate conditions and even fail to provide expected performance when the conditions are beyond typical ranges. Such sensitivity of buildings to atypical climate conditions is becoming more critical considering that due to climate change the frequency and intensity of extreme climate conditions is increasing. This thesis provides an overview of the risks induced by climate change on the performance of buildings and provide a method for protection against future climate uncertainty.

The first step towards protection against climate uncertainty is to identify the climate conditions that a building might face during its life span. The work identifies a prospect of climate conditions for built environment as: climate normals or typical climate conditions and climate extremes. Climate extremes are distinguished into two: foreseeable extreme conditions and unforeseeable extreme events. It further discusses to which extent these conditions can be considered during the design phase of buildings. After identifying the possible climate conditions, a work was set to create a framework that conceptualise protection for buildings against all these conditions. After reviewing the concepts and definitions provided in the literature, the two concepts of “robustness” and “resilience” were found appropriate for the aimed framework. According to the defined framework, the concept of robustness is the most proper to deal with typical and foreseeable extreme climate conditions, where in this concept the main focus is on reducing the sensitivity of performance under presence of source of uncertainty. The discussion on protection against unforeseeable extreme events falls into the concept of resilience, where withstanding and recovery mechanisms should be considered and was out of scope of this thesis. Based on the framework a climate robust building is “a building that, while in operation, can provide its performance requirements with a minimum variation under typical and foreseeable extreme climate conditions.”

In the second step, a total of 74 representative weather files are synthesized for city of Geneva to account for future foreseeable extreme conditions together with typical climate conditions. The aim is to investigate the impacts of these conditions on the energy performance of single buildings and their combination to create a virtual neighborhood. The results showed, depending on the type of building, the relative change of peak load for cooling demand under near future can be up to 28.5% higher for extreme conditions compared to typical conditions. Furthermore, the results for the neighborhood demonstrate the

critical situation that an energy network may face due to increased peak load under extreme climatic conditions. It is concluded that only those weather files that take into consideration both typical and extreme conditions are the most reliable for providing representative boundary conditions to test the energy robustness of buildings under future climate uncertainties.

In the final step, a method is proposed in this work, in which three future weather files including typical, extreme warm and extreme cold conditions are used in a simulation-based optimization process. The method allows architects and engineers to effectively consider future climate uncertainties during the design phase and achieve solutions with robust energy performance against these uncertainties. Using only three weather files make the process feasible and computationally inexpensive. To test the effectiveness of the method, the primary energy use of an obtained optimum solution is calculated for the 74 weather files. According to the results, the performance of the optimum solution not only has 81.5% lower variation (less sensitivity to climate uncertainty) but at the same time 14.4% lower mean value of energy use in comparison to a solution that is compliant with a recent construction standard (ASHRAE 90.1-2016). Less sensitivity to climate uncertainty means better robustness against climate change and simultaneously keeping a high performance. The simplicity and the low computational demand of the process ascertain the feasibility and applicability of this method. The approach can be used at any stage of design process and can help architects and engineers to improve robustness of their design against future climate uncertainties.

Nomenclature and acronyms

AR	Augmented Reality
BCCR	Bjerknes Centre For Climate Research
BIM	Building Information Modelling
BPS	Building Performance Simulation
CDD	Cooling Degree Days
ECY	Extreme Cold Year
EPW	Energyplus Weather file
EWY	Extreme Warm Year
GA	Genetic Algorithm
GCM	General Circulation Model
HDD	Heating Degree Days
IAQ	Indoor Air Quality
IGDG	Italian Climatic Data Collection "Gianni De Giorgio"
IPCC	Intergovernmental Panel For Climate Change
IWEC	International Weather For Energy Calculations
LT	Long-Term
MOGA-II	Multi-objective Genetic Algorithm
MSD	Mean Squared Deviation
MT	Medium-Term
NCEI	National Centers For Environmental Information
NSGA-II	Fast Non-Dominated Sorting Genetic Algorithm
NT	Near-Term
nZEB	Nearly Zero-Energy Building
PE	Primary Energy
RCA4	Rossby Centre Regional Atmospheric Climate Model
RCM	Regional Climate Model
RCP	Representative Concentration Pathway
RDO	Robust Design Optimization
S/N	Signal-To-Noise Ratio
SD	Standard Deviation
SRES	Special Report On Emissions Scenarios
TDY	Typical Downscaled Year
TMY	Typical Meteorological Year
UNISDR	United Nations Office For Disaster Risk Reduction
WMO	World Meteorological Organization

Appended papers

I. Moazami, Amin; Carlucci, Salvatore; Causone, Francesco; Pagliano, Lorenzo. “Energy retrofit of a day care center for current and future weather scenarios.” Procedia Engineering 2016; 145:1330-7.

II. Pagliano, Lorenzo; Carlucci, Salvatore; Causone, Francesco; Moazami, Amin; Cattarin, Giulio. “Energy retrofit for a climate resilient child care centre.” Energy and Buildings 2016; 127:1117-32.

III. Moazami, Amin; Carlucci, Salvatore; Geving, Stig. “Critical Analysis of Software Tools Aimed at Generating Future Weather Files with a view to their use in Building Performance Simulation.” Energy Procedia. 2017;132:640-5.

IV. Moazami, Amin; Nik, Vahid M.; Carlucci, Salvatore; Geving, Stig. “Impacts of future weather data typology on building energy performance – Investigating long-term patterns of climate change and extreme weather conditions.” Applied Energy. 2019;238:696-720.

V. Moazami, Amin; Carlucci, Salvatore; Geving, Stig. “Robust and resilient buildings: A framework for defining the protection against climate uncertainty.” Submitted to IAQVEC 2019 conference in Bari, Italy

VI. Moazami, Amin; Carlucci, Salvatore; Nik, Vahid M.; Geving, Stig. “Towards climate robust buildings: an innovative method for designing buildings with robust energy performance under climate change.” Submitted to Journal of Energy and Buildings

Declaration of Authorship

The thesis work is done by the thesis author and is main author and responsible for the writing of papers, setting up simulations and analysis of the results for **paper I, paper III, paper IV, paper V** and **paper VI** that are appended to the thesis. For **paper II**, the author of thesis as co-author had major contribution in writing the methodology, results and discussion parts and was the main responsible for modeling the building and performing simulations and calibration. The thesis author also participated in monitoring campaign that was set up in the building for collecting necessary data for model calibration. Four of the **Papers I**, **II**, **III** and **IV** have been published before the thesis submission and the remaining **Papers V** and **VI** have been submitted to the IAQVEC 2019 conference and Energy and Buildings journal respectively. The role of co-authors in the thesis and the appended papers is as follow:

- Salvatore Carlucci as co-supervisor and co-author provided inputs regarding simulations, inputs on designing research studies and cases to be investigated, gave inputs on the analysis of the results and proof reading of the **Papers I** to **VI**.
- Vahid M. Nik as co-author in **Paper IV** and **VI** synthesized the RCM climate and their representative data sets, helped with writing some of the Matlab code and assessment of results, supervised structuring the research work and helped with writing the article.
- Lorenzo Pagliano and Francesco Causone as co-authors of **Paper I** and **II** provided access to the data for the case study building in Milan, and provided inputs on the analysis of the results and with proof reading.
- Giulio Cattarin as co-author of **Paper II** wrote the introduction and background and contributed in proof reading.
- Stig Geving as the main supervisor contributed to discussions regarding the results obtained, scientific input from his expertise, quality control on the scientific content and proof reading of **Papers III** to **VI**.

Preface

This PhD thesis is the result of more than three years researching, developing and improving methods for mitigation of climate change impacts on the performance of buildings. It started in August 2015 and ended in April 2019. It was conducted at the Norwegian University of Science and Technology (NTNU), Department of Civil and Environmental Engineering (IBM).

This research work would not be possible without kindness, patience, support and expertise of many people. I want to thank everyone but only can mention some of them here.

First of all, I truly would like to thank my supervisors: Stig Geving and Salvatore Carlucci who trusted me in the first place. I remember how during my interview for the PhD position suddenly the sky turned dark. It was a total solar eclipse on March 20, 2015 and I guess we all took it as a good sign! Both Stig and Salvatore were always present to help me with my doubts and questions. I am grateful that I had the chance to work with them. I have learned many things both professionally and personally from them.

I also would like to say thank you to our amazing administration team at IBM: Kjerstina, Maria, Elin, Marit, Tone, Wenche and Carine for their kind supports and our head of the department Carl Thodesen for all his encouragements.

First part of my thesis evolved from collaboration with eERG research group at Politecnico di Milano. I would like to thank Lorenzo Pagliano, Francesco Causone and Marco Pietrobon for allowing me to take part in their research project and having access to the collected data from the child care centre in Milan.

In the third year of my research, I had opportunity to spend a total of two months at Chalmers University of technology, where I was given chance to develop ideas and work with Vahid M. Nik. I would like to thank Vahid for all the meetings and discussions we had and for all I learned from him on the topic of climate change impact assessment and acquisition of data from climate models.

Last, but definitely not least, I thank my parents and my brother Abdolreza for their unquestioned love and supports. They always tried to keep me calm and make me smile in the hardest moments. I want to dedicate this work to my parents: Mehdi and Maryam, and my brother: Abdolreza, whom I can’t thank enough for all they have done for me.

Contents

1 Introduction 10
1.1 Background 10
1.2 Evolution of the project work 10
1.3 Objectives of the study and research questions 15
1.4 Thesis outline 16
2 Methodology 19
3 Prospect of climate conditions for built environment 21
3.1 Climate normal and typical climate conditions 21
3.2 Climate change and foreseeable extreme conditions 22
3.3 Unforeseeable extreme events with disaster impacts 22
3.4 Full prospect of climate conditions for built-environment 24
4 Climate modelling 26
4.1 Climate models 26
4.2 Climate model uncertainty 26
5 Conceptual objectives for protection of built-environment against climate uncertainty .. 29
5.1 Uncertainty in modelling built-environment 29
5.2 Positioning robustness and resilience in a framework for protection against climate change 33
6 Climate change impacts on building performance 35
6.1 Weather files for BPS 35
6.1.1 Weather files representing future typical conditions 36
6.1.2 Weather files representing future typical and extreme conditions 38
6.1.3 Credible weather data sets for climate change impacts assessment 39
6.2 Impacts of climate change on case-study buildings 42
6.2.1 Retrofit design of an existing buildings 43
6.2.2 ASHRAE reference buildings 44
6.2.3 Virtual neighborhood 49
7 Robust energy performance under climate change 53
7.1 Concept of robust design and its application in built environment 53
7.2 Simulation-based optimization method for design of energy-efficient buildings with robust energy performance 56
7.2.1 Formulating the objective functions 57
7.2.2 Building energy model 60
7.2.3 Formulation of optimization process 60

7.3 Assessment of optimization strategies 66
8 Conclusions 70
9 References 72
10 Individual papers 78

1 Introduction

1.1 Background

In the developed countries, more than 87% of the time is spent indoor [1] and this is accompanied with a rapid increase of population living in the urban areas [2].Thus, the role of buildings and their indoor environment is becoming increasingly important. This role becomes even bolder with the recent researches demonstrating high correlation between indoor environment quality and health and well-being of the occupants, and hence their productivity [3]. In addition, there are requirements by regional and national standards and laws to ensure that energy-efficiency in buildings is taken into account while providing a high indoor air quality (IAQ) [4]. In this regard, numerical models and simulation tools such as Building Performance Simulation (BPS) allow the designers to simulate their design concepts and check their compliance with the requirements. Even though these tools had played a central role in achieving high performance in building designs, it is still a major challenge to keep the performance as expected once these designs are constructed. Such a performance gap between the expected level of performance and the actual performance has been discussed and demonstrated in the literature [5-7]. One of the main sources of this discrepancy are the factors that are difficult to predict during the design phase. Climate is an example of that, while its impact on buildings performance has proved to be prominent, it is very difficult to properly consider it in the simulation and design process [8]. In this PhD work, the impacts of climate on building performance is firstly discussed, following by an overview of the main challenges as well as main methods for presenting climate uncertainty in the design process of buildings. At the end a methodology is provided that allow architects and engineers to effectively consider future climate uncertainties during the design phase and achieve solutions that their performance are least sensitive to these uncertainties, or as it will be defined later, are more robust.

1.2 Evolution of the project work

Climate conditions are key input parameters for BPS, but traditionally and for simplification, a typical climate condition is used to represent the most likely condition that a building will experience. The justification for using most likely climate scenarios based on historical data in decision making process has failed to address the natural variability of climate and the increasing recognition of changes in the climate patterns [9]. In the recent years, the increasing impact of climate change and the need for understanding possible future climate evolutions has led to developments of climate models to simulate sophisticated earth climate system. The output data of climate models is downscaled to a set of hourly data gathered to represent one year, which is then formatted in a weather file suitable to be used in BPS [10]. Such weather file allows assessing the impacts of climate change on building performance and therefore can be used for better addressing the protection of buildings against climate change. While data from climate models are available, there is little-to-

nothing done in current standards and building regulations to set principles for assessment of climate change impacts and to support the design of buildings protected against them.

In the first stage of this PhD work, one of the methods for generating future weather files was used to study the impacts of climate change on the performance of a deep energy retrofit design of an existing child care center. The design of the renovation was targeting the achievement of a nearly zero-energy building (nZEB) with no active cooling during summer. This study was the base for several subsequent research questions that have been later answered during this PhD work.

In the following sections, how the research questions and objectives of this study were set, what challenges were faced during this period, and how these challenges have been addressed is briefly described.

As mentioned, the first phase of the study started by evaluating a deep energy retrofit of a child care center in Milan (Italy) under current and future weather scenarios. The retrofit design was developed by a group of building physicists and designers at Politecnico di Milano using an existing weather file, built from the historical observations recorded in 20-years from 1951 to 1970. The main goal of the design was to achieve nZEB with high indoor thermal comfort, while using no means of active cooling during summer. This goal was achieved through the effective exploitation of diurnal and nocturnal natural ventilative cooling strategies by automated windows opening and protecting the building from excessive incoming solar gains by operating properly automated shading devices. As part of the PhD work, the task was identifying to what extent the choices that were made on the basis of 20-year average historical data may succeed to provide acceptable energy and indoor environmental performance throughout the future decades [11], [12]. For this task, a software tool that is based on a method called "*morphing*" was used to generate future weather files for the years 2030, 2050 and 2080. This method is later described in detail and is the most commonly used to downscale the monthly future climate data of a climate model to the temporal resolution suitable for BPS. This study was published in a conference paper with a subsequent Journal paper as follow:

- **Paper I**: Moazami, Amin; Carlucci, Salvatore; Causone, Francesco; Pagliano, Lorenzo. ***Energy retrofit of a day care center for current and future weather scenarios***. Procedia Engineering 2016; 145:1330-7.

- **Paper II**: Pagliano, Lorenzo; Carlucci, Salvatore; Causone, Francesco; Moazami, Amin; Cattarin, Giulio. ***Energy retrofit for a climate resilient child care centre***. Energy and Buildings 2016; 127:1117-32.

The results of this study showed the following impacts on the design due to climate change:

- The installation of active cooling systems is required for coping with harsher summers in the future
- The nZEB target will not be achieved in the future
- The building can demonstrate a substantial shift from the energy need for space heating to a higher request of energy need for space cooling.

This study raised two further questions which became the base for the next stages of the PhD work:

- Although morphing method is one of the most commonly used approaches in the literature, the significance of mentioned impacts raised following question: how credible are the weather files generated using this approach?
- In the study, the ability of the design to keep its expected performance under future scenarios was evaluated; it was named as "*climate resilient building*". Due to vagueness in the building science literature, the choice of the term "*resilience*" raised two more questions: Is it the proper term in this case? How to distinguish between this concept and other concepts that are used in the literature for the protection of built-environment against the impacts of climate change?

To answer the first question, an extensive study was performed on the available methodologies for generating future weather files, suitable for use in BPS. In this process, the authors realized that there is a lack of studies in which the performances of major available methods are compared, and the impacts of using them on energy calculation of buildings are assessed. This study was performed, and the results were published in the Journal of Applied Energy (Paper V), which is described later in this section. In order to proceed with this study, weather files generated based on all major methods were required. Nonetheless it was realised that this task is challenging. To understand the challenge, the source of data for future climate needs to be introduced first.

Global Climate Models (GCMs) are the main source of our understanding of the future evolution of climate and are some of the most complex numerical models that exist. These models consist of several climate system components (atmosphere, ocean, land surface, snow and sea ice) and it describes the dynamics between them. The earth's energy balance between these components is the base for climate projections and generation of future climate data. GCMs are run on supercomputers with thousands of processors [13] and the output data requires petabytes of data storage. These models have quite coarse spatial resolutions (100-300 km) and their outputs are usually stored in monthly or daily temporal resolutions. The first challenge is that such resolutions are not suitable for BPS, which requires local climate data with hourly or sub-hourly time resolution. Furthermore, the following variables are the

minimum that are required to create weather files for use in BPS, which is not often that all are available in climate model datasets:

- Air Temperature
- Relative Humidity
- Global Radiation
- Diffuse Horizontal Radiation
- Direct Normal Radiation
- Wind Speed
- Atmospheric pressure

Several methods are developed to downscale climate models data to a suitable temporal and spatial resolution. The two main approaches are: statistical downscaling and dynamical downscaling. The statistical downscaling method such as morphing [14] is based on simple transformation algorithms. The algorithms apply changes based on monthly trends and variations of GCM outputs on the values of a local weather file, therefore they operate only a temporal downscaling. Due to simplicity of the method and availability of local weather files, this approach is one of the most commonly used approaches in literature [15]. There are several tools that generate future weather files based on this method. Two main software tools based on morphing method and today are available on the market were critically compared and analysed in the paper:

- **Paper III**: Moazami, Amin; Carlucci, Salvatore; Geving, Stig. ***Critical Analysis of Software Tools Aimed at Generating Future Weather Files with a view to their use in Building Performance Simulation.*** Energy Procedia. 2017;132:640-5.

The results suggest that, depending on the purpose of the design, care should be taken in using the above-mentioned tools. One of these tools was the one used for generating the future weather files of the first two papers.

In the other approach which is dynamical downscaling, future climate data with higher resolutions for a specific region is generated by modelling climate system of that region and nest it into a GCM (i.e. using the outputs of GCM as boundary conditions). These models are called Regional Climate Models (RCMs) and the outputs of RCMs have suitable spatial resolution for buildings design purpose and can be run in high temporal resolution. The challenge is that these outputs require extensive storage space to for them to be recorded, and like GCMs they are also mainly stored with a monthly, daily or 6-hour resolution. In order to further downscale RCM data into suitable resolution, one should ask an institute that has an RCM, to perform the simulation and store the required data in the requested higher resolution.

For the purpose of the work and to acquire RCM data for Norway with suitable temporal resolution, a negotiation with the Bjerknes Centre for Climate Research (BCCR) institute started. The centres key area of research is natural variability in the Earth system and man-made climate change (www.bjerknes.uib.no). Unfortunately, the institute did not have all the necessary meteorological variables stored at hourly resolution. Due to time and resource limitation the idea was dropped and a collaboration with Chalmers University of Technology was initiated. Through this collaboration, RCM data for two locations: Stockholm and Geneva became available. These data were at suitable resolution to create future weather files for BPS. The city of Geneva was chosen and a dataset of future weather files based on all major methods of downscaling were created. Geneva was chosen due to the possibility of having cold winters and warm summers.

These data were then converted to weather files with format suitable for BPS. This allowed comparing the relative performance of major available methods for generating future weather files. These files were then used for climate change impact assessment of individual buildings and a neighbourhood in Geneva. The study was published as follow:

- **Paper IV**: Moazami, Amin; Nik, Vahid; Carlucci, Salvatore; Geving, Stig. ***Impacts of future weather data typology on building energy performance – Investigating long-term patterns of climate change and extreme weather conditions***. Applied Energy. 2019;238:696-720.

The work aimed at answering two research questions: does a method of generating future weather files for building performance simulation bring advantages that cannot be provided by other methods? And what type of future weather files enable building engineers and designers to more credibly test robustness of their designs against climate change?

According to the results of this study, all the methods provide enough information to study the long-term impacts of climate change on average. But only those weather files generated based on dynamical downscaling and that take into consideration both typical and extreme conditions are the most reliable for providing representative boundary conditions to test the energy robustness of buildings under future climate uncertainties.

The next step was on proper use of the term “resilience” for the concept of protection against climate change. During the course of the PhD work, it was realized that there is a lack of precise definitions for the concept of protecting the built-environment against climate uncertainty. Several attributes were found in literature. Some of the common terms were: adaptable buildings [16], resilient buildings [17], robust buildings [18], responsive buildings [19]. However, the first step towards protection against climate uncertainty is to identify the climate conditions that a building might face during its life span. Chapter 3 is allocated to provide a prospect of climate conditions for built-environment and to which extend these

conditions can be considered during the design phase of buildings. Through this prospect typical and extreme climate conditions were defined and the extremes were distinguished into two: foreseeable extreme conditions and unforeseeable extreme events. More details are provided in Chapter 3. After identifying the possible climate conditions, a work was set to create a framework that conceptualise protection for buildings against all these conditions. After reviewing the concepts and definitions provided in the literature, the two concepts of *robustness* and *resilience* were found appropriate for the aimed framework. The literature review process and the development of this framework are described in Chapter 5 and the work was published in the following paper:

- **Paper V**: Moazami, Amin; Carlucci, Salvatore; Geving, Stig. ***Robust and resilient buildings: A framework for defining the protection against climate uncertainty.*** (Submitted to IAQVEC 2019 conference, Bari, Italy.)

Finally, the generated weather files representing future typical and extreme conditions, and the defined framework, allowed undertaking the final research question: how is it possible to design buildings with robust performance under climate change? In this regard, a methodology was developed, to empower architects and engineers to achieve building designs with robust energy performance under the future climate uncertainty. The concept of robustness used in this method is in agreement with the defined framework in Chapter 5. The results of this study were presented in the following paper:

- **Paper VI:** Moazami, Amin; Carlucci, Salvatore; Nik, Vahid; Geving, Stig. ***Towards climate robust buildings: an innovative method for designing buildings with robust energy performance under climate change***. (Submitted to Journal of Energy and Buildings)

The method uses three weather files representing future typical and extreme climate conditions in a simulation-based optimization process. More details of the methodology are provided in Chapter 7.

In the following sections, the objectives, research questions and methodologies for this project are briefly described.

1.3 Objectives of the study and research questions

The purpose of this PhD project is to create an automated and algorithm-driven optimization workflow for architects and engineers, which can be used during the design phase to achieve energy-efficienct buildings with robust energy performance under future climate uncertainty. The following two objectives are addressing this purpose:

- The work ought to provide architects and engineers a good insight on methods for generating future weather files, and on which future weather data typology serves better their design purpose.
- The work ought to provide architects and engineers a workflow coherent with the proposed definitory framework to achieve building designs with robust performance under climate change.

The research objectives have been developed into the following research questions:

- What is the prospect of future climate conditions acting on the built-environment? (Chapter 2)
- How the protection of the built-environment against future climate conditions be schematized? (Chapter 5, Paper V)
- What type of future weather files enables to increase the credibility of BPS outcomes under future climate conditions? (Chapter 4, Section 6.1, Paper III and Paper IV)
- Which are the impacts of climate change on the performance of buildings in terms of energy use and thermal comfort? (Section 6.2, Paper I, Paper II and Paper IV).
- How is it possible to design buildings with robust energy performance under future climate uncertainties? (Chapter 7 and Paper VI).

1.4 Thesis outline

This thesis consists of seven chapters and five publications:

Chapter 1 is the introduction which gives brief description about background, aims and evolution of the research work. It also interconnects the publications together in a logical structure.

Chapter 2 provides a prospect for all climate conditions that a building can experience during its life span.

Chapter 4 describes climate modelling and the uncertainty associated to climate projections.

Chapter 5 is about concepts and definitions realised for full protection of built-environment against all future climate conditions.

Chapter 6 describes the implication of climate data in BPS and impact assessment of climate change on the performance of buildings.

Chapter 7 describes the simulation-based optimization method developed in this project to achieve energy-robustness for buildings under presence of climate uncertainties.

Chapter 8 contains main findings, concluding remarks and suggestion for future works.

Paper I and Paper II focus on a deep retrofit design of a real case building and assess the impact of future climate conditions on its energy and thermal comfort performance.

Paper III makes a comparison of two software tools to generate future projection weather data based on statistical downscaling.

Paper IV provides an overview of the major approaches to create future weather data sets based on the statistical and dynamical downscaling of climate models and it investigates the importance of typical and extreme future weather conditions on the energy performance of buildings.

Paper V reviews the concepts of robustness and resilience and organizes them into a framework that clarifies their relationships in the protection of buildings against climate uncertainties.

Paper VI presents a methodology using simulation-based optimization, which allows designers to optimize their solutions for energy-robustness under changing climate.

A schematic overview of the thesis is presented in Figure 1.

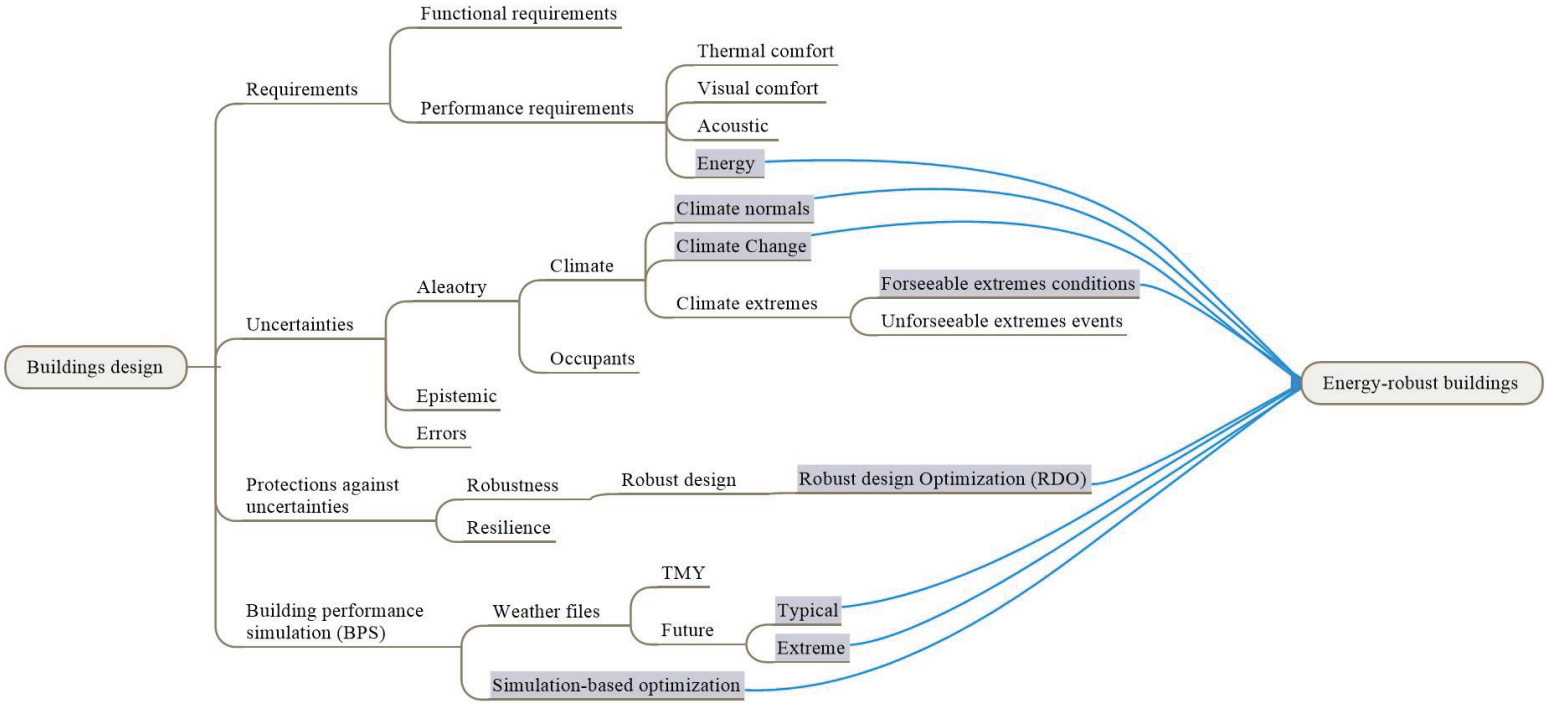

Figure 1 Schematic overview of the thesis and the covered areas.

2 Methodology

The first step of the research was to demonstrate the importance of future climate data as an input for design of high-performance buildings. For this purpose, in collaboration with Politecnico di Milano, a retrofit design of an existing child care center was considered to be evaluated under future climate data. The design was originally based on a weather file representing typical weather condition, generated from historical data, and aimed for renovating the building to become nZEB. A numerical model of the existing building was created based on data collected from site survey, interviews with teachers and some standard values. The model was then calibrated against measured delivered energy and indoor air temperatures following the ASHRAE Guideline 14 [20]. This model was used to refine the refurbishment concept of the building, and finally to estimate the performance of the renovated building under current typical and future typical weather scenarios. A software tool called CCWorldWeatherGen was used to generate future weather files using the morphing method. The generated future weather files were used to assess the performance of the building in terms of thermal comfort and energy. The work was published in two papers [21], [11].

After studying the climate change impacts on a real case building using statistically downscaled climate data, the collaboration with Chalmers University gave the chance of having access to dynamically downscaled climate data. These data were generated by Rossby Centre Regional Atmospheric Climate Model (RCA4). RCA4 is a regional climate model (RCM) that was used to dynamically downscale climate data from four different GCMs to the spatial resolution of 12.5 km^2 and the hourly temporal resolution [22]. Using these dynamically downscaled data in addition with statistically downscaled data, a weather data sets of 74 future weather files were generated for the city of Geneva (Switzerland) ready to use in BPS [15]. Representative weather files were synthesized to account for extreme conditions together with typical climate conditions. The weather files were applied to energy simulation of 16 ASHRAE standard reference buildings. The reference buildings were simulated in isolation, and in combination to create a virtual neighbourhood. A simulation workflow was implemented in the multidisciplinary design optimization platform modeFRONTIER coupled with MATLAB for post-processing of the output data. This was used to simulate the full set of 16 building models under the 74 generated future weather files, giving a total of 1 184 simulation runs. This allowed investigating the impacts of all major future weather data typology on building energy performance. The work is published in a journal paper [15].

From the literature review, the two concepts of robustness and resilience were found most relevant to create a framework for describing the protection of the built environment under all climate conditions that are identified in Chapter 5.

In the final stage of the project, we specifically referred to an algorithm-driven multi-objective robust design optimization whose goal consists in identifying a set of optimal

building design solutions to achieve energy-efficient with robust energy performance under climate uncertainty. The set of design solutions make the buildings to have high-energy performance and low performance-variability while climate uncertainty is present. It implies low energy use and a minimum sensitivity to the disturbance. The presence of climate uncertainty is the source of variation in primary energy use for the building. The specific robust design optimization problem was formulated with two objectives. The design effect of these two objectives is to narrow the distribution of the primary energy and shift the mean of the distribution close to the target value (ideally zero). To apply climate as source of performance variability, the triple method is adapted. In this method, the distribution of climate scenarios is represented with only three weather files: TDY, EWY and ECY. The TDY file represents the most likely climate evolution, and EWY and ECY are the extreme warm and cold climate evolutions respectively.

A case-study building model is used to run three different optimization configurations. To conduct the optimization tasks, the dynamic energy simulation engine EnergyPlus [23] was integrated into the modular environment for process automation and optimization in the engineering design process modeFRONTIER [24], which embeds a multi-objective optimization engine that integrates several optimization algorithms and sampling strategies.

3 Prospect of climate conditions for built environment

This section tries to identify a prospect of climate conditions for buildings. The first step towards protection against climate uncertainty is to identify the climate conditions that a building might face during its lifespan. The following definitions provided by World Meteorological Organization (WMO), Intergovernmental Panel for Climate Change (IPCC) and United Nations Office for Disaster Risk Reduction (UNISDR) can provide a platform for depicting this prospect:

- ***Climate normals*** as defined by WMO are "averages of climatological data computed for the following consecutive periods of 30 years: 1 January 1981 to 31 December 2010, 1 January 1991 to 31 December 2020, etc."

- **Climate extreme** defined by IPCC as "the occurrence of a value of a weather or climate variable above (or below) a threshold value near the upper (or lower) ends of the range of observed values of the variable".

- ***Climate change*** defined by IPCC as "A change in the state of the climate that can be identified (e.g., by using statistical tests) by changes in the mean and/or the variability of its properties and that persists for an extended period, typically decades or longer. Climate change may be due to natural internal processes or external forcings, or to persistent anthropogenic changes in the composition of the atmosphere or in land use."

Although nowadays, decision-makers are provided with data on climate normals and also projections of climate changes according to generated data by climate models [15], there are climate conditions that occur far beyond observed or expected ranges. These extreme events are unforeseeable and can lead to disaster impacts.

- ***Disaster impacts*** are defined by UNISDR as "the total effect, including negative effects (e.g., economic losses) and positive effects (e.g., economic gains), of a hazardous event or a disaster. The term includes economic, human and environmental impacts, and may include death, injuries, disease and other negative effects on human physical, mental and social well-being".

3.1 Climate normal and typical climate conditions

The WMO has been providing climate normals at monthly scale for the last 82 years. They first calculated climate normals for the period of 1901-1930 and updated them every 30 years [9]. As they are meant to be, these data provide decision makers and stakeholders a representative image of climate conditions in a given location. The climate normals are based on a stationary assumption of climate. Stationarity assumption is considering that natural systems fluctuate within an unchanging envelope of variability [25]. However, the observed climate change has shown that the assumption of stationarity for climate cannot be taken for

granted and climate normals do not provide a complete image of possible future climate for a location.

3.2 Climate change and foreseeable extreme conditions

As stated by IPCC [26], the mean (i.e. the climate normals) and the variability of climate is changing over time, therefore, in any decision-making process, it is important to account for these changes over several decades to come. Apart from long-term patterns of climate change, the short-term changes that induce climate extremes have to be considered. Observations show a more frequent and more intense occurrence of climate extremes [27].

The Swiss Federal Office of Meteorology and Climatology (MeteoSwiss) provides climate indicators that characterize the climate, indicators such as hot days, frost days and tropical nights. These are also used to communicate how climate is changing. Hot days are defined as "*days in which the temperature rises above 30 °C*", frost days are defined as "*days on which the temperature dips below 0 °C*", and tropical nights are defined as "*days on which the temperature does not dip below 20 °C*". Table 1 shows the numbers of hot days and tropical nights during 92 days of summer (1st June-31st August) for the city of Geneva according to climate normal and three climate extreme summers.

Table 1 Comparison of the number of hot days and tropical nights for the extremely hot summer of 2003, 2017 and 2018 in Geneva.

		Number of hot days	**Number of tropical nights**
Climate normals[1]	1961-1990	10.4	0.1
	1981-2010	14.7	0.4
Observed climate extremes[2]	Summer 2003	51	4
	Summer 2017	30	4
	Summer 2018	33	1

The above table demonstrate how the number of hot days and tropical nights for climate normal (averaged over 30-year period) has increased from 1961-1990 to 1981-2010, which shows the change in the mean of climate. The table also reveals how the averaging process of calculating climate normals misses important information on climate extremes. A decision maker would not be informed that values up to 3 times the normal values can occur although there are historical records of such values.

3.3 Unforeseeable extreme events with disaster impacts

Climate extremes can become unforeseeable extreme events with disaster impacts through two mechanisms:

Mechanism 1: Cities are complex systems, and, during an extreme event, some functionalities disrupt as a result of a chain of small events. An example is the failure of a power grid during a heat wave. This failure is typically the result of several smaller events:

1. Extremely high temperatures can last from days to weeks. This cause peak loads to be much higher both in magnitude and duration [28].
2. Extremely high temperatures cause reduction of the thermal capacity of the transmission lines that applies more stress on the power grid [29].
3. Heat waves are usually accompanied by stationary high-pressure zones, resulting in light winds at the surface and, therefore, reduced wind generation by wind turbines [29].
4. Increased air temperature has a derating effect on gas-turbines, which causes a reduction in capacity and the efficiency of these systems [30].
5. During heat wave 2003, French nuclear power plants operated at much lower capacity due to very low river water levels and also high temperature of the water leaving cooling towers exceeded environmental safety levels [31].

This chain of events and high demands for a period of time implies high stress on the grid, which can lead to unforeseeable failure of the grid system and so:

6. No electricity leaves thousands of buildings without any means of mechanical cooling, potentially causing a fatal situation for the elderly, very young, or chronically ill people, as it occurred during the 2003-heat wave in Europe when thousands of people died [32].

The climate extremes experienced during the summer of 2003 led to disaster impacts with a high number of heat-related deaths in France [33] and in Switzerland [34] including Geneva. In Table 1, Although there is a substantial difference in number of hot days between the summer of 2003 with those of 2017 and 2018, the scale of the impacts was much higher than this difference, in other words, during the 2003 heatwave, the extreme conditions were coupled with other small events that in a domino effect ended to a disaster impact. Climate extremes increase the probability of disaster impacts, but it is almost impossible to predict which outcome will occur due to a number of involved factors characteristic of each urban system. The best description of such conditions is given in the following proverb[35]:

"*For want of a nail the shoe was lost,*

For want of a shoe the horse was lost,

For want of a horse the rider was lost,

For want of a rider the battle was lost,

For want of a battle the kingdom was lost,

And all for the want of a horseshoe nail."

The loss of one horseshoe might be insignificant, but it could indirectly cause the loss of a war, and is almost impossible to predict which outcome will occur.

The frequency and intensity of climate extremes occurrence is increasing [36] and consequently the number of disaster impacts are on the rise. Figure 2 demonstrates for each year in the United States the number of weather and climate disasters with overall losses of more than $1 billion. An increase in the number of such events is evident. Part of this increase is due to expansion of urban areas, which means more people and infrastructures are exposed to damage during these events [37].

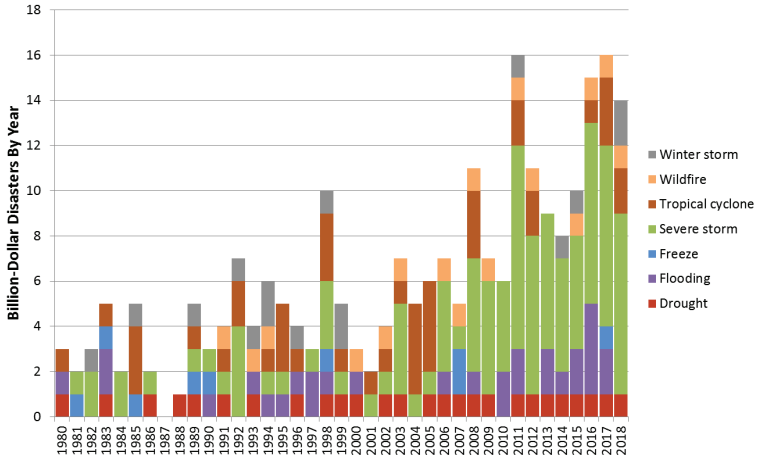

Figure 2 Yearly occurrence of extreme events in the United States (as of 7 July 2017) whose impacts cost greater than 1 billion. NOAA National Centers for Environmental Information (NCEI) U.S. Billion-Dollar Weather and Climate Disasters (2019). https://www.ncdc.noaa.gov/billions/

Mechanism 2: Climate extremes can also cause disaster impacts as they occur in an unpredictable scale of magnitude for a given location. An example of this failure mechanism is the hurricane Maria that made landfall on Puerto Rico on Wednesday, September 20, 2017. It caused several casualties and estimated damage of $ 90 billion [38]. On the island of Puerto Rico during 48 hours of the event, it was recorded a maximum wind speed of 61.2 m/s and a maximum precipitation rate of 163.6 mm/h [39]. To provide a benchmark, the American Meteorological Society classifies a precipitation rate above 7.6 mm/h as *heavy rainfall* [40]. Thus, the peak value of the precipitation rate in Porto Rico during the hurricane Maria was more than twentyfold what is expected to be heavy rainfall.

3.4 Full prospect of climate conditions for built-environment

From above, a complete prospect of climate conditions for a location can be realised as: climate normals, climate change, foreseeable climate extremes and unforeseeable extreme events with disaster impacts.

Given a prospect of climate conditions, first, the available climate modelling technology that provides future climate data is discussed in Chapter 4. Based on the available data on historical and future climate conditions and the above prospect, in the second stage, a framework is conceptualized to represent the building's protection against all identified climate conditions. This framework is presented in Chapter 5. In Chapter 6, the methodologies to use data from climate models and generate future weather files for BPS are briefly described. And last, generated future weather files are used to assess the impacts of future climate on the performance of buildings at an individual building scale and a neighbourhood scale in the second part of Chapter 6.

4 Climate modelling

4.1 Climate models

Climate models are our most advanced tools to enhance our understanding of climate behaviour on long-term and short-term time scales. So called Global Climate Models (GCMs) are complex mathematical modelling of the earth climate system. They include different components for land surface, atmosphere, ocean and sea ice and simulate their interactions [41]. Such complex models require enormous computational power and data storage space, which is provided by supercomputers today. GCM outputs represent averages over a region or the entire globe with a spatial resolution in the range of 100-300 km^2 and a monthly temporal resolution[15]. For higher resolutions, the regional climate models (RCMs) are used, which downscale the results of GCMs to a specific region and with higher temporal resolution. Climate models are feed with several climate forcings. A climate forcing is "*an energy imbalance imposed on the climate system either externally or by human activities. Examples include changes in solar energy output, volcanic emissions, deliberate land modification, or anthropogenic emissions of greenhouse gases, aerosols, and their precursors.*" [42]. Changes in climate forcings will result in having different outcomes from GCMs and RCMs. To determine these forcings, IPCC created a number of possible scenarios of future anthropogenic greenhouse gas emissions based on given socio-economic storylines that are used as inputs for modelling climate in the future. The first set of scenarios were introduced in the IPCC Special Report on Emissions Scenarios (SRES) in 1996 [43], [44]. Later, in 2014, the IPCC adopted a new series of emission and concentration scenarios called "Representative Concentration Pathways (RCPs)".

4.2 Climate model uncertainty

Climate models are all verified models and validated against past climate conditions [45]. GCMs are usually run for very long-time periods (even more than one thousand years) before industrialization. The major point is to verify the models concerning the performance and evolution of the climate system. The verified models will then set to run from 1870, picking initial conditions and future climate scenarios. Afterwards, what we see as future conditions is a function of the evolution of the climate model affected by the initial and boundary conditions. Once the model is verified, it means the outcomes for any period are verified and it cannot be said that a far future period is less/more uncertain than a near future.

A common method to deal with the uncertainty of climate projections is to perform several climate simulations and creating ensemble [46]. This is the same way IPCC uses to provide information on the uncertainty of the projections. Figure 3 presents the near-term projections resulted from aggregating the outcomes of several climate models. This figure is provided by IPCC Fifth Assessment Report [47] and the link to the figure is given in the caption.

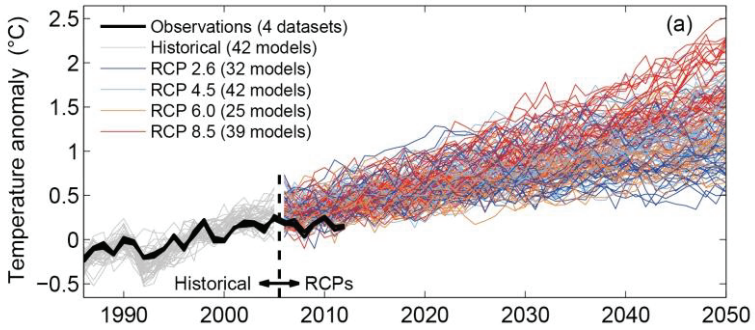

Figure 3 Gobal mean temperature near-term projections relative to 1986-2005 (http://www.climatechange2013.org/images/figures/WGI_AR5_Fig11-25.jpg)[47]

The dynamically downscaled data used in the PhD project were derived from four climate models tested under two emission scenarios: CNRM and ICHEC under RCP 8.5 and RCP 4.5, and IPSLm and MPIM under RCP 8.5. This gives an ensemble of six combinations. This means the uncertainty associated to climate modelling were taken into account (using simulation data from a combination of 4 climate models and 2 emission scenarios). Definitely more combinations would give more information on the uncertainty. In total, the weather files used in this study were generated based on SRES A2, RCP 4.5 and RCP 8.5 scenarios of IPCC. These emission scenarios cover the possible range of projections provided by IPCC that pass global warming of 1.5 °C with respect to the pre-industrial levels, by 2100. For better comparison of scenarios, following graph brought here from an article [48] published in Nature (Figure 4), which demonstrate the global temperature changes relative to 1986–2005 for different scenarios of IPCC. The yellow highlighted area is not in the original graph. It is added for better visualization of area covered by the three considered emission scenarios mentioned above.

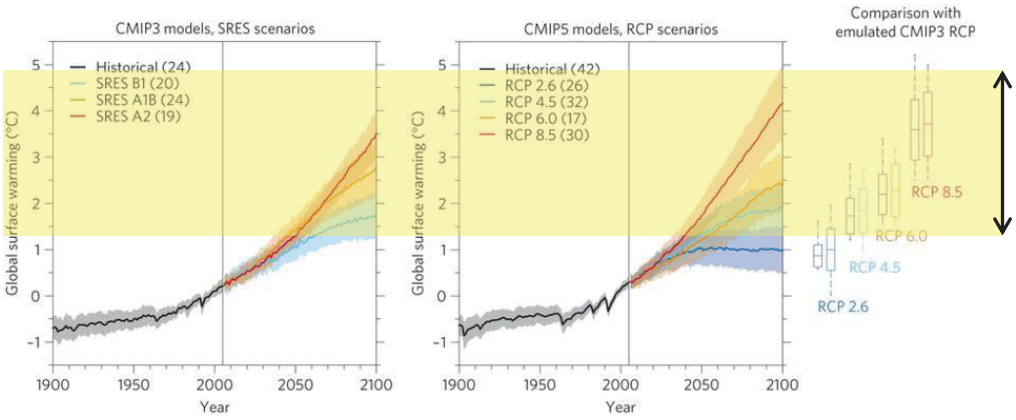

Figure 4 Global temperature change (mean and one standard deviation as shading) relative to 1986–2005 for the SRES scenarios run by CMIP3 and the RCP scenarios run by CMIP5. The number of models is given in brackets. The box plots (mean, one standard deviation, and minimum to maximum range) are given for 2080–2099 for CMIP5 (colours) and for the MAGICC model calibrated to 19 CMIP3 models (black), both running the RCP scenarios. [48]

Description of scenarios used in this project is given below:

- ***SRES A2***: "The A2 storyline and scenario family describes a very heterogeneous world. The underlying theme is self-reliance and preservation of local identities. Fertility patterns across regions converge very slowly, which results in continuously increasing global population. Economic development is primarily regionally oriented and per capita economic growth and technological change are more fragmented and slower than in other storylines." [43]
- ***RCP 4.5***: "It is a stabilization scenario where total radiative forcing is stabilized to 4.5 W/m^2 before 2100 by employment of a range of technologies and strategies for reducing greenhouse gas emissions." [49]
- ***RCP 8.5***: "The RCP 8.5 is characterized by rising radiative forcing pathway leading to 8.5 W/m^2 by 2100. The underlying scenario drivers and resulting development path are based on the SRES A2 scenario." [49]

The availability of generating possible future climate conditions adding to the recorded climate data allows us to have a good coverage of the prospect of climate condition that was described in Chapter 3. The climate normal can be calculated for past, current and future while considering climate change. There is also data available for climate extremes, the observed conditions and foreseeable future conditions. But as mentioned before, unforeseeable extreme events are unpredictable. In the following chapter, a conceptual framework for protection of built-environment against all climate conditions is proposed and described.

5 Conceptual objectives for protection of built-environment against climate uncertainty

5.1 Uncertainty in modelling built-environment

There are several studies showing that the buildings do not perform as they were expected to do, once they are in operation [5-7]. The sources of discrepancies can be due to simplifications and numerical approximation of modelling tools [50], human errors during the construction or poor quality of construction [51], and operational factors such as occupant behaviour and weather conditions [52], etc. The causes of discrepancy in buildings performance can be categorized in three types: epistemic uncertainties, aleatory uncertainties and errors. They are defined as:

- **Epistemic uncertainty**: "a potential deficiency that is due to a lack of knowledge. It can arise from assumptions introduced in the derivation of the mathematical model used or simplifications related to the correlation or dependence between physical processes." [53]
- **Error**: "A discrepancy between a computed, observed or measured value or condition and the true, specified or theoretically correct value or condition" [54]
- **Aleatory uncertainty**: "is said to arise due to the inherently random or variable nature of a quantity, or the (usually unknown) system underlying it." [50]

Epistemic uncertainties in building modelling can be reduced by improvement of numerical models, calibration using additional experimental observations, and providing better information [55]. *Human Errors* can be minimized by the use of technological advancements such as Building Information Modelling (BIM) [56] and Augmented Reality (AR) [57], and offsite or prefabricated construction technologies [58]. These technologies can reduce the gap between the expected simulated quality and the quality of constructed building. The third type, *aleatory uncertainty*, due to its inherent randomness and natural variability, is irreducible and cannot be eliminated [59]. So far, the common approach to deal with this type of uncertainty in BPS is to consider a most likely scenario. For example, occupants are normally simulated with a fixed schedule [60] as the most probable occupancy scenario. Using typical meteorological year (TMY) weather files is another example of counting for the most likely conditions [61]..

After the buildings are built, they are expected to perform as designed. This from the traditional perspective of reliability, where a system is considered reliable if it performs as expected in a stable environment with stable requirements [62]. However, for buildings in real-life conditions, the stability of the environment and requirements cannot be guaranteed. The environmental conditions for a building are changing constantly due to presence of aleatory uncertainties such as climate and occupant's behaviour. While the other uncertainties can be reduced, aleatory uncertainties are irreducible. This means these uncertainties cannot

be eliminated and the only way to deal with them is to include them in the modelling i.e. to evaluate and design buildings under presence of aleatory uncertainties.

Designing under presence of aleatory uncertainties is not a new concept and has begun a standard procedure in other industries since long time, but it has not been yet applied in buildings industry. The idea of this concept is that instead of eliminating the source of uncertainty, assuming or forcing that the inputs are deterministic, this source is presented as noise during the design phase and the goal is to achieve a design solution which has a performance with minimum sensitivity to the presence of noise. This process is called "robust design" and was introduced first by Taguchi in the 1940s [63].

With the focus on climate as an aleatory uncertainty and inspired by the concept of robust design, during this PhD work, a novel methodology is developed for achieving buildings design with robust energy performance under presence of climate uncertainty. In this method, both climate normals (typical climate conditions) and foreseeable climate extremes based on historical and future generated climate data are used. These conditions are introduced as noise into BPS, and an algorithm-driven and simulation-based optimization process is built for achieving design solutions with minimum sensitivity to the presence of the noise. The methodology for considering climate uncertainty as noise in BPS and formulation of the optimization is described in detail in section 7.

Although climate robust buildings provide performance that is insensitive to typical and predictable extreme conditions (see results provided in section 7.3), these buildings cannot be considered as protected against the unforeseeable extreme events (described in section 3.3). Protection against such events requires a different approach that discusses possible failure mechanism in case of occurrence and also a recovery mechanism. This concept in the literature is mainly referred to as "resilience". For a better understanding, Table 2 provides the commonly discussed concepts of robustness and resilience both in buildings design and system design.

Next section organises the concepts into a framework that clarifies their relationships, and protection of buildings against all climate conditions is discussed.

Table 2 Definitions provided in buildings design's literature for the concepts of robustness and resilience

Ref.	Definition	Ability	Source of Uncertainty
	Robustness		
[64]	"The measure by which the indoor environment of a building lives up to its design purpose when it is used by occupants in a real-life situation."	Lives up to its design purpose	Occupants in a real-life situation
[65]	"The sensitivity of identical performance indicators of a building design for errors in the design assumptions."	Insensitivity	Errors in the design assumptions
[66]	"A building that shows little variation in performance despite of variable occupant's behavior."	Little variation	Occupant's behavior
[67]	"A building that is not negatively affected by changes in operation parameters."	Not negatively affected	Changes in operation parameters
[68]	"Robust solution is insensitive to climate change uncertainties."	Insensitivity	Climate change uncertainties
[69]	"Buildings whose performances show little variations with alternating occupant behavior patterns."	Little variations	Occupant behavior patterns
	Resilience		
[70]	"A resilient built environment as one designed, located, built, operated, and maintained in a way that maximizes the ability of built assets, associated support systems (physical and institutional) and the people that reside or work within the built assets, to withstand, recover from, and mitigate the impacts of threats."	Withstand, recover, mitigate	Impacts of threats
[71]	"Buildings resilience could be seen as an ability to withstand the effects of earthquakes, extreme winds, flooding and fire, and their ability to be quickly returned to normal use after such event."	Withstand, quickly returned to normal	Earthquakes, extreme winds, flooding, fire
[72]	"A building's ability to withstand severe weather and natural disasters along with its ability to recover in a timely and efficient manner if it does incur damages."	Withstand, recover in a timely and efficient manner	Severe weather and natural disasters
[73]	"Resilience in terms of cities generally refers to the ability to absorb, adapt and respond to changes in an urban system"	Absorb, adapt, respond	Changes in an urban system
[74]	"The capacity of the city (built infrastructure, material flows, social functioning, etc.) to undergo change while still maintaining the same structure, functions and feedbacks, and therefore identity."	Undergo change while maintaining the structure, functions and feedbacks	NA

Table 3 Definitions provided in system design's literature for the concepts of robustness and resilience

Ref.	Definition	Ability	Source of Uncertainty
	Robustness		
[75]	*Insensitivity to anticipated risks.*	Insensitivity	Anticipated risk
[76]	*Capable of accommodating unforeseeable changes in the operating environment*	accommodating	Unforeseeable changes in the operating environment
[77]	*Insensitivity to both expected and unexpected variations*	Insensitivity	Expected and unexpected variations
[78]	*The ability of a system to continue to operate correctly across a wide range of operational conditions*	Continue to operate correctly	Wide range of operational conditions
[79]	*The ability of a technical system to maintain its stated performance level in the presence of fluctuations in primary and secondary inputs, the environment and in human operation*	Maintain its stated performance level	Fluctuations in the environment and in human operation
[80]	*The ability of a system to absorb change*	Absorb	Change
[81]	*The potential for system success under varying future circumstances or scenarios.*	System success	Varying future circumstances or scenarios
[62]	*The ability of a system, as built/designed, to do its basic job in uncertain or changing environments*	To do its basic job	Uncertain or changing environments
	Resilience		
[82]	*Ability to anticipate, prepare for, and adapt to changing conditions and withstand, respond to, and recover rapidly from disruptions through sustainable, adaptable, and holistic planning and technical solutions*	Anticipate, prepare, adapt, withstand, respond, recover rapidly	Changing conditions, disruptions
[83]	*Potential to sustain development by responding to, and shaping, change in a manner that does not lead to the loss of future options.*	Sustain, respond, shape, change	Future options
[84]	*The ability to withstand a severe/extreme event (shock) and recover*	Withstand, recover	Severe/ extreme event
[85]	*The ability of a system to return to its original (or desired) state after being disturbed*	Return to its original (or desired) state	Being disturbed
[86]	*The capacity to cope with unanticipated dangers after they have become manifest*	Cope	Unanticipated dangers
[87]	*A system that is able to adjust its functioning prior to, during, or following changes and disturbances, so that it can continue to perform as required after disruption or major mishap, and in the presence of continuous stress*	Adjust its functioning, continue to perform as required	Changes, disturbances, disruption, major mishap, continuous stress
[88]	*Withstand[ing] a major disruption within acceptable degradation parameters and to recover within an acceptable cost and time*	Withstand, recover	Major disruption

5.2 Positioning robustness and resilience in a framework for protection against climate change

1) Table 2 allows identifying two aspects for both robustness and resilience concepts: (1) the nature of their considered uncertainties, and (2) the required attributes for the protection against these uncertainties.

In the case of robustness, the considered uncertainties are "uncertainties during operation" and the main attribute is the "insensitivity" of the system/building performance to the presence of those uncertainties. For buildings, the main focus is on aleatory uncertainties such as occupants and climate.

In the case of robustness, the considered uncertainties are "uncertainties during operation" and the main attribute is the "insensitivity" of the building performance to the presence of those uncertainties. For buildings, the main focus is on aleatory uncertainties such as occupant behavior and actions and climate. In the case of resilience, although the considered uncertainties are "uncertainties during operation", the focus is on "major disruptions or shocks", which can be the unforeseeable extreme events described in section 3.3. These types of events, as mentioned earlier, can lead to disaster impacts (please refer to section 2). For this reason, the required attributes can be summarized as "withstand, absorb and recover". Thus, if a building is robust, it is likely that it will withstand and absorb the shock better than a non-robust building. However, an unforeseeable extreme event can still cause the building to fail. For the aforementioned matters, the following two definitions are provided in this PhD work..

- **Definition 1**: A robust building is a building that, while in operation, can provide its performance requirements with a minimum variation in a continuously changing environment.
- **Definition 2**: A resilient building is a building that not only is robust but also can fulfill its functional requirements during a major disruption. Its performance might even be disrupted but has to recover to an acceptable level in a timely manner in order to avoid disaster impacts. (disaster impact is defined in Chapter 3).

The *functional requirements* defines what a building has to do, and the *performance requirements* determines how well a functional requirement has to be done [89].

Following these definitions and considering the prospect of climate conditions for built-environment that were identified in section 3.4, a framework can be realised for protection of built-environment against all climate conditions. The concepts of robustness and resilience now can be clearly related and differentiated within this framework. For a better understanding, the framework is depicted in Figure 5.

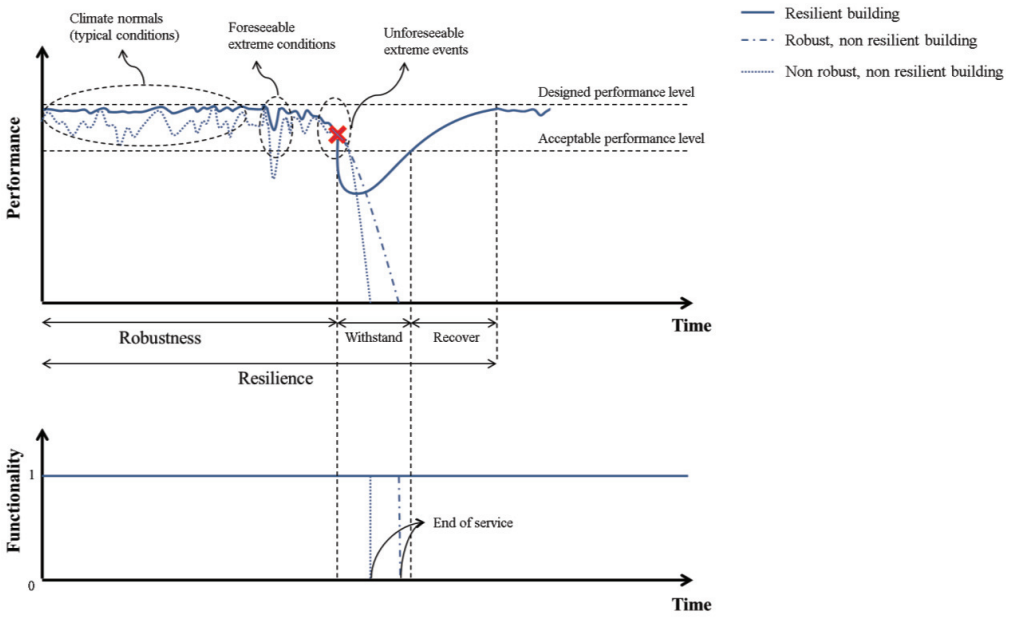

Figure 5 Framework for protection of built-environment against all climate conditions.

Based on this framework:

- A fully protected built-environment against climate change means: while in operation, it can provide a designed performance level with minimum variation under typical and foreseeable extreme conditions, and in case of unforeseeable extreme events, it can maintain its functionality during the event with acceptable performance level and is able to recover to its designed performance level after the event: in other words, the built-environment is protected under climate normal and foreseeable and unforeseeable climate extremes.

6 Climate change impacts on building performance

6.1 Weather files for BPS

Environmental data with high temporal resolution are required for BPS [3]. These data are provided by files that contain values for 8760 hours of a year. The BPS tool that was used in this project for energy calculation of the buildings is called EnergyPlus [23]. An EnergyPlus Weather (EPW) file contains hourly values of several climate variables, such as: air temperature, relative humidity, solar radiation, wind speed, etc. Figure 6 shows hourly climate data presented in EPW file format for the city of Geneva. The first 8 lines, includes information on the location, design conditions, ground temperature, etc.

```
LOCATION,GENEVA,-,CHE,IWEC Data,067000,46.25,6.13,1.0,416.0
DESIGN CONDITIONS,1,Climate Design Data 2009 ASHRAE Handbook,,Heating,1,-6.9,-4.8,-11,1.5,-4.8,-9.1,1.8,-2.9,11.3,1.6,9.5,3.1,2.3,240,Cooling,7,11.5,30.8,19.3,29,18.8,27.2,
TYPICAL/EXTREME PERIODS,6,Summer - Week Nearest Max Temperature For Period,Extreme,7/ 6,7/12,Summer - Week Nearest Average Temperature For Period,Typical,7/20,7/26,Winter -
GROUND TEMPERATURES,3,.5,,,,2.79,2.05,3.37,5.43,10.84,15.02,17.83,18.69,17.23,13.99,9.66,5.64,2,,,,5.53,4.20,4.48,5.57,9.19,12.46,15.08,16.49,16.19,14.35,11.37,8.20,4,,,,7.
HOLIDAYS/DAYLIGHT SAVINGS,No,0,0,0
COMMENTS 1,"IWEC- WMO#067000 - Europe -- Original Source Data (c) 2001 American Society of Heating, Refrigerating and Air-Conditioning Engineers (ASHRAE), Inc., Atlanta, GA
COMMENTS 2, -- Ground temps produced with a standard soil diffusivity of 2.3225760E-03 {m**2/day}
DATA PERIODS,1,1,Data,Sunday, 1/ 1,12/31
1984,1,1,1,60,C9C9C9C9*0?9?9?9?9?9?9?9A7A7A7A7A7*0E8*0*0,-2.4,-4.9,81,98100,0,1415,236,0,0,0,0,0,0,0,250,1.0,0,0,2.8,22000,0,999999099,0,0.0980,0,88,0.000,0.0,0.0
1984,1,1,2,60,C9C9C9C9*0?9?9?9?9?9?9?9*0B8B8B8B8*0*0E8*0*0,-1.8,-3.7,85,98100,0,1415,239,0,0,0,0,0,0,0,250,0.8,0,0,3.2,22000,9,999999999,0,0.0980,0,88,0.000,0.0,0.0
1984,1,1,3,60,C9C9C9C9*0?9?9?9?9?9?9?9*0B8B8B8B8*0*0E8*0*0,-1.4,-2.9,88,98100,0,1415,241,0,0,0,0,0,0,0,250,0.7,0,0,3.6,22000,9,999999999,0,0.0980,0,88,0.000,0.0,0.0
1984,1,1,4,60,C9C9C9C9*0?9?9?9?9?9?9?9A7A7A7A7A7A7*0E8*0*0,-1.4,-2.6,90,98100,0,1415,241,0,0,0,0,0,0,0,240,0.5,0,0,4.0,22000,0,999999099,0,0.0980,0,88,0.000,0.0,0.0
1984,1,1,5,60,C9C9C9C9*0?9?9?9?9?9?9?9*0B8B8B8B8*0*0E8*0*0,-1.5,-2.6,91,98100,0,1415,241,0,0,0,0,0,0,0,240,1.2,0,0,3.0,22000,9,999999999,0,0.0980,0,88,0.000,0.0,0.0
1984,1,1,6,60,C9C9C9C9*0?9?9?9?9?9?9?9*0B8B8B8B8*0*0E8*0*0,-1.7,-2.6,93,98100,0,1415,240,0,0,0,0,0,0,0,240,1.9,0,0,2.0,22000,9,999999999,0,0.0980,0,88,0.000,0.0,0.0
1984,1,1,7,60,A7A7E8E8*0?9?9?9?9?9?9?9A7A7A7A7A7A7*0E8A7*0,-1.8,-3.0,90,98100,0,1415,239,0,0,0,0,0,0,0,240,2.6,0,0,1.0,22000,0,999999099,0,0.0980,0,88,0.000,0.0,0.0
1984,1,1,8,60,B8C8E8B8*0?9?9?9?9?9?9?9*0B8B8B8B8*0*0E8*0*0,-1.4,-2.6,90,98100,0,1415,241,0,0,0,0,0,0,0,240,1.7,0,0,0.7,22000,9,999999999,0,0.0980,0,88,0.000,0.0,0.0
1984,1,1,9,60,B8C8E8B8*0H9H9H9I9I9I9I9*0B8B8B8B8*0*0E8*0*0,-1.0,-2.3,90,98100,37,1415,243,11,0,11,1200,0,1200,340,240,0.9,0,0,0.4,22000,9,999999999,0,0.0980,0,88,0.000,0.0,
1984,1,1,10,60,A7A7E8E8*0G9G9G9I9I9I9I9A7A7A7A7A7A7*0E8*0*0,-0.6,-2.0,89,98100,211,1415,244,89,53,81,9700,3800,9000,1770,0,0.0,0,0,0,0.1,22000,0,999999099,0,0.0980,0,88,0.000
1984,1,1,11,60,B8C8E8B8*0H9H9H9I9I9I9I9*0B8B8B8B8*0*0E8*0*0,0.1,-1.3,89,98000,360,1415,258,186,361,94,19400,28800,12400,1740,0,0.3,3,3,0.1,22000,9,999999999,0,0.0980,0,88,0
1984,1,1,12,60,B8C8E8B8*0H9H9H9I9I9I9I9*0B8B8B8B8*0*0E8*0*0,0.9,-0.4,91,98000,458,1415,272,197,130,155,21400,11500,17900,3500,0,0.7,7,7,0.1,22000,9,999999999,0,0.0980,0,88,
1984,1,1,13,60,A7A7E8E8*0G9G9G9I9I9I9I9A7A7A7A7A7A7*0E8*0*0,1.6,0.5,92,97900,497,1415,294,77,0,77,9100,0,9100,3280,240,1.0,10,10,0.1,15,0,999999599,0,0.0980,0,88,0.000,0.0,
1984,1,1,14,60,B8C8E8B8*0H9H9H9I9I9I9I9*0B8B8B8B8*0*0E8*0*0,1.8,0.7,92,97900,475,1415,295,72,0,72,8500,0,8500,3060,240,1.2,10,10,0.1,15,9,999999999,0,0.0980,0,88,0.000,0.0,
1984,1,1,15,60,B8C8E8B8*0H9H9H9I9I9I9I9*0B8B8B8B8*0*0E8*0*0,2.0,0.9,92,97800,393,1415,296,55,0,55,6500,0,6500,2300,240,1.3,10,10,0.1,15,9,999999999,0,0.0980,0,88,0.000,0.0,
1984,1,1,16,60,A7A7E8E8*0G9G9G9I9I9I9I9A7A7A7A7A7A7*0E8*0*0,2.2,1.1,92,97700,257,1415,297,30,0,30,3500,0,3500,1200,240,1.5,10,10,0.1,15,0,999999599,0,0.0980,0,88,0.000,0.0,
1984,1,1,17,60,B8C8E8B8*0H9H9H9I9I9I9I9*0B8B8B8B8*0*0E8*0*0,1.9,0.8,93,97800,78,1415,296,6,0,6,700,0,700,220,240,1.2,10,10,0.1,15,9,999999999,0,0.0980,0,88,0.000,0.0,0.0
1984,1,1,18,60,B8C8E8B8*0?9?9?9?9?9?9?9*0B8B8B8B8*0*0E8*0*0,1.5,0.5,93,97800,0,1415,294,0,0,0,0,0,0,0,240,0.8,10,10,0.1,15,9,999999999,0,0.0980,0,88,0.000,0.0,0.0
1984,1,1,19,60,A7A7E8E8*0?9?9?9?9?9?9?9A7A7A7A7A7A7*0E8A7*0,1.2,0.2,93,97800,0,1415,292,0,0,0,0,0,0,0,320,0.5,10,10,0.1,15,0,999999599,0,0.0980,0,88,0.000,0.0,0.0
1984,1,1,20,60,B8C8E8B8*0?9?9?9?9?9?9?9*0B8B8B8B8*0*0E8*0*0,0.7,-0.3,92,97800,0,1415,289,0,0,0,0,0,0,0,320,0.7,10,10,0.1,15,9,999999999,0,0.0980,0,88,0.000,0.0,0.0
1984,1,1,21,60,B8C8E8B8*0?9?9?9?9?9?9?9*0B8B8B8B8*0*0E8*0*0,0.3,-0.9,91,97800,0,1415,287,0,0,0,0,0,0,0,320,0.8,10,10,0.1,15,9,999999999,0,0.0980,0,88,0.000,0.0,0.0
1984,1,1,22,60,A7A7E8E8*0?9?9?9?9?9?9?9A7A7A7A7A7A7*0E8*0*0,-0.2,-1.2,92,97800,0,1415,285,0,0,0,0,0,0,0,310,1.0,10,10,0.1,15,0,999999599,0,0.0980,0,88,0.000,0.0,0.0
1984,1,1,23,60,B8C8E8B8*0?9?9?9?9?9?9?9*0B8B8B8B8*0*0E8*0*0,-0.5,-1.4,92,97800,0,1415,283,0,0,0,0,0,0,0,310,1.0,10,10,0.1,15,9,999999999,0,0.0980,0,88,0.000,0.0,0.0
1984,1,1,24,60,B8C8E8B8*0?9?9?9?9?9?9?9*0B8B8B8B8*0*0E8*0*0,-0.7,-1.7,92,97800,0,1415,282,0,0,0,0,0,0,0,310,1.0,10,10,0.1,15,9,999999999,0,0.0980,0,88,0.000,0.0,0.0
```

Figure 6 sample file header and hourly data of 1st January in the EPW file format for the city of Geneva

Conventionally, the one-year data in a weather file are extracted from 20-30 years of historical recorded data, which represents represent the typical weather condition for a specific location. This is similar to the concept of generating climate normals by WMO (described in section 2). A method developed by Hall et al. [61] is used for creating this one-year hourly data called typical meteorological year (TMY). In this method a TMY is derived from 30 years of weather data recordings. Climate data for January in a TMY is copied directly from a historical January data that has the closest match to the 30-year average condition for January. This process is replicated for the other months to produce 12 months of the typical weather year. Same as climate normals, typical weather files are meant to provide a representative image of climate condition for a location. As it was discussed and shown for climate normals in section 2, typical weather files also cannot provide a complete image of possible future climate for a location. This can cause a design that is developed based on considering only typical condition, to perform unreliably during operation when the conditions are different. This issue was highlighted in this project and more details are given in the following sections.

6.1.1 Weather files representing future typical conditions

Global climate models (GCMs) data need to be downscaled to a regional location and hourly time scale to be able to be used in BPS. The two major downscaling methods are: statistical and dynamical or hybrid. Hybrid downscaling is when the statistical methods are used to further downscale the data from RCMs in case they are not at suitable resolution for BPS. Following graph (Figure 7) shows the downscaling processes to downscale climate data from GCM and generate future climate data to be used in BPS:

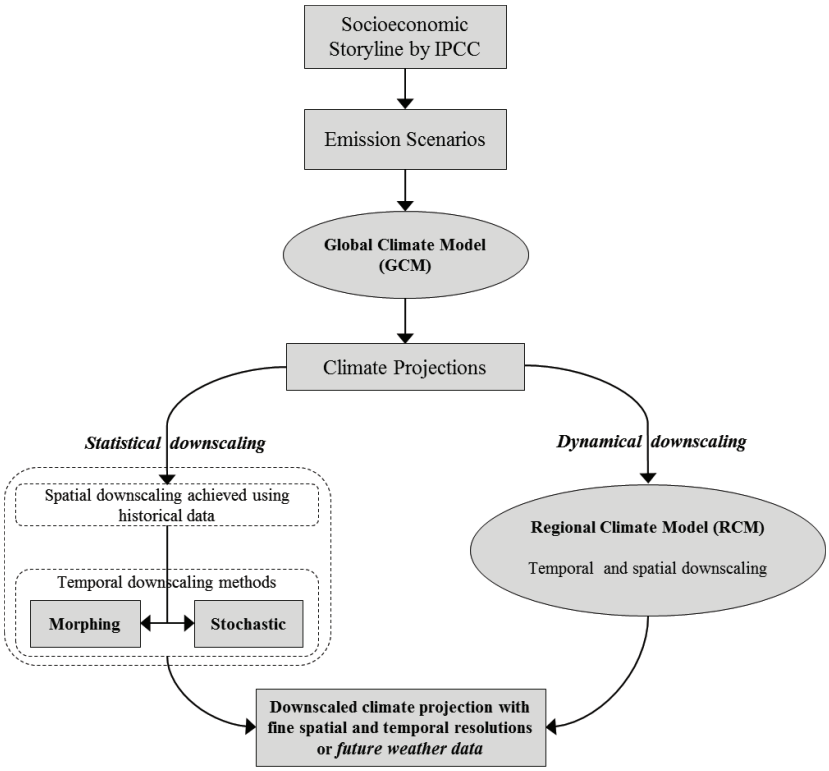

Figure 7. Flowchart of different approaches for preparing climate projection data with fine spatial and temporal resolution suitable to generate future weather files for BPS.

To better understand the state-of-the-art for climate change impacts assessment on buildings, we draw on the literature and selected 111 articles. Data presented in Figure 8 were extracted from the analysis of 111 scientific papers detected after querying the Web of Science and Scopus databases. All these papers have been published after 2001. As shown in this figure, with regards to the downscaling methods used for preparing weather files, 52% (58 articles) are based on statistically downscaled data, 13% (14 studies) used dynamical downscaling and 25% (28 articles) used the hybrid method. Finally, 10% of the studies (11 articles) used recorded data, which means they used recorded data of an extreme year for example the year 2003 in Europe to study the impact of extreme conditions.

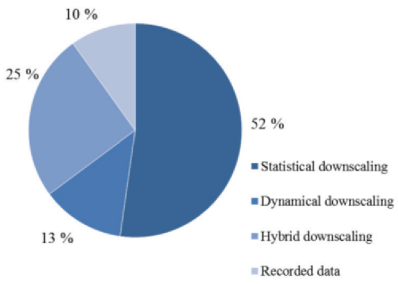

Figure 8 Analysis of literature that used BPS to assess the impact of climate change on the performance of the buildings (111 articles)

The above results shows that statistical downscaling of GCMs is the most common method used for generating future climate data at suitable resolution for BPS. Between the statistical methods, "morphing" is one of the frequently used methods in literature for climate change impact assessments [90]. The morphing method allows downscaling the monthly mean climate data that is created by a GCM to a future hourly weather data, by applying three transforming functions: shifting, stretching and the combination of shifting and stretching, on a baseline (hourly data of a typical weather file). Two software tools, namely CCWorldWeatherGen and WeatherShift™ use morphing method to transform typical weather files into future weather files in the EPW format. Figure 9 shows, the hourly differences between the values of future weather data and the values of the baseline weather file. E.g. the pattern of shifting transformation can clearly be seen in generated data from WeatherShift™ for dry bulb temperature, or for relative humidity in case of CCWorldWeatherGen.

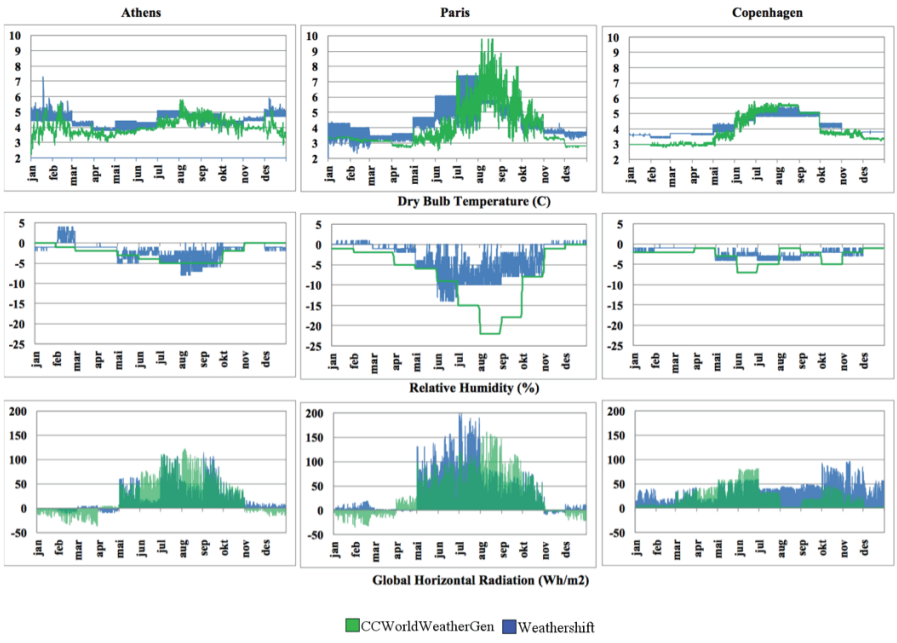

Figure 9 Hourly differences between the values of projected weather data and the values of the reference IWEC weather file.

These types of files are generated under the assumption that short-term future weather patterns will follow the same pattern and climate variability as historical weather data. They therefore cannot represent probable future extreme conditions due to climate change. Conversely, the weather files generated using dynamical downscaling are not constrained by historical data. To better illustrate the difference between the two types of weather data, the hourly outdoor dry-bulb temperature for one day (1st February as an example) is plotted in for statistically downscaled data weather files and one dynamically downscaled data weather file, and compared with a TMY.

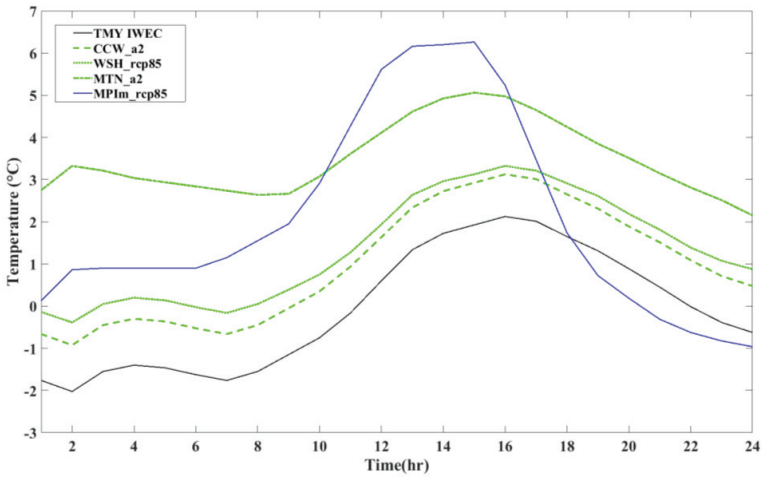

Figure 10 Hourly outdoor dry-bulb temperature for one day (1st February as an example) are plotted for three weather files of statistical group (in green) and one weather file of the dynamical group (in blue) and compared to TMY (in black).

As expected, the hourly temperature profiles of statistically downscaled type, the CCW_a2[1], WSH_rcp85[2] and MTN_a2[3], have a very similar pattern to the TMY file with a higher average temperature. However, the dynamically downscaled type, The MPIm_rcp85[4], does not match the other profiles. This again points to the fact that weather files generated using statistical methods cannot represent short-term variations of climate conditions induced by climate change.

6.1.2 Weather files representing future typical and extreme conditions

Albeit considering extreme conditions in the design process seems to be obvious, the analysis of 111 scientific papers demonstrated otherwise. It showed that 66% of the studies

[1] CCW_a2: weather file generated by statistically downscaling using CCWorldWeatherGen tool based on SRES A2 emission scenario

[2] WSH_rcp85: weather file generated by statistically downscaling using WeatherShift tool based on RCP 8.5 emission scenario

[3] MTN_a2: weather file generated by statistically downscaling using Meteonorm tool based on SRES A2 emission scenario

[4] MPIm_rcp85: weather file generated by dynamically downscaling of MPIm GCM outputs based on RCP 8.5 emission scenario

(73 articles) are based on only typical future climate conditions and only 34% (38 articles) considered extreme conditions in theirs studies. Figure 11, shows these results.

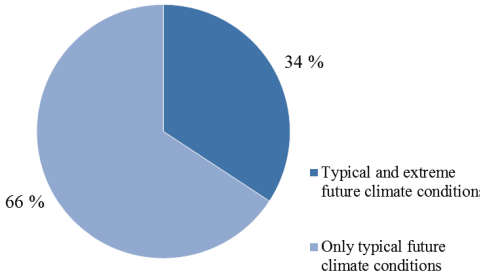

Figure 11 Analysis of literature that used BPS to assess the impact of climate change on the performance of the buildings (111 articles)

tyåpucalwas proposed by Nik [22]. The method is based on synthesizing one typical and two extreme (cold and warm) data sets: Typical Downscaled Year (TDY), Extreme Cold Year (ECY) and Extreme Warm Year (EWY). The process for creating a TDY starts by following the method for creating a TMY file, except that just one climate variable (dry-bulb temperature) is considered in the selection of typical months instead of four. A similar procedure is used to create ECY and EWY data sets. However, instead of looking for the least absolute difference, the years with the maximum (for ECY) and minimum (for EWY) absolute difference are selected as the years representing the extreme temperatures for each month. Nik showed that by considering TDY, ECY and EWY together (which is called Triple), it is possible to achieve a probability distribution of future conditions which is very similar to the full set of 30 years RCM data.

It was mentioned in Section 4.2 that it is necessary to consider several climate scenarios instead of just one scenario in the impact assessment on buildings, due to significant uncertainties in climate modelling. The method developed by Nik [22] was used to overcome the challenge of climate uncertainties, the method synthesizing one set of representative weather files that takes into consideration several climate scenarios (e.g. in [22], five climate scenarios were considered – i.e. 5×30 years of data for a 30-year time span – and TDY, ECY and EWY were synthesized). This allows an impact assessment to be performed under both typical and extreme conditions with a minimum number of required simulation runs and in which climate uncertainty is also taken into account.

6.1.3 Credible weather data sets for climate change impacts assessment

The above methods were used, which provided 72 future weather files for the city of Geneva as shown in Table 4. A total of 74 files were used in this study, including two TMY weather files.

Table 4. Weather files generated for the city of Geneva and used in this study.

Method	Tool/GCM/RCM	Emission scenario	Number of weather files	Adopted term
Statistical	CCWorldWeatherGen	A2	3*	CCW_a2
	WeatherShift	RCP 8.5	3	WSH_rcp85
	Meteonorm	A2	3	MTN_a2
Dynamical-typical	MPIM-RCA4	RCP 8.5	3	MPIM_TDY_rcp85
	IPSLm-RCA4	RCP 8.5	3	IPSLm_TDY_rcp85
	ICHEC-RCA4	RCP 8.5, RCP 4.5	3×2	ICHEC_TDY_rcp85 ICHEC_TDY_rcp45
	CNRM-RCA4	RCP 8.5, RCP 4.5	3×2	CNRM_TDY_rcp85 CNRM_TDY_rcp45
	Multi GCMs-RCA4	RCP 8.5+RCP 4.5	3	$TDY_{Multiple}$
Dynamical-extreme	MPIM_RCA4	RCP 8.5	3×2	MPIM_ECY_rcp85 MPIM_EWY_rcp85
	IPSLm_RCA4	RCP 8.5	3×2	IPSLm_ECY_rcp85 IPSLm_EWY_rcp85
	CNRM_RCA4	RCP 8.5, RCP 4.5	3×4	CNRM_ECY_rcp85 CNRM_EWY_rcp85 CNRM_ECY_rcp45 CNRM_EWY_rcp45
	ICHEC_RCA4	RCP 8.5, RCP 4.5	3×4	ICHEC_ECY_rcp85 ICHEC_EWY_rcp85 ICHEC_ECY_rcp45 ICHEC_EWY_rcp45
	Multi GCMs_RCA4	RCP 8.5+RCP 4.5	3×2	$ECY_{Multiple}$ $EWY_{Multiple}$

* refers to three time periods: near-term (NT), medium-term (MT) and long-term (LT); one weather file for each period.

Boxplots of the outdoor dry-bulb air temperature of 74 weather files are plotted in Figure 12. This figure reveals a pattern of continuous increase in the average dry-bulb temperature from NT[5] to MT[6] and LT[7], and for all future weather files. The slope of increase is greater for

[5] Refer to Near-Term future projected period (more details are provided in paper IV)

[6] Refer to Medium-Term future projected period (more details are provided in paper IV)

[7] Refer to Long-Term future projected period (more details are provided in paper IV)

weather files with A2 and RCP 8.5 emission scenarios than for RCP 4.5, which is in agreement with the GCM projections for these scenarios. An increasing trend exists for all generated weather files. However, the maximum values of typical future weather files only get close to the historical observed value of maximum temperature under LT. This reveals the weakness of typical weather files in representing extreme conditions, as discussed before. For extreme weather data sets, the distribution of EWY series for the RCP8.5 scenario is close to the observed maximum daily temperatures and the ECY series of RCP4.5 is close to the distribution of observed minimum daily temperatures. Using Multi-Scenario files therefore improves the coverage of both maximum and minimum borders of the distributions for dry-bulb temperature. These files approximately cover the distributions of all other dynamical data group files. This means that it is possible to reduce the number of simulations by using Multi-Scenario weather files instead of several weather files (six in this case) with different climate scenarios, as was shown in [22] and [91].

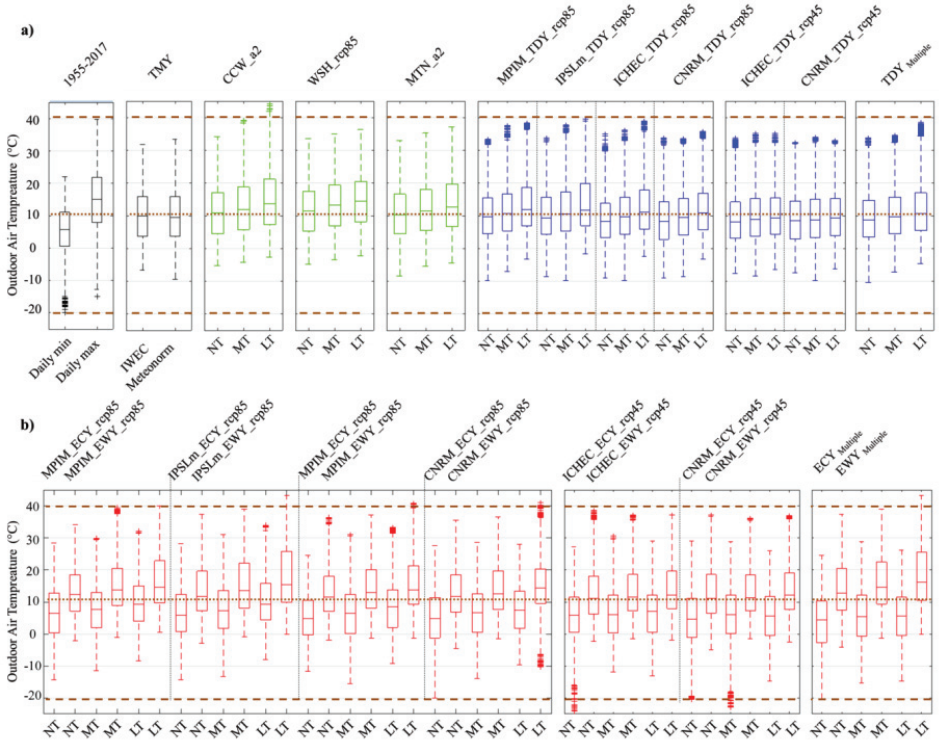

Figure 12 Boxplots of the outdoor dry-bulb air temperature for the weather files. The dashed lines show the lower whiskers for minimum daily temperature and the upper whiskers of the maximum daily temperature and the horizontal dotted brown lines show the average according to recorded data from 1955 to 2017 of Genève-Cointrin weather station. a) Historical observed data and typical weather data sets, b) extreme weather data sets.

In Table 1 we compared climate normals with extreme summer recorded data using number of hot days and tropical nights, which showed how the averaging process of

generating climate normals neglect climate extremes. Here in Table 5 extreme summer recorded data are compared to calculated values for the same period for two TMY weather files (IWEC and Meteonorm), and one typical ($TDY_{Multiple}$) and one extreme warm ($EWY_{Multiple}$) weather file from dynamical groups; both for near-term (NT: 2010-2039) future.

Table 5. Comparison of the number of hot days (Tmax ≥30°C) and tropical nights (Tmin ≥ 20°C) for the extremely hot summer of 2003 in Geneva calculated from different weather data sets.

		Number of hot days	**Number of tropical nights**
Climate normals	1961-1990	10.4	0.1
	1980-2010	14.7	0.4
TMY	IWEC	8	1
	Meteonorm	4	3
Future Near-Term (NT)	$TDY_{Multiple}$	10	0
	$EWY_{Multiple}$	54	13
Observed climate extremes	Summer 2003	51	4
	Summer 2017	30	4
	Summer 2018	33	1

It can be highlighted from Table 5 that only the $EWY_{Multiple}$ weather file value is comparable with the number of hot days that occurred during the heat waves in Geneva. The climate normals and the typical weather files are far from observed values. The above example reveals how the averaging process, both for current and future weather data, can result in missing extreme values. It therefore shows how systems designed taking into consideration only typical conditions could become a costly mistake (due to under-dimensioning).

6.2 Impacts of climate change on case-study buildings

The 111 articles describe earlier in section 6.1.1, were also analysed for performance metrics used in these studies, which are demonstrated in Figure 13. The results show the majority of the studies focused on the impact of climate change on energy and thermal performance (89%) with 48% on energy, 21% on thermal comfort and overheating risk and 20% on both energy and comfort. 11% of the studies used other metrics such as: equivalent carbon dioxide emissions, mould growth risk, etc.

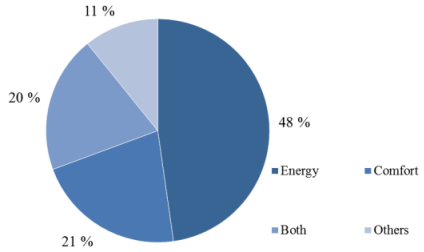

Figure 13 Analysis of literature that used BPS to assess the impact of climate change on the performance of the buildings (111 articles)

In this project, even though the impacts of climate change on thermal comfort were studied and presented in Paper I and II, but the main focus of the thesis was on energy performance.

6.2.1 Retrofit design of an existing buildings

The work started by looking at the impacts of climate changes on energy performance of retrofit design of an existing building with the aim of becoming nZEB. The existing building is a child care center built in the 80s.

Figure 14: (left) Picture of the southwest façade; (right) kindergarten plan view including the five monitored rooms.

A pre-retrofit energy model was created and calibrated in order to provide reliable simulation outcomes. The model was first calibrated on the basis of measured monthly delivered energy for heating in a conditioned mode, then the best building variant after the first calibration was refined further by a second calibration, where it was operated in a free-running mode. The benchmark of the second calibration was the hourly indoor air temperature. The indoor environmental conditions of the building were monitored from July 2014 to July 2015. Figure depicts the comparison between the simulated and the measured indoor air temperature in Room 4.

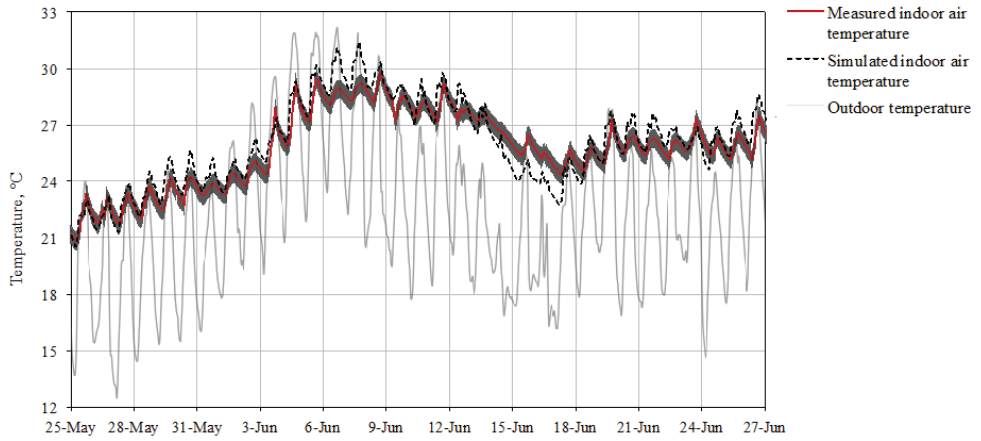

Figure 5: Comparison of the simulated and monitored indoor air temperatures in Room 4. The shaded area represents a measurement uncertainty of ±0.5 °C.

After calibrating the pre-retrofit model, the post-retrofit model of the building was built and simulated under current typical (IGDG) and future typical weather conditions.

Figure 12 shows the yearly heating and cooling energy need for space heating and cooling throughout the whole building under the four climatic scenarios.

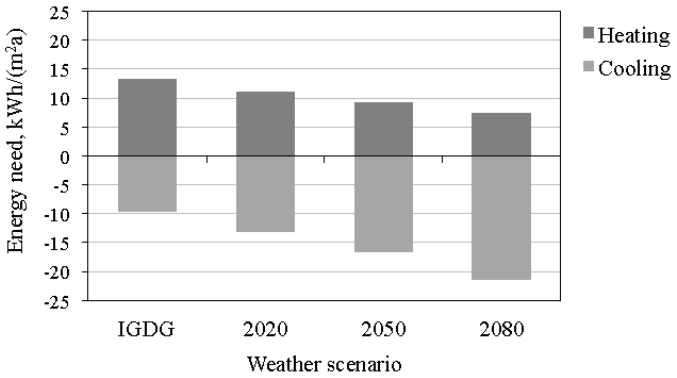

Figure 15 Yearly energy need for space heating and cooling per unit of net floor area.

The analysis showed that in future weather conditions a substantial shift from heating energy needs to cooling energy needs would be registered in building operations in a temperate climate such as Milan, Italy, which is a winter dominated climate nowadays. More details of analysis and results are provided in following references: [11, 12, 21, 92].

6.2.2 ASHRAE reference buildings

After preparing the 74-file weather data set, these weather files were used to assess the methods for generating typical and extreme future weather files and their impacts on building energy performance. To avoid having biased results because of the building type/model, to

minimize the probable uncertainties because of the energy simulation models and to provide generalizable outcomes, we chose the widely used commercial reference building benchmark models provided by ASHRAE 90.1[93]. The suite provides a simulation bench test to compare the relative impact of using the generated weather file on energy performance of various building types. Technical descriptions of the selected building envelope components, used in building models, are given in ref. [15]. The suite is a collection of standardized building models with realistic building characteristics and includes 16 buildings of different types and dimensions (Figure 16).

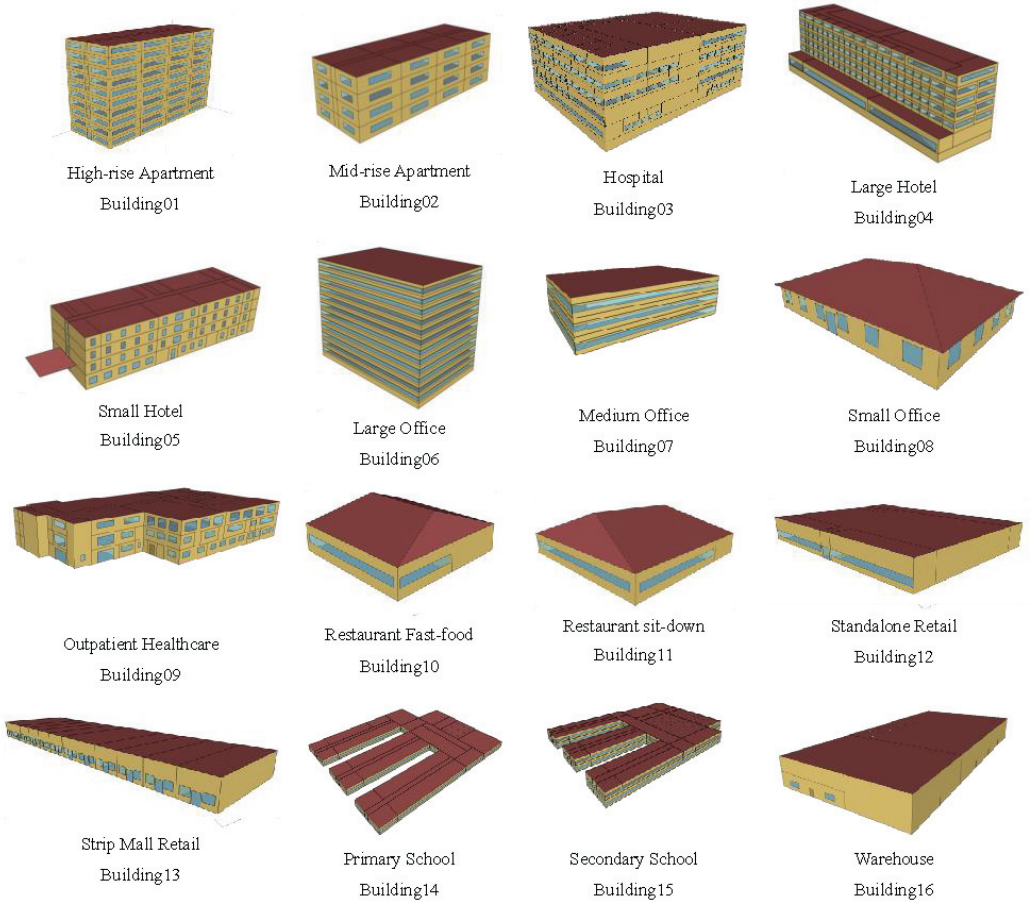

Figure 16 Reference building models from the ASHRAE Standard 90.1.

A simulation workflow was implemented in the multidisciplinary design optimization platform modeFRONTIER [24] coupled with MATLAB for post-processing of the output data (the implemented workflow in modeFRONTIER is shown in Figure 17). This was used to simulate the full set of 16 building models under the 74 generated future weather files, giving a total of 1 184 simulation runs

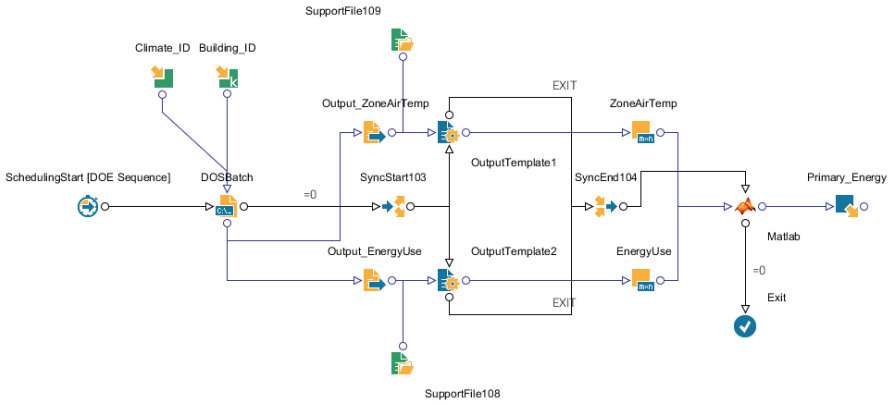

Figure 17 workflow implemented in modeFRONTIER

modeFRONTIER used the algorithm presented in Figure 18 to perform the simulations.

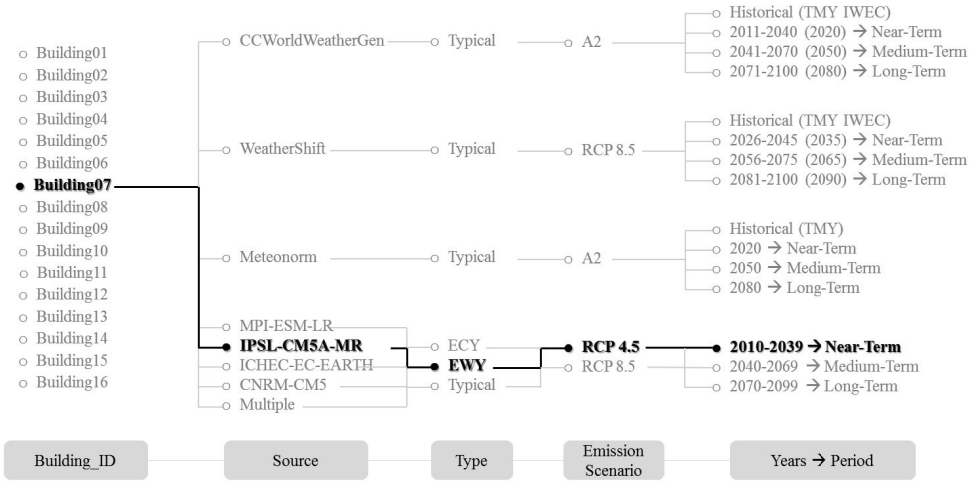

Figure 18. Configuration of simulation runs of 16 reference buildings under the generated future weather files. Simulation of building number 07, Medium Office, using weather file 'IPSL_EWY_rcp45_NT.epw' is highlighted as an example.

The weather data set included typical and extreme future weather data and the results are presented in the following.

First, the hourly primary energy need for space heating and cooling per square meter for the 16 reference buildings are calculated for one year under typical weather data sets. Figure 19 shows the distribution of calculated values for all the buildings. The above weather data sets allow considering the uncertainty of climate projections into energy calculations. The span of values resulted from simulations under these weather files, shows the uncertainty of buildings energy performances in future following IPCC emission scenarios (please see Figure 4 in section 4.2).

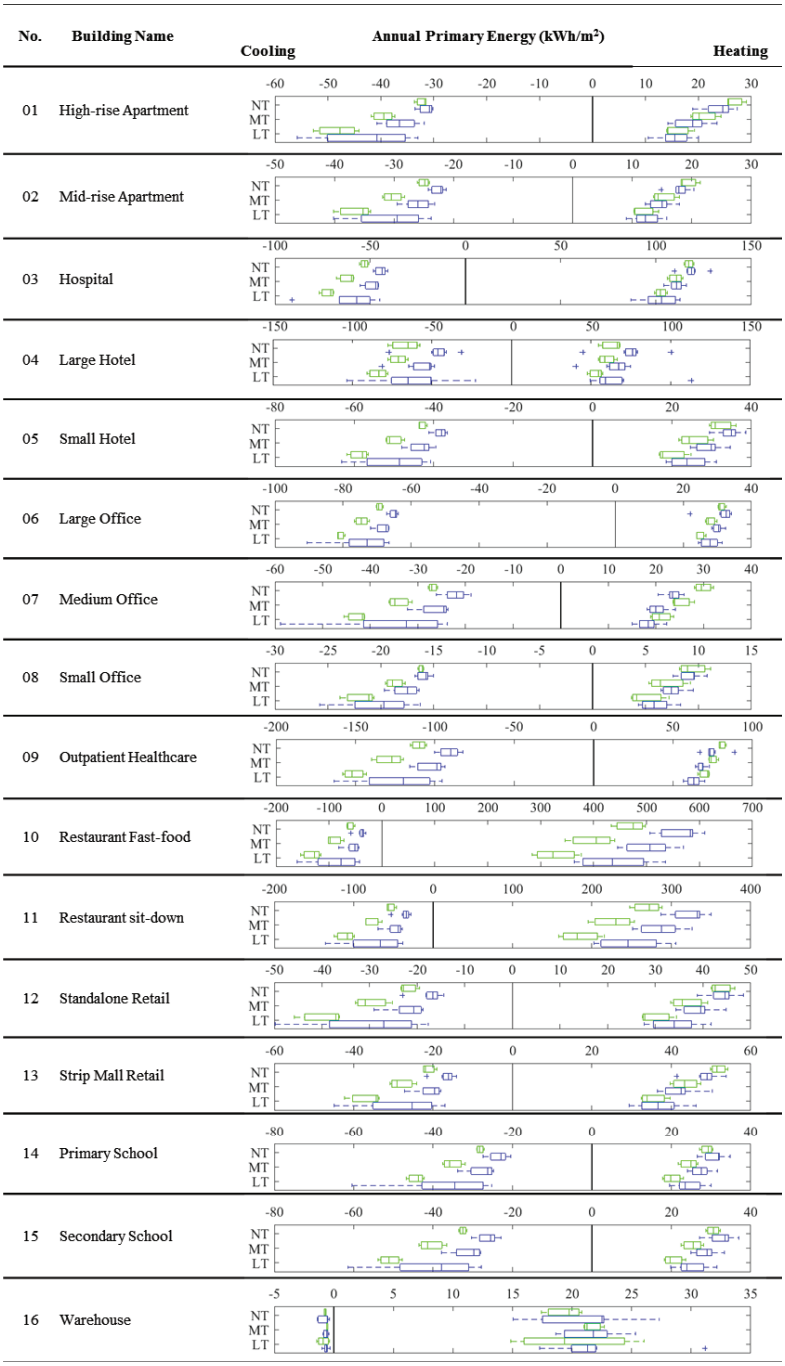

Figure 19. The boxplots present the distribution of values for the calculated annual primary cooling energy (negative values) and primary heating energy (positive values) under typical weather data sets for all 16 reference buildings. Values of the dynamical data group are presented in blue and the statistical data group in green.

The boxplots in Figure 19 for both statistical and dynamical under all NT, MT and LT of each building shows that the fast food restaurant has the largest range of primary energy. The range of values for this building is approximately 280-610 kWh/m^2/a for space heating and 30-160 kWh/m^2/a for space cooling. The reason for this can be the high ventilation rate of restaurant buildings compared to other buildings. The hospital has a relatively small range for primary energy for space heating (~ 85-130 kWh/m^2/a) and space cooling (~ 40-90 kWh/m^2/a). This is probably due to equipment energy use and other energy end-uses than heating, cooling and ventilation predominating in this building.

Overall, the shifting impact on primary cooling energy and primary heating energy is present for all buildings except building number 16 (warehouse). This might show that climate conditions are not the dominant force driving the energy performance of this building. For some buildings, a heating-load dominated building under NT furthermore becomes a cooling-load dominated building under MT or LT. Examples of this are buildings number 14 and 15 (primary and secondary schools) as discussed also in section 6.2.1 for the case study in Milan. This reveals that both methods are able to provide enough information to show a shift in the energy use of the buildings.

The span of values for the annual primary energy increases from near-term (NT) to long-term (LT). This is due to the fact that as the time horizon increases, emission scenarios diverge. For example, the distance between projected global mean temperature under RCP4.5 and RCP8.5 is increasing by evolution of time. Otherwise, the uncertainty of near-term trajectories is the same as of long-term, as discussed in section 4.2.

Second, the peak loads of the cooling demand with the date and time of occurrence for each of the 16 buildings under typical and extreme warm conditions were considered. *Table 6* presents the magnitude of the peaks and the time in which they occur. The peak values for $EWY_{Multiple}$ compared to $TDY_{Multiple}$ ranges from a 2 % increase for the hospital to a 28.5 % increase for the sit-down restaurant. The findings from Table 6 illustrate the importance of considering extreme conditions and the usefulness of the suggested approach in ensuring a robust design of buildings and energy systems for the future.

Table 6. Value of Peak cooling demand and the date-time of occurrence under NT for all buildings and the virtual neighborhood, values for dynamical-typical and dynamical-extreme are presented and compared.

Building name	Dynamical-typical $TDY_{Multiple}$		Dynamical-extreme $EWY_{Multiple}$		Peak cooling load relative change $EWY_{Multiple}$ to $TDY_{Multiple}$ (%)
	Peak load for cooling (kW)	Date-Time	Peak load for cooling (kW)	Date-Time	
High-rise Apartment	59.97	19 Jul-17:00	62.27	24 Jul-19:00	3.8 %
Mid-rise Apartment	18.76	19 Jul-15:00	21.22	27 Jul-15:00	13.1 %
Hospital	235.01	20 Jun-15:00	239.67	24 Jul-15:00	2.0 %
Large Hotel	147.61	28 Jul-19:00	172.21	19 Jul-16:00	16.7 %
Small Hotel	34.71	19 Jul-16:00	38.06	27 Jul-16:00	9.6 %
Large Office	430.21	20 Jun-17:00	453.95	24 Jul-15:00	5.5 %
Medium Office	63.03	19 Jul-15:00	70.55	27 Jul-16:00	11.9 %
Small Office	5.00	19 Jul-16:00	5.47	27 Jul-16:00	9.5 %
Outpatient Healthcare	93.32	20 Jun-15:00	100.82	7 Jul-16:00	8.0 %
Restaurant Fast-food	11.30	19 Jul-13:00	14.16	3 Jul-18:00	25.4 %
Restaurant sit-down	17.96	19 Jul-12:00	23.08	3 Jul-18:00	28.5 %
Standalone Retail	34.69	19 Jul-15:00	42.29	27 Jul-15:00	21.9 %
Strip Mall Retail	30.57	19 Jul-15:00	38.64	27 Jul-15:00	26.4 %
Primary School	97.27	20 Jun-15:00	109.06	13 Jun-15:00	12.1 %
Secondary School	316.51	20 Jun-15:00	348.09	13 Jun-15:00	10.0 %
Warehouse	5.54	19 Jul-16:00	6.78	27 Jul-17:00	22.5 %

6.2.3 Virtual neighborhood

A combination of the 16 buildings was used to virtually model a neighborhood. We looked at the neighborhood of Champel in Geneva to get an idea of the scale of such a neighborhood, which has a total building area of 328 105 m^2 [94]. The distribution of the areas occupied by the buildings in the canton of Geneva was used to distribute the 16 buildings based on type. In the canton, 64 % of buildings are residential and 36 % are non-residential and mixed-use buildings [95]. The above assumptions gave the virtual neighborhood created for this study, which had a total energy reference area of 414 341 m^2, 64.3 % residential buildings and 35.7 % non-residential buildings. The composition of the virtual neighborhood is presented in Table 7. This composition was used only to assess the magnitude of impacts at the neighborhood

scale. The spatial attributes of a neighborhood (organization of the buildings and infrastructure between) are not within the scope of this paper.

Table 7. Composition of the 16 ASHRAE standard 90.1 reference buildings in the virtual neighborhood for city of Geneva.

Building number	Name	floor Area of Thermally conditioned space [1] (m^2)	Number of floors	Number of thermal zones [2]	Windows-to-wall ratio [3]	Number of building type in the neighborhood [4]	Percentage of floor area in the whole neighborhood [5]
Building01	High-rise apartment	7059.9	10	80	30%	20	37.8 %
Building02	Mid-rise apartment	2824.0	4	32	20%	35	26.5 %
Building03	Hospital	22436.2	5	162	16%	1	5.4 %
Building04	Large hotel	10736.3	6	195	30.2%	1	2.6 %
Building05	Small hotel	3725.1	4	54	10.9%	2	1.9 %
Building06	Large office	46320.4	12	74	37.5%	1	11.2 %
Building07	Medium office	4982.2	3	18	33%	3	3.6 %
Building08	Small office	511.0	1	6	20.1%	5	0.6 %
Building09	Outpatient healthcare	3804.0	3	118	20%	1	0.9 %
Building10	Restaurant fast-food	232.3	1	2	14%	8	0.4 %
Building11	Restaurant sit-down	511.2	1	2	17.1%	3	0.4 %
Building12	Standalone retail	2294.0	1	5	7.1%	1	0.6 %
Building13	Strip mall retail	2090.3	1	10	10.5%	1	0.5 %
Building14	Primary school	6871.0	1	25	35%	1	1.7 %
Building15	Secondary school	19592.0	2	46	33%	1	4.7 %
Building16	Warehouse	4835.1	1	3	0.7%	1	1.2 %

[1] Defined by ISO 52000-1:2017 [96] as: heated and/or cooled space.

[2] Number of thermal zones in the energy model.

[3] Defined by ASHRAE 90.1 [97] as: The ratio of vertical fenestration areas to the gross above-grade wall area.

[4] Number of each building type in the virtual neighborhood.

[5] Percentage of each building type in the total floor area of the neighborhood.

As shown in Table 6, the need for air conditioning increases dramatically during extreme hot conditions. This high demand can last for days to weeks. Additionally, as mentioned before in section 3.3, high demand and low energy production during extreme conditions, in a chain of smaller events can lead to the failure of power system, as in the 2006 heat wave in New York City [98].

Electrical power demand of the virtual neighborhood under typical and extreme conditions was calculated to illustrate such risks at the urban scale. Figure 20 shows the power demand for the neighborhood during the week of the peak loads for $EWY_{Multiple}$ compared to TMY and $TDY_{Multiple}$ under NT. Electric power demand was calculated by adding up for each hour the delivered energy for total electricity for all the buildings in the neighborhood.

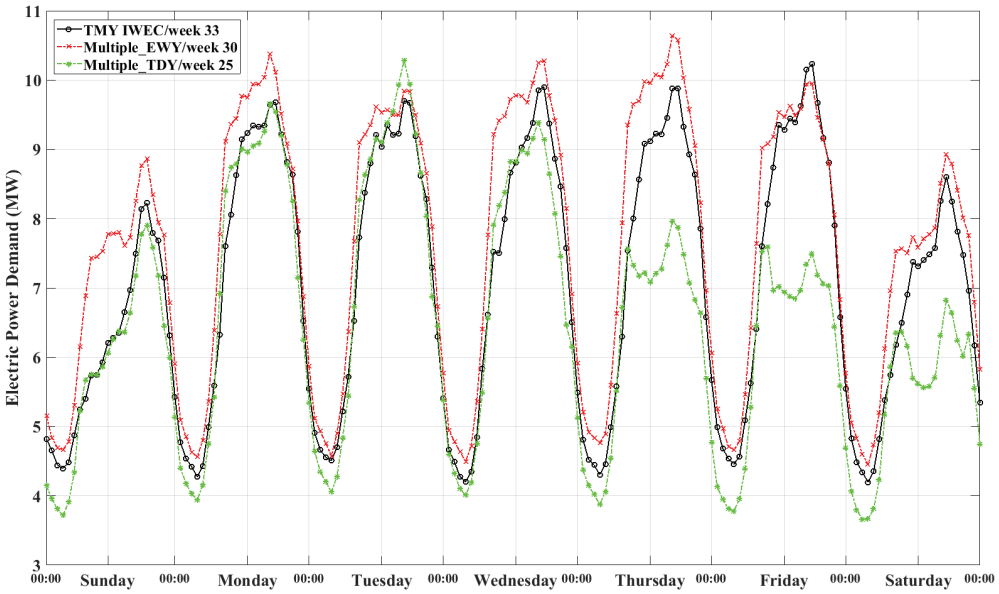

Figure 20. The electrical load profile of virtual neighborhood for a peak summer week in Geneva, considering historical typical weather year (TMY), future typical weather year (TDYMultiple) and future extreme warm weather year (EWYMultiple) under NT.

The criticality is during the peak load hours, which are from 2:00 pm to 6:00 pm on weekdays and 4:00 pm to 9:00 pm during the weekend, in the case of the virtual neighborhood. The so-called peak-load power plants are usually used to cater for the demand peaks. They have a relatively high fuel cost compared with base-load power plants and they are started up whenever there is a spike in demand and stopped when the demand recedes. For the neighborhood, the peak value of 10.23 MW is registered for TMY on Friday 18 August at 5:00 pm. This value for $TDY_{Multiple}$ is slightly higher than TMY and is 10.29 MW on Tuesday 20 June at 4:00 pm. The peak values for the extreme case $EWY_{Multiple}$ is above 10.28 MW for 4 days, the highest value being 10.64 MW on Thursday 27 July at 4:00 pm. The hourly electricity demand during the days of extreme conditions furthermore stays above values of typical conditions for almost the whole week. The peak electricity demand values for the neighborhood for $EWY_{Multiple}$ under MT and LT are 11.01 MW and 11.95 MW respectively. This means that the value of peak electricity demand can increase by 4.0 %, 7.6 % and 16.8 % for extreme conditions under NT, MT and LT in relation to the TMY IWEC value. Power plants can, as described before, suffer reductions in efficiency during extreme conditions (heat waves), with a consequential reduction in the capacity of the energy system to cover peaks.

Taking into account these issues and looking into the increase in electricity demand for the virtual neighborhood under extreme conditions, it might become a challenge for the energy system of this neighborhood to cover the margin, especially in the likely event of a reduction in generation capacity. The simulation test bench used in this study is developed based on the 2013 version of the ASHRAE 90.1 standard, which means the models are compliant with a recent energy code. Therefore, the above impacts can be magnified considerably if considering presence of older buildings with envelopes that have lower thermal performance; hence their energy performance is more sensitive to climate conditions. The single most marked observation that emerges from data comparison is the importance of considering extreme conditions to assure the robustness of the designed buildings or energy systems.

7 Robust energy performance under climate change

In the previous chapters, the concept of robustness against climate uncertainties in buildings was defined as:

- A robust building is a building that, while in operation, can provide its performance requirements with a minimum variation in a continuously changing environment..

It was also shown that foreseeable climate normals and extreme conditions can be presented in BPS with three weather files TDY, ECY and EWY.

However, there is little-to-nothing done in current design methodologies, standards and building regulations to set principles for design or assessment of building's performance robustness. In this chapter, a methodology based on the above concepts is developed, which allows designers achieving solutions with minimum energy performance variation under climate normals and extreme conditions.

7.1 Concept of robust design and its application in built environment

Robust design was first introduced in the 1940s to improve the quality of products in industrial engineering, but this discipline has been applied in various design areas since then. Inspired by the work of Taguchi [63], a large attention was given to application of this concept in the industrial sector. Since then, this discipline has been adopted in wide range of industries. Taguchi defined robustness as "*the state where the technology, product, or process performance is minimally sensitive to factors causing variability (either in the manufacturing or user's environment) and aging at the lowest unit manufacturing cost*" [99]. In other words, "*a product or process is said to be robust when it is insensitive to the effect of source of variability, even though the sources themselves have not been eliminated*" [100]. Robust design is a general concept applicable to all design procedures when uncertainty is taken into account. The aim is minimizing the sensitivity of product's performance to the presence of uncertainties in real world conditions.

This concept can be transferred from industrial product to buildings simply by considering the target value as any desired performance indicator (e.g., the indoor thermal comfort condition, the indoor daylight performance or the maximum delivered energy) and noise factor as any variable that cause deviations in the performance of a building during its operation (e.g. weather conditions).

Robust design of a product involves factors that are defined as follow [101]:

- *Control factors (or Design variables),* are variables that have to be specified by the designer;
- *Noise factors* are uncertain parameters that designer cannot control (only the statistical characteristics of noise factors that are expected in production or in actual use of the product can be known or specified);

- *Target value (Signal factor),* is set by regulations or user of the product to express the desired value for the response of the product;
- *Response* is the output of the product with the presence of noise.

One application of robust design is in car manufacturing and specifically in car packaging design, where the target is achieving high spatial and ergonomic efficiency for the cars. For example in a study [102] for an ergonomic robust design of car packaging, the *seat cushion angle, steering-wheel-to-BOF (ball of foot) distance,* etc. were considered as control factors, the *anthropometric variability* was considered as noise factor and the response was *comfort loss* of the occupants. The aim of a robust design is to set optimal control factors in which the variation of response from the target value to be minimum under presence of noise factors. To explain the procedure of the robust design, a block diagram representation of a product [101] is shown in Figure 21.

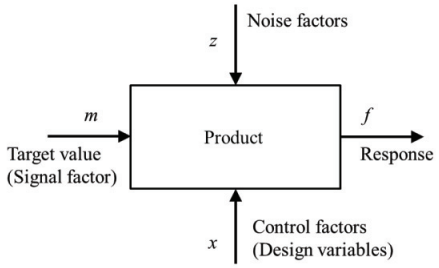

Figure 21 Block diagram of a product: P diagram

A robust design problem is a multi-objective optimization problem. The objectives are to reduce variation of the response while the mean is shifted to a target value (Figure 22).

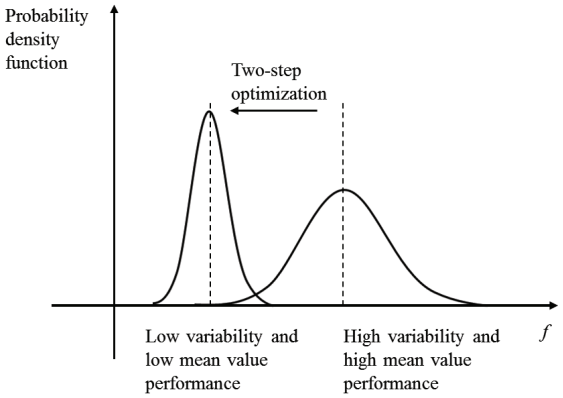

Figure 22: Robust design applied to buildings performance where the smaller mean and variation of response f is the better.

Based on this process, Taguchi developed the signal-to-noise ratio (S/N) that is a key metric used to perform the first step of the optimization process. During this step, the S/N gets maximized that is equivalent to minimizing the sensitivity of the response to the noise factors [100].

$$S/N = 10log_{10}\left[{\mu^2}/{\sigma^2}\right] \quad (1)$$

S/N is proportional to the base 10 logarithm of the ratio between the squared of the signal factors (μ) and the squared of the noise factors (σ). Adding logarithm to the metric was proposed by Taguchi and puts the S/N ratio into *decibels* units (*dB*) [100]. Taguchi described that a metric for robust design should have four properties [100]:

1. The metric should reflect the variability in the response.
2. The metric should be independent of adjustment of the mean.
3. The metric should measure relative quality.
4. The metric should not induce unnecessary complications, such as control factors interactions.

Robust design process originally was formulated in a way that the process can be performed with minimum cost and resources. This was due to high costs of experimental tests and also limited computational powers for running simulations. Taguchi used *orthogonal array* that is a method for setting experiments with only fraction of the full combinations [100]. But with the availability of better numerical models and high computational power, this concept was later introduced in simulation-based optimization process, and is referred to as robust design optimization (RDO) [103]. In other words, RDO is when the concept of robust design is added to the conventional optimization [104, 105]. In conventional optimization, the deterministic approach does not consider the impact of unavoidable uncertainties (noise factors) associated with the input design variables in real engineering environment. This results in optimum solutions that their performance measure is sensitive and can vary significantly due to distribution of noise factors. The design problems of buildings engineering also can be formulated as RDO problems, where the objective is to achieve a performance measure (e.g. energy) with minimum sensitivity to a noise factor (e.g. climate).

For this study, a number of design variables for an office building are optimized to achieve a minimum variation of its energy performance under the disturbance of mutable climate variables. In this case, the noise factor is climate change and the objectives of RDO scheme are to minimize mean energy performance while minimizing energy performance variability under climate change. Inspired by the work of Taguchi, two metrics (two objective functions) were developed for an optimization process that results in solutions with minimum variation

in energy performance of a building under presence of climate uncertainty. The first objective is a S/N ratio metric customize for the purpose of this study that fulfil the four properties described earlier. The second objective focuses on minimizing the energy use. These metrics are introduced in 7.2.1.

Theoretically, in order to take into account climate uncertainty, it is possible today to run a design under 100 of years of consistent climate data representing past recorded data and future possible climate scenarios. The availability of these data makes it possible to study the sensitivity of a design or to look for design alternative that demonstrate minimum sensitivity to climate conditions. However, this means that at each step of optimization, hundreds of simulation runs should be performed to be able to calculate the RDO objectives. The optimization scheme may therefore become infeasible due to high computational cost. The following example helps to grasp a feeling of the time and the computation resources that are required to consider all possible scenarios and minimize mean and variation of energy performance under these scenarios. Let's consider 30 years of future climate data with an ensemble of 4 scenarios (two GCM-RCMs and two emission scenario) are generated while 30 years of historical data are also available. These provide 150 years of climate data. In the case of running the optimization process, each optimization step will contain 150 annual simulations. In other words, for an optimization process of 1000 evaluations, 150000 simulation runs are required. Considering that each simulation takes 1 minute and the possibility of four parallel simulations, the optimization process will take around 26 days. The required time-scale is not feasible in buildings design practice.

In order to overcome this issue, the triple method described in section 6.1.2 is used in this study. This approach allows allows applying climate change as noise factor in simulations by only using three weather files (three-year of climate data). This means, the simulation runs of the mentioned example reduce to 3000 (1000 evaluation × 3 simulation runs using TDY, ECY and EWY weather files), and as a result optimization process will require 12.5 hours.

7.2 Simulation-based optimization method for design of energy-efficient buildings with robust energy performance

This specific robust design optimization problem can be formulated as:

$$\min_{x \in \mathbb{R}^n} \{f_1(\boldsymbol{x}, \boldsymbol{u}_i), f_2(\boldsymbol{x}, \boldsymbol{u}_i)\} \tag{2}$$

$$g_i(\boldsymbol{x}, \boldsymbol{u}_i) \leq 0 \quad \forall \boldsymbol{u}_i \in \mathcal{U}_i, \quad i = 1, \dots, r \tag{3}$$

$$x_L \leq x \leq x_U \tag{4}$$

where $\boldsymbol{x}$ is the vector of design variables, $f_1(\boldsymbol{x}, \boldsymbol{u}_i)$ and $f_2(\boldsymbol{x}, \boldsymbol{u}_i)$ are the objective functions, $g_i(\boldsymbol{x}, \boldsymbol{u}_i)$ are inequality constraints subject to the uncertainty parameters that can take any arbitrary values in the *uncertainty domain* $\mathcal{U}_i \subseteq \mathbb{R}^m$. Using this formalism, the goal

of this robust design optimization problem is to find a set of $X(\mathcal{U}_i)$ (i.e. the set of the minimum-cost building variants) among all the available building variants which are feasible considering all the noises factors $\boldsymbol{u}_i \in \mathcal{U}_i$

$$X(\mathcal{U}_i) = \{x | g_i(\boldsymbol{x}, \boldsymbol{u}_i) \leq 0 \quad \forall \boldsymbol{u}_i \in \mathcal{U}_i, \quad i = 1, \dots, r\}. \tag{5}$$

The design effect of these two objectives, as shown in Figure 22, is a narrow distribution of primary energy with the mean value close to the target value (ideally zero). Optimizing $f_1(\boldsymbol{x}, \boldsymbol{u}_i)$ will minimize the sensitivity of performance to the noise and is a measure of robustness. Optimizing $f_2(\boldsymbol{x}, \boldsymbol{u}_i)$ will minimize the primary energy use and is a measure of energy-efficiency. These effects are visualized in Figure 23.

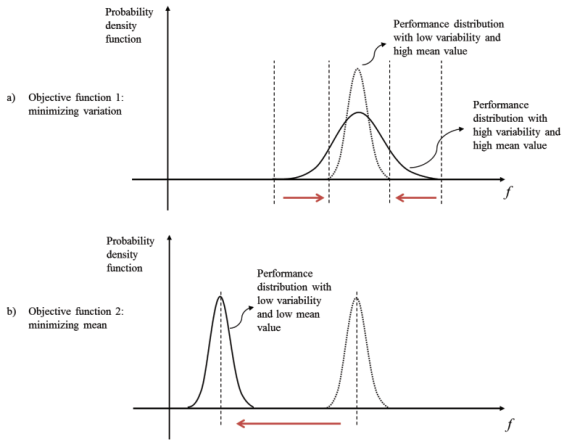

Figure 23 visualization of the designed effects of the two objective functions

7.2.1 Formulating the objective functions

As mentioned before, the focus of this study is to achieve robustness against climate uncertainty. In this regard, the achieved distribution of energy performance shown in Figure 23 is only due to variations of climate. To apply climate as source of performance variability, as described in section 6.1.2, the triple method is adapted. EWY and ECY. Reminding that the TDY file represents the most likely climate evolution and EWY and ECY are the extreme warm and cold climate evolutions, $PE_{TDY,i}$, $PE_{ECY,i}$ and $PE_{EWY,i}$ are the primary energy use (PE) calculated for the time-step i using the TDY, EWY and ECY weather files.

To develop a custom S/N ratio for the specific task of this study, the four properties described in section 7.1 were considered as a guideline. The first property is to define a metric that *reflects the variability in the response*. Accordingly, the mean squared deviation (MSD) is calculated, which is the average squared differences between $PE_{ECY,i}$ and $PE_{EWY,i}$ values with $PE_{TDY,i}$ as reference values. Considering $PE_{TDY,i}$ as reference values, this function can be used to measure how far the values of $PE_{ECY,i}$ and $PE_{EWY,i}$ are from these reference values as measure of variability. The second property requires the metric to be *independent of*

adjustment of the mean. For this reason, a second objective function was introduced. In this objective, calculated value of $PE_{TDY,i}$ is separately minimized, which makes the first objective being independent of the adjustment of $PE_{TDY,i}$. For the third property, *the metric should measure relative quality,* the S/N is calculated as relative change of $PE_{TDY,i}$ squared to MSD. At the final step, adding logarithm to the metric was proposed by Taguchi and puts the S/N ratio into *decibels* units (dB) [100]. With this transformation, the multiplicative changes in the metrics are transformed to additive changes, which helps reduce the effect of interactions between the design variables. It means the influence of each design variable is independent of the effects of the other design variables, which fulfils the fourth property. This metric is formulated as objective function n.1 and is descried below. By minimizing the first objective, the difference of energy performance under extreme and typical is minimized, which means the sensitivity of response to the changing of climate is minimized, while simultaneously the second objective minimize the annual primary energy $PE_{TDY,i}$, which is the annual total primary energy required by the building under average conditions (TDY). These objectives are formulated as below:

Objective function n.1: the purpose of $f_1(\boldsymbol{x}, \boldsymbol{u}_i)$ is to squeeze the energy performances calculated using EWY and ECY towards the one calculated using TDY. In this regard MSD is defined as:

$$MSD = \frac{1}{2p}\sum_{i=1}^{p}\left[\left(PE_{ECY_{(\boldsymbol{u}_1),i}} - PE_{TDY_{(\boldsymbol{u}_1),i}}\right)^2 + \left(PE_{EWY_{(\boldsymbol{u}_1),j}} - PE_{TDY_{(\boldsymbol{u}_1),i}}\right)^2\right] \quad (6)$$

Following Eq. (1) for S/N ratio and in order to maintain the usual convention according to which an optimization is a minimization process, S/N is negated when used as objective function. Therefore, $f_1(\boldsymbol{x}, \boldsymbol{u}_i)$ is:

$$f_1(\boldsymbol{x}, \boldsymbol{u}_i) = -10log_{10}\left[\frac{\left(PE_{TDY_{(\boldsymbol{u}_1),i}}\right)^2}{MSD}\right] \quad (7)$$

Where p is the the temporal resolution of data. For example, if one is interested in yearly energy performance and calculates it accumulating 12 monthly values, p has to be set at 12. If one is interested in the yearly energy performance calculated over hourly values, p has to be set at 8760; otherwise, for daily energy performance calculated over the 24 hours in a day, p has to be set at 24. Minimizing $f_1(\boldsymbol{x}, \boldsymbol{u}_i)$ results in minimizing the sensitivity of the response (energy use) to the variability of noise (climate conditions).

Objective function n.2: The purpose of $f_2(\boldsymbol{x}, \boldsymbol{u}_i)$ is to reduce a building's energy performance under the most likely climate conditions that are represented by the TDY weather file. It is the annual total primary energy required by the building under TDY. The two objective functions can be formulated as:

$$f_2(\boldsymbol{x}, \boldsymbol{u}_i) = \sum_{i=1}^{p} PE_{TDY(\boldsymbol{u}_1),i} \tag{8}$$

Where p is the the temporal resolution of data. For example, if one is interested in yearly energy performance and calculates it accumulating 12 monthly values, p has to be set at 12. If one is interested in the yearly energy performance calculated over hourly values, p has to be set at 8760; otherwise, for daily energy performance calculated over the 24 hours in a day, p has to be set at 24.

With the two objectives described above, it is now possible to conceptualize an RDO process in which climate uncertainty is introduced as noise factor in simulations by only using three weather files. In this process, objective function n.1 minimize the deviation between responses under extremes and average conditions. Objective function n.2 brings the primary energy with the mean value close to the target value (ideally zero). The concept is visualized in Figure 24 for two time-steps during heating period and during cooling period.

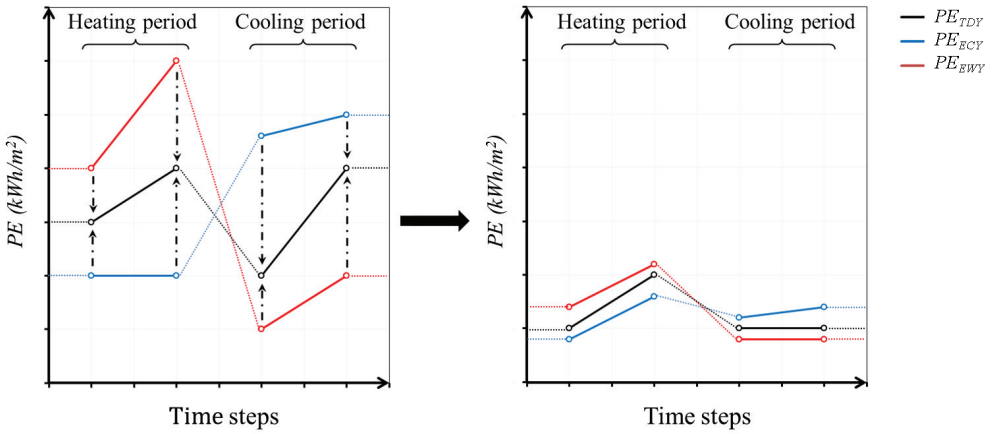

Figure 24 The concept of robust design optimization using three weather files: TDY, ECY and EWY

The above formulation allows performing robust design optimization at different temporal resolutions. This feature is required because the effect of a noise factor on the performance variability of a building system varies according to its typical response time. For example, when optimizing building envelope properties, one would need to consider the seasonal effect of climate variation, so the monthly resolution might be appropriate; otherwise, if someone

want to optimize building's devices such as automated shadings, the temporal resolution of climate variation has to be finer, e.g. day or hour. For this reason, in the development of the optimization process, two set of design variables were considered: building envelope properties and control settings. Two configurations based on these two groups were designed for optimization process (see section 7.2.3). Before moving to the formulation of optimization process, in the following section the energy models and design variables that are considered for this study are briefly described.

7.2.2 Building energy model

The small office building from ASHARE 90.1 reference buildings (please see section6.2.2) was chose for this study. The reference models are provided in three categories: "*new construction*", "*post-1980*" and "*pre-1980*" (existing buildings constructed in or after 1980 and before 1980). The *new construction* models are modified according to recent editions of ASHRAE 90.1 Standard [97]. For the purpose of this study, two base-case were considered; one from *new construction* category complying with ASHRAE 90.1-2016 standard and one from *post-1980* category. These cases are called "2016-compliant base-case" representing a newly built building quality and "1980-compliant base-case" representing an existing building quality. It allows assessing energy robustness of models representing newly built and existing old buildings under climate uncertainty. This case-study also shows the potential improvement by "robustifying" the energy performance of buildings.

The considered input variables for the target building are divided to two groups: building envelope properties and control settings. Building envelope properties involves six categories: windows' U-value, windows' SHGC, windows' solar transmittance, building surfaces' solar absorptance, thermal resistance of insulation layers and building's infiltration rate. The control settings include: cooling setpoint, heating setpoint and shading setpoint. Most of the input variables were divided into sub-variables according to different directions. A total of 15 variables were finally determined.

7.2.3 Formulation of optimization process

As mentioned above, building systems are characterized by different response times, thus in order to identify reliable values for the input variables considering the appropriate time effect of the noise factor, a two-step optimization process was designed. First, a monthly resolution was used to account for the seasonal effect of climate variation, and yearly primary energy was used to optimize the building envelope properties. Second, an hourly resolution was used to account for short-term weather evolution, and daily primary energy was used to optimize building's control settings such as the maximum irradiance incident on a window for lowering automated solar shadings. In addition, this two-step optimization process will provide an insight whether, to design an energy robust building, it is sufficient to apply only optimal control settings without improving the building envelope or vice versa, or whether both strategies were important, but there might be a priority option between them. Of course, in the context of a building refurbishment, the deployment of optimum control settings

requires less interventions and costs, while the renovation of the building envelope may require a large capital investment. For the mentioned reasons, two different optimization configurations were developed. To conduct the optimization tasks, the dynamic energy simulation engine EnergyPlus [23] was integrated into the modular environment for process automation and optimization in the engineering design process modeFRONTIER [24], which embeds a multi-objective optimization engine that integrates several optimization algorithms and sampling strategies..

7.2.3.1 Configuration no.1: Optimization of the building envelope

In this task, only input variables related to thermal properties of the building envelope are optimized for robustness. The noise factor applied is the weather file used for running the simulation. Two different weather files were used to represent the extreme climate conditions, specifically EWY and ECY. The optimization process was performed for both NSGA-II and MOGA-II. The parameter settings of the algorithms are important for their performance. Hamdy et al. [106] recommended that the minimum required number of evaluations for optimization of building energy models is 1400-1800. The population size for population-based optimizations is recommended to be 2-4 times the number of design variables [107]. Following the recommendations, for each algorithm 1620 evaluations were considered by using population size of 27 (3×9 design variables) and number of generations equal to 60. The initial population is generated based on random sequence. For the other settings, the default values were kept unchanged. These settings are reported in Table 8. During each evaluation, three energy simulations are run (using the EWY, ECY and TDY files) to calculate the two objective functions in Eq.(7) and Eq.(8).

Table 8 Parameter settings the selected optimization algorithms

Optimization algorithm	No. of evaluations	Simulation resolution	*p*	No. of runs	population size	No. of generations	Probability of cross-over	Probability of mutation
NSGA-II	1620	Monthly	12	1	27	60	0.9	1.0
MOGA-II	1620	Monthly	12	1	27	60	0.5	0.1

The flowchart of the process and the implemented correspondent workflow in modeFRONTIER are presented in Figure 25.

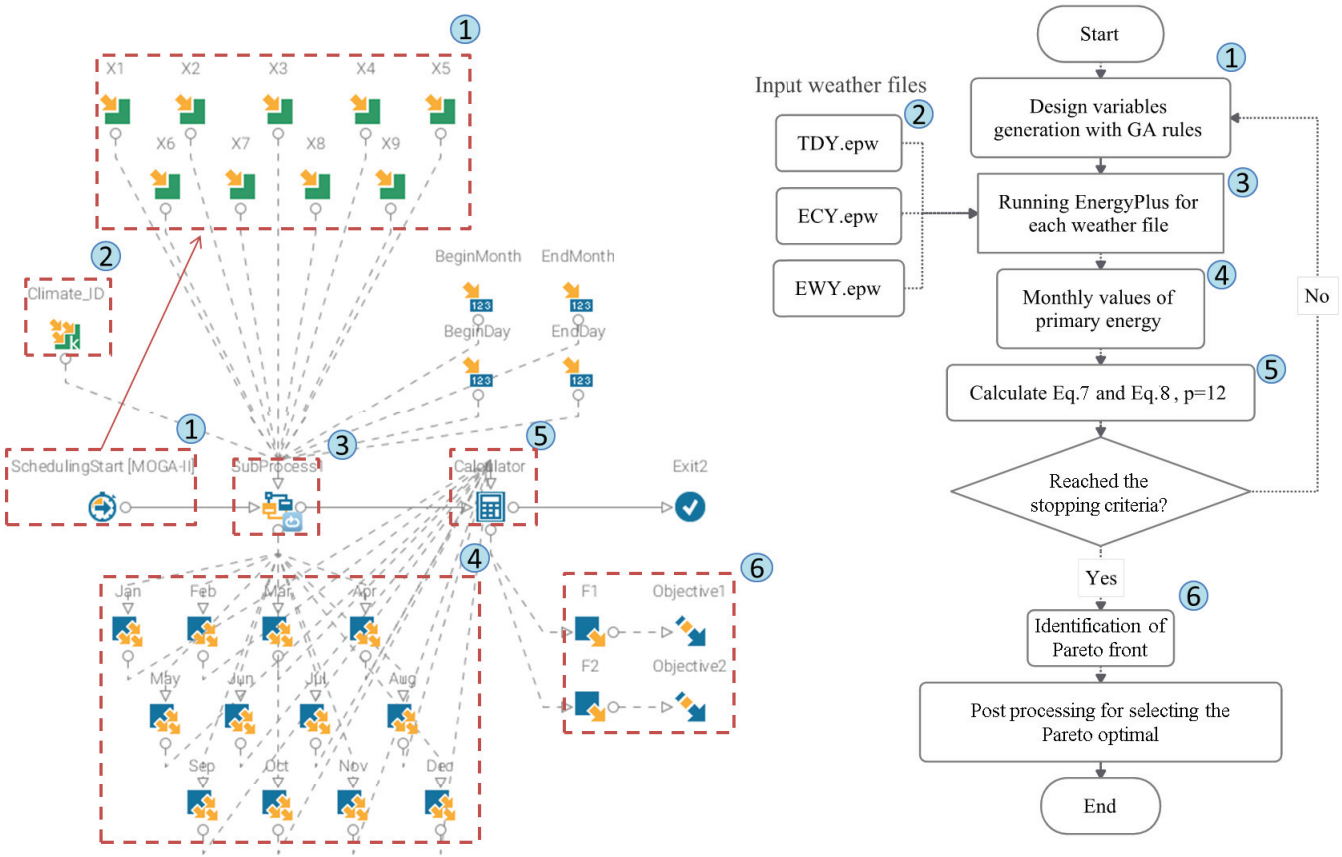

Figure 25 The implemented workflow of optimization process in modeFRONTIER for configuration no.1. The flowchart describes the flow of information during the process.

For the purpose of this work Genetic Algorithm (GA) is used for the multi-objective optimization. GA is the most common optimization strategy used in building performance analysis [108]. modeFRONTIER provides both Fast Non-dominated Sorting Genetic Algorithm (NSGA-II) algorithm [109] and Multi-Objective Genetic Algorithm (MOGA-II) [110]. MOGA-II is an improved version of MOGA [111]. To decide which optimization algorithm is best suited, in the first optimization process, both the algorithms were used with similar initial population. MOGA-II found providing better results and was chosen for the second optimization process.

The multi-objective optimization process results in a two-dimensional solution space with a Pareto frontier. Figure 26 demonstrate the strategy used in this study for post-processing and selecting the Pareto optimal. In this method, the Pareto frontier is normalized to zero-one interval ($0 \leq f_i^t(x) \leq 1$) using following transformation [112]:

$$f_i^t(x) = \frac{f_i(x) - f_i^{min}}{f_i^{max} - f_i^{min}} \tag{9}$$

With f_i^{max} and f_i^{min}, the maximum and minimum of $f_i(x)$, $x \in \mathbb{R}^s$. Then the closest point to the utopia point ($f_1 = 1$ and $f_2 = 0$) is chosen as the optimal solution. This method was used because the significance of both objective functions was considered equal and also the values of the two objective functions were expressed in different orders of magnitude.

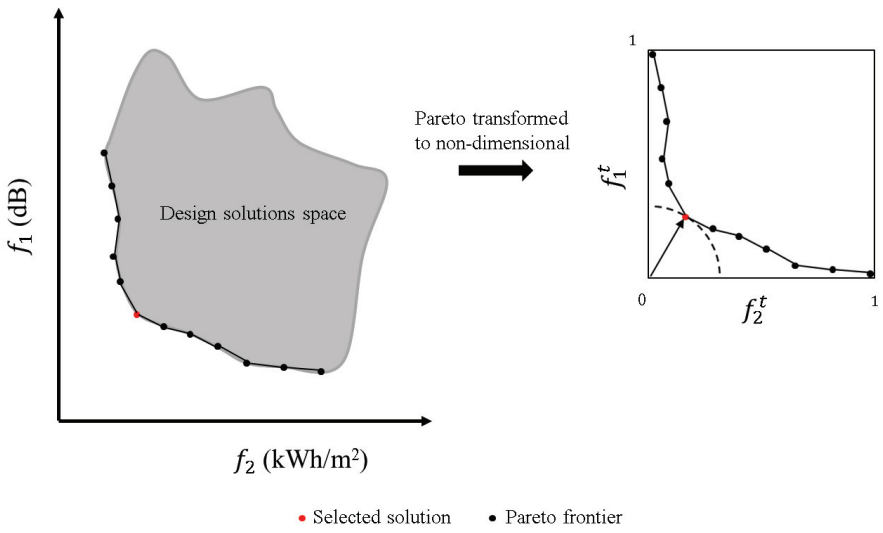

Figure 26 The approach for selection of the best solution from the Pareto

The first optimization round was performed to find optimal values for the building envelope properties (2016-EnvelopeOpt). Figure 27 shows the scatterplot of the simulated building variants using MOGA_II and NSGA_II algorithms, which are represented on the plan of the two objective functions. MOGA_II demonstrate a better performance by covering a larger area of the design space and providing Pareto frontier closer to the utopia point.

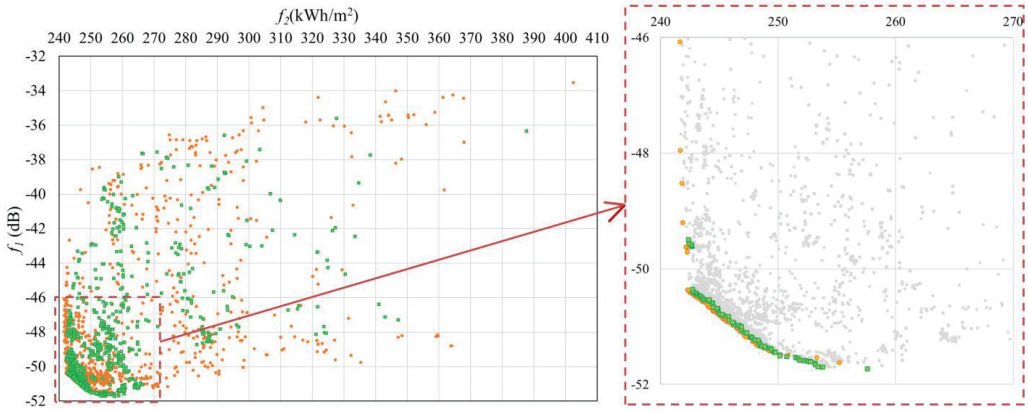

Figure 27 Scatter plot for the optimization of building envelope properties (in orange are building variants using MOGA_II algorithm and in green the ones based on NSGA_II algorithm).

The optimal solution is selected from the Pareto frontier using the approach described earlier. In this approach, first the Pareto frontier is normalized to values between zero and one, and then the solution with minimum distance to ideal point is selected as optimal solution. The normalized Pareto frontier and the selected solution are shown in Figure 28.

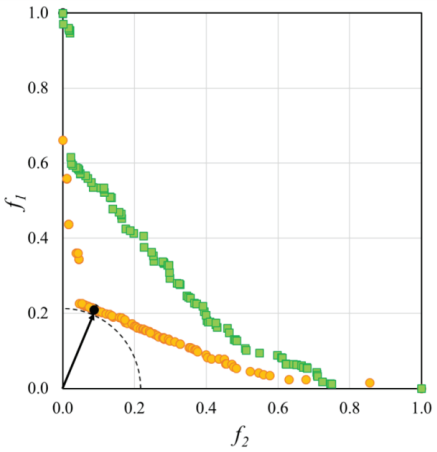

Figure 28 Normalized Pareto frontier with the selected optimal solution in black (in orange are normalized Pareto frontier using MOGA_II algorithm and in green the ones provided by NSGA_II algorithm).

7.2.3.2 Configuration no.2: Optimization of the control settings

The second process involves optimization of daily control setting using TDY, ECY and EWY based on hourly typical and extreme values (see section 6.1.2). The configuration differs from the first because the input variables related to thermal properties of building envelope are excluded and only the control settings are considered in the optimization run that uses the same noise of the configuration no.1. The optimization is performed for each day of

the year using MOGA_II algorithm, but the number of evaluations is now 48, while the probability of directional cross-over and the probability of mutation are kept the same. The initial population with 6 designs is generated using a random sequence and the number of generations is set to 8. These values were set using trials and errors to perform the process with an acceptable convergence level and feasible time. Figure 29 shows an optimization evolution for one day as an example. In each evaluation, 3 energy simulations were run under the three weather files. A total of 365 optimizations were performed to find optimum control settings for each day of the year, with objective functions set according to Eq.(7) (p=24) and Eq.(8). The last solution at each optimization is considered as optimum control setting for that day.

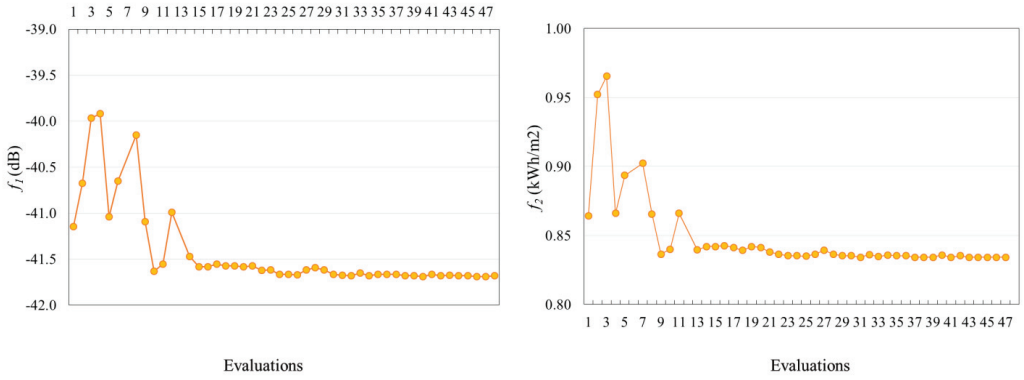

Figure 29 Evolution of objective functions. Example of optimizing control settings for a day.

Figure 30 demonstrate the flowchart of the optimization process for the above configuration.

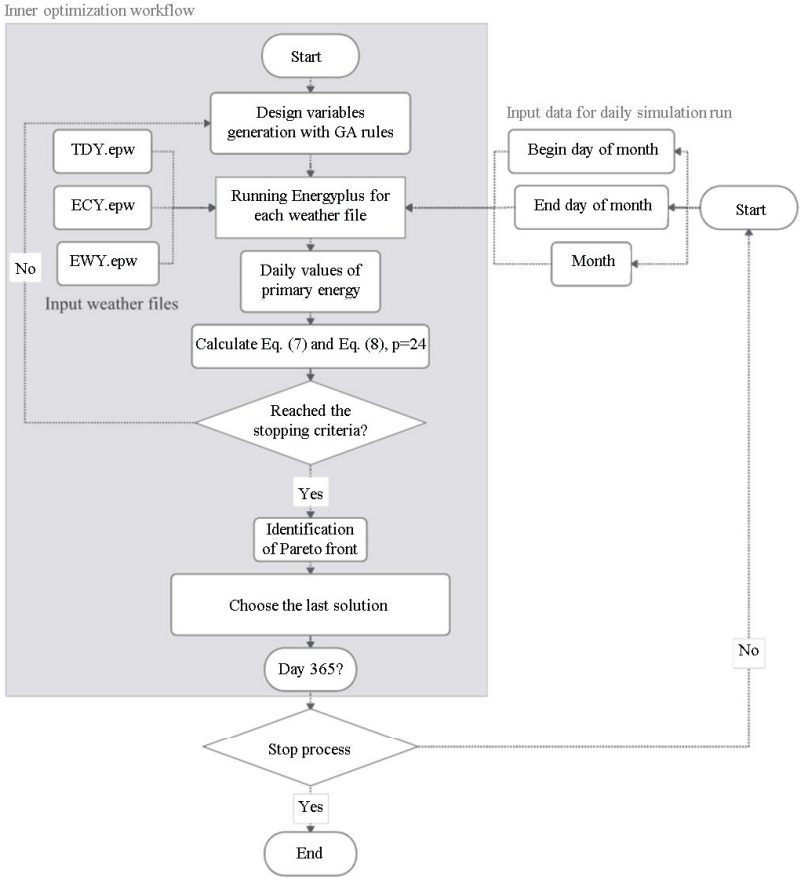

Figure 30 Flowchart of the optimization process implemented in modeFRONTIER for configuration no.2

7.3 Assessment of optimization strategies

Six cases were designed to render the impacts of each group of design variables on the energy-robustness and energy-efficiency of base-cases. First on a newly built building, the aforementioned optimization process applied to the base-case building model compliant to the 2016 requirements.

1. *2016-base*: It is the 2016-compliant base-case model with fixed values of heating and cooling setpoints and no automated solar shadings.

Three cases were developed to identify the most effective optimization strategy:

2. *2016-EnvelopeOpt:* The building envelope properties of the 2016-base model are changed to their optimum values, but the control settings are not optimized;

3. *2016-ControlOpt:* Automated solar shading is added to the 2016-base model and optimum daily *values* are used for setting the setpoint values for space heating and cooling and solar shading control;
4. *EnvelopeOpt+ControlOpt:* Both envelope properties and control settings of 2016-base are replaced with optimum values.

Afterwards, the existing building that we assumed to be compliant to 1980s quality standards considered for the purpose of optimization. It should be noted that the exclusive optimization of the building envelope without the upgrade of the HVAC systems may not be compatible with the latest legislative requirements (e.g., in Europe the Directive on energy performance of buildings), and the lifecycle of an HVAC system, in any case, is not longer than 30 years. Therefore, if we renovate a 1980-compliant base-case building by upgrading the HVAC systems to recent requirements (let's say 2016) and optimize the building envelope to maximize its energy-robustness and energy-efficiency, we obtain the previously mentioned *Envelope optimized-2016-case*. Furthermore, if we optimize both the envelope properties and the control settings, we obtain the *EnvelopeOpt+ControlOpt*. Thus, we will study the case where an existing building gets enhanced by optimizing its control settings that would require a little investment.

5. *1980-base:* The building model has the same geometry of the 2016-base, but its constructions are set according to typical 1980s quality standards.

Therefore, an additional case will be studied:

6. *1980-ControlOpt:* Automated solar shading is added to 1980-base model, and optimum daily values are used for setting the setpoint values for space heating and cooling and solar shading control.

Finally, in order to test the effectiveness of the proposed method and demonstrate the most energy-robust building variant against climate change among the solutions, all of them are tested against a weather file dataset made of 74 representative weather files generated for the city of Geneva (see section 6.1.3).

This assessment methodology is applied to identify the most effective optimization strategy to render a new building with robust energy performance under against climate change and to measure the robustness potential. After performing all the optimizations (more details are provided in Paper VI), the six cases are assessed considering their robustness against climate change. Each case underwent 74 annual simulations using 74 representative weather files. Figure 31 shows the results of this assessment, which are distribution of 74 values of primary energy calculated for each case under 74 different weather files, including typical and extremes.

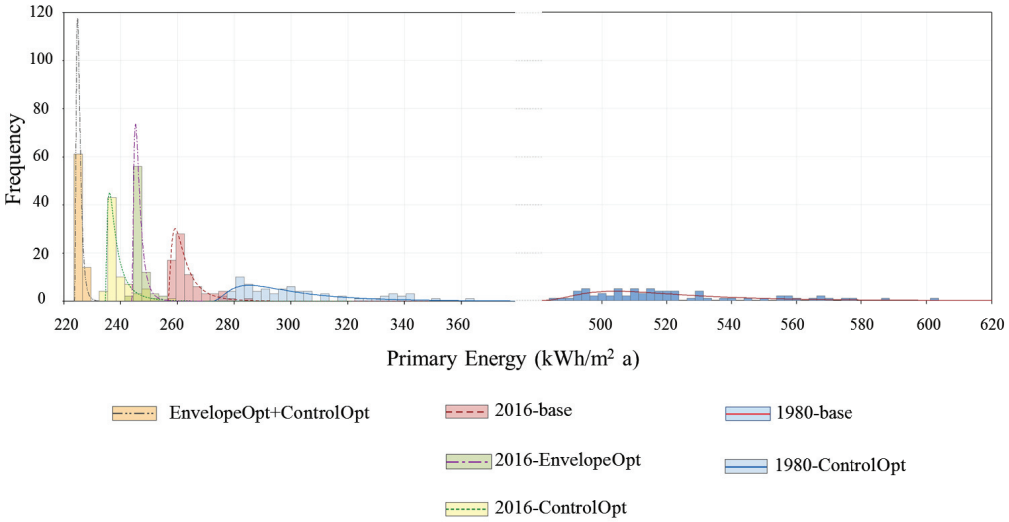

Figure 31 Qualitative distributions comparison of the six cases. For better readability the distribution of 1980-base-case is separated from other cases .

Figure 31 demonstrates the primary energy use of 1980-base case has significantly high sensitivity to the changing climate following by cases 1980-ControlOpt, 2016-base, 2016-EnvelopeOpt, 2016-ControlOpt and EnvelopeOpt+ControlOpt. The statistics calculated based on 74 values of primary energy calculated for each case are presented in Table 9. On the right side of the table the relative changes (%) of mean and standard deviation (SD) of all cases are compared to their values calculated for 1980-base and 2016-base cases.

Table 9 Descriptive statistics based on 74 calculated primary energy use for each case.

Cases	Primary energy use (kWh/m2)					Relative Change (%) to 1980-base value		Relative Change (%) to 2016-base value	
	Mean	SD	Min	Median	Max	Mean	SD	Mean	SD
1980-base	521.7	26.3	485.1	514.7	602.4	0.0%	0.0%	98.1%	354.5%
1980-ControlOpt	301.8	21.4	275.4	296.5	363.5	-42.1%	-18.7%	14.6%	269.6%
2016-base	263.4	5.8	257.1	260.7	284.0	-49.5%	-78.0%	0.0%	0.0%
2016-ControlOpt	239.4	4.6	234.9	237.5	257.1	-54.1%	-82.4%	-9.1%	-19.9%
2016-EnvelopeOpt	246.7	2.1	244.2	246.2	254.6	-52.7%	-92.1%	-6.3%	-64.0%
EnvelopeOpt+ControlOpt	225.5	1.1	223.9	225.1	228.9	-56.8%	-95.9%	-14.4%	-81.5%

Looking deeper into the results, the distribution of 2016-CotrolOpt has lower mean than 2016-EnvelopeOpt but with longer tail, that actually covers the distribution of 2016-EnvelopeOpt case. This means, although EnvelopeOpt case has higher energy demand but the demand is more predictable under extreme conditions than 2016-CotrolOpt case. Comparing 1980-base and 1980-ControlOpt, optimum control settings cause significant reduction in the mean of primary energy use, but the variation remains significantly high and unreliable during extreme climate conditions. However, the highest value of 1980-CotrolOpt case is still lower than the lowest value of 1980-base case, which means a significant improvement only by applying minimum intervention using optimum control settings. EnvelopeOpt+ControlOpt case has very narrow distribution in compare to other cases and at the same time with the lowest mean value.

Looking into statistics provided in Table 9, the calculated standard deviation of EnvelopeOpt+ControlOpt case, is around 5 times (81.5 %) smaller than 2016-base case and almost 24 times (95.9 %) smaller than 1980-base case. It points to a significant reduction of variability in the primary energy use, while having the lowest mean value of primary energy use. This makes EnvelopeOpt+ControlOpt case not only the most energy-efficient case but also the case with most robust energy performance. It demonstrates the effectiveness of the proposed method for designing buildings with robust energy performance under future climate uncertainties.

Furthermore, according to the results, shading and control settings has the highest impact on energy-efficiency. In other words, by adjusting the cooling- and heating-setpoints to optimum values as well as the solar incident setpoint for shading, it is possible to significantly reduce the primary energy use under typical conditions. While optimizing the building envelope properties effectively reduces f_1, which means the solution has lower variability in its response when exposed to extreme conditions and as a result better robustness of energy performance.

8 Conclusions

An energy retrofit design for a child care centre in Milan targeting very high energy and indoor environment performances developed on the basis of a typical weather file of today was studied. The results showed that the choices that were made on the basis of typical climate conditions may fail to provide acceptable energy and indoor environmental performance throughout the future decades.

In another study performed during this PhD work, 74 weather data sets for Geneva were synthesized and applied to the energy simulation of 16 ASHRAE standard reference buildings, single buildings and their combination to create a virtual neighborhood. The dynamical and statistical methods for downscaling the outputs of GCMs were used for preparing the weather data sets to account for extreme conditions together with typical climate conditions. According to the results, for the near-term future, the range of relative change of peak load for cooling demand under extreme conditions shows an increase of 2 % to 28.5 %, compared to typical conditions depending on the building type. Furthermore, the analysis of the virtual neighborhood revealed that the peak electric power demand for the neighborhood can increase by 4.0 %, 7.6 % and 16.8 % under near-term, medium-term and long-term future for extreme conditions in relation to the value calculated using the TMY file. These results underline the importance of considering extreme conditions in studying the impacts of climate change on single buildings and larger spatial scales (e.g. urban and city scales) and preparing urban energy systems for future conditions.

In conclusion, the above studies provided further evidence that proper weather data sets based on high resolution data from climate models and several climate scenarios, including extreme conditions, are required to empower building engineers and architects to test their design solutions under future climate uncertainties. It was also noticed that a large part of literature with focus on the impacts of future climate conditions on the performance of buildings are from the UK, where such weather files are readily accessible for several locations. It shows that the availability of such files is crucial and requires efforts at national levels. Only this type of approach will involve more experts into the discussion of finding solutions that guarantee a more robust and climate resilient built environment in the future.

For better protection of buildings against climate change, this work propose a robust design optimization (RDO) workflow, where the aim is to achieve an optimum solution that it’s energy performance has minimum sensitivity to climate variations. The key to the feasibility of the method is considering climate variations by using only three weather files that represent typical (TDY), extreme warm (EWY) and extreme cold (ECY) weather conditions. A multi-objective optimization process was configured with two objective functions. Minimization of the two objective functions provided in this study, ensures having a building with low energy use under most likely conditions and minimum variation when the conditions change or become extreme. This method applied on the the small office building model from ASHARE 90.1 reference buildings models, and for the city of Geneva. After

performing all the optimizations, the design solutions were assessed for their robustness against climate change. Each design solution underwent 74 annual simulations using 74 representative weather files for Geneva.The results demonstrated that by having optimum daily setpoint temperatures for cooling and heating, and solar incident setpoint for shading, it is possible to reduce significantly the primary energy use under typical conditions. While optimizing the building envelope properties reduce significantly the variability of performance under changing climate conditions including extremes. And finally, by optimizing both the envelope properties and the control settings, the most energy-efficient solution with robust energy performance was achieved. According to the results, the performance of the optimum solution not only had 81.5% lower variation (less sensitivity to climate uncertainty) but at the same time 14.4% lower mean value of energy use in comparison to a solution that was compliant with a recent construction standard (ASHRAE 90.1-2016). Less sensitivity to climate uncertainty means better robustness against climate change and simultaneously keeping a high performance.

This PhD work is a step towards practical tools for designing climate robust buildings, and as demonstrated, efforts at national levels for developing standardised weather data sets representing typical and extreme conditions is crucial for such purpose. The simplicity and the low computational demand of the process ascertain the feasibility and applicability of this method. The approach can be used at any stage of the design process and can help architects and engineers to improve robustness of their design against future climate uncertainties. The work is easily extensible to develop further robust design methods for other sources of variations than climate and other target performances than energy.

9 References

[1] Klepeis NE, Nelson WC, Ott WR, Robinson JP, Tsang AM, Switzer P, et al. The National Human Activity Pattern Survey (NHAPS): a resource for assessing exposure to environmental pollutants. Journal of Exposure Science and Environmental Epidemiology. 2001;11:231.

[2] United Nations DoEaSA, Population Division (2018). World Urbanization Prospects: The 2018 Revision, Online Edition. Available from https://esa.un.org/unpd/wup/Publications. 2018.

[3] Hensen JL, Lamberts R. Building performance simulation for design and operation: Routledge; 2012.

[4] ASHRAE. Standard 62.1-2016. Ventilation for acceptable indoor air quality. American Society of Heating, Refrigerating, and Air-Conditioning Engineers, Inc: Atlanta, GA. 2016.

[5] Menezes AC, Cripps A, Bouchlaghem D, Buswell R. Predicted vs. actual energy performance of non-domestic buildings: Using post-occupancy evaluation data to reduce the performance gap. Applied Energy. 2012;97:355-64.

[6] Bartlett K, Brown C, Chu A-M, Ebrahimi G, Gorgolewski M, Hodgson M, et al. Do our green buildings perform as intended. World Sustainable Building Conference (SBE2014)2014.

[7] Li P, Froese TM, Brager G. Post-occupancy evaluation: State-of-the-art analysis and state-of-the-practice review. Building and Environment. 2018;133:187-202.

[8] de Wilde P, Coley D. The implications of a changing climate for buildings. Building and Environment. 2012;55:1-7.

[9] Arguez A, Vose RS. The Definition of the Standard WMO Climate Normal: The Key to Deriving Alternative Climate Normals. Bulletin of the American Meteorological Society. 2011;92:699-704.

[10] Herrera M, Natarajan S, Coley DA, Kershaw T, Ramallo-González AP, Eames M, et al. A review of current and future weather data for building simulation. Building Services Engineering Research and Technology. 2017;38:602-27.

[11] Moazami A, Carlucci S, Causone F, Pagliano L. Energy Retrofit of a Day Care Center for Current and Future Weather Scenarios. Procedia Engineering. 2016;145:1330-7.

[12] Pagliano L, Carlucci S, Causone F, Moazami A, Cattarin G. Energy retrofit for a climate resilient child care centre. Energy and Buildings. 2016;127:1117-32.

[13] Balaji V, Maisonnave E, Zadeh N, Lawrence BN, Biercamp J, Fladrich U, et al. CPMIP: measurements of real computational performance of Earth system models in CMIP6. Geoscientific Model Development. 2017;10:19-34.

[14] Belcher SE, Hacker JN, Powell DS. Constructing design weather data for future climates. Building Services Engineering Research and Technology. 2005;26:49-61.

[15] Moazami A, Nik VM, Carlucci S, Geving S. Impacts of future weather data typology on building energy performance – Investigating long-term patterns of climate change and extreme weather conditions. Applied Energy. 2019;238:696-720.

[16] Kinnane O, Grey T, Dyer M. Adaptable housing design for climate change adaptation. Proceedings of the Institution of Civil Engineers-Engineering Sustainability. 2017;170:249-67.

[17] Lomas KJ, Ji YC. Resilience of naturally ventilated buildings to climate change: Advanced natural ventilation and hospital wards. Energy and Buildings. 2009;41:629-53.

[18] Nik VM, Mata É, Kalagasidis AS. A statistical method for assessing retrofitting measures of buildings and ranking their robustness against climate change. Energy and Buildings. 2015;88:262-75.

[19] Bodach S, Lang W, Hamhaber J. Climate responsive building design strategies of vernacular architecture in Nepal. Energy and Buildings. 2014;81:227-42.

[20] Ansi/Ashrae. Standard Method of Test for the Evaluation of Building Energy Analysis Computer Programs. Atlanta (GA), USA: American Society of Heating, Refrigerating and Air-Conditioning Engineers; 2011.

[21] Causone F, Carlucci S, Moazami A, Cattarin G, Pagliano L. Retrofit of a kindergarten targeting zero energy balance. IBPC 20152015.

[22] Nik VM. Making energy simulation easier for future climate – Synthesizing typical and extreme weather data sets out of regional climate models (RCMs). Applied Energy. 2016;177:204-26.

[23] Crawley DB, Lawrie LK, Winkelmann FC, Buhl WF, Huang YJ, Pedersen CO, et al. EnergyPlus: Creating a new-generation building energy simulation program. Energy and Buildings. 2001;33:319-31.

[24] Esteco S. ModeFRONTIER 2014 User's Manual. 2014.

[25] Milly PCD, Betancourt J, Falkenmark M, Hirsch RM, Kundzewicz ZW, Lettenmaier DP, et al. Stationarity Is Dead: Whither Water Management? Science. 2008;319:573-4.

[26] Field CB, Barros V, Stocker TF, Dahe Q. Managing the risks of extreme events and disasters to advance climate change adaptation: special report of the intergovernmental panel on climate change: Cambridge University Press; 2012.

[27] Fischer EM, Knutti R. Anthropogenic contribution to global occurrence of heavy-precipitation and high-temperature extremes. Nature Clim Change. 2015;5:560.

[28] Lu N, Wong P, Leung L, Scott M, Taylor T, Jiang W, et al. The impact of climate change on US power grids. Proceedings of the 2 climate change technology conference: CCTC 20092009.

[29] Ke X, Wu D, Rice J, Kintner-Meyer M, Lu N. Quantifying impacts of heat waves on power grid operation. Applied Energy. 2016;183:504-12.

[30] Najjar YSH. Efficient use of energy by utilizing gas turbine combined systems. Applied Thermal Engineering. 2001;21:407-38.

[31] De Bono A, Peduzzi P, Kluser S, Giuliani G. Impacts of summer 2003 heat wave in Europe. United Nations Environment Programme Retrieved from https://wwwunisdrorg/files/1145_ewheatwaveenpdf. 2004.

[32] Robine J-M, Cheung SLK, Le Roy S, Van Oyen H, Griffiths C, Michel J-P, et al. Death toll exceeded 70,000 in Europe during the summer of 2003. Comptes Rendus Biologies. 2008;331:171-8.

[33] Vandentorren S, Suzan F, Medina S, Pascal M, Maulpoix A, Cohen J-C, et al. Mortality in 13 French Cities During the August 2003 Heat Wave. American Journal of Public Health. 2004;94:1518-20.

[34] Grize L, Huss A, Thommen O, Schindler C, Braun-Fahrlander C. Heat wave 2003 and mortality in Switzerland. Swiss medical weekly. 2005;135:200-5.

[35] contributors W. For Want of a Nail. Wikipedia, The Free Encyclopedia.

[36] Christensen JH, Krishna Kumar K, Aldrian E, An S-I, Cavalcanti IFA, de Castro M, et al. Climate Phenomena and their Relevance for Future Regional Climate Change. In: Stocker TF, Qin D, Plattner G-K, Tignor M, Allen SK, Boschung J, et al., editors. Climate Change 2013: The Physical Science Basis Contribution of Working Group I to the Fifth Assessment Report of the Intergovernmental Panel on Climate Change. Cambridge, United Kingdom and New York, NY, USA: Cambridge University Press; 2013. p. 1217–308.

[37] Bouwer LM. Have disaster losses increased due to anthropogenic climate change? Bulletin of the American Meteorological Society. 2011;92:39-46.

[38] Kishore N, Marqués D, Mahmud A, Kiang MV, Rodriguez I, Fuller A, et al. Mortality in Puerto Rico after Hurricane Maria. New England journal of medicine. 2018;379:162-70.

[39] National Aeronautics and Space Administration (NASA), Maria (Atlantic Ocean), accessed on March 23rd, 2019. https://www.nasa.gov/feature/goddard/2017/maria-atlantic-ocean.

[40] Glossary, Meteorology. "American Meteorological Society." Accessed on 23rd March 2019. http://glossary.ametsoc.org/wiki/Rain.

[41] Stocker TF, Qin D, Plattner G-K, Tignor M, Allen SK, Boschung J, et al. Climate change 2013: The physical science basis. Intergovernmental Panel on Climate Change, Working Group I Contribution to the IPCC Fifth Assessment Report (AR5)(Cambridge Univ Press, New York). 2013;25.

[42] Council NR, Committee CR. Radiative forcing of climate change: Expanding the concept and addressing uncertainties: National Academies Press; 2005.

[43] Nakicenovic N, Alcamo J, Grubler A, Riahi K, Roehrl R, Rogner H-H, et al. Special report on emissions scenarios (SRES), a special report of Working Group III of the intergovernmental panel on climate change: Cambridge University Press; 2000.

[44] Carter T. General guidelines on the use of scenario data for climate impact and adaptation assessment. In: (TGICA) TGoDaSSfIaCA, editor.: Intergovernmental Panel on Climate Change; 2007.

[45] Uppala SM, Kållberg P, Simmons A, Andrae U, Bechtold VDC, Fiorino M, et al. The ERA-40 re-analysis. Quarterly Journal of the royal meteorological society. 2005;131:2961-3012.

[46] Kjellström E, Nikulin G, Hansson U, Strandberg G, Ullerstig A. 21st century changes in the European climate: uncertainties derived from an ensemble of regional climate model simulations. Tellus A: Dynamic Meteorology and Oceanography. 2011;63:24-40.

[47] Stocker T. Climate change 2013: the physical science basis: Working Group I contribution to the Fifth assessment report of the Intergovernmental Panel on Climate Change: Cambridge University Press; 2014.

[48] Knutti R, Sedláček J. Robustness and uncertainties in the new CMIP5 climate model projections. Nature Clim Change. 2013;3:369.

[49] van Vuuren DP, Edmonds J, Kainuma M, Riahi K, Thomson A, Hibbard K, et al. The representative concentration pathways: an overview. Climatic Change. 2011;109:5.

[50] Rastogi P. On the sensitivity of buildings to climate - the interaction of weather and building envelopes in determining future building energy consumption: EPFL; 2016.

[51] Bordass B. Energy performance of non-domestic buildings: closing the credibility gap. in Proceedings of the 2004 Improving Energy Efficiency of Commercial Buildings Conference: Citeseer; 2004.

[52] Macdonald IA. Quantifying the Effects of Uncertainty in Building Simulation: University of Strathclyde; 2002.

[53] Iaccarino G. Quantification of Uncertainty in Flow Simulations Using Probabilistic Methods: Stanford University; 2008.

[54] IEC. 60050-191: International electrotechnical vocabulary: Chapter 191: Dependability and quality of service. International Electrotechnical Commission, Geneva. 1990.

[55] ANSI/ASHRAE 140. Standard Method of Test for the Evaluation of Building Energy Analysis Computer Programs. Atlanta (GA), USA: American Society of Heating, Refrigerating and Air-Conditioning Engineers; 2011. p. 272.

[56] Ham Y, Golparvar-Fard M. Mapping actual thermal properties to building elements in gbXML-based BIM for reliable building energy performance modeling. Automation in Construction. 2015;49:214-24.

[57] Ham Y, Golparvar-Fard M. EPAR: Energy Performance Augmented Reality models for identification of building energy performance deviations between actual measurements and simulation results. Energy and Buildings. 2013;63:15-28.

[58] Pan W, Gibb AGF, Dainty ARJ. Strategies for Integrating the Use of Off-Site Production Technologies in House Building. Journal of Construction Engineering and Management. 2012;138:1331-40.

[59] C.J. Hopfe, Uncertainty and sensitivity analysis in building performance simulation for decision support and design optimization, Ph.D, Eindhoven University of Technology. 2009.

[60] Delzendeh E, Wu S, Lee A, Zhou Y. The impact of occupants' behaviours on building energy analysis: A research review. Renewable and Sustainable Energy Reviews. 2017;80:1061-71.

[61] Hall IJ, Prairie R, Anderson H, Boes E. Generation of a typical meteorological year. Analysis for solar heating and cooling. San Diego, CA, USA: Sandia Labs., Albuquerque, NM (USA); 1978.

[62] Chalupnik MJ, Wynn DC, Clarkson PJ. Comparison of ilities for protection against uncertainty in system design. Journal of Engineering Design. 2013;24:814-29.

[63] Taguchi G. Introduction to quality engineering: designing quality into products and processes. 1986.

[64] Leyten JL, Kurvers SR. Robust indoor climate design. 12th International Conference on Indoor Air Quality and Climate 2011, June 5, 2011 - June 10, 2011. Austin, TX, United states: International Society of Indoor Air Quality and Climate; 2011. p. 1025-30.

[65] Hoes P, Hensen JLM, Loomans MGLC, de Vries B, Bourgeois D. User behavior in whole building simulation. Energy and Buildings. 2009;41:295-302.

[66] Fabi V, Buso T, Andersen RK, Corgnati SP, Olesen BW. Robustness of building design with respect to energy related occupant behaviour. IBPSA. Chambery, France2013. p. 1999-2006.

[67] Palme M, Isalgue A, Coch H, Serra R. Energy consumption and robustness of buildings. CESB. Prague, Czech republic: Czech Technical University; 2010. p. 1-12.

[68] Chinazzo G, Rastogi P, Andersen M. Robustness assessment methodology for the evaluation of building performance with a view to climate uncertainties. IBPSA. Hyderabad, India2015. p. 947-54.

[69] Buso T, Fabi V, Andersen RK, Corgnati SP. Occupant behaviour and robustness of building design. Building and Environment. 2015;94:694-703.

[70] Bosher L. Introduction: the need for built-in resilience. Hazards and the Built Environment: Routledge; 2008. p. 21-37.

[71] Faller G. The resilience of timber buildings. SEMC. Cape Town, South africa: Taylor & Francis - Balkema; 2013. p. 1845-9.

[72] Champagne CL, Aktas CB. Assessing the Resilience of LEED Certified Green Buildings. In: Chong O, Parrish K, Tang P, Grau D, Chang J, editors. Icsdec 20162016. p. 380-7.

[73] Desouza KC, Flanery TH. Designing, planning, and managing resilient cities: A conceptual framework. Cities. 2013;35:89-99.

[74] Pearson LJ, Pearson L, Pearson CJ. Sustainable urban agriculture: stocktake and opportunities. International Journal of Agricultural Sustainability. 2010;8:7-19.

[75] Floricel S, Miller R. Strategizing for anticipated risks and turbulence in large-scale engineering projects. International Journal of project management. 2001;19:445-55.

[76] Olewnik A, Brauen T, Ferguson S, Lewis K. A Framework for Flexible Systems and Its Implementation in Multiattribute Decision Making. Journal of Mechanical Design. 2003;126:412-9.

[77] Bates RA, Kenett RS, Steinberg DM, Wynn HP. Achieving robust design from computer simulations. Quality Technology & Quantitative Management. 2006;3:161-77.

[78] Gribble SD. Robustness in complex systems. Hot Topics in Operating Systems, 2001 Proceedings of the Eighth Workshop on: IEEE; 2001. p. 21-6.

[79] Andersson P. Robustness of Technical Systems in Relation to Quality, Reliability and Associated Concepts. Journal of Engineering Design. 1997;8:277-88.

[80] Yassine AA. Investigating product development process reliability and robustness using simulation. Journal of Engineering Design. 2007;18:545-61.

[81] Bettis RA, Hitt MA. The new competitive landscape. Strategic management journal. 1995;16:7-19.

[82] National Laboratory of the US Department of Energy, Resilience Roadmap: https://www.nrel.gov/resilience-planning-roadmap/, accessed on 15th March 2019.

[83] Berkes F, Colding J, Folke C. Navigating social-ecological systems: building resilience for complexity and change: Cambridge University Press; 2008.

[84] Faller G. The resilience of timber buildings. 5th International Conference on Structural Engineering, Mechanics and Computation, SEMC 2013, September 2, 2013 - September 4, 2013. Cape Town, South africa: Taylor & Francis - Balkema; 2013. p. 1845-9.

[85] Christopher M, Rutherford C. Creating supply chain resilience through agile six sigma. Critical eye. 2004;7:24-8.

[86] Wildavsky AB. Searching for safety: Transaction publishers; 1988.

[87] Hollnagel E, Nemeth CP, Dekker S. Resilience Engineering Perspectives, Volume 1: Remaining sensitive to the possibility of failure: Ashgate; 2008.

[88] Haimes YY, Crowther K, Horowitz BM. Homeland security preparedness: Balancing protection with resilience in emergent systems. Systems Engineering. 2008;11:287-308.

[89] Wilde Pd. Building Performance Analysis: Wiley-Blackwell; 2018.

[90] Moazami A, Carlucci S, Geving S. Critical Analysis of Software Tools Aimed at Generating Future Weather Files with a view to their use in Building Performance Simulation. Energy Procedia. 2017;132:640-5.

[91] Nik VM. Application of typical and extreme weather data sets in the hygrothermal simulation of building components for future climate – A case study for a wooden frame wall. Energy and Buildings. 2017;154:30-45.

[92] Causone F, Moazami A, Carlucci S, Pagliano L, Pietrobon M. Ventilation strategies for the deep energy retrofit of a kindergarten. AIVC 20152015.

[93] Deru M, Field K, Studer D, Benne K, Griffith B, Torcellini P, et al. US Department of Energy commercial reference building models of the national building stock. 1617 Cole Boulevard Golden, Colorado: National Renewable Energy Laboratory; 2011.

[94] Mohajeri N, Gudmundsson A, Scartezzini J-L. Statistical-thermodynamics modelling of the built environment in relation to urban ecology. Ecological Modelling. 2015;307:32-47.

[95] Khoury J. Assessment of Geneva multi-family building stock: main characteristics and regression models for energy reference area determination. SCCER Future Energy Efficient Buildings & Districts (http://www.sccer-feebd.ch/); 2016.

[96] ISO C. ISO 52000-1:2017. Energy performance of Buildings—Overarching EPB assessment–Part 1: General framework and procedures.

[97] ASHRAE AS. Standard 90.1-2004, Energy standard for buildings except low rise residential buildings. American Society of Heating, Refrigerating and Air-Conditioning Engineers, Inc; 2004.

[98] Luber G, McGeehin M. Climate Change and Extreme Heat Events. American Journal of Preventive Medicine. 2008;35:429-35.

[99] Taguchi G, Chowdhury S, Taguchi S. Robust engineering: learn how to boost quality while reducing costs & time to market: McGraw-Hill Professional Pub; 2000.

[100] Fowlkes WY, Creveling CM. Engineering Methods for Robust Product Design: Using Taguchi Methods in Technology and Product Development: Addison-Wesley Publishing Company; 1995.

[101] Phadke MS. Quality engineering using robust design: Prentice Hall PTR; 1995.

[102] Lanzotti A. Robust design of car packaging in virtual environment. International Journal on Interactive Design and Manufacturing (IJIDeM). 2008;2:39-46.

[103] Park G-J, Lee T-H, Lee KH, Hwang K-H. Robust Design: An Overview. AIAA Journal. 2006;44:181-91.

[104] Gorissen BL, Yanıkoğlu I, den Hertog D. A practical guide to robust optimization. Omega. 2015;53:124-37.

[105] Gabrel V, Murat C, Thiele A. Recent advances in robust optimization: An overview. European Journal of Operational Research. 2014;235:471-83.

[106] Hamdy M, Nguyen A-T, Hensen JLM. A performance comparison of multi-objective optimization algorithms for solving nearly-zero-energy-building design problems. Energy and Buildings. 2016;121:57-71.

[107] Mauro GM, Hamdy M, Vanoli GP, Bianco N, Hensen JL. A new methodology for investigating the cost-optimality of energy retrofitting a building category. Energy and Buildings. 2015;107:456-78.

[108] Nguyen A-T, Reiter S, Rigo P. A review on simulation-based optimization methods applied to building performance analysis. Applied Energy. 2014;113:1043-58.

[109] Deb K, Agrawal S, Pratap A, Meyarivan T. A fast elitist non-dominated sorting genetic algorithm for multi-objective optimization: NSGA-II. International conference on parallel problem solving from nature: Springer; 2000. p. 849-58.

[110] Rigoni E, Poles S. NBI and MOGA-II, two complementary algorithms for Multi-Objective optimizations. Dagstuhl Seminar Proceedings: Schloss Dagstuhl-Leibniz-Zentrum für Informatik; 2005.

[111] Fonseca CM, Fleming PJ. Genetic Algorithms for Multiobjective Optimization: FormulationDiscussion and Generalization. Icga: Citeseer; 1993. p. 416-23.

[112] Augusto OB, Bennis F, Caro S. A new method for decision making in multi-objective optimization problems. Pesquisa Operacional. 2012;32:331-69.

10 Individual papers

Paper I

Available online at www.sciencedirect.com

ScienceDirect

Procedia Engineering 145 (2016) 1330 – 1337

Procedia Engineering

www.elsevier.com/locate/procedia

International Conference on Sustainable Design, Engineering and Construction

Energy retrofit of a day care center for current and future weather scenarios

Amin Moazami[a*], Salvatore Carlucci[a], Francesco Causone[b], Lorenzo Pagliano[b]

[a]*NTNU Norwegian University of Science and Technology, Department of Civil and Transport Engineering, Trondheim, Norway*
[b]*end-use Efficiency Research Group, Department of Energy, Politecnico di Milano, Milano, Italy*

Abstract

Many scientific evidences have shown that Earth's climate is rapidly changing. By 2050, European Union is aiming to significantly reduce greenhouse gas emissions (GHG) in the building sector. Achieving this target might help the mitigation of global warming, but the climate change seems inevitable. This means that both new and refurbished buildings should be able to face those conditions that they are going to experience during their lifetime. Therefore, any building design should be checked both for current and future climate scenarios. This study describes the use of a downscaling method named *morphing* to generate future weather scenarios and intends to support the design process of a deep energy retrofit of a day care center in order to improve the energy and thermal comfort performance of the building under the current and future weather scenarios. The retrofit concept of the building also includes hybrid ventilation, automated solar shading, lighting controls and renewable energy generation systems.

© 2016 The Authors. Published by Elsevier Ltd. This is an open access article under the CC BY-NC-ND license (http://creativecommons.org/licenses/by-nc-nd/4.0/).
Peer-review under responsibility of the organizing committee of ICSDEC 2016

Keywords: Climate change, climate change adaptation, climate resilience, future weather scenario, net-zero energy buildings.

1. Introduction

The 195 countries were participating in the 2015 United Nations Climate Change Conference (COP 21) in Paris recently agreed on a set of global actions to limit the global warming below 1.5 °C with respect to the pre-industrial period [1]. The recent assessment report by the Intergovernmental Panel on Climate Change (IPCC) highlights the

* Corresponding author. Tel.: +47 40476475.
E-mail address: amin.moazami@ntnu.no

1877-7058 © 2016 The Authors. Published by Elsevier Ltd. This is an open access article under the CC BY-NC-ND license (http://creativecommons.org/licenses/by-nc-nd/4.0/).
Peer-review under responsibility of the organizing committee of ICSDEC 2016
doi:10.1016/j.proeng.2016.04.171

considerable technological, economics and institutional challenges that are required to achieve this goal [2]. Moreover, designers and managers of the built environment have to take into account the forthcoming changes since the global warming can cause extreme conditions such as summer overheating and a substantial shift from space heating to space cooling both for existing and new buildings in temperate, winter-dominated climates [3]. IPCC developed future climate scenarios based on possible future GHG emissions. These scenarios are considered as most likely future global conditions. In order to make these scenarios suitable for the building sector, local scenarios are required. Belcher et al. [4], developed a methodology called 'morphing' that generates future weather scenarios with an hourly resolution from general circulation models of the atmosphere, which have a monthly resolution. In this work, three different future weather scenarios for the city of Milan in Italy were developed using IPCC scenarios and the morphing method. Such three scenarios, namely 2020, 2050, and 2080, are used to assess the deep energy retrofit design of a day care center [5], against future climate change. To date, in the design process of high-performance buildings, typical meteorological year are mostly used, and little attention has been reserved to future weather projections. Robert and Kummert [6] have shown that a net-zero energy building, designed under typical weather conditions, can miss the net-zero energy target in future projected years. The focus of this paper is to evaluate the behavior of a net-zero energy day care center under future weather scenarios, in terms of energy and thermal comfort. To this aim, the long-term thermal discomfort indices proposed in the European standard EN 15251 [7] are used to assess indoor thermal comfort conditions and suitable climate severity indices have been applied to characterize the severity of the future weather scenarios.

Nomenclature

ASHRAE	American society of heating, refrigerating, and air-conditioning engineers
BPS	Building performance simulation
CDD	Cooling degree-day
COP	Conference of the Parties
CV(RMSE)	Coefficient of variation of the Root mean square error
HadCM3	UK Met Office Hadley Centre coupled model version 3
HDD	Heating degree-day
HVAC	Heating ventilation and air conditioning
IPCC	Intergovernmental panel on climate change
MBE	Mean bias error
PV	Photovoltaic
SRES	Special report on emission scenarios
TMY	Typical meteorological year

2. Materials and methods

A deep energy retrofit of a day care center was supported by building performance simulation (BPS) to improve the energy and thermal comfort performance of the building and to achieve the net zero energy balance under the current, typical and future weather scenarios.

First, an environmental monitoring of the building allowed to identify the most important deficiencies of the existing building and address the retrofitting concept. Then, BPS was used to support the retrofit design of a day care center and the consequent decision-making process. A model of the existing building was created and calibrated against both monthly measured delivered energy and hourly indoor air temperature [3]. Then, several refurbishment options were implemented in the model and compared in order to identify the best options to apply into the final retrofitting concept of the building, which includes hybrid ventilation, automated solar shading, lighting controls and a photovoltaic (PV) generation systems. The model of the existing building (also referred as the pre-retrofit model) was after that used as the reference to evaluate the energy saving and the thermal enhancement of the post-retrofit building under typical, current and future weather scenarios.

2.1. The case study: the day care center of Via Feltrinelli 11

The day care center is a one-story rectangular building located in Via Feltrinelli 11 in Milan, Italy. It has two 44-meter-long façades on southwest and northeast and two 23-meter-long façades on southeast and northwest. The building has a total gross area of 944 m^2 and a net floor area of 855 m^2. Around 58% of the net floor area is dedicated to the children activities and the remaining are staff and service areas. The total heated volume of the building is 3422 m^3, and the building is characterized by surface to volume ratio (S/V) equal to 0.77 m^2/m^3. Table 1 reports the designed values of the opaque and glazing components of the building envelope implemented in the numerical models representing the existing building and the retrofitting concept.

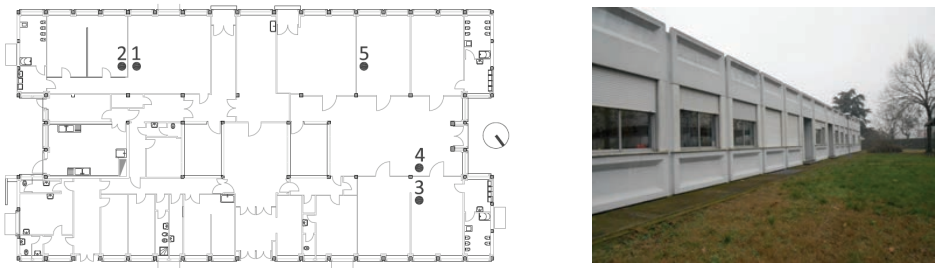

Fig. 1. (a) Kindergarten plan view including the five monitored rooms; (b) picture of the southwest facade.

Table 1. Descriptions of the building envelope opaque and glazing components of the pre- and post- retrofit models.

Building envelope component	Description of the existing components	Pre-retrofit estimated U-value, W/(m^2K)	Post-retrofit calculated U-value, W/(m^2K)
Roof	Pre-cast concrete slab	1.3	0.10
Vertical opaque wall	Pre-cast concrete panel	1.2	0.10
Floor (facing an unheated basement)	Pre-cast concrete slab	1.3	0.30
Windows	Clear double glazing + Aluminum frame without thermal break	5.8	0.73

2.2. Environment monitoring of the building

Currently, a natural gas boiler with metal radiators for heating are installed in the day care center, and no active cooling system is available. The occupants manually operate the windows to refresh indoor air all year round and cool down the building during summer days. In order to evaluate the thermal quality of the building envelope of the existing building, an inspection with an infrared thermal camera was performed during winter 2014. The analysis clearly showed a poor thermal resistance of the envelope due to a very low thermal insulation and the existence of noteworthy thermal bridges. The indoor environmental conditions of the building are under monitoring since July 2014; it was therefore possible to note a very high drop of indoor air temperature (Figure 2b) during the Christmas holidays of 2014, because the heating system was switched off and the building envelope performance are poor. Carbon dioxide concentration was monitored in Room 4 (Figure 2a) to assess indirectly indoor air quality in the building. The result shows noticeable peaks after September with values considerably higher than the reference value of 700 ppm above the 400 ppm background level recommended by the standard ASHRAE 62 [8]. The recorded data shows that the buildings clearly needs a better ventilation strategy [9].

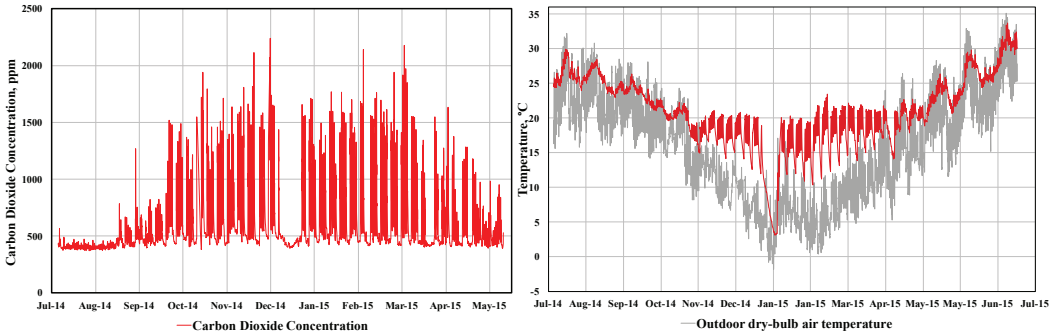

Fig. 2. (a) Carbon dioxide concentration in Room 4; (b) Air temperature in Room 4 versus outdoor air temperature.

2.3. Modeling and simulation of the pre- and post-retrofit numerical models of the building

Modeling and simulation of the building were performed in the whole-building dynamic software EnergyPlus [10], version 8.3.0.1. Within the capability of EnergyPlus, the building model was created to reproduce in detail the geometry of the existing building, and the algorithms were selected in order to reproduce accurately physical phenomena. Two rounds of simulations were carried out, one for the pre-retrofit building model and the second for the post-retrofit building model to assess both the building models under typical, current, and future weather scenarios.

Regarding the existing building, it was modeled without mechanical ventilation and cooling systems, and, hence, the whole building was modeled to be passively operated during summertime. According to the Italian law DPR 412 [11], in Milan, heating systems can be turned on during the period ranging from 15th October to the 15th April. This period was adopted to schedule the operation of the heating system, and, during the rest of the year, the model was simulated in free-running mode. The heating set-point temperature was set according to the design values recommended by EN 15251 and based on the Fanger comfort model. The internal gains are heat produced by occupants, electrical equipment, and artificial lighting. Then, the pre-retrofit model was calibrated to provide consistent and reliable simulation outcomes. Two calibration processes were carried out, following the ASHRAE Guideline 14 [12]. In the beginning, the pre-retrofit model was calibrated based on the monthly measured delivered energy. The model was then refined with a second calibration using hourly measured indoor air temperature as the benchmark.

The post-retrofit building was simulated in two configurations: the first configuration assumes that no mechanical cooling system is installed, and the building is in free-running during summertime while the second one assumes that an ideal reversible air-to-air heat pump is installed. Hence, the building is mechanically conditioned throughout the year. The cooling set-point temperature is set according to the design values recommended by EN 15251 and based on the Fanger comfort model. In the two post-retrofit building models, a PV system is included. The generation system is assumed to be adequate to meet the net-zero energy target expressed in primary energy and calculated on a yearly basis.

2.4. Generation of the future weather scenarios

In this paper, the approach proposed by Jentsch et al. [13] is adopted. They developed a tool called CCWorldWeatherGen that provides future weather projections with an hourly resolution. Such future weather data are suitable for being used in BPS. The calculation method implemented in this tool uses three factors: first, the A2 emission scenario that is developed by the Special report on emission scenarios (SRES) of IPCC working group 3 [2]. Second, the *UK Met Office Hadley Centre Coupled Model version 3* (HadCM3) [14], and third, a downscaling method called *morphing*, which was introduced by [4]. This calculation method is applied in the Typical Meteorological Year (TMY) file to obtain hourly weather data for the three future scenarios in 2020, 2050 and 2080.

In summary, five different scenarios are created: the typical weather file (TMY), the monitored weather file for the year 2014, and three weather projections for the years 2020, 2050, and 2080. For each scenario, heating degree-day (HDD) and cooling degree-day (CDD) are calculated and used to evaluate their climate severity (Table 2).

Table 2. Comparison of climate severity of the typical, current and future weather scenarios.

Parameter (unit of measure)	TMY	2014	2020	2050	2080
HDD (°C h)	3002	2274	2718	2384	1988
CDD (°C h)	3	45	26	116	289

2.5. Assessment of the energy and thermal performance of the building models

Since the existing building is operated in free-running mode during summer, to assess the enhancement of the post-retrofit concept a long-term thermal discomfort index is used for the thermal comfort assessment [15]. The *Percentage out of range* method, proposed by the European standard EN 15251, was used to assess the building thermal performance, although it is characterized by some limitations [16,17]. It calculates the percentage of occupied hours when the indoor operative temperature falls outside of a given thermal comfort category. This index is symmetrical, i.e. it measures both overheating and undercooling occurrences [17]. Moreover, EN 15251 suggests the use of Category I for spaces occupied by very sensitive and fragile people, such as day care centers.

For the second configuration of the post-retrofit model, since the building is assumed fully conditioned, the energy needs for space heating and cooling, before and after the retrofit, are compared in the typical, current and the three future weather scenarios.

3. Results and discussion

The calibrated model of the existing building reproduces the general thermal behavior of the actual building with a good agreement (Figure 3). The calibration process comprised two subsequent calibrations. The first calibration was based on monthly energy use over a 1-year period (2014) and showed a Mean bias error (MBE) and a Coefficient of variation of the Root mean square error (CV(RMSE)) equal respectively to MBE = 3.7 % and CV(RMSE) = 11.6 %. According to ASHRAE Guideline 14, a numerical model can be considered calibrated if MBE and CV(RMSE) are lower than 5% and 15% correspondingly, for monthly data. In order to further refine the model and to reduce the uncertainty, a second calibration run was carried out for the hourly indoor air temperature measured in Room 4. In the second run, the best building variant showed MBE = 0.8 % and CV(RMSE) = 4.2 %. ASHRAE Guideline 14 recommends that MBE has to be lower than 10% and CV(RMSE) has to be lower than 30% for hourly data. Therefore, the model is also calibrated in terms of hourly temperatures. For further details on the calibration procedure of the model, please refer to [3].

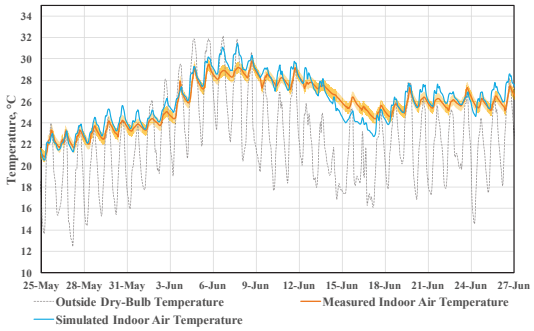

Fig. 3. Comparison of simulated and monitored indoor air temperatures in Room 4. The shaded area is the measurement uncertainty of ±0.5 ºC.

3.1. Post-retrofit model simulated in free-running mode during summer under typical and future weather scenarios

In this first simulation round, the building has been simulated in free-running during the period 15th May to 15th September. The obtained results provide information on the period in which the building might experience thermal discomfort due to overheating. Figure 4 shows the indoor operative temperature contrasted with the exponentially-weighted running mean outdoor temperature only for the occupied hours. Although the Category I is suitable for a day care center according to EN 15251, all three categories proposed by such standard are depicted in Figure 4, to show the effect that the selection of the comfort category can have on the building assessment [18]. According to the simulations, the energy retrofit design concept for the existing day care center performs quite well concerning the overheating issue during the summer period under the current year (2014), TMY and 2020 scenarios. In 2050 and 2080 scenarios the temperature falls outside the upper thresholds of the comfort categories.

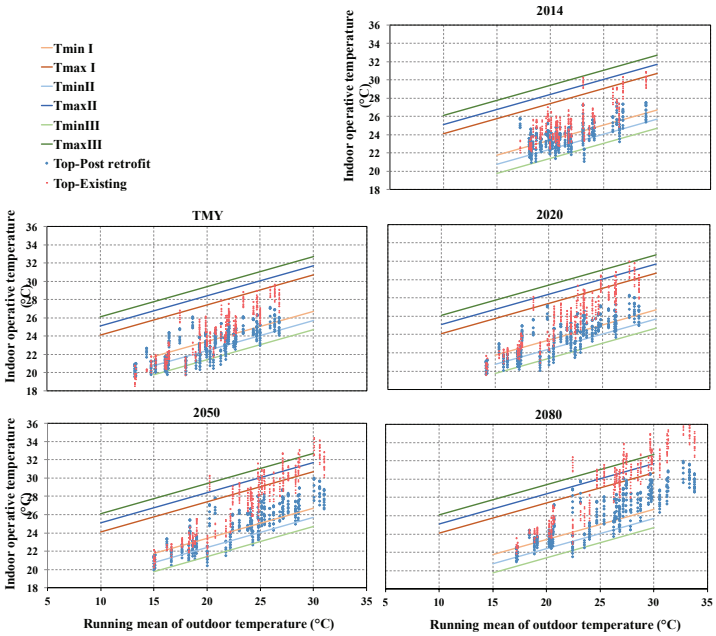

Fig. 4. Comparison of the running mean of the outdoor temperature and the indoor operative temperature in the five weather scenarios. In red the conditions referring to the existing building model and in blue the conditions referring to the retrofitted building model.

According to the 2050 and 2080 projections, it is expected that the running mean of outdoor temperature will fall outside the applicability domain of the adaptive thermal comfort model as proposed by EN 15251. Furthermore, considering both upper and lower overshoots, the total amount of hours out of Category-I range increases drastically in the 2080 scenario, but the percentage of undercooling tends to decrease for future weathers accordingly to the global warming predictions.

Figure 5 presents the difference between the pre- and post-retrofit situation of respectively primary energy usage (ΔPE) and absolute difference of long-term thermal discomfort index (ΔLDI). It can be seen that the gain of energy performance between the post-retrofit and pre-retrofit conditions reduces in the future warmer conditions, whereas the thermal discomfort difference value increases considerably. It means that the post-retrofit building shows not only a much better energy performance but also a much lower occurrence of overheating conditions compared to the existing building, particularly under future climate scenarios.

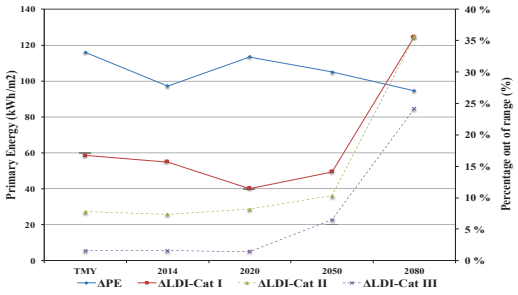

Fig. 5. Difference of primary energy usages (ΔPE) and absolute difference of long-term discomfort index (ΔLDI) of pre- and post-retrofit models

3.2. Post-retrofit model simulated in conditioning mode under typical and future weather scenarios

The second round of simulations considers the post-retrofit building model fully conditioned throughout the year by assuming the installation of an ideal system that guarantees the achievement of the heating and cooling set-point temperatures. Figure 6 shows primary energy disaggregated by energy service for the whole building in the five weather scenarios under study. The primary energy conversion factors are assumed to be symmetric for the electricity delivered from the grid to the building and for the electricity generated by the photovoltaic (PV) system i.e. 2.18 kWh_{PE}/kWh_{el} [19]. Considering the TMY scenario, a PV system with a total capitation area of 120 m^2 and a nominal efficiency of 13% was required to balance (over one year) the whole building primary energy.

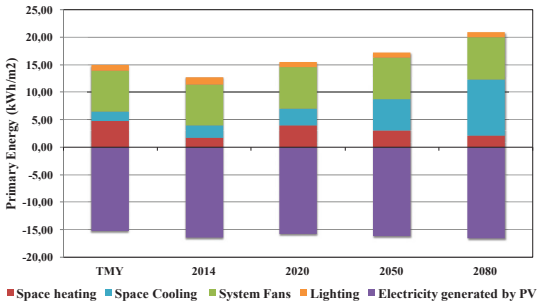

Fig. 6. Primary energy breakdown of the post-retrofit building including electricity generated by the PV system.

Energy simulation indicates that global warming could determine, in Milan, a shift from heating dominance to cooling dominance. Furthermore, although the energy need for heating will decrease, the overall energy usage of the building will increase. Furthermore, in 2050 and 2080, the post-retrofit building concept might not be anymore compliant with the net-zero energy target if the capitation area of the PV system is not increased. Moreover, it is worth to be reminded that the performance decay of the PV system has not been modeled.

4. Conclusions

The energy retrofit project for a day care center targeting the net zero primary energy balance and high indoor environment quality has been developed on the base of a TMY weather file. Such weather scenario synthesizes climate in the recent past, 1951-1970. Energy simulation of the pre- and post- retrofit building models were carried out under five weather scenarios: TMY, current (2014), and three future weather scenarios (2020, 2050 and 2080) projected according to the methodology proposed by [13]. The objective of the analysis was to investigate whether the chosen energy concepts that were selected on the base of typical/past climate conditions would be resilient to

future expected climate change. The study showed that the retrofitting concept of the building including hybrid ventilation, automated solar shading, lighting controls, renewable energy generation systems and improvement of the building envelope thermal resistance may result quite robust in the mid-term also in free-running during summertime. However, in the long-term, to face climate change effects, the installation of an active cooling system might be necessary. Regarding the assessment of the long-term thermal discomfort condition in a building, our analysis suggests that care should be taken in using symmetric indexes, since a design strategy targeting to reducing overcooling occurrences in the present weather might make the building less resilient to overheating in future climate conditions.

Acknowledgements

The authors would like to thank the Department of School Construction and the Office for EU Affairs of the Municipality of Milano, ROCKWOOL Italia and Askeen for the collaboration on this project. The study was partially developed within the EU-GUGLE project funded by Seventh Framework Programme under grant agreement n. 314632.

References

[1] Paris Agreement - European Commission. http://ec.europa.eu/clima/policies/international/negotiations/future/index_en.htm (accessed January 15, 2016).
[2] Edenhofer, O., R. Pichs-Madruga, Y. Sokona, E. Farahani, S. Kadner, K. Seyboth, A. Adler, I. Baum, S. Brunner, P. Eickemeier, B. Kriemann, J. Savolainen, S. Schlömer, C. von Stechow, T. Zwickel and J.C. Minx (eds.), 2014: Climate Change 2014: Mitigation of Climate Change Contribution of Working Group III to the Fifth Assessment Report of the Intergovernmental Panel on Climate Change, IPCC, Cambridge University Press, Cambridge, United Kingdom and New York, NY, USA, 2014.
[3] F. Causone, S. Carlucci, A. Moazami, G. Cattarin, L. Pagliano, Energy retrofit for a climate resilient kindergarten, Energy and Buildings, under review.
[4] S.E. Belcher, J.N. Hacker, D.S. Powell, Constructing design weather data for future climates, Build. Serv. Eng. Res. Technol. 26, 2005, 49–61. doi:10.1191/0143624405bt112oa.
[5] F. Causone, S. Carlucci, A. Moazami, G. Cattarin, L. Pagliano, Retrofit of a Kindergarten Targeting Zero Energy Balance, Energy Procedia. 78, 2015, 991–996. doi:10.1016/j.egypro.2015.11.039.
[6] A. Robert, M. Kummert, Designing net-zero energy buildings for the future climate, not for the past, Build. Environ. 55, 2012, 150–158.
[7]CEN, Indoor Environmental Input Parameters for Design and Assessment of Energy Performance of Buildings Addressing Indoor Air Quality, Thermal Environment, Lighting and Acoustics, in, European Committee for Standardization, Brussels, Belgium, 2007.
[8] ASHRAE, ASHRAE Standard 62.1-2013, Ventilation for Acceptable Indoor Air Quality (ANSI Approved), 2013.
[9] F. Causone, A. Moazami, S. Carlucci, L. Pagliano, M. Pietrobon, Ventilation strategies for the deep energy retrofit of a kindergarten, in: Proceeding 36th AIVC - 5th TightVent 3rd Venticool Conf., Madrid, 2015.
[10] D.B. Crawley, L.K. Lawrie, F.C. Winkelmann, W.F. Buhl, Y.J. Huang, C.O. Pedersen, et al., EnergyPlus: creating a new-generation building energy simulation program, Energy Build. 33 ,2001, 319–331. doi:10.1016/S0378-7788(00)00114-6.
[1] Presidente della Repubblica, Regolamento recante norme per la progettazione, l'installazione, l'esercizio e la manutenzione degli impianti termici degli edifici ai fini del contenimento dei consumi di energia, in attuazione dell'art. 4, comma 4, della L. 9 gennaio 1991, n. 10, in, Gazzetta Ufficiale della Repubblica Italiana S.O., DPR n. 412, 26/08/1993.
[12] ASHRAE, Guideline 14 - Measurement of Energy and Demand Savings, 8400, American Society of Heating, Refrigerating, and Air-Conditioning Engineers, 2002.
[13] M.F. Jentsch, P.A.B. James, L. Bourikas, A.S. Bahaj, Transforming existing weather data for worldwide locations to enable energy and building performance simulation under future climates, Renew. Energy. 55, 2013, 514–524. doi:10.1016/j.renene.2012.12.049.
[14] F.R. Met Office, Met Office Hadley Centre for Climate Science and Services, Met Off, http://www.metoffice.gov.uk/climate-guide/science/science-behind-climate-change/hadley (accessed October 29, 2015).
[15] S. Carlucci, Thermal Comfort Assessment of Buildings, Springer, London, 2013.
[16] S. Carlucci, L. Pagliano, A. Sangalli, Statistical analysis of the ranking capability of long-term thermal discomfort indices and their adoption in optimization processes to support building design, Build. Environ. 75, 2014, 114–131.[17] S. Carlucci, L. Pagliano, A review of indices for the long-term evaluation of the general thermal comfort conditions in buildings, Energy and Buildings, 53, 194-205, 2012.
[18] A. Sfakianaki, M. Santamouris, M. Hutchins, F. Nichol, M. Wilson, L. Pagliano, et al., Energy consumption variation due to different thermal comfort categorization introduced by European standard EN 15251 for new building design and major rehabilitations, Int. J. Vent. 10, 2011, 195–204.
[19] Pacheco Torgal F, Mistretta M, Kaklauskas A, Granqvist CG, Cabeza LF. Nearly Zero Energy Building Refurbishment: A Multidisciplinary Approach. London: Springer; 2013.

Paper II

Energy and Buildings 127 (2016) 1117–1132

Contents lists available at ScienceDirect

Energy and Buildings

journal homepage: www.elsevier.com/locate/enbuild

Energy retrofit for a climate resilient child care centre

Lorenzo Pagliano[a], Salvatore Carlucci[b], Francesco Causone[a], Amin Moazami[b,*], Giulio Cattarin[a]

[a] end-use Efficiency Research Group (eERG), Department of Energy, Politecnico di Milano, Via Lambruschini 4, 20156, Milano, Italy
[b] NTNU Norwegian University of Science and Technology, Department of Civil and Transport Engineering, Trondheim, Norway

ARTICLE INFO

Article history:
Received 5 November 2015
Received in revised form 25 April 2016
Accepted 29 May 2016
Available online 3 June 2016

Keywords:
Climate change
Climate change adaptation
Climate resilience
Energy retrofit
Future weather scenarios
Resilient building
Comfort models
Comfort categories
Long-term thermal discomfort indices
Energy need for heating or cooling

ABSTRACT

Climate scientists have developed and refined climate change models on a global scale. One of the aims of these models is to predict the effects of human activities on climate, and thus the delivery of information that is useful to devise mitigation actions. Moreover, if they can be properly downscaled to a regional and local level, they might be useful to deliver support for adaptation actions. For example, they may be used as an input for the better design of the features of buildings in order to make them resilient to climate modification, e.g., able to passively control heat flows to produce comfortable indoor conditions not only in the present climate, but also in future climate conditions. Taking into account the future weather scenarios that show an increase in the global temperature and climate severity, a likely consequence on building energy use will be a substantial shift from space heating to space cooling, and potentially uncomfortable thermal conditions during the summer will became a major challenge, both for new and existing buildings. In this paper, a deep energy retrofit of a child care centre located in Milan (Italy) is analysed on the basis of future weather scenarios; the analysis aims to identify to what extent choices that are made nowadays on the basis of a typical meteorological year may succeed to provide acceptable energy and indoor environmental performance throughout the future decades. The analysis confirms that climate change might require the installation of active cooling systems to compensate for harsher summer conditions over a long-term horizon, however, in the mid-term, passive cooling strategies combined with envelope refurbishment may still guarantee thermally comfortable conditions, and they will reduce energy cooling needs when active cooling is eventually installed.

© 2016 Elsevier B.V. All rights reserved.

1. Introduction

The average temperature of our planet is increasing rapidly. According to the analysis performed by NASA in 2015, the year 2014 was the warmest on record (since 1880), and this trend is expected to continue over the long term [1]. At the beginning of 2016, NOAA and NASA reported that 2015 was by far the hottest year on record globally. NOAA [2] also reported that "During December [2015], the average temperature across global land and ocean surfaces was 2.00 °F (1.11 °C) above the 20th century average. This was the highest for December in the 1880–2015 record, surpassing the previous record of 2014 by 0.52 °F (0.29 °C). The December temperature departure from average was also the highest departure among all months in the historical record and the first time a monthly departure has reached +2 °F from the 20th century average". The working groups of the Intergovernmental Panel on Climate Change (IPCC) have developed scenarios for both contaminant emissions and global warming [3,4]; these scenarios are able to describe the likely average global conditions in the future. However, local climate scenarios are required in order to design our built environment to be able to withstand future weather conditions. ASHRAE fundamentals 2009 states in Chapter 14: "The evidence is unequivocal that the climate system is warming globally (IPCC 2007). The most frequently observed effects relate to increases in average, and to some degree, extreme temperatures" [5]; and it reports the results obtained by Thevenard [6] according to which design condi-

Abbreviations: ASHRAE, American Society of Heating Refrigerating and Air Conditioning Engineers; CSI, Climatic Severity Index; CO_2, carbon dioxide; CDD, cooling degree-days; HDD, heating degree-days; GCM, general circulation model; GCSI, Global Climate Severity Index; HadCM3, UK Met Office Hadley Centre Coupled Model version 3; HVAC, heating ventilation and air conditioning; IAQ, indoor air quality; IPCC, Intergovernmental Panel on Climate Change; NASA, National Aeronautics and Space Administration; NOAA, National Oceanic and Atmospheric Administration (USA); TMY, typical meteorological year; TRY, typical reference year; IGDG, Italian climatic data collection "Gianni De Giorgio".

* Corresponding author.
E-mail address: amin.moazami@ntnu.no (A. Moazami).

http://dx.doi.org/10.1016/j.enbuild.2016.05.092
0378-7788/© 2016 Elsevier B.V. All rights reserved.

tions, heating degree days and cooling degree days were all found to have significantly modified values.

By adopting the *morphing* methodology presented by Belcher et al. [7], three different future weather scenarios were developed for the city of Milano, and the deep energy retrofit design of a child care centre [8,9] was assessed against them, in order to evaluate the building resilience to future local climate change.

2. Background

The Italian educational buildings stock consists of 52 000 buildings, of which about 63% were constructed before 1973 [10], the year of the first oil crisis, which provided the initial *stimulus* towards the introduction of energy efficiency targets in building regulations. The energy retrofit of such a large and old building stock, which is mostly owned by local governments, can yield significant improvements in energy efficiency (EE). Constructions from before the first Italian law on energy performance in buildings (Law n. 373/1976), especially in the 50′s and 60′s, are characterised typically by a very poor performance. Hence, the case study presented in this paper, the retrofit of a building that was constructed in the 80′s, might provide a conservative estimation of the energy savings that could potentially be obtained if a similar retrofit strategy were applied to buildings constructed between the 50′s and 70′s. However, also the envelope of the pre-retrofit child care centre, analysed here, presents a poor thermal performance, as indicated in Table 1.

Educational buildings capable of high energy performance have been built in the last decades, sometimes showing problematic issues on the side of thermal comfort (TC) and indoor air quality (IAQ) [11]. For example, higher ventilation rates in order to improve IAQ imply more energy use, and care in design and control is needed to find a sensible balance. A potential 'EE-TC-IAQ dilemma' in high-performance educational buildings in the Netherlands has been analysed through measurements and surveys and it is presented in [12].

Another challenge is that even high-performance buildings and zero-energy buildings are designed using current or historical data such as typical weather data files e.g. Typical Reference Year (TRY), Typical Meteorological Year (TMY) and, in the case of Italy, weather files of the Italian Climatic data collection "Gianni De Giorgio" (IGDG), all of which are based on weather data parameters measured in a time span of the order of twenty years in the past [13]. This results in a lack of analysis of the behaviour of those buildings during their lifetime where climate patterns might be significantly different from present and past patterns. In order to contribute in filling this gap, this paper focuses on the resilience assessment of a high-performance retrofit for a child care centre against future weather scenarios. To achieve this aim, in parallel to an analysis of energy performances, the long-term thermal discomfort indices proposed in the European standard EN 15251 [14] are used to assess the indoor thermal comfort conditions, and suitable climate severity indices have been applied to characterise the severity of a few future weather scenarios.

2.1. Climate severity

Phillips and Crowe [15] define climate severity as "an unfavourable aspect of climate that arises as a consequence of certain adverse climate elements, occurring either singularly or in combination, and persisting beyond some minimum duration and/or at an intensity above some critical threshold". It was also pointed out that "duration, frequency, extremes and variability are important statistics that should be considered part of any scheme that attempts to quantify the unfavourable aspects of climate" [15]. One of the first examples is the *Climatic Severity Index* (CSI) that was proposed by Markus et al. [16], which defines, by a single number on a dimensionless scale, "the stress placed on a building's energy system by any given climatic *stimulus*".

For the specific case of buildings, the climate severity can be expressed in various ways. A particularly simple way is by using the *Heating degree-days* (HDD) *index*, i.e. the cumulative number, computed over a year under 'representative' weather, of the products of a time interval (a day) and the sole positive difference between an outdoor reference temperature (below which a building needs to be heated[1]) and the outdoor air temperature. In case a conventional value for the *building balance-point temperature* is assumed, e.g., 18 °C in Europe and 65°F in the USA, the number of HDDs becomes independent of the features of the building and can be used as a concise description of the cold season climate; it is often used for climatic classification purposes in legislation [17]. The great diffusion of mechanical cooling systems fostered the definition of a similar index for the warm season, i.e. the *Cooling degree-days* (CDD). However, not all of the national legislations have included a classification of climatic zones for cooling needs [18]. The heating and cooling degree-days, based on a conventional choice of the building balance-point temperature, have the advantage of being independent from the specific building features and being easily available, see e.g., [19]. Caution should be used anyway, and one should check how the tabulated values are calculated for both the reference temperature and the time step for calculations (hourly, daily) [20], since these may differ from country to country. Moreover, degree-days cannot capture the dynamic effects due to solar irradiance (excluding the indirect effect on external temperature), which depend on many factors including the building's orientation, the window-to-wall ratio, the optical properties of the glazing systems (including fixed/movable solar shading devices), the thermal mass of the building etc. Thus, degree-day analysis can lead to large deviations when compared to energy simulations [21]. More detailed methods have been developed in order to include the building thermal dynamics during the whole year in a single value metric. For example, Burmeister and Keller [22] and Keller and Magyari [23] propose an ordinary differential equation for an energy balance of the indoor air temperature, which includes information on the thermal mass, the thermal transmittance of the external walls, the air change rate and the total solar energy transmittance of transparent elements, condensed into three parameters named the *generalised loss-factor*, the *time constant* and the *gain-to-loss ratio*. The equation also includes a building-specific meteorological function, which depends on the external air temperature, the solar irradiance on the façade and the gain-to-loss ratio. The model allows for the calculation of the free-running temperature of a room, and it helps when making decisions at an early-design stage, when it is still not possible or desirable to handle a large number of parameters. The objective is to "arrive at the lowest possible energy consumption of a room, construct it in a way, that its free-run-temperature[2] remains the most part of the year within the comfort range [. . .]. This strategy minimises not only the energy need but also the peak powers needed for heating and/or cooling" [23].

In recent years, an Italian research group led by Terrinoni developed a new index that tackles the climate severity of the summer season [18,24,25]. The proposed *Summer CSI* is determined from hourly calculations and takes into account the outdoor air

[1] This temperature is called the *building balance-point temperature* and it is defined as the value of the outdoor air temperature at which, for a specified value of indoor temperature (set-point), the total heat loss is equal to the free heat gain (from occupants, lights, sun etc.). The building balance-point temperature is a consequence of the functions and features of the building rather than just the outdoor weather conditions.

[2] Note of the authors: usually the *free-run-temperature* mentioned here is generally called *free-running temperature* in the literature.

Table 1
Description and properties of building envelope components in the pre- and post-retrofit configurations.

Building envelope component	Pre-retrofit (calculated) U-value, W/(m^{2}K)	Post-retrofit (design) U-value, W/(m^{2}K)
Roof	1.30	0.09
Vertical opaque wall	1.20	0.09
Window (glazing plus frame)	5.80	0.73
Floor (facing an unheated basement)	1.30	0.30

temperature, specific humidity and solar irradiation. The energy requirement for cooling a space is normalised with respect to the main characteristics of the building (geometrical dimensions, global thermal transmittance and thermal capacity), thus being independent from the characteristics of the building, and linearly dependent on the climatic variables.

In the study by Sánchez et al. [26], the climate severity metrics for winter and summer were assessed as the ratio between the heating or cooling energy needs of a certain building and the needs that the same building has in a reference site. The indices are functions of the heating or cooling degree-days and the mean accumulated global radiation over a horizontal surface. The methodology was developed in particular for assessing the influence of the *urban heat island* effect on a building's energy use. With a similar definition, Salmerón et al. [27] introduce the *Global Climate Severity Index*, combining the heating and cooling end-uses and weighting them in terms of primary energy and of carbon dioxide (CO_2) emissions.

2.2. Building resilience to future weather scenarios

The CSI and its following modifications were introduced to assess the performance of a building in the typical climate; however, as the consequences of climate change become more and more evident at a local level, the research interest now includes a medium-to-long-term perspective. Given the lifetime of a building, predictions show that it will experience substantial climatic change, and thus modelling for design and compliance to national guidance should be completed using both typical and future weather scenarios [28]. Although de Wilde and Tian [29] remarked that the HVAC systems are likely to be replaced every 15–20 years, a time span in which the gradual effects of climate change might not yet play a relevant role, this is only true for the generation components of those systems. Distribution and terminal devices usually have a longer life; the life of opaque and transparent building envelope elements are generally even longer, and the latter elements should, hence, be dimensioned to be able to perform their function in future climate scenarios.

Throughout the last decades, researchers have proposed various ways to assess how buildings will react to climate. As pointed out in [28], "the overwhelming majority of studies on the impact of climate change on buildings thus far look at relatively straightforward performance indicators: energy use for heating, energy use for cooling, and building overheating. Both energy uses are often combined into one figure for overall energy use, or annual carbon emissions".

Two main approaches can be followed, which could be denominated general and building-specific.

The former proposes indices that are not strictly related to the analysed building and rely on simple correlations and the global thermal performance parameters of buildings. For example, Burmeister and Keller [22] trace back the thermal behaviour of a room to three parameters: the generalised loss-factor (accounting for the heat losses through the envelope and the ventilation/infiltration rate), the time constant and the (solar) gain-to-loss ratio. The impact of these parameters can be studied without detailing, e.g. the stratigraphy of the opaque components or the optical properties of the transparent elements. The strength of this approach is evidently the attempt to gain early hints that can guide the pre-design phase of a building.

The latter focuses on the analysis of one or a few case studies or of ideal typical buildings, and it relies on dynamic thermal simulation to obtain yearly time series for present and future climate conditions. This approach needs a more detailed description of the building's characteristics, and thus it cannot be suitable in a pre-design phase. However, it can enable a deeper understanding of the thermal dynamics of specific parts of the analysed thermal system (meaning the building envelope and its services), and it may also offer insights to guide a generalisation process for a broader building stock. For example, Wang and Chen [30] analysed the change in the energy requirement for space cooling in buildings in 15 different US cities that are located in seven climate zones by the decade throughout the 2080s. In particular, the typical buildings in this study were an apartment, a hospital, a hotel, a single-family house, a small and a medium-sized office, a restaurant, a mall and a school.

Although these indices are mostly dedicated to assess energy use, they should always be accompanied by an indication of the thermal comfort levels that are expected to be experienced by the occupants, in particular when dealing with sensitive and fragile persons as e.g. handicapped, sick, very young children and elderly persons [31]. As reported in [28], "some work is emerging that suggests a need to study alternative or more refined metrics"; for example the work done by Lomas and Ji [32] that correlates resilience of passively cooled buildings to their life expectancy.

Thermal comfort assessments for the future climate cannot usually take into consideration the full spectrum of outdoor conditions, due to the inevitable inaccuracy of predictions. Probably one of the most complex thermal comfort-based index proposed so far is the *Climate Severity Index* by Murdock et al. [33,34], which comprises indicators for winter discomfort (wind chill, length of winter and severity of winter) and summer discomfort (Humidex, length of summer, warmth of summer, dampness), as well as psychological factors (darkness, sunshine, wet days and fog), hazards (e.g., strong winds, thunderstorms and snowfall) and outdoor mobility (e.g., restricted visibility). Evidently, this index was not intended to only be used for indoor thermal comfort assessments, and it has a more general focus on perceived 'weather-related' well-being. While offering a good attempt at a comprehensive evaluation of the impact of climate severity on personal thermal comfort, the index presents drawbacks, such as the need for very advanced weather predictions and the strong impact of weighting coefficients when combining factors in the global index.

In the field of indoor thermal comfort assessment, the general trend is to adopt long-term thermal discomfort metrics (e.g., [31]), such as indices that refer to thermal comfort models or simpler criteria that compute the number of hours outside certain fixed temperature ranges. In general, more than fifteen long-term thermal discomfort indices are available in literature and standards, and they can be grouped into four homogeneous categories: percentage indices, cumulative indices, risk indices and averaging indices [35]. Unfortunately, their assessment capabilities are not aligned and the selection of the index strongly influences the assessment [36]. In the present paper, the thermal resilience of a building under varying climatic conditions is evaluated by means of all-year,

Fig. 1. Southwest façade of the child care centre.

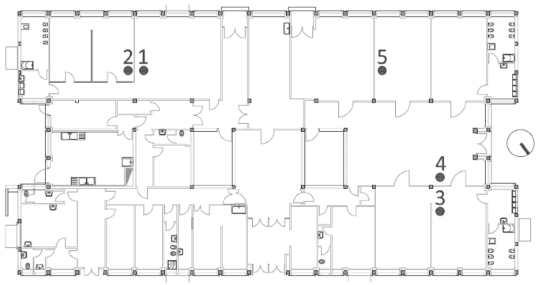

Fig. 2. Building plan view including the five monitored rooms.

whole-building, and dynamic simulations; and it is expressed in terms of:

- The energy need for space heating and cooling[3] under typical and future weather scenarios.
- The indoor operative temperature in free-running conditions under typical and future weather scenarios.

3. Case study: the comprehensive energy retrofit of a child care centre

The object of the analysis is a child care centre that is occupied by children who are 3–36 months old. It was built in the '80s in Milan, Italy [8,9]. It is a one-story building with a simple rectangular base (44 m long and 23 m wide); the longest sides are facing south-west and north-east (Figs. 1 and 2). Around 58% of the ground floor is dedicated to children activities, and the rest is used for staff and service areas. The building has: a gross floor area of 944 m^2; a net floor area of 855 m^2; a gross heated volume of 3422 m^3 and a shape factor (S/V) equal to 0.77 m^2/m^3.

The existing building is a typical heavy-prefabricated facility, made of precast concrete panels that include a thin layer of polystyrene foam. The U-value of the walls before the retrofit is estimated to be about 1.0 W/(m^2 K). After the retrofit the façade will be covered with prefabricated wooden modules. The modules are highly insulated (with approximately 35–38 cm of mineral wool) and include mechanical ventilation and automated solar shading devices. The U-value of the external walls after the retrofit will be in the order of 0.1 W/(m^2 K).

The existing roof is a pitched metallic plate with no insulation, placed upon a horizontal concrete slab (Predalles system). The metallic plate will be removed and a new insulation layer will be laid on the existing slab (approximately 38–40 cm of mineral wool). After the retrofit the U-value of the roof will be in the order of 0.1 W/(m^2 K).

The existing floor has been constructed using a precast concrete slab with a linoleum finishing. The whole floor is above a basement space that is not heated. An insulation layer 10 cm to 15 cm thick will be added to the side of the slab that is facing the basement in order to reach a U-value of 0.3 W/(m^2 K).

The existing windows are made of an air-filled double glazing unit, $U_g \approx 3$ W/(m^2 K), with aluminium frames without thermal breaks, $U_f \approx 6$ W/(m^2 K). In addition to the low thermal performance, the low airtightness of the existing windows causes a high infiltration loss. During the retrofit, new high-performance windows (with an overall thermal transmittance $U_w = 0.73$ W/(m^2 K)) will be integrated in the prefabricated façade modules.

A natural gas boiler for heating is currently installed in the child care centre in combination with metal radiators, whereas a connection to the local district heating system will be provided after the retrofit.

No mechanical ventilation system is currently available in the building, and the ventilation is accomplished by the manual operation of the windows. A new decentralised mechanical ventilation system coupled with highly-efficient double-flow heat recovery units with a nominal sensible recovery efficiency of 0.80 will be installed inside the prefabricated façade.

The building's indoor conditions were monitored from July 2014 to July 2015 (Figs. 3 and 4), and the building envelope was checked with an infrared thermal camera. During the Christmas holidays there was a large drop in the indoor temperature, and similar rapid temperature drops appeared over winter weekends and during the night-time when the heating system was off. This is evidence of the poor thermal features of the building envelope (Fig. 3).

CO_2 concentration was monitored in Room 4 (Fig. 4), which is a common space where children play and spend a large part of their time. Throughout August the building is unoccupied, therefore, the recorded average value of 400 ppm may be considered as the average background outdoor CO_2 level. After September, noticeable peaks have been recorded in the room, with values that substantially exceed the reference value of 700 ppm above the background level [39], i.e. beyond 1100 ppm. This evaluation should be made under steady-state conditions, however, the recorded peaks go far beyond the threshold, showing that the building needs a better ventilation strategy.

The amount of delivered energy[4] [37,38] to heat the space and produce hot water was gathered from energy bills for the heating seasons from 2008 to 2015, showing an average yearly value (normalised with respect to the net floor surface of the treated zones) of 130 kWh/(m^2 a) for heating and 30 kWh/(m^2 a) for hot water. Delivered energy for heating shows considerable variations from year to year as a function of the different climate severities. The delivered energy in the form of electricity for the seasons from 2012 to 2014 was on average 35 kWh/(m^2 a).

The data for the delivered energy, derived from the bills and the indoor environment monitoring data, are coherent with the low

[3] The *energy need for heating or cooling* is defined in EN ISO 13790 [37]. and EN 15603 [38] as "heat to be delivered to, or extracted from, a conditioned space to maintain the intended temperature conditions during a given period of time".

[4] *Delivered energy* is defined in ISO 13790 [37] and EN 15603 [38] as "energy, expressed per energy carrier, supplied to the technical building systems through the system boundary, to satisfy the uses taken into account (heating, cooling, ventilation, domestic hot water, lighting, appliances etc.) or to produce electricity".

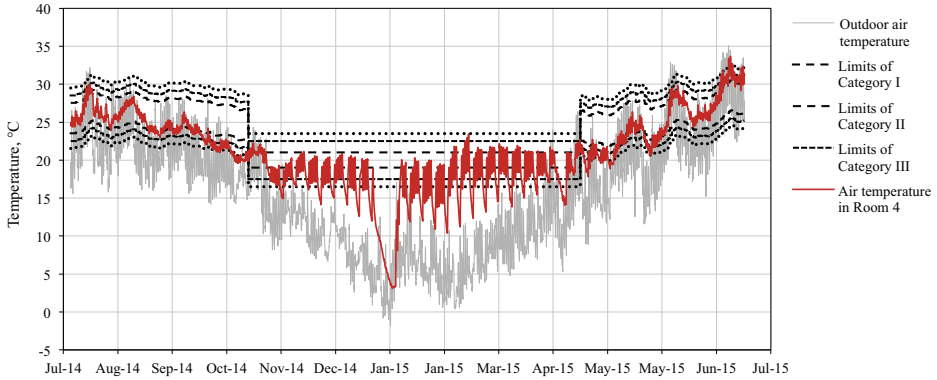

Fig. 3. Outdoor air temperature and indoor air temperature in Room 4 (used as a proxy of the operative temperature) compared to the operative temperature ranges for comfort categories according to standard EN 15251.

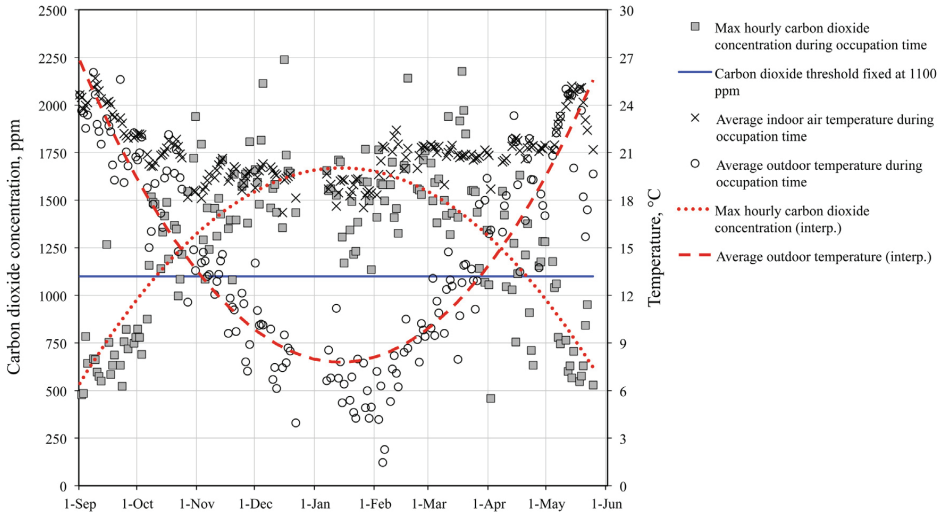

Fig. 4. For each day: maximum hourly CO_2 concentration level in Room 4 during occupation hours; indoor and outdoor air temperature values averaged over the occupied hours.

thermal performance of the existing building envelope components (Table 1) and heating and lighting systems; furthermore, no solar control strategy has been implemented in the existing building, and this clearly contributes to overheating during the hot periods. Finally, the child care centre shows poor ventilation management and a potential low level of indoor air quality (IAQ).

The energy retrofit strategy was, therefore, defined by means of an integrated design process involving the architects of the Municipality of Milan and the authors, which analysed existing constraints and targeted the following goals:

- Reducing the energy need for space heating.
- Reducing all of the energy uses by improving the efficiency of the building's systems.
- Adopting passive strategies for cooling whenever possible, while avoiding the installation of active cooling systems.
- Installing new grid-connected renewable energy generation systems.
- Improving IAQ by installing highly-efficient decentralised ventilation systems, and by implementing an effective ventilation strategy.
- Ensuring adequate thermal comfort conditions all-year long.
- Reducing construction time to limit the disturbance or interruption of the educational service.

4. Methodology

Building performance simulation is a powerful technique to support not only the design of a new building, or the refurbishment of an existent one, but also in the operation, diagnostics, commissioning and evaluation of the building's performance. In this work, simulation has been used to compare various energy saving measures and refurbishment options in order to guide the definition of the energy concept.

A numerical model of the existing building was created and calibrated against measured delivered energy and indoor air temperatures, then used to define the refurbishment concept of the building, and finally to estimate the performance of the renovated

building under typical and future weather scenarios in free-running and conditioned modes.

4.1. Numerical model calibration

Building performance simulation tools are increasingly versatile and are able to implement a considerable number of physical models and several numerical resolution schemes. Their potential for delivering useful forecasts of energy and comfort performances is only tackled through skilled modelling choices and an accurate calibration process. Indeed, the building performance simulation models that are not calibrated or calibrated only based on a single benchmark such as energy use or indoor air temperature, can be significantly unreliable [40]. Calibration is a process where the results of a simulation are compared with measured data to improve the agreement of the simulation outcomes with respect to a chosen set of benchmarks through the adjustment of independent parameters that are implemented in the building model. Though calibration is fundamental, at present there are no internationally-agreed requirements for evaluating the goodness-of-fit of a building energy model, but a few recommendations have been proposed in guidelines, such as the ASHRAE Guideline 14 [41]. The guideline introduces three basic methods to estimate energy use and savings that result from the efficiency measures: the whole building approach, the retrofit isolation approach and the whole building calibrated simulation approach (calibrated simulation). The latter approach considers using simulation programs for the energy modelling of pre- and post-retrofit buildings. The proposed set-up for the calibration by ASHRAE is:

1. Produce a calibrated simulation plan.
2. Collect data from the field.
3. Create a numerical model of the building.
4. Compare simulation model output to measured data.
5. Refine model until an acceptable calibration is achieved.
6. Produce baseline and post-retrofit models.
7. Estimate savings.
8. Report on observations and savings.

The ASHRAE Guideline 14 uses two indices to evaluate the goodness-of-fit of the building energy model: the Mean bias error, *MBE*, and the Coefficient of variation of the Root mean square error, *CV*(*RMSE*).

MBE is a non-dimensional measure of the overall bias error between the measured and simulated data in a known time resolution, and it is usually expressed as a percentage:

$$MBE \equiv \frac{\sum_{i=1}^{N_p}(m_i - s_i)}{\sum_{i=1}^{N_p} m_i}\,[\%] \tag{1}$$

where m_i ($i = 1, 2, \ldots, N_p$) are the measured data, s_i ($i = 1, 2, \ldots, N_p$) are the simulated data at time interval i and N_p is the total number of the data values.

CV(*RMSE*) represents how well the simulation model describes the variability in the measured data. It is defined as:

$$CV\,(RMSE) \equiv \frac{1}{\bar{m}}\sqrt{\frac{\sum_{i=1}^{N_p}(m_i - s_i)^2}{N_p}}\,[\%] \tag{2}$$

where, besides the quantities already introduced in Eq. (1), $\bar{m}$ is the average of the measured data values.

The evaluation of the accuracy of a building energy simulation model is made according to the model's conformity with the recommended criteria for *MBE* and *CV*(*RMSE*). According to the ASHRAE Guideline 14, the simulation model is considered calibrated if it has MBE that is not larger than 5%, and *CV*(*RMSE*) that is not larger than 15%, when the monthly data are used for the calibration, and MBE not larger than 10% and *CV*(*RMSE*) not larger than 30% when the hourly data are used for the calibration.

In the present work, in order to get a reliable building energy model, and to increase the accuracy of the estimation of the building's performance, the pre-retrofit model of the building underwent two subsequent calibrations. The building model was first calibrated on the basis of the building's measured monthly energy use for heating in conditioned mode, then it was refined in free-running with a second calibration with respect to monitored hourly indoor air temperatures in a selected thermal zone of the building (Room 4). In both calibrations the input weather file for the simulations was constructed by collecting and formatting the data of a weather station in Milano-Bovisa that is in a similar position with respect to the city centre. The weather data were recorded during the same time-interval of the monitored data for the energy use and indoor temperature.

The calibration process requires the identification of those input variables that, at the same time, are affected by uncertainty and can significantly impact on the chosen benchmark. Then, a scale of variation has to be identified for each of them according to the boundary conditions. Table 2 reports the five input variables, the scale of variation and the step size tested in the first calibration.

In order to identify the independent variables that, at the same time, influence the energy and thermal performances of the building and that are mostly affected by uncertainty, we referred to Hopfe [42], who identified through a sensitivity analysis the most influencing variables on both energy performance and thermal discomfort. However, in the present case study of calibration: the room size is fixed and it is not a design variable; the type of windows, the power density of the electric equipment and electric lighting and the number of occupants in the building have been precisely quantified with surveys and an energy audit, and hence they are not sources of significant uncertainty [8]. Therefore, the calibration process focused on testing independent variables that describe infiltration rates, the thickness of the insulating layer of opaque envelope components and, we also added, the global seasonal efficiency of the heating system. As for air infiltration, the ranges of variation of the flow coefficient and flow exponent were set according to the values reported in Tables A1, A2 and A3 of Annex A. The thickness of the insulating layer was based on geometric constraints due to the entire thickness of the components, which were measured during the energy audit. Finally, the range of variation of the global seasonal efficiency of the heating system was deduced from calculations based on the Italian standard UNI TS 11300-2 [43] according to the components that are actually installed in the building. Table 2 presents the independent variables, their range of variation and the step size used in the monthly energy calibration.

According to the calibration problem described in Table 2, a problem space of 1875 building variants was investigated.

The second calibration inherited the model from the first calibration, and it was based on the air temperature monitored in Room 4 (Fig. 2) from the 15th May to the 15th July. This period was specifically chosen because the pre-retrofit building was in free-running from the 15th April to the 15th October. Also in the designed post-retrofit model, the building is assumed to be in free-running from the 15th April to the 15th October. Three input variables were chosen. Table 3 shows the independent variables, the range of variation and the steps adopted in the second calibration based on hourly temperatures.

The indoor air temperature is used as the control parameter for the control strategies of the solar shading and window opening devices, since in the pre-retrofit situation both adaptation possibilities are manually operated by the teachers on the basis of their personal feelings about the indoor thermal condition. The range of the variations was deduced from the analysis of the monitored data.

Table 2
Input variables for calibration based on monthly values of delivered energy.

Source of uncertainty	Independent variables (unit of measure)	Range of variation
Air-leakage of joints between building envelope components	Flow coefficient ($kg\,s^{-1}\,m^{-1}$ crack @ 1 Pa) Flow exponent (non-dimensional)	{Very poor, Poor, Medium}[a]
Insulation thickness	Wall insulation (cm) Roof insulation (cm) Floor insulation (cm)	{1, 2, 3, 4, 5} {1, 2, 3, 4, 5} {1, 2, 3, 4, 5}
Heating system	Global seasonal efficiency (%)	{45, 49, 53, 57, 61}

[a] See Annex A for the specific values of Flow coefficient and Flow exponent implemented in the simulations.

Table 3
Input variables for calibration based on the hourly indoor measured air temperature in Room 4.

Source of uncertainty	Independent variables (unit of measure)	Range of variation
Control strategy of solar shading devices	Indoor air temperature (°C)	{22, 23, 24, 25, 26}
Control strategy of window opening	Indoor air temperature (°C)	{22, 23, 24, 25, 26}
Occupancy	Number of occupants in Room 4 (people)	{20, 25, 30, 35, 40}

The number of occupants in Room 4 is affected by a wide day-by-day variability; hence, from a survey of the building staff and from the analysis of the measured CO_2 concentrations, the daily values were deduced and used as the range of variation in the calibration process.

According to the calibration problem described in Table 3, a problem space of 125 building variants was investigated.

4.2. Future weather scenarios

The Special report on emission scenarios (SRES) of IPCC working group 3 provides four storylines followed by four scenario families for the future climate, and IPCC working group 1 developed *General Circulation Models* (GCM) as tools for simulating the response of the global climate system to the increase of greenhouse gas concentrations [4]. The combination of GCMs and SRES scenarios are used to predict the future climate. Each storyline considers different future directions. They cover a variety of future characteristics such as social, economical and technological changes. In this paper, we adopted the approach presented by Jentsch et al. [44], who developed a tool called *CCWorldWeatherGen* that provides hourly future weather data that is suitable for building performance simulation. The calculation principles of this tool are based on the A2 emission scenario developed by SRES, the *UK Met Office Hadley Centre Coupled Model version 3* (HadCM3) [45] and a downscaling method called *morphing*, proposed by Belcher et al. [7]. HadCM3 is one of the major GCMs that supports the IPCC reports, and the combination of this model with the A2 emission scenario is one of the most widely used combinations in climate predictions [13]. The A2 represents a very heterogeneous world with continuously increasing global population, regional economic development and technological change that is fragmented and slower than in other scenarios. This scenario has a continuous increase in greenhouse gas emission that causes the increase of temperature with best estimate of 3.4 °C at 2090–2099 relative to 1980–1999 [46].

The morphing method allows to downscale the monthly mean predicted data that is created, in this case by HadCM3, to a future hourly weather data, by applying three transforming functions on a 'baseline' hourly weather data file, e.g., a typical meteorological year (having TMY or other equivalent format): shifting, stretching and the combination of shifting and stretching.

Shifting is used when the climate change scenario requires an absolute change to the mean. It has an additive formulation and it adds the HadCM3 predicted absolute monthly mean change (Δx_m) to the TMY hourly data (x_0):

$$x = x_0 + \Delta x_m \tag{3}$$

Shifting is, for example, used to adjust atmospheric pressure.

Stretching has a multiplicative formulation and scales the TMY hourly data (x_0) by a HadCM3 predicted relative monthly mean change (α_m). α_m is a fractional change between the future monthly values and the existing TMY data according to HadCM3.

$$x = \alpha_m x_0 \tag{4}$$

Stretching is used, for example, when there is a change to either the mean or the variance. The *combination of shifting and stretching* is a linear combination of the two previous transforming functions:

$$x = x_0 + \Delta x_m + \alpha_m \left(x_0 - x_{0,m}\right) \tag{5}$$

The *combination of shifting and stretching* is used when the *morphing* has to be applied to both the mean and the variance of the hourly weather data, for example, in the case of temperature shift, by adding the HadCM3 predicted absolute monthly mean change, it is stretched by the monthly diurnal variation of this parameter. More detailed information is available in Ref [7].

In our case a typical weather data file from Milano-Linate from the Italian Climatic data collection "Gianni De Giorgio" (IGDG) was downloaded from Ref. [47] and used as a baseline. The above method was applied on this file to obtain hourly weather data for the three future scenarios in the years 2020, 2050 and 2080. For each scenario, the cooling potential of night natural ventilation was evaluated by calculating the number of summer night hours when the outdoor air temperature falls below 20 °C. Moreover, the HDD and CDD values were calculated and compared to evaluate the severity of the different scenarios (Table 4).

4.3. Set-up of the building energy simulations

The dynamic energy simulation of the building was performed using the software EnergyPlus [48], version 8.3.0.1. Each released version of EnergyPlus undergoes two major types of validation tests [49]: analytical tests, according to ASHRAE Research Projects 865 and 1052, and comparative tests, according to the ANSI/ASHRAE 140 [50] and IEA SHC Task34/Annex43 BESTest method. The building model was set-up with the aim to reproduce the actual geometry of the building in detail, and the algorithms were selected, among the ones available within EnergyPlus, with the aim

Table 4
Comparison of the climate severity of the typical and future weather scenarios and assessment of the cooling potential of night natural ventilation.

	Weather scenario			
Parameter (unit of measure)	IGDG	2020	2050	2080
$HDD_{20\,°C}$ (°C h)	3002	2718	2384	1988
$CDD_{26\,°C}$ (°C h)	3	26	116	289
Night hours when outdoor air temperature is below 20 °C (h)	468	368	266	168

to represent physical phenomena as accurately as possible, to the expense of computing time.

In detail, the update frequency to calculate sun paths was set to 1 day. The heat conduction through the opaque envelope was calculated via the finite difference method with a 3-min time step [51]. The natural convection heat exchange coefficient near the external and internal surfaces were calculated via the adaptive convection algorithm [52], to meet the local conditions of each surface of the model. We chose an initialisation period of 25 days, rather than the default value of seven days, to reduce the effect of the thermal initialisation of the model. The voluntary ventilation and involuntary air infiltration were calculated with the *AirflowNetwork* module to better estimate the contribution of natural ventilation due to both infiltration and opening of the windows.

Two sets of simulations were carried out. During the first set, the model was simulated in free-running mode to assess the performance of the building envelope by itself, and passive strategies in the typical (IGDG) and in the future climates. Then, the second set was simulated adding to the model an ideal active system which ensures that indoor operative temperature is maintained at the chosen winter and summer set-point temperatures during occupation hours. According to the Italian law [17], in Milan, the heating season ranges from the 15th October to the 15th April. No indication is provided by legislation on the length and start date of the cooling season. Following the analysis and suggestions in [53], the authors decided to use the period from the 15th May to the 30th September as the 'summer' period, this being the time interval in which the 15-day mean sol-air temperature is higher than the summer set-point temperature. Furthermore, the building was considered unoccupied during all national holidays, weekends, and during August due to the summer vacation, according to the actual schedule.

In the pre-retrofit model used for the monthly energy calibration, the heating set-point for the indoor air temperature was set to 21 °C according to the data gathered from the building survey.

In the post-retrofit model used in a conditioned mode for the climate resilience assessment, (i) the heating set-point for the indoor air temperature was set to 20 °C according to the requirement set by the Italian law DPR 412 [17], and (ii) the cooling set-point for the indoor operative temperature was set to 24 °C, taking as reference Table A3 of EN 15251; the rationale for this choice is discussed in the next paragraphs.

There is ample debate and continuous progress on thermal comfort models and their implications on building design, which eventually will translate into a further revision of the standards (both EN and ASHRAE). Among the open issues one might list:

- The Fanger model was derived on the base of a necessary condition of thermal balance and additional conditions, namely two correlations, obtained by observing subjects in thermal comfort. One correlation relates mean skin temperature and activity level, and the second relates evaporative heat loss and metabolic activity. The two correlations were derived by analysing data regarding American college-age subjects in controlled climate chamber (no quantitative correlation index was given) and later compared with similar experiments involving 128 Danish college-age subjects with a mean age of 23 years and 128 elderly subjects with a mean age of 68 years. Specific data regarding small children were not part of the dataset [54]. Therefore, van Hoof [55] underlines that "the PMV model applies to healthy adult people and cannot, without corrections, be applied to children, older adults and the disabled". Some studies that have been published recently deal with the comfort perception and preference by children attending kindergarten or primary school [56–59]. In general, they point to a possible lower acceptance of warm conditions by children compared with adults, but the conclusions are based on various methodological attempts to translate the ASHRAE comfort sensation questionnaire in terms and images accessible to children (hence potentially affected by some semantic distortion) and on corrections to take into account differences in metabolic rate and body area between children and adults. The need for further research is proposed in the cited papers, and none of them reports evaluations on children 3–36 months old.
- From statistical analysis of the recognised international thermal comfort survey databases (ASHRAE RP-884 database, SCATs the *Smart Controls And Thermal Comfort database*, BCC *Berkeley City Center project database*), some researchers have suggested that the EN 15251 category I, ranging between PMV values −0.2 and +0.2 (which is called category A in ISO standards), might be too narrow to actually be perceived by subjects [60]. The authors conclude that: "In an analysis of high-quality field studies, the three classes do not exhibit different comfort/acceptability outcomes. The tightly air-temperature-controlled space (class A) does not provide higher acceptability for occupants than non-tightly air-temperature-controlled spaces (class B and C)."
- On the same issue of the operational significance of Category A, Alfano et al. [61] performed an analysis of uncertainty based on error propagation assuming the sensors accuracy required by EN ISO 7726. They conclude that: "the PMV range required by A-category can be practically equal to the error due to the measurements accuracy and/or the estimation of parameters affecting the index itself [62]; as a matter of fact, the errors accepted by EN ISO 7726 in terms of required accuracy give large errors in the PMV value, as in Fig. 2". The cited Figure does indeed report uncertainties in the PMV value of the order of 0.8–1.1, that is comparable with the widths of the two widest categories: Category II and III defined respectively by the limits $-0.5 < PMV < +0.5$ and $-0.7 < PMV < +0.7$.

One consequence of this debate might have been the fact that in EN 15251 the Category I, rather than being implicitly proposed as the one of highest comfort levels as in ISO 7730, has been proposed for "very sensitive and fragile persons with special requirements like handicapped, sick, very young children and elderly persons" [63]. However, no statistical analysis is proposed in EN 15251 to support the applicability of Category I to sensitive and fragile people.

While a deeper understanding about comfort categories and children thermal sensations and expectations is being developed, in everyday practice a designer has anyway to choose a reasonable set point during the warm season. A national design value for the cooling set-point is not available in Italy; the value of 24.0 °C for indoor operative temperature was adopted for this analysis. This value was chosen taking into account Table A2 of EN 15251 entitled

Recommended indoor temperatures for energy calculations, which recommends indoor temperature be in the range 22.5–24.5 °C for kindergartens in Category I, assuming clothing insulation of 0.5 clo and a metabolic rate of 1.4 met correspondent to standing-walking activity.

4.4. Thermal comfort assessment of the post-retrofit building model

A few long-term thermal discomfort indices proposed by the EN 15251 are used to assess the performance of the post-retrofit building model operated in free-running mode. Specifically, the Percentage outside the range method and the Degree hours criterion are suitable to that purpose. The former provides a quantification of the fraction of time during which the indoor operative temperatures exceed the given thresholds that depend on the chosen comfort category. This index is symmetrical, i.e. it measures both overheating and undercooling occurrences. The Degree hours criterion provides a quantification of the magnitude of the overheating phenomenon by summing over the considered period, for each occupation hour, the product of time and the temperature difference of the indoor temperature from the upper temperature limit of the chosen comfort category. This index is asymmetrical, i.e. it measures only the magnitude of overheating occurrences. For a more detailed description of the indices refer to Ref [35].

In the case where the post-retrofit building model is conditioned, an ideal system provides all of the energy needs required to meet the winter and summer set-point temperatures. The performance of the building in the typical and future climate scenarios is assessed using as a metric the energy need for heating and cooling (that is the energy to be delivered to the conditioned spaces in order to meet the thermal comfort conditions specified in Section 4.3).

5. Results and discussion

First, the results of the calibration of the numerical model are presented to show the reliability of the subsequent analyses. Then, the thermal behaviour of the post-retrofit building model in free-running mode under typical and future weather scenarios is proposed in order to assess how long the building might be operated in a purely passive way without affecting the thermal comfort conditions of the occupants. These results also highlight the evolution of the building's passive behaviour in future weather scenarios, where, progressively, the summer overheating issue will become dominant. Since the results show that the building cannot rely solely on passive strategies (currently because of space heating, and in the future also because of space cooling), the energy need for heating and cooling the building is calculated assuming that the building is in a fully conditioned mode. These analyses show how the energy need for space heating and cooling will probably vary in future scenarios, implying significant challenges for designers and building managers.

5.1. Calibration of the pre-retrofit building model

The pre-retrofit model was calibrated in order to provide reliable simulation outcomes. Two calibration processes were carried out in order to increase its estimation accuracy. Specifically, the model was first calibrated on the basis of measured monthly delivered energy for heating in a conditioned mode, then the best building variant after the first calibration was refined further by a second calibration, where it was operated in a free-running mode. The benchmark of the second calibration was the hourly indoor air temperature that was measured in Room 4.

The results of the first calibration are: *MBE* and *CV*(*RMSE*) of the monthly delivered energy over the calibration period (year 2014) for the pre-retrofit model are equal to 3.7% and 11.6%, respectively, hence the model satisfies the criteria recommended by the ASHRAE Guideline 14 for the monthly data.

Then, the final combination of the best values for the independent variables provided values of *MBE* and *CV*(*RMSE*) equal to 0.8% and 4.2%, respectively. Therefore, the model can be considered calibrated according to the ASHRAE Guideline 14. Table 5 reports the values of the independent variables resulting form the calibration process. Table 1 summarises the thermal performance of the building elements of the calibrated building model.

Fig. 5 depicts the comparison between the simulated and the measured indoor air temperature in Room 4.

The calibrated model of the pre-retrofit building reproduces the general thermal behaviour of the actual building with a good agreement, and it catches the main peaks. It is characterised by slightly wider fluctuations and a more rapid variation of the indoor air temperature as a consequence of sudden changes in the outdoor air temperature than the actual building. This can partly be explained by the lower thermal inertia considered in the model compared to reality, since furniture and equipment were not modelled. After the second calibration, the refined model is used as a baseline to support the design of the retrofit and create the post-retrofit building model.

5.2. Performance of the post-retrofit building model under current and future weather scenarios

After calibrating the pre-retrofit model, the post-retrofit model of the building was built and simulated under typical (IGDG) and future weather scenarios. The performance of the post-retrofit building was evaluated by first assuming that the building is operated in free-running mode by evaluating the long-term thermal discomfort indices that are proposed by EN 12521 (the *Percentage outside the range method* and the *Degree hours criterion*), then in conditioned mode by calculating the energy needs for heating and cooling.

5.2.1. Post-retrofit model simulated in free-running mode

The building has been simulated in free-running mode, i.e. keeping both the heating and the cooling systems off for the whole year. The internal gains, i.e. the heat produced by the occupants and the internal electrical loads for lighting and appliances, are taken into account in the simulations. The obtained results provide information on the periods in which the building might potentially work in free-running mode, and the frequency and intensity of overheating throughout the whole year.

Fig. 6 shows, only for the hours when the school is occupied, the indoor operative temperatures in the building (averaged over all of the occupied zones) obtained by simulation using the IGDG weather file and the weather projections for 2020, 2050 and 2080, which were plotted against the running mean of the external temperature[5] over the entire year. The hourly indoor operative temperatures are compared to the EN 15251 comfort thresholds for Categories I, II and III for the warm period of the year.

As discussed in the previous parts of this paper, the child care centre is occupied by children who are 3–36 months old and the information on thermal comfort for this age range is scarce and it has not yet been incorporated into thermal comfort models. Hence the data obtained for the simulations over the IGDG and future

[5] The *running mean of the external temperature* is defined in EN 15251 as the "exponentially weighted running mean of the daily mean external air temperature" [14].

Table 5
Values of the independent variables that characterise the calibrated building variant.

Source	Independent variables (unit of measure)	Scale of variation	Best value
Air-leakage of joints between building envelope components	Flow coefficient (kg s^{-1} m^{-1} crack @ 1 Pa)	{Very poor, Poor, Medium}	Poor
	Flow exponent (non-dimensional)		
Insulation thickness	Wall insulation (cm)	{1, 2, 3, 4, 5}	2
	Roof insulation (cm)	{1, 2, 3, 4, 5}	2
	Floor insulation (cm)	{1, 2, 3, 4, 5}	3
Heating system	Global seasonal efficiency (%)	{45, 49, 53, 57, 61}	53
Control strategy of solar shading devices	Indoor air temperature (°C)	{22, 23, 24, 25, 26}	24
Control strategy of window opening	Indoor air temperature (°C)	{22, 23, 24, 25, 26}	25
Occupancy	Number of occupants in Room 4 (people)	{20, 25, 30, 35, 40}	25

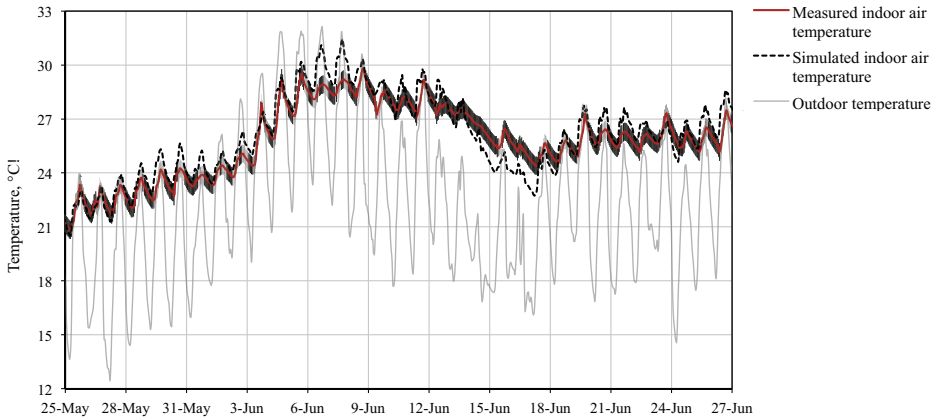

Fig. 5. Comparison of the simulated and monitored indoor air temperatures in Room 4. The shaded area represents a measurement uncertainty of ±0.5 °C.

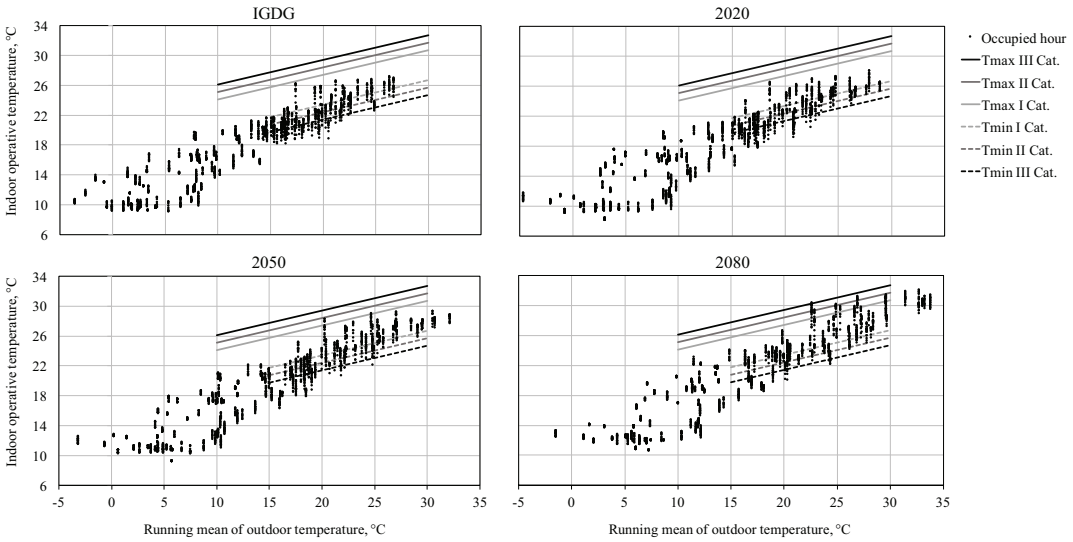

Fig. 6. Indoor hourly operative temperature versus the running mean of daily outdoor temperature with the building operated in free-running mode, under typical (IGDG) and future weather scenarios (2020, 2050, 2080).

weather scenarios are not only compared to Category I suggested in EN 15251 for "very sensitive and fragile persons" [14], but also to the other two categories.

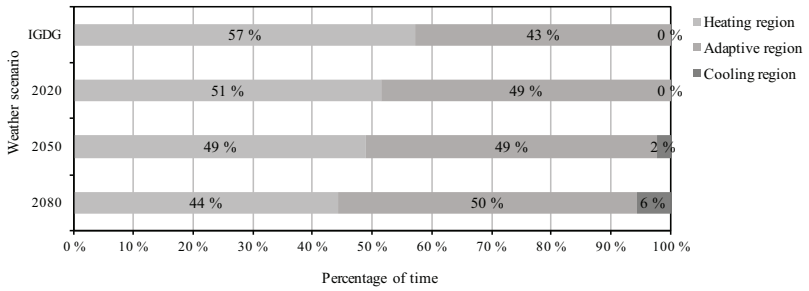

Fig. 7. Percentage of time over the entire year when the running mean of the outdoor temperature falls into the region where the European adaptive comfort can be used, into the active heating region and into the active cooling region.

According to the simulations, the energy concept developed for the retrofit of the building works quite well with respect to overheating during the summertime in the typical weather file (IGDG) scenario and under a near future scenario (2020); whereas the indoor temperature is outside the upper thresholds of the comfort categories in the 2050 and 2080 scenarios, but only for a few hours. However, when considering both the upper and lower thresholds, the amount of hours when the indoor operative temperature is outside the adaptive comfort categories is quite large. In order to quantify this behaviour, Fig. 7 shows the percentage of hours when the running mean of the outdoor temperature falls inside or outside of the range of the running mean of the outdoor temperature where the EN adaptive comfort model is applicable. Three regions are identified in this way: a heating region where the running mean of the outdoor temperature is lower than 15 °C, an adaptive region where it is between 15 and 30 °C, and a cooling region where it is higher than 30 °C.

The simulations under the future scenarios show a significantly important reduction in the hours when active heating is required (44% of time in 2080 compared to 57% in IGDG scenario), and an interesting expansion of the period when the EN adaptive comfort model can by applied (50% in the 2080 scenario versus 43% in the IGDG scenario). Finally, the 2050 and 2080 scenarios show that in 2% and 6% of the occupied hours, respectively, the running mean of the outdoor temperature falls outside of the domain of the adaptive model on the upper side. During this time the EN adaptive comfort model cannot be used any more, and an active cooling system should be used to ensure thermal comfort conditions. Therefore, PMV has to be used again, according to EN 15211, with a consequent problem in the discontinuity of design implications and temperature set-points, as already discussed in Ref. [64].

Free-running indoor conditions change considerably in future climates, as shown in the cumulative distribution of the indoor operative temperatures that are presented in Fig. 8.

Focusing on the summer period, defined here as ranging from the 15th May to the 30th September, Fig. 9 shows the outcome of the Percentage Outside of the Range Method, which quantifies to what extent the average indoor operative temperature falls within the boundaries of the EN 15251′s comfort categories during occupied hours.

It might appear surprising that the percentage of the occupied hours when the indoor operative temperature falls inside Category I significantly increases (from 35% to 74%) in the future weather scenarios. However, since the Percentage Outside of the Range Method is a symmetric long-term thermal discomfort index, it records both the occurrences due to overheating and those due to undercooling. In order to better understand the source of thermal discomfort, the frequency of overheating and undercooling referring to all of the three comfort categories are represented separately in Fig. 10.

Limited to the climate of Milan, during the summertime and with the post-retrofit building being operated in free-running mode, when the indoor operative temperature falls outside of a given comfort category, in most of the cases, the cause of the thermal discomfort is due to undercooling, defined as the condition when the indoor operative temperature is below the lower limit of a given comfort category. Only in the 2050 and 2080 scenarios, and with respect to Category I and II, the occurrence of indoor operative temperatures that are above the upper limit of those comfort categories are found as the source of thermal discomfort for a maximum of 5% of the occupied hours. If a designer were to try to optimise the building using this index under the IGDG scenario, he/she might be brought to select, for example, a configuration of the envelope with a lower performance than considered here (in order to shift all of the indoor temperatures during the summer upwards, under the IGDG scenario). This would have the drawback of increasing the risk and occurrence of overheating when the weather evolves to a warmer configuration in the future, as noticed in [64]. Symmetry of comfort category is reported in both EN 15251 and ASHRAE 55, but it seems to be more of a result of assumptions [65], than the outcome of statistical analyses. Indeed, a certain deviation from symmetry in thermal preferences was already found by Nicol and Humphreys [66]. Furthermore, one might argue that overcooling might be easier to manage than overheating, via adaptations in clothing in the first hours of the morning, and, in this particular building, by adopting a finer control of the night cooling ventilation.

Fig. 11 shows the intensity of the deviation quantified by the degree hours criterion proposed by EN 15251. It is an asymmetrical index, since it cumulates only degree hours of exceedance above the upper threshold of a given comfort category (during the summer) or it cumulates only the degree hours of exceedance below the lower limit of a given comfort category (during the winter).

According to the simulations and the assumed morphing transformation of the weather, the post-retrofit building model performs considerably well in the summer conditions, and, even in 2080, the overheating issues appear to be limited with only a few occurrences in July. However, it should be considered that the thermal discomfort is assessed using the adaptive comfort model, thus the lower and upper temperature thresholds vary according to the running mean of the outdoor temperature, which is rising in future weather scenarios, i.e. 2020, 2050 and 2080. However, the improvements of the thermal comfort models are outside of the scope of this paper. As for the long-term indexes, our analysis suggests that care should be taken in using the symmetric indexes, since focusing on overcooling in the present weather might make the building less resilient to overheating in the future climate conditions. This reinforces the need to verify if the assumption of symmetry of the thermal comfort categories with respect to the optimal comfort

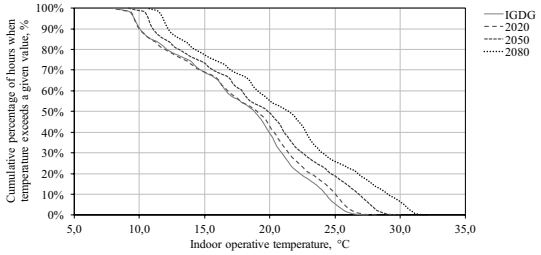

Fig. 8. Cumulative representation of hourly values of indoor operative temperature (averaged over all occupied zones) of the entire year, for post retrofit model in free-running mode in the four weather scenarios.

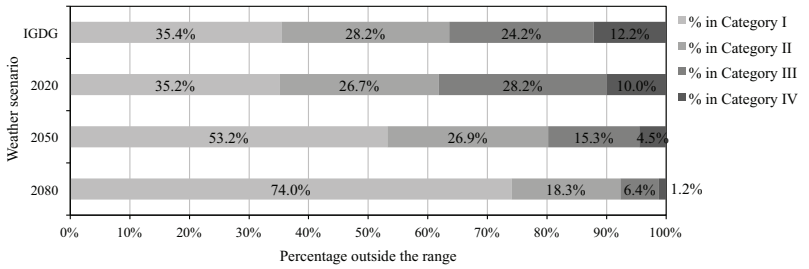

Fig. 9. Thermal comfort footprint representing the percentage of occupied hours indoor when the average operative temperature is within the boundaries of the comfort categories proposed by EN 15251 under the IGDG and the future weather scenarios for the post-retrofit building model in free-running mode in the period from 15th May to 30th September.

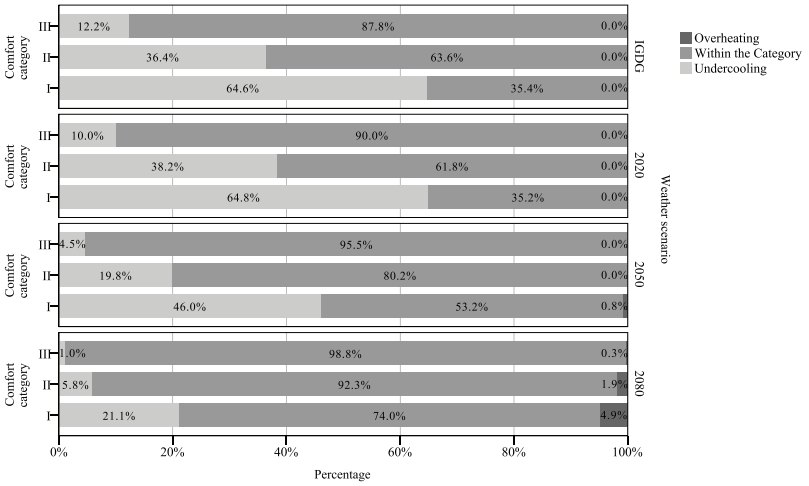

Fig. 10. Percentage of hours with overheating or undercooling occurrences referred to the adaptive comfort categories I, II and III under IGDG and future weather scenarios for the post-retrofitted building model in free-running mode.

temperature is reliable, or if amendments might be required on this point.

Even with a high-performance envelope and well-designed passive techniques, the introduction of an active cooling system (either vapour compression, solar assisted absorption, evaporative or combinations) might become necessary as the climate gets warmer and there are fewer opportunities for free-cooling with natural ventilation [67]. However, the simulations lead to conclude that the post-retrofit building model will be able to run in purely free-running mode during the summer (given the uncertainty related to the prediction of future weather conditions) for the next 30 years approximately, while later on it could operate in a mixed-mode after the installation of a cooling system, i.e. exploiting the remaining free-cooling potential and relying on the active system for critical conditions.

Ideally, the design of a new building or a retrofit should be conducted with this long-term vision, including, from the start, passive physical features that are able to make the building's fabric resilient to future weather and a plan for installing a cooling system when it eventually becomes necessary. For example, in the case of new

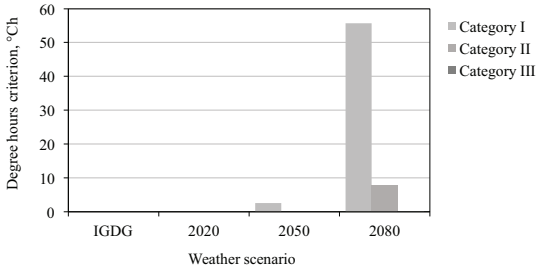

Fig. 11. Degree hours criterion for summer (only overheating occurrences are counted) for the three adaptive comfort categories in the four simulated scenarios.

constructions, one might foresee and allow for the technical spaces required for the later installation of radiant technologies and a mechanical ventilation system. However, one should also consider that, in the next 30 years, cooling technologies might evolve significantly, making it hard to determine now which systems (for generation, distribution and diffusion) would be an optimal choice in the future.

5.2.2. Post-retrofit model simulated in a conditioned mode

The second set of simulations considers the building operated in a conditioned mode for both the winter and the summer periods assuming that the required energy is provided by an ideal system. Therefore, the second set of simulations allows for the estimation of the energy need for heating and cooling required by the building to maintain the set-point temperatures mentioned in Section 4.3 throughout the year.

Fig. 12 shows the yearly energy need for space heating and cooling throughout the whole building under the four climatic scenarios under study.

When the climate evolves to a warmer configuration, the energy need for space heating is reduced, whereas the energy need for space cooling increases. Table 6 reports the yearly energy need for heating and cooling under the future weather scenarios, and their percentage variations calculated with respect to the situation corresponding to IGDG.

Fig. 12 and Table 6 show that the total energy need of the building will shift towards space cooling as the climate gets warmer. Also the national energy demand might shift from natural gas (which is typically used for heating in Italy) to electric energy, to an extent dependent on which fraction of active cooling will be realised via compression cooling. Moreover, the whole energy need for space conditioning (heating plus cooling) will increase up to 25% in 2080 with respect to the IGDG scenario, and it will take an even higher impact if it is considered in terms of primary energy. Therefore, it is of national interest to manage the actual primary energy demand of the building sector in the coming years, which will be influenced not only by the performance of the building envelope and energy systems, but also by the evolution and the penetration of renewable generation technologies, as well as by the efficiency of the electric grid.

6. Conclusions

An energy retrofit project for a child care centre targeting very high energy and indoor environment performances has been developed on the basis of a typical (IGDG) weather file. IGDG and TMY weather files were built using data from the climate conditions of past decades. The building model has been simulated taking into consideration the future weather scenarios developed according to the *morphing* methodology applied to the IGDG file. The objective of the analysis was to investigate whether the chosen energy concept would be resilient to the expected future climate changes.

The analysis showed that the design approach based on the substantial exploitation of passive strategies and the improvement of envelope thermal resistance and solar protections may result quite robust in the mid-term weather scenario, justifying the initial capital investment. In the long-term weather scenario, however, in order to be able to cope with the warmer outdoor conditions, the building will probably have to integrate an active cooling system (compression, absorption, evaporative etc.), hopefully optimised to operate in a mixed-mode with natural ventilation.

As for the use of the long-term thermal discomfort indexes, our analysis suggests that symmetric indexes should be used with caution as for the summer season, since focusing on overcooling in present weather might make the building less resilient to overheating in the future climate conditions. Rather, the physical features allowing the building to manage the summer loads should be installed and their exploitation graduated through controls to follow the evolution of the climate. There might also be scope for further analysis on whether the long-term thermal discomfort indexes should consider comfort categories that are strictly symmetrical with respect to the optimal comfort temperature.

In general, the analysis showed that in future weather conditions a substantial shift from heating energy needs to cooling energy needs would be registered in building operations in a temperate climate such as Milan, Italy, which is a winter dominated climate nowadays. A higher shift might be expected at lower latitudes, and should be considered by designers.

A design shift from 'static' buildings into buildings that can respond and adapt to climate change is therefore required. Moreover, it should also be considered that the applicability of the comfort models available nowadays to child care centres and kindergartens presents several limitations. The Fanger model was developed in climate chambers through interviews with young adults. The adaptive model is suggested by EN15251 "for human occupancy with mainly sedentary activities and dwelling, where there is easy access to operable windows and occupants may freely adapt their clothing to the indoor and/or outdoor thermal conditions" [14], but young children do not have the same opportunities as adults regarding behavioural adjustment, physiological acclimatisation and psychological habituation, as classified by Brager and de Dear [68], to adapt to the thermal environment. For example, they do not have direct control over operable windows, and cannot easily adjust their clothing or get themselves hot and cold food and drinks. In addition, they present a higher metabolic level when compared to sedentary adults, given both by physiological aspects and by activities/games performed at the care centre. Thus, the most important adaptive measures are due to their teachers, who need to take decisions for the whole classroom, e.g., the operation of windows and the scheduling of activities.

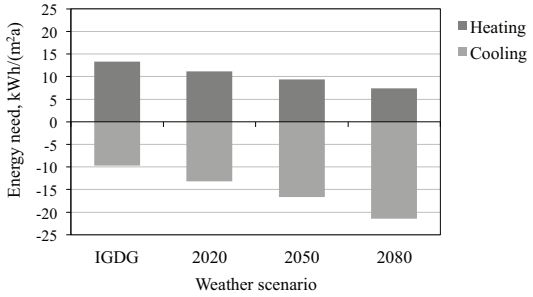

Fig. 12. Yearly energy need for space heating and cooling per unit of net floor area.

Table 6
Yearly energy need for space heating and cooling for the post-retrofit building model under future weather scenario and percentage variations with respect to IGDG.

	Weather scenario			
Parameter, unit of measure	IGDG	2020	2050	2080
	Heating			
Energy need, (kWh $m^{-2}a^{-1}$)	13.4	11.2	9.4	7.5
Variation with respect to IGDG (%)	–	−16%	−30%	−45%
	Cooling			
Energy need, (kWh $m^{-2}a^{-1}$)	9.7	13.3	16.8	21.6
Variation with respect to IGDG (%)		+37%	+73%	+123%
	Heating and cooling			
Energy need, (kWh $m^{-2}a^{-1}$)	23.1	24.5	26.2	29.1
Variation with respect to IGDG (%)	–	+6%	+13%	+25%

Considering this, the reported results might be slightly optimistic and the need for an active cooling system could be required earlier in buildings that are occupied by children, compared to offices or other kinds of buildings. Meanwhile, there is probably a need to improve the adaptive and the thermal comfort models in general, and the long-term thermal discomfort indexes, in order to provide the designers with better analysis tools to address climate change in buildings design. Refinements of thermal comfort categories and guidelines on their applicability in various conditions will be important both for the comfort objectives and for the energy containment objectives of the design process [69].

Acknowledgements

The authors would like to thank the Department of School Construction and the Office for EU Affairs of the Municipality of Milano for the collaboration on this project. The study was partially developed within the EU-GUGLE project funded by Seventh Framework Programme under grant agreement n. 314632. Finally, the authors are presently contributing to the on-going work for developing better evaluation criteria for hybrid or mixed-mode buildings and fostering an evolution of standards on adaptive thermal comfort within the EBC Annex 69 entitled *Strategy and Practice of Adaptive Thermal Comfort in Low Energy Buildings*, and would like to thank all the participants of the Annex for the important *stimuli* received during the realisation of the work presented in this paper.

Annex A. —Crack templates

Table of data with flow coefficient, *C*, and flow exponent, *n*, are presented for the following components: windows, doors, walls, roof and floor.

The crack characteristics of windows and doors are normalised by opening perimeter lengths. Porosity of walls, roof and floor has been modelled as a single equivalent crack for each component

Table A1
Predefined crack template values—Very poor.

Component	Flow coefficient ($kg\,s^{-1}\,m^{-1}$crack @ 1 Pa)	Flow Exponent (non-dimensional)
Internal windows	0.0030	0.60
External windows	0.0030	0.60
Internal doors	0.0030	0.60
External doors	0.0030	0.66
Internal walls	0.0190	0.75
External walls	0.0004	0.70
Roof	0.0030	0.70
Floor	0.0002	0.70

Table A2
Predefined crack template values—Poor.

Component	Flow coefficient ($kg\,s^{-1}\,m^{-1}$crack @ 1 Pa)	Flow Exponent (non-dimensional)
Internal windows	0.00180	0.60
External windows	0.00100	0.60
Internal doors	0.02000	0.60
External doors	0.00180	0.66
Internal walls	0.00500	0.75
External walls	0.00020	0.70
Roof	0.00015	0.70
Floor	0.00020	0.70

Table A3
Predefined crack template values—Medium.

Component	Flow coefficient ($kg\,s^{-1}\,m^{-1}$crack @ 1 Pa)	Flow Exponent (non-dimensional)
Internal windows	0.00014	0.65
External windows	0.00140	0.65
Internal doors	0.02000	0.60
External doors	0.00140	0.65
Internal walls	0.00300	0.75
External walls	0.00010	0.70
Roof	0.00010	0.70
Floor	0.00090	0.70

.

References

[1] NASA's Goddard Institute for space Studies (GISS), Five-Year Global Temperature Anomalies from 1880 to 2014 (2014).
[2] Global Analysis—Annual 2015 | National Centers for Environmental Information (NCEI) http://www.ncdc.noaa.gov/sotc/global/201513, (2015) (accessed 05.03.16.).
[3] IPCC, IPCC Special Report on Emissions Scenarios (SRES): Summary for Policymakers, a Special Report of IPCC Working Group III Intergovernmental Panel on Climate Change, IPCC, Geneva, Switzerland, 2000.
[4] D.J. Griggs, M. Noguer, Climate change 2001: the scientific basis. Contribution of working group I to the third assessment report of the intergovernmental panel on climate change, Weather 57 (2002) 267–269, http://dx.doi.org/10.1256/004316502320517344.
[5] ASHRAE, ASHRAE Handbook: Fundamentals, American Society of Heating Refrigeration and Air-Conditioning Engineers, 2009.
[6] D. Thevenard, Influence of long-term trends and period of record selection on the calculation of climatic design conditions and degree days, ASHRAE Trans. 116 (2010) 447–460.
[7] S.E. Belcher, J.N. Hacker, D.S. Powell, Constructing design weather data for future climates, Build. Serv. Eng. Res. Technol. 26 (2005) 49–61, http://dx.doi.org/10.1191/0143624405bt112oa.
[8] F. Causone, S. Carlucci, A. Moazami, G. Cattarin, L. Pagliano, Retrofit of a kindergarten targeting zero energy balance, in: Proceeding 6th Int Build. Phys. Conf., Turin, 2015.
[9] F. Causone, A. Moazami, S. Carlucci, L. Pagliano, M. Pietrobon, Ventilation strategies for the deep energy retrofit of a kindergarten, in: Proceeding 36th AIVC—5th TightVent 3rd Venticool Conf, Madrid, 2015.
[10] CRESME, RIUSO03 Ristrutturazione edilizia riqualificazione energetica rigenerazione urbana, Centro Ricerche Economiche Sociali di Mercato per l' Edilizia e il Territorio, 2014.
[11] R. Becker, I. Goldberger, M. Paciuk, Improving energy performance of school buildings while ensuring indoor air quality ventilation, Build. Environ. 42 (2007) 3261–3276, http://dx.doi.org/10.1016/j.buildenv.2006.08.016.
[12] W. Zeiler, G. Boxem, Net-zero energy building schools, Renew. Energy 49 (2013) 282–286, http://dx.doi.org/10.1016/j.renene.2012.01.013.
[13] A. Robert, M. Kummert, Designing net-zero energy buildings for the future climate, not for the past, Build. Environ. 55 (2012) 150–158, http://dx.doi.org/10.1016/j.buildenv.2011.12.014.
[14] CEN, EN 15251, Indoor environmental input parameters for design and assessment of energy performance of buildings addressing indoor air quality, in: Thermal Environment, Lighting and Acoustic, Comité Européen de Normalisation (CEN), Bruxelles, 2007.
[15] D.W. Phillips, R.B. Crowe, Canada: atmospheric environment service., climate severity index for Canadians, Environment Canada, Atmospheric Environment Service, Downsview, Ont, 1984.
[16] T.A. Markus, J.A. Clarke, E.N. Morris, T.G. Collins, The influence of climate on housing: a simple technique for the assessment of dynamic energy behaviour, Energy Build. 7 (1984) 243–259, http://dx.doi.org/10.1016/0378-7788(84)90029-X.
[17] Presidente della Repubblica, Regolamento recante norme per la progettazione, l'installazione, l'esercizio e la manutenzione degli impianti termici degli edifici ai fini del contenimento dei consumi di energia, in: Attuazione Dell'art. 4, Comma 4, Della L. 9 Gennaio 1991, n. 10. 26 Agosto 1993, Gazzetta Ufficiale della Repubblica Italiana S.O., 1993.
[18] A. Federici, D. Iatauro, C. Romeo, L. Terrinoni, P. Signoretti, Climatic Severity Index: definition of summer climatic zones in Italy through the assessment of air conditioning energy need in buildings, in: RHEVA Word Congr Int. Conf. on IAQVEC, Prague, 2013.
[19] Solar Energy Research Institute (SERI), Solar Radiation Energy Resource Atlas of the United States, Report SERI/SP-642-1037, Solar Energy Research Institute (SERI), Washington D.C, 1981.
[20] J.F. Kreider, P. Curtiss, A. Rabl, Heating and Cooling of Buildings: Design for Efficiency, McGraw-Hill, 2002.
[21] M.J. Scott, L.E. Wrench, D.L. Hadley, Effects of climate change on commercial building energy demand, Energy Sources 16 (1994) 317–332, http://dx.doi.org/10.1080/00908319408909081.
[22] H. Burmeister, B. Keller, Climate surfaces: a quantitative building-specific representation of climates, Energy Build. 28 (1998) 167–177, http://dx.doi.org/10.1016/S0378-7788(98)00012-7.
[23] B. Keller, E. Magyari, A universally valid strategy for low energy houses, Renew. Energy 401–406 (1998).
[24] L. Terrinoni, Report RSE/2009/204—Un approccio razionale alla definizione delle zone climatiche di un territorio per la regolamentazione dei consumi energetici derivanti dalla climatizzazione degli edifici: dai gradi-giorno invernali agli indici di severità climatica all weather (2009).
[25] L. Terrinoni, P. Signoretti, D. Iatauro, C. Romeo, A. Federici, Definition, Analysis and Application of a Climatic Severity Index Aimed at Zoning The Italian Territory for Summer Air Conditioning of Buildings, ENEA, Energia Ambiente e Innovazione, 2012.
[26] F. Sánchez, J. Salmerón, S. Álvarez, A new methodology towards determining building performance under modified outdoor conditions, Build. Environ. 41 (2006) 1231–1238, http://dx.doi.org/10.1016/j.buildenv.2005.05.035.
[27] J.M. Salmerón, S. Álvarez, J.L. Molina, A. Ruiz, F.J. Sánchez, Tightening the energy consumptions of buildings depending on their typology and on climate severity indexes, Energy Build. 58 (2013) 372–377, http://dx.doi.org/10.1016/j.enbuild.2012.09.039.
[28] P. de Wilde, D. Coley, The implications of a changing climate for buildings, Build. Environ. 55 (2012) 1–7, http://dx.doi.org/10.1016/j.buildenv.2012.03.014.
[29] P. de Wilde, W. Tian, Management of thermal performance risks in buildings subject to climate change, Build. Environ. 55 (2012) 167–177, http://dx.doi.org/10.1016/j.buildenv.2012.01.018.
[30] H. Wang, Q. Chen, Impact of climate change heating and cooling energy use in buildings in the United States, Energy Build. 82 (2014) 428–436, http://dx.doi.org/10.1016/j.enbuild.2014.07.034.
[31] K.J. Lomas, R. Giridharan, Thermal comfort standards, measured internal temperatures and thermal resilience to climate change of free-running buildings: a case-study of hospital wards, Build. Environ. 55 (2012) 57–72, http://dx.doi.org/10.1016/j.buildenv.2011.12.006.
[32] K.J. Lomas, Y. Ji, Resilience of naturally ventilated buildings to climate change: advanced natural ventilation and hospital wards, Energy Build. 41 (2009) 629–653, http://dx.doi.org/10.1016/j.enbuild.2009.01.001.
[33] T.Q. Murdock, R.J. Lee, E. Barrow, F. Zwiers, I. Rutherford, Methodology and Technical Report for Scenarios of the Climate Severity Index, Canadian Institute for Climate Studies Report, 2001, 69 pp.
[34] T. Murdock, Scenarios of the Canadian climate severity index, in: Canadian Institute for Climate Studies, Ouranos derived Data and Climatic Indices Meeting, Montréal, 2003.

[35] S. Carlucci, L. Pagliano, A review of indices for the long-term evaluation of the general thermal comfort conditions in buildings, Energy Build. 53 (2012) 194–205.
[36] S. Carlucci, L. Pagliano, A. Sangalli, Statistical analysis of the ranking capability of long-term thermal discomfort indices and their adoption in optimization processes to support building design, Build. Environ. 75 (2014) 114–131.
[37] CEN, ISO 13790:2008, Energy Performance of Buildings—Calculation of Energy Use for Space Heating and Cooling, Comité Européen de Normalisation (CEN), 2008.
[38] CEN, EN 15603, Overall Energy Use and Definition of Energy Ratings, Comité Européen de Normalisation (CEN), 2008.
[39] ASHRAE, ASHRAE Standard 62. 1–2013 Ventilation for Acceptable Indoor Air Quality (ANSI Approved), ASHRAE, 2013.
[40] F. Roberti, U.F. Oberegger, A. Gasparella, Calibrating historic building energy models to hourly indoor air and surface temperatures: methodology and case study, Energy Build. 108 (2015) 236–243, http://dx.doi.org/10.1016/j.enbuild.2015.09.010.
[41] ASHRAE, ASHRAE GUIDELINE 14–2002 Measurement of Energy and Demand Savings, 8400, ASHRAE, 2002.
[42] C.J. Hopfe, Uncertainty and Sensitivity Analysis in Building Performance Simulation for Decision Support and Design Optimization, Ph.D., Eindhoven University of Technology, 2009.
[43] UNI, UNI TS 11300 Energy Performance of Buildings Part 2: Evaluation of Primary Energy Need and of System Efficiencies for Space Heating and Domestic Hot Water Production, Ente Nazionale Italiano di Unificazione (UNI), Milano, 2008.
[44] M.F. Jentsch, P.A.B. James, L. Bourikas, A.S. Bahaj, Transforming existing weather data for worldwide locations to enable energy and building performance simulation under future climates, Renew. Energy 55 (2013) 514–524, http://dx.doi.org/10.1016/j.renene.2012.12.049.
[45] F.R. Met Office, Met Office Hadley Centre for Climate Science and Services, Met Off, 2010, http://www.metoffice.gov.uk/climate-guide/science/science-behind-climate-change/hadley (accessed 29.10.15.).
[46] Intergovernmental Panel on Climate Change, Fourth Assessment Report: Climate Change 2007: Synthesis Report: Summary for Policymakers, Intergovernmental Panel on Climate Change, 2007.
[47] EnergyPlus Energy Simulation Software: Weather Data, (n.d.), http://apps1.eere.energy.gov/buildings/energyplus/weatherdata_about.cfm, (accessed 03.11.15.).
[48] D.B. Crawley, L.K. Lawrie, F.C. Winkelmann, W.F. Buhl, Y.J. Huang, C.O. Pedersen, R.K. Strand, R.J. Liesen, D.E. Fisher, M.J. Witte, J. Glazer, EnergyPlus: creating a new-generation building energy simulation program, Energy Build. 33 (2001) 319–331, http://dx.doi.org/10.1016/S0378-7788(00)00114-6.
[49] US-DoE, Testing and Validation EnergyPlus Energy Simulation Software, 2012, http://apps1.eere.energy.gov/buildings/energyplus/energyplus_testing.cfm, (accessed 19.04.14.).
[50] ASHRAE, ANSI/ASHRAE 140, Standard Method of Test for the Evaluation of Building Energy Analysis Computer Programs Atlanta (GA), USA, American Society of Heating, Refrigerating and Air-Conditioning Engineers, 2011.
[51] G. Beccali, M. Cellura, V.L. Brano, A. Orioli, Is the transfer function method reliable in a European building context? A theoretical analysis and a case study in the south of Italy, Appl. Therm. Eng. 25 (2005) 341–357, http://dx.doi.org/10.1016/j.applthermaleng.2004.06.010.
[52] US-DoE, InputOutput Reference: The Encyclopedic Reference to EnergyPlus Input and Output, U.S. Department of Energy, 2010.
[53] S. Carlucci, Thermal Comfort Assessment of Buildings, Springer, London, 2013.
[54] P.O. Fanger, Thermal Comfort-Analysis and Applications in Environmental Engineering, Danish Technical Press, Copenhagen, 1970.
[55] J. Van Hoof, Forty years of Fanger's model of thermal comfort: comfort for all? Indoor Air 18 (2008) 182–201, http://dx.doi.org/10.1111/j.1600-0668.2007.00516.x.
[56] S. ter Mors, J.L.M. Hensen, M.G.L.C. Loomans, A.C. Boerstra, Adaptive thermal comfort in primary school classrooms: creating and validating PMV-based comfort charts, Build. Environ. 46 (2011) 2454–2461, http://dx.doi.org/10.1016/j.buildenv.2011.05.025.
[57] D. Teli, M.F. Jentsch, P.A.B. James, Naturally ventilated classrooms: an assessment of existing comfort models for predicting the thermal sensation and preference of primary school children, Energy Build. 53 (2012) 166–182, http://dx.doi.org/10.1016/j.enbuild.2012.06.022.
[58] K. Fabbri, Thermal comfort evaluation in kindergarten: PMV and PPD measurement through datalogger and questionnaire, Build. Environ. 68 (2013) 202–214, http://dx.doi.org/10.1016/j.buildenv.2013.07.002.
[59] H. Yun, I. Nam, J. Kim, J. Yang, K. Lee, J. Sohn, A field study of thermal comfort for kindergarten children in Korea: an assessment of existing models and preferences of children, Build. Environ. 75 (2014) 182–189, http://dx.doi.org/10.1016/j.buildenv.2014.02.003.
[60] E. Arens, M.A. Humphreys, R. de Dear, H. Zhang, Are class A temperature requirements realistic or desirable? Build. Environ. 45 (2010) 4–10, http://dx.doi.org/10.1016/j.buildenv.2009.03.014.
[61] F. d'Ambrosio Alfano, E. Ianniello, B.I. Palella, G. Riccio, Thermal comfort design in indoor environments: a comparison between EU and USA approaches, Proc. Healthy Build. 2 (2006) 1–6.
[62] G. Alfano, F.R. d'Ambrosio, G. Riccio, Sensibility of the PMV index to variations of its independent variables, in: Proc. Therm. Comf. Stand. 21st Century April, Windsor, 2001, pp. 158–165.
[63] CEN, ISO 7730, Ergonomics of the Thermal Environment—Analytical Determination and Interpretation of Thermal Comfort Using Calculation of the PMV and PPD Indices and Local Thermal Comfort Criteria, Comité Européen de Normalisation (CEN), 2005.
[64] L. Pagliano, P. Zangheri, Comfort models and cooling of buildings in the Mediterranean zone, Adv. Build. Energy Res. 4 (2010) 167–200, http://dx.doi.org/10.3763/aber.2009.0406.
[65] S. Attia, S. Carlucci, Impact of different thermal comfort models on zero energy residential buildings in hot climate, Energy Build. 102 (2015) 117–128, http://dx.doi.org/10.1016/j.enbuild.2015.05.017.
[66] F. Nicol, M. Humphreys, Maximum temperatures in European office buildings to avoid heat discomfort, Sol. Energy 81 (2007) 295–304, http://dx.doi.org/10.1016/j.solener.2006.07.007.
[67] F. Causone, Climatic potential for natural ventilation, Archit. Sci. Rev. 59 (3) (2015) 218–228 http://dx.doi.org/10.1080/00038628.2015.1043722.
[68] G.S. Brager, R.J. de Dear, Thermal adaptation in the built environment: a literature review, Energy Build. 27 (1998) 83–96.
[69] A. Sfakianaki, M. Santamouris, M. Hutchins, F. Nichol, M. Wilson, L. Pagliano, W. Pohl, J.L. Alexandre, A. Freire, Categorization introduced by european standard en 15251 for new building design and major rehabilitations, Int. J. Ventilation 10 (2) (2011) 195–204.

Paper III

Available online at www.sciencedirect.com

ScienceDirect

Energy Procedia 00 (2017) 000–000

Energy Procedia

www.elsevier.com/locate/procedia

11th Nordic Symposium on Building Physics, NSB2017, 11-14 June 2017, Trondheim, Norway

Critical Analysis of Software Tools Aimed at Generating Future Weather Files with a view to their use in Building Performance Simulation

Amin Moazami[a]*, Salvatore Carlucci[a], Stig Geving[a]

[a]*NTNU Norwegian University of Science and Technology, Department of Civil and Environmental Engineering, Trondheim, Norway*

Abstract

Two software tools, namely CCWorldWeatherGen and WeatherShift™, are today available on the market and enable individual end-users, to generate future projection weather data that can be used for executing building performance simulation. These software tools have been developed based on different assumptions. Therefore, the outputs of the two tools were generated and compared both graphically and using statistical methods to get to a better understanding of their differences and, hence, to identify possible consequences when applied to building performance simulation. The results suggest that, depending on the purpose of the design, care should be taken in using the above-mentioned tools.
© 2017 The Authors. Published by Elsevier Ltd.
Peer-review under responsibility of the organizing committee of the 11th Nordic Symposium on Building Physics.

Keywords: Future weather generation tools, building performance simulation, climate change, future weather data

1. Introduction

In 1976 National Climatic Data Center (NCDC) [1] provided one of the first weather data sets, called test reference year (TRY) to be used in building performance simulation. Since then many attempts have been made by several organizations to create worldwide weather data sets such as WYEC, TMY, CWEC and CTZ that are readily accessible for users of energy simulation tools [2]. But the increasing recognition of climate change and its impact on built environment [3] has added a new dimension to this challenge, which is the increasing need for future

* Corresponding author. Tel.: +0-000-000-0000 ; fax: +0-000-000-0000 .
E-mail address: author@institute.xxx

1876-6102 © 2017 The Authors. Published by Elsevier Ltd.
Peer-review under responsibility of the organizing committee of the 11th Nordic Symposium on Building Physics.

projection weather data sets for the local climates. To tackle this challenge, several methods have been developed. Guan [4] reviewed the methods used to prepare future weather data for the study of the impact of climate change on buildings. One of the practical and frequent used methods is to impose the predicted future climate data generated by a general circulation model (GCM) on the current typical weather data such as typical meteorological year (TMY) for a specific location. Since the output of GCMs are expressed with a monthly resolution and monthly values are not suitable for building performance simulation (BPS) purposes, Belcher et al. [5] introduced a downscaling method named morphing. Jentsch et al. [6] discuss the general validity of the morphing method and state that the extensive use of this method in the UK and its acceptance by the Chartered Institution of Building Services Engineers (CIBSE) [7] give some confidence in its principal applicability. However, De Dear [8] questions this method by highlighting its limitations and in general the uncertainties associated with all climatic impact research.

The present study has three purposes. First, it provides users of BPS with the general idea of mentioned concepts and processes on generating future weather data. Second, it presents a comprehensive statistical analysis of the outputs from the two future weather generator tools available today on the market, CCWorldWeatherGen [6] and WeatherShift™ [9], which allows exploring relationships and differences among the data samples. Third, the study warns modellers that, since only a few variables are modified by one of the tools and the other is developed on an older IPCC report, these tools have to be used carefully and consciously.

2. Methodology

In order to give an overview of the two future weather generator tools and estimate the implications of their use in BPS, foremost, the background and calculation assumptions made for their development are described in Section 2.1 and 2.2. Next, three European capitals are used to represent diverse climate conditions in Europe. Accordingly, in Section 2.3, three future projected periods are considered, namely near-term (NT), medium-term (MT) and long-term (LT). The two tools generated the three future projected periods for each of the three selected cities. Finally, Section 2.4 presents the statistical metrics that are used to quantify the changes and differences in the output of the two tools.

2.1. CCWorldWeatherGen tool

In 2000, the Intergovernmental Panel on Climate Change (IPCC) published a special report on the emission scenarios (SRES) that provided projections of possible future climate change. These scenarios were used in the third and fourth assessment reports, respectively mentioned hereby AR3 [10] and AR4 [11]. Based on AR3 and AR4, Jentsch et al. [6] published their work on providing a methodology based on morphing technique for generation of future weather data for worldwide locations. The standard weather file formatted according to the EnergyPlus Weather (EPW) was selected as the baseline weather data for conducting the morphing procedure. EPW files are freely available for worldwide locations, which is as well one of the key attractiveness of this method.

Jentsch et al. [6] reviewed six GCMs under AR3 and 23 GCMs under AR4, which were available on the IPCC online data distribution center [12] by the time. They found that the most suitable GCM for applying their method was HadCM3 [13] for A2 emission scenario [10]. HadCM3 output is expressed as relative changes with respect to the data gathered in the period ranging from 1961 to 1990 that is taken as a timeframe. The tool job is to superimpose this relative change on the meteorological parameters stored in an EPW file format.

In this study, weather files from international weather for energy calculation (IWEC) database are considered. IWEC database has been derived from measured weather data from 1982 to 1999, which is a different timeframe than HadCM3. According to Jentsch [6], this means that morphed weather files created using this EPW data are expected to overestimate the effect of climate change for the given location. Based on the above-mentioned methodology, the Sustainable energy research group (SERG) at Southampton university introduced a Microsoft® Excel based tool called 'The climate change world weather generator (CCWorldWeatherGen)' [14]. The tool is freely available and it allows users to generate future weather files for worldwide locations within three time slices: 2011-2040 ('2020s'), 2041-2070 ('2050s') and 2071-2100 ('2080s') relative to baseline period (1961-1990). It transforms EPW files template into future weather data always in the EPW format ready for use in BPS tools. More details on generation of climate parameters for EPW future weather data can be find in [15] and [5].

2.2. WeatherShift™

In their fifth assessment report, AR5 [16], IPCC identified new "benchmark emission scenarios" referred as representative concentration pathways (RCPs). Based on two of the RCP emission scenarios (4.5 and 8.5), Arup and Argos Analytics has developed a tool named 'WeatherShift™' [17] that applies the morphing procedure on the outcomes of 14 GCMs (out of approximately 40 models) available under AR5 [18]. The tool provides future projection weather data for three time periods – 2026-2045 (referred as '2035s'), 2056-2075 (referred as '2065s'), 2081-2100 (referred as '2090s') relative to the baseline period 1976-2005 – and two emission scenarios – RCP8.5 and RCP4.5 – of the IPCC's AR5. Moreover, WeatherShift™ provides a cumulative distribution function (CDF) that is constructed for each variable using linear interpolation between the model values [9]. This method was introduced earlier from UK Climate Impact Programme (UKCIP) for the UK Climate Projections [19]. The CDF enables users to decide a probability assigned to the projections. In order to make comparable the outcomes of the two weather generation tools, the RCP8.5 is used in the WeatherShift™ that is the highest emission scenario of AR5, which is in accordance with the A2 scenario used by SERG in the CCWorldWeatherGen. For the probability level, we chose 50% value, which means the median or as referred by UKCP09 as central estimate. Table 1 contrasts the different assumptions used in the two tools.

Table 1. Differences between the two tools.

	CCWorldWeatherGen	WeatherShift™
Projected time periods	2020, 2050, 2080	2035, 2065, 2090
IPCC Report	AR3 (2001), AR4 (2007)	AR5 (2014)
GCM(s)	HadCM3	14 models
IPCC emission scenario(s)	A2	RCP4.5, RCP8.5
Downscaling method	Morphing	Morphing
Baseline period	1961-1991	1986-2005

2.3. Projected periods

The two tools use different time slices as described before. For the simplicity of this study, three projection periods – near-term (NT) projection, medium-term (MT) projection and long-term (LT) projection – have been used. The terminology was adopted from IPCC's AR5 (2014), and are used accordingly instead of 2020, 2050, 2080 for CCWorldWeatherGen and 2035, 2065, 2090 for WeatherShift™ tool.

2.4. Statistical analysis

Statistical analysis was carried out on all the parameters contained in the EPW files using the software package IBM® SPSS® Statistics version 24. For the first step of the analysis, all the parameters contained in the EPW file were tested for normality using the Kolmogorov-Smirnov statistic given the sample size. Since the result of the test for all the parameters showed a non-normal distribution for $p \leqslant 0.05$, non-parametric statistic methods were adopted to explore the differences among different sets of data. Secondly, to estimate the statistical significance of the differences between the baseline IWEC files and the generated future weather files, the Mann-Whitney U test was used. This test is the non-parametric test equivalence of the t-test for independent samples. Instead of comparing means of the two groups, as in the case of the t-test, the Mann-Whitney U test actually compares medians. If the significance level (p) provided by the Mann-Whitney U test is higher than 0.05 there is statistically significant difference between the two tested independent samples.

Thirdly, to quantify the magnitude of the differences, the effect size (ES) was calculated. According to Cohen [20], ES is some specific nonzero value and the larger this value, the greater the degree to which the phenomenon under study is manifested, which in our case is a statistically significant difference. The effect size is defined as

$$r = \frac{z}{\sqrt{N}} \tag{1}$$

Where r is the effect size, z is the statistic's value and N is the sample size. According to Cohen [20], ES is considered large if the value of r is larger than 0.5, medium if it is in the range between 0.5 and 0.1, and low if is lower than 0.1.

The key variables considered for this assessment are dry bulb temperature, relative humidity and global horizontal radiation.

3. Results

The first step aimed at characterizing the data samples. As mentioned before the output of the tools are in EPW format, which contains several meteorological parameters in hourly values for an entire year. All meteorological failed the Kolmogorov-Smirnov normality test and are hence are not normally distributed. For this reason, data is described using the median and the interquartile range instead of using the mean and the standard deviation and is represented graphically using a boxplot. As an example, Figure 1 shows the distribution of the three key variables plotted solely for Paris in the three future projection weather scenarios as generated by the two tools. It allowed us to have a quick scan of the differences.

Figure 2 shows, for the three key variables in the three selected locations, the hourly differences between the values of the long-term projected weather data and the values of the reference IWEC weather file. Pattern of the differences of the two tools emerge and show a substantial different implementation of the morphing method in the two tools. Next, the Mann-Whitney U test was used to estimate quantitatively the magnitude of the difference between the reference IWEC file and the future projection weather files. Table 2 reports the effect size of the changes as a result of this analysis.

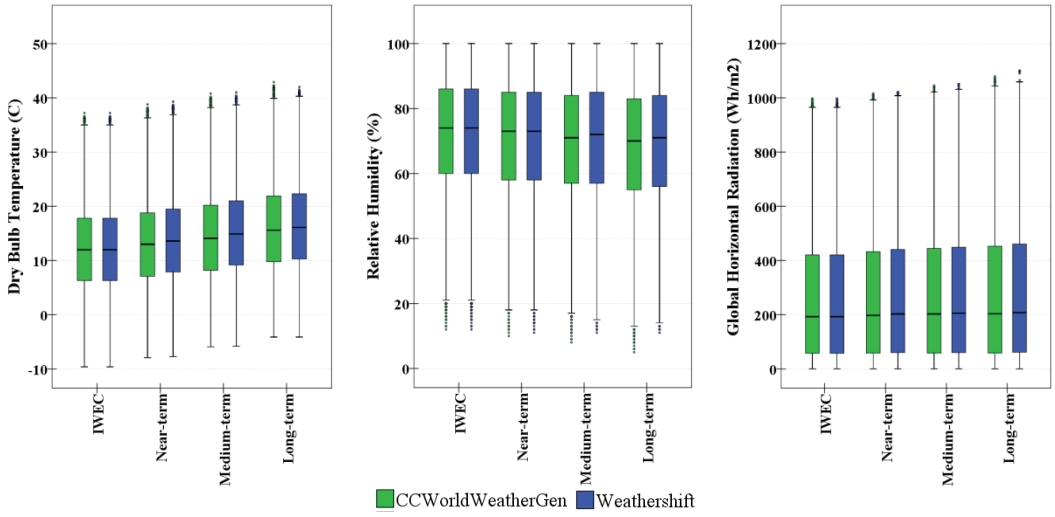

Fig. 1. Comparison of the outcomes of the two weather generation tools for the three meteorological parameters for the city of Paris.

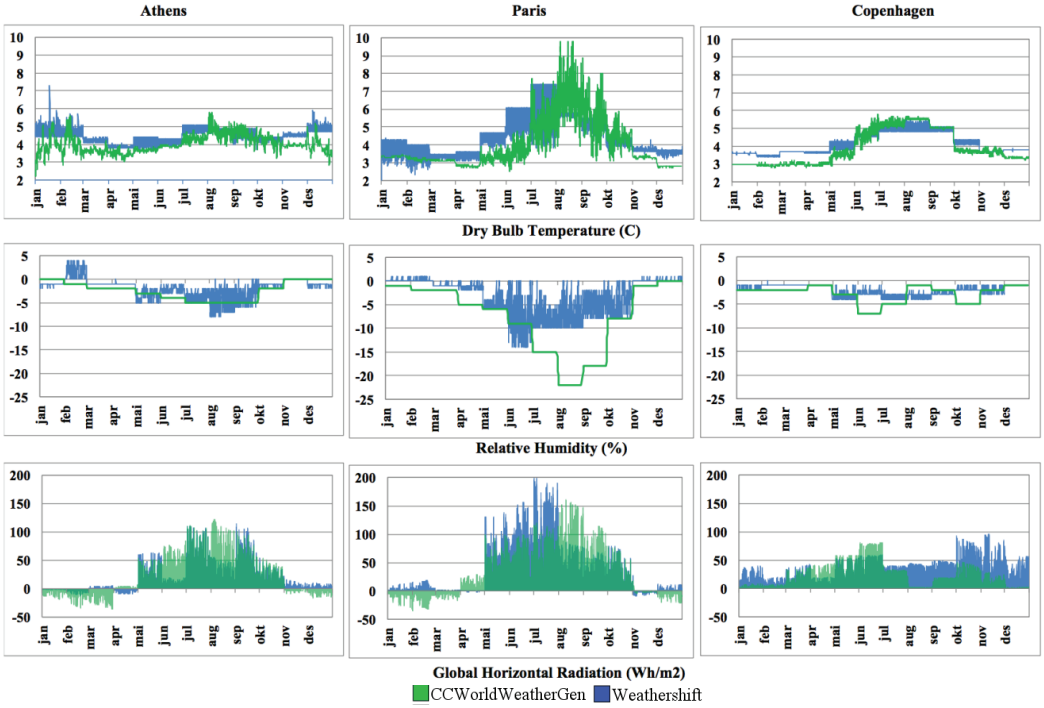

Fig. 2. Hourly differences between the values of the long-term projected weather data and the values of the reference IWEC weather file

Table 1. Comparison of the changes with respect to the reference IWEC file and indication of the effect size of the change.

EPW Parameters	CCWorldWeatherGen									WeatherShift								
	Near-Term			Medium-Term			Long-Term			Near-Term			Medium-Term			Long-Term		
	Athens	Paris	Copenhagen	Athens	Paris	Copenhagen	Athens	Paris	Copenhagen	Athens	Paris	Copenhagen	Athens	Paris	Copenhagen	Athens	Paris	Copenhagen
Dry Bulb Temperature (°C)	✓	✓	✓	✓	✓	✓	✓	✓	✓	✓	✓	✓	✓	✓	✓	✓	✓	✓
Dew Point Temperature (°C)	✓	✓	✓	✓	✓	✓	✓	✓	✓	✓	✓	✓	✓	✓	✓	✓	✓	✓
Relative Humidity (%)	✓	✓	✓	✓	✓	✓	✓	✓	✓	✓	✓	✓	✓	✓	✓	✓	✓	✓
Atmospheric Pressure (Pa)	✓	✓	✓	✓	✓	✓	✓	✓	✓	✓	✓	✓	✓	✓	✓	✓	✓	✓
Extraterrestrial Horizontal Radiation (Wh/m^2)	✓	✓	✓	✓	✓	✓	✓	✓	✓	-	-	-	-	-	-	-	-	-
Horizontal Infrared Radiation Intensity from Sky (Wh/m^2)	✓	✓	✓	✓	✓	✓	✓	✓	✓	-	-	-	-	-	-	-	-	-
Global Horizontal Radiation (Wh/m^2)	✓	✓	✓	✓	✓	✓	✓	✓	✓	✓	✓	✓	✓	✓	✓	✓	✓	✓
Direct Normal Radiation (Wh/m^2)	✓	✓	✓	✓	✓	✓	✓	✓	✓	✓	✓	✓	✓	✓	✓	✓	✓	✓
Diffuse Horizontal Radiation (Wh/m^2)	✓	✓	✓	✓	✓	✓	✓	✓	✓	✓	✓	✓	✓	✓	✓	✓	✓	✓
Global Horizontal Illuminance (lux)	✓	✓	✓	✓	✓	✓	✓	✓	✓	-	-	-	-	-	-	-	-	-
Direct Normal Illuminance (lux)	✓	✓	✓	✓	✓	✓	✓	✓	✓	-	-	-	-	-	-	-	-	-
Diffuse Horizontal Illuminance (lux)	✓	✓	✓	✓	✓	✓	✓	✓	✓	-	-	-	-	-	-	-	-	-
Zenith Luminance (Cd/m2)	✓	✓	✓	✓	✓	✓	✓	✓	✓	-	-	-	-	-	-	-	-	-
Wind Direction (deg)	-	-	-	-	-	-	-	-	-	-	-	-	-	-	-	-	-	-
Wind Speed (m/s)	✓	✓	✓	✓	✓	✓	✓	✓	✓	✓	✓	✓	✓	✓	✓	✓	✓	✓
Total Sky Cover (.1)	✓	✓	✓	✓	✓	✓	✓	✓	✓	-	-	-	-	-	-	-	-	-
Opaque Sky Cover (.1)	✓	✓	✓	✓	✓	✓	✓	✓	✓	-	-	-	-	-	-	-	-	-
Precipitable Water (mm)	-	-	-	-	-	-	-	-	-	-	-	-	-	-	-	-	-	-
Days Since Last Snow	-	-	-	-	-	-	-	-	-	-	-	-	-	-	-	-	-	-
Liquid Precipitation Depth (mm)	-	-	-	-	-	-	-	-	-	-	-	-	-	-	-	-	-	-

- No model implemented in the tool
✓ No statistically significant change
✓ Statistically significant change - Small ES
✓ Statistically significant change - Medium ES
✓ Statistically significant change - Large ES

4. Discussion and Conclusion

The direct comparison of the distributions of values generated by the two future weather generation tools displays little differences between them (Figure 1), but, Figure 2 shows very different patterns in application of the morphing method although both tools recur to the same method to downscale the monthly values generated by the GCMs.

After the comparison in Table 2, the two tools demonstrate to be substantially different and Weathershift™ only modifies the most important meteorological parameters (dry bulb temperature, dew point temperature, relative humidity, atmospheric pressure, global horizontal radiation, direct normal radiation, diffuse horizontal radiation, and wind speed). This aspect is of major importance when a modeler (designer, consultant, etc.) want to test the performance of a model that uses one of the other meteorological variables under future weather scenarios. Furthermore, Table 2 shows that a change in a variable might be not statistically significant in the near-term, but becomes statistically significant in medium-term and long-term, for example the global horizontal radiation in case of Paris for CCWorldWeatherGen or in case of Athens for WeatherShift™. The effect size of climate change increases for higher latitudes, that is, although the net increase in temperature in Copenhagen is lower than in Athens, the relative temperature rise will be higher in the former city.

References

[1] NCDC. Test Reference Year (TRY), Tape Reference Manual. Asheville, North Carolina: National Climatic Data Center, U.S. Department of Commerce; 1976.
[2] Crawley DB. Which weather data should you use for energy simulations of commercial buildings? In: ASHRAE, editor. ASHRAE Transactions. Atlanta1998. p. 498–515.
[3] Wilby RL. A Review of Climate Change Impacts on the Built Environment. Built Environment. 2007;33(1):31-45.
[4] Guan L. Preparation of future weather data to study the impact of climate change on buildings. Building and Environment. 2009;44(4):793-800.
[5] Belcher SE, Hacker JN, Powell DS. Constructing design weather data for future climates. Building Services Engineering Research and Technology. 2005;26(1):49-61.
[6] Jentsch MF, James PAB, Bourikas L, Bahaj AS. Transforming existing weather data for worldwide locations to enable energy and building performance simulation under future climates. Renewable Energy. 2013;55:514-24.
[7] Jake Hacker RC, Anastasia Mylona, Chartered Institution of Building Services Engineers. Use of climate change scenarios for building simulation: the CIBSE future weather years. London: CIBSE; 2009. 36 p.
[8] Dear RD. Adapting buildings to a changing climate: but what about the occupants? Building Research & Information. 2006;34(1):78-81.
[9] Robert Dickinson BB, editor Generating future weather files for resilience. International Conference on Passive and Low Energy Architecture, PLEA 2016 - Cities, Buildings, People: Towards Regenerative Environments; 2016; Los Angeles.
[10] IPCC. IPCC special report on emissions scenarios (SRES): summary for policymakers. Geneva, Switzerland: a special report of IPCC Working Group III Intergovernmental Panel on Climate Change; 2000.
[11] IPCC. Climate change 2007: the physical science basis. Contribution of working group I to the fourth assessment report of the intergovernmental panel on climate change. Cambridge, New York: Cambridge University Press; 2007.
[12] IPCC Data distribution centre (DDC) [Available from: http://www.ipcc-data.org].
[13] Met Office Hadley Centre for Climate Science and Services 2010 [Available from: http://www.metoffice.gov.uk/climate-guide/science/science-behind-climate-change/hadley].
[14] Climate Change World Weather File Generator for Worldwide Weather Data – CCWorldWeatherGen: Sustainable Energy Research Group; [Available from: http://www.energy.soton.ac.uk/ccworldweathergen].
[15] Jentsch MF, Bahaj AS, James PAB. Climate change future proofing of buildings-Generation and assessment of building simulation weather files. Energy and Buildings. 2008;40(12):2148-68.
[16] Edenhofer O PMR, Sokona Y , Farahani E, Kadner S, Seyboth K, Adler A, Baum I, Brunner S, Eickemeier P, Kriemann B, Savolainen J, Schlömer S, Stechow C von, Zwickel T, Minx J.C. Climate Change 2014: Mitigation of Climate Change Contribution of Working Group III to the Fifth Assessment Report of the Intergovernmental Panel on Climate Change, IPCC. Cambridge, New York; 2014.
[17] WeatherShift [Available from: http://www.weather-shift.com].
[18] Luke Troup DF. Morphing Climate Data to Simulate Building Energy Consumption. The ASHRAE and IBPSA-USA SimBuild 2016: Building Performance Modeling Conference; Utah2016.
[19] Phil Jones CK, Colin Harpham, Vassilis Glenis, Aidan Burton. UK Climate Projections science report: Projections of future daily climate for the UK from the Weather Generator. University of Newcastle; 2009.
[20] Cohen J. The Concepts of Power Analysis. Statistical Power Analysis for the Behavioral Sciences (Revised Edition): Academic Press; 1977. p. 1-17.

Paper IV

Applied Energy 238 (2019) 696–720

Contents lists available at ScienceDirect

Applied Energy

journal homepage: www.elsevier.com/locate/apenergy

Impacts of future weather data typology on building energy performance – Investigating long-term patterns of climate change and extreme weather conditions

Amin Moazami[a], Vahid M. Nik[b,c,d,*], Salvatore Carlucci[a], Stig Geving[a]

[a] NTNU Norwegian University of Science and Technology, Department of Civil and Environmental Engineering, 7491 Trondheim, Norway
[b] Division of Building Physics, Department of Building and Environmental Technology, Lund University, 223 63 Lund, Sweden
[c] Division of Building Technology, Department of Civil and Environmental Engineering, Chalmers University of Technology, 412 58 Gothenburg, Sweden
[d] Institute for Future Environments, Queensland University of Technology, Garden Point Campus, 2 George Street, Brisbane, QLD 4000, Australia

HIGHLIGHTS

- Assessing the methods for generating typical and extreme future weather files.
- Typical weather data sets can only predict long-term variations of climate.
- Extreme weather files are needed to assess short-term variations such as heatwaves.
- Extreme weather files are needed for a robust design in building and urban scales.
- Using only typical data underestimates peak load calculations considerably.

ARTICLE INFO

Keywords:
Future weather files
Typical and extreme weather conditions
Climate uncertainty
Building performance simulation
Climate change
Statistical and dynamical downscaling of climate models

ABSTRACT

Patterns of future climate and expected extreme conditions are pushing design limits as recognition of climate change and its implication for the built environment increases. There are a number of ways of estimating future climate projections and creating weather files. Obtaining adequate representation of long-term patterns of climate change and extreme conditions is, however, challenging. This work aims at answering two research questions: does a method of generating future weather files for building performance simulation bring advantages that cannot be provided by other methods? And what type of future weather files enable building engineers and designers to more credibly test robustness of their designs against climate change? To answer these two questions, the work provides an overview of the major approaches to create future weather data sets based on the statistical and dynamical downscaling of climate models. A number of weather data sets for Geneva were synthesized and applied to the energy simulation of 16 ASHRAE standard reference buildings, single buildings and their combination to create a virtual neighborhood. Representative weather files are synthesized to account for extreme conditions together with typical climate conditions and investigate their importance in the energy performance of buildings. According to the results, all the methods provide enough information to study the long-term impacts of climate change on average. However, the results also revealed that assessing the energy robustness of buildings only under typical future conditions is not sufficient. Depending on the type of building, the relative change of peak load for cooling demand under near future extreme conditions can still be up to 28.5% higher compared to typical conditions. It is concluded that only those weather files generated based on dynamical downscaling and that take into consideration both typical and extreme conditions are the most reliable for providing representative boundary conditions to test the energy robustness of buildings under future climate uncertainties. The results for the neighborhood explaining the critical situation that an energy network may face due to increased peak load under extreme climatic conditions. Such critical situations remain unforeseeable by relying solely on typical and observed extreme conditions, putting the climate resilience of buildings and energy systems at risk.

* Corresponding author at: Division of Building Physics, Department of Building and Environmental Technology, Lund University, 223 63 Lund, Sweden.
E-mail addresses: amin.moazami@ntnu.no (A. Moazami), vahid.nik@byggtek.lth.se, vahid.nik@chalmers.se, vahid.nik@qut.edu.au, nik.vahid.m@gmail.com (V.M. Nik), salvatore.carlucci@ntnu.no (S. Carlucci), stig.geving@ntnu.no (S. Geving).

https://doi.org/10.1016/j.apenergy.2019.01.085
Received 3 September 2018; Received in revised form 14 December 2018; Accepted 15 January 2019
0306-2619/ © 2019 Elsevier Ltd. All rights reserved.

Nomenclature

AR	IPCC Assessment Report
ASHRAE	American Society of Heating, Refrigerating, and Air-Conditioning Engineers
BPS	Building performance simulation
ECY	Extreme Cold Year
EPW	EnergyPlus Weather
EWY	Extreme Warm Year
GCM	Global Climate Model or General Circulation Model
IPCC	Intergovernmental Panel for Climate Change
IPCC DDC	IPCC Data Distribution Center
IWEC	International Weather for Energy Calculations
PNNL	Pacific Northwest National Laboratory
RCM	Regional Climate Model
RCP	Representative Concentration Pathway
SRES	Special Report on Emission Scenarios
TDY	Typical Downscaled Year
TMY	Typical Meteorological Year
UKCP09	UK Climate Projections 2009
XMY	Extreme Meteorological Year

1. Introduction

Building performance simulation (BPS) empowers designers to evaluate a proposed design under the probable climate conditions that a building will face during its lifetime. Weather data defines the external boundary conditions for a numerical building model. Detailed weather data that, as a minimum, includes daily and hourly resolution is required to properly describe the dynamic energy behavior of a building. There have been many attempts over the last 40 years by a number of organizations to create standardized weather files for thousands of locations on the planet [1]. These files are readily accessible to users and have formats that are suitable to be directly used in energy simulation tools [2]. Weather files are usually built upon recordings of actual historical weather data. Different weather files may, however, have different baseline observation periods. These standardized weather files provide BPS users with a single-year of typical weather data that represent typical regional climate conditions, based on a continuous time span of 20 or 30 years of historical observed data. These weather data sets are widely used and represent average conditions well enough. They, however, to a large extent fail to represent extreme weather conditions and to project future conditions, especially at the hourly temporal resolution, as it has been shown by several studies [3–6]. As a result, a number of methods have been developed to create future weather files for BPS. These have been discussed in a review paper by Herrera et al. [7]. The future weather files are used to study the impacts of climate change on building performance, numerous works on this having been published. Yau and Hasbi [8] reviewed the climate change impacts on commercial buildings and arrived at the trivial conclusion that, in general, buildings in regions with a projected increase in temperature will, in the future, require more energy for space cooling and less energy for space heating. Other studies revealed similar conclusions for case-study buildings in Austria [9], Italy [10], United States [11], China [12], and other locations around the globe. de Wilde and Coley [13] discuss the relationship between climate change and buildings and conclude that the majority of studies on the impact assessment of climate change on buildings look at few performance indicators, such as energy use for space heating and cooling, and the risk of overheating. There are, however, studies of the hygrothermal performance of buildings under future climatic conditions [14], which investigate performance indicators that highly correlate with air temperature and moisture content [15], and that take into account several climate indices such as air temperature, relative humidity, solar radiation and cloudiness [16].

The Intergovernmental Panel for Climate Change (IPCC) created a number of possible scenarios of future anthropogenic greenhouse gas emissions based on given socio-economic storylines, to project future changes in climate for impact and adaptation assessment. The first set of scenarios were introduced in the IPCC Special Report on Emissions Scenarios (SRES) in 1996 [17,18]. Later, in 2014, the IPCC adopted a new series of emission and concentration scenarios called "Representative Concentration Pathways (RCPs)" [19]. These emission scenarios are the input data used to provide initial conditions for the so-called General Circulation Models or Global Climate Models (GCMs), which are today's most complex quantitative models for forecasting climate change. GCM outputs represent averages over a region or the entire globe with a spatial resolution in the range of 100–300 km^2 and a monthly temporal resolution. These data resolutions are not suitable for direct use in BPS tools that require local weather data with hourly or sub-hourly resolution. Therefore, GCM data need to be downscaled to the appropriate spatial and temporal resolution. Indeed, all future weather information with a spatial resolution of less than 100 km^2 and temporal resolution less than monthly values has been through a downscaling process [20]. There are two main approaches to downscale GCM outputs and generating data with a finer temporal and spatial resolution. These are dynamical and statistical downscaling. After the downscaling process, the generated years of weather data need to be formatted according to a precise template to be readable by BPS tools. One common approach is the method developed by Hall et al. [21] for creating a typical meteorological year (TMY), which is derived from 30 years of weather data recordings. January for the TMY is copied directly from the historical January data that has the closest match to the 30-year average condition for January. This process is replicated for

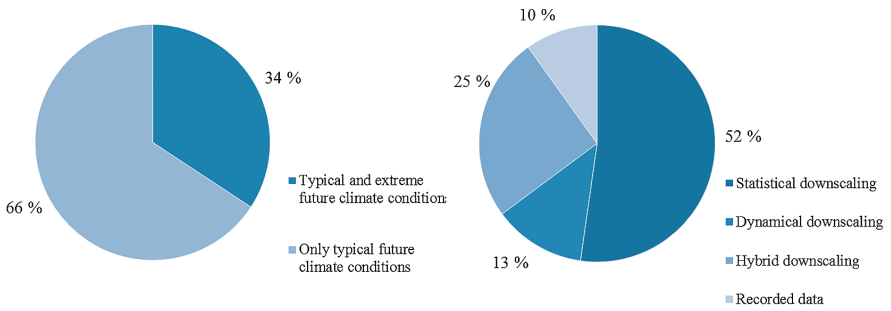

Fig. 1. Analysis of literature that used BPS to assess the impact of climate change on the performance of the buildings (111 articles).

the other months to produce 12 months of the typical weather year. Subsequently, some methods, for example the spline method, are then adopted to smooth and link together the twelve monthly weather data series. One of the main disadvantages of this method on climate change impact assessment is its averaging nature: the generation of a typical weather year neglects extreme weather conditions. We, in the last decade, have experienced some of the warmest years on record [22]. Such conditions highlight the importance of considering extreme conditions in the design and adaptation process of buildings and energy systems for the future conditions. A probabilistic forecast indicates a warmer than normal period for 2018–2022, temporarily reinforcing the long-term global warming trend and increasing the likelihood of intense to extreme temperatures, as happened in summer 2018 in Europe [23]. Failure in climate change adaptation can lead to costly short- and long-term issues [24], such as blackouts due to energy supply disruption [25]. Power failures can leave thousands of buildings without electricity or any means of space cooling, which can be fatal for the elderly, very young, or the chronically ill people. The heat wave of the summer of 2003 in Europe caused more than 70 000 heat-related deaths [26]. This is becoming increasingly important as the number of elderly people continues to rise and the predicted occurrence of heat waves increases [27]. These problems partly are arising from the fact that existing buildings are not designed for atypical conditions, and their expected performance is based on most-likely conditions. It makes their performance to fluctuate significantly when outdoor climate conditions fall out of typical conditions. That is why during a heat wave the electricity demand soars and causes the energy systems at risk of failure. Unfortunately, only a minority of scientific works and professional practices test their building design under conditions that include extremes. We draw on the literature and selected studies that used BPS to assess the impact of climate change on the performance of the buildings (Fig. 1).

Fig. 1 was developed from the analysis of 111 scientific papers detected after querying the Web of Science and Scopus databases. All these papers have been published after 2001 and are listed in Appendix A. Albeit considering extreme conditions in the design process seems to be obvious due to the increase in their frequency of occurrence and magnitude and also the high cost of possible damages, but according to Fig. 1, 66% of the studies (73 articles) are based on only typical future climate conditions. Furthermore, with regards to the downscaling methods used for preparing weather files, 52% (58 articles) are based on statistically downscaled data, 13% (14 studies) used directly data from RCMs and 25% (28 articles) used the hybrid method. These methods are described further in this study. Finally, 10% of the studies (11 articles) used recorded data, which means they used recorded data of an extreme year such as that of 2003 in Europe to study the impact of extremes conditions. It is worth highlighting that 38% of all the 111 studies (42 articles) corresponding to 55% of all the studies that consider extremes (21 out of 38 articles) are from the UK where *Test reference year* (TRY) weather files representing future typical conditions and *near extreme Design Summer Year* (DSY) weather files are provided at national level. These files are generated using data from the UK Climate Projections (UKCP) project [28]. Therefore, it seems that if reliable future weather data sets are available at a national level, the tendency to be used in building studies is very high.

As mentioned, adequate representation of long-term patterns of climate change and extreme conditions is challenging, as there are a number of ways of estimating future climate projections and creating weather files. This study provides an overview of the major approaches for creating future weather data sets based on statistical and dynamical downscaling of climate models. For the first time, the effects of using major available approaches for generating future weather files are studied on the calculation of energy performance of buildings. The building models were simulated in isolation and combined to create a virtual neighborhood representing a neighborhood in Geneva. The investigation critically analyzes the magnitude of the difference between impact assessments carried out using weather data generated by dynamical and statistical downscaling methods. It also investigates the possibility and importance of using extreme weather years in BPS at both the building and neighborhood scales. This will allow understanding the magnitude of the risk induced at large scale by not taking into account possible future climate extremes. The main objective of this study is to provide insight on which is the most reliable future weather generation method to use in building energy simulations, enabling engineers and designers to test their building designs and achieve designs that are less sensitive and more robust against climate changes.

A total number of 74 future weather data files, which include typical and extreme weather years, were generated for the city of Geneva, Switzerland, to be used in the investigation. Geneva was chosen due to the availability of the data and the possibility of having cold winters and warm summers. Geneva furthermore reached a temperature record of 41.5 °C (+5.4 °C above the average temperature) during the summer heat wave in Europe of 2003 [29]. This makes an interesting site to investigate in this work. The generated weather files were used to simulate 16 commercial reference buildings proposed by the ASHRAE Standard 90.1. Each of the buildings was simulated using the 74 weather files, which resulted in a total of 1184 simulation runs. Afterwards, a virtual neighborhood was also created using a combination of the 16 buildings for a total of 85 buildings, to evaluate the impact of the weather file typology on estimating the energy demand at the neighborhood scale.

This paper is divided into five sections. Section 2 provides a short background on downscaling GCM outputs to generate future weather files to us in BPS (Section 2.1), and to creating typical and extreme weather data sets (Section 2.2). Section 3 explains the methodology used for performing the analysis applied in this study, details of the generated weather files, building models, and virtual neighborhood being given in Sections 3.1, 3.2.1 and 3.2.2 respectively. Results are presented and discussed in Section 4, followed by Conclusions in Section 5.

2. Preparing future weather data sets

2.1. Downscaling global climate models

Global climate models (GCMs) are numerical models of the physical processes that characterize the global climate system, including the atmosphere, oceans, cryosphere and land surface [30]. These models are validated against past climate conditions to check if they can simulate the evolution of the climate system by means of running re-analyses like ERA-40 for validation. ERA-40 is a re-analysis of meteorological observations from September 1957 to August 2002 produced by the European Centre for Medium-Range Weather Forecasts (ECMWF) [31]. Once the model is verified and validated, it will set to run (usually from 1870), picking initial conditions and forced by emissions scenarios or Representative Concentration Pathways (RCPs), which are based on different greenhouse gas emission scenarios developed by IPCC [20]. Results of GCMs are expressed at the global or continental scale, and typically use long temporal resolutions such as monthly, seasonal or annual periods. These scales are too coarse for many applications and particularly for the building performance assessment. Direct use of the GCM output in impact assessment is therefore not recommended due to recognized biases [32]. Buildings are affected by the local climate, and some assessment methods may require environmental data even at the sub-hourly resolution [33]. Future weather data sets at finer temporal and spatial resolutions than those provided by GCMs are required to meet the needs of building engineers and designers. As previously mentioned, there are two main approaches to generating future weather data series. These are *dynamical downscaling* and *statistical downscaling*. There is a third approach that consists of a combination of the two approaches and is referred as *hybrid*

downscaling.

The flowchart in Fig. 2 displays the usual steps of the downscaling process available today.

The downscaling process of GCMs provides climate data with higher spatial and temporal resolutions. The procedure hence requires additional information and assumptions, which typically result in a propagation of uncertainties. There are also a number of GCMs developed by different institutes, generating future climate projections. The chaotic nature of the climate system limits accurate interannual prediction of global temperatures [23]. There are several uncertainties that affect any impact assessment of climate change, such as uncertainties in the historical relationship between temperature variability and economic growth, the spatial pattern temperature change associated with the level of aggregate emissions, and the future rate and pattern of economic development [34]. Therefore, probabilistic approaches are usually taken into account for the impact assessment of climate change, considering several climate scenarios and uncertainties. The existence of several models and uncertainties in simulating future climatic conditions is an important challenge which should be considered in impact assessment in all fields. This has been thoroughly investigated in previous works [14,16,35]. There is significant confidence that climate models provide reliable quantitative estimates of future climate change. This confidence comes from the fact that models are based on accepted physical principles and also from their ability to regenerate observed patterns of current climate and past climate change [36].

2.1.1. Dynamical downscaling

Dynamical downscaling derives local or regional climate information using a Regional Climate Model (RCM). RCMs are numerical models that require explicitly specified boundary conditions from a GCM, or an observation-based data set (re-analysis). They simulate "atmospheric and land surface processes, while accounting for high-resolution topographical data, land-sea contrasts, surface characteristics, and other components of the Earth-system" [37]. RCMs generate climate information at a much finer resolution than GCM, down to 2.5 km^2 [38]. This method has many advantages. It however also requires a considerable amount of computational power and large storage for the creation of the data sets. An RCM is nested into a GCM. The overall quality of the outputs is therefore tied to the accuracy of the underlying GCM [39]. Efforts were therefore made to quantify these uncertainties by combining different GCM-RCM pairings and performing series of simulations called 'ensembles'. Examples of such efforts are the ENSEMBLES [40] and EURO-CORDEX [41] projects. The need to consider several climate scenarios rather than just one scenario in the impact assessment of buildings has been highlighted in previous studies [42,16]. The Rossby Centre Regional Atmospheric Climate Model (RCA4) is used in this study. RCA4 has been running for the European CORDEX domain at two different horizontal resolutions, 50 km^2 and 12.5 km^2. Downscaling of the ERA-Interim reanalysis data are used to evaluate model performance in the recent past climate [43]. The verification process has been performed for the historical period 1961–2005 for which historical forcing was applied [44]. The model is then used to perform simulations for different future scenarios in which RCP scenarios have been applied to prescribe future radiative forcing. For the purpose of this work, the output data from the combination of four GCMs downscaled by RCA4 and forced by two different RCPs (4.8 and 8.5) are used. The details are given in Section 3.1.4.

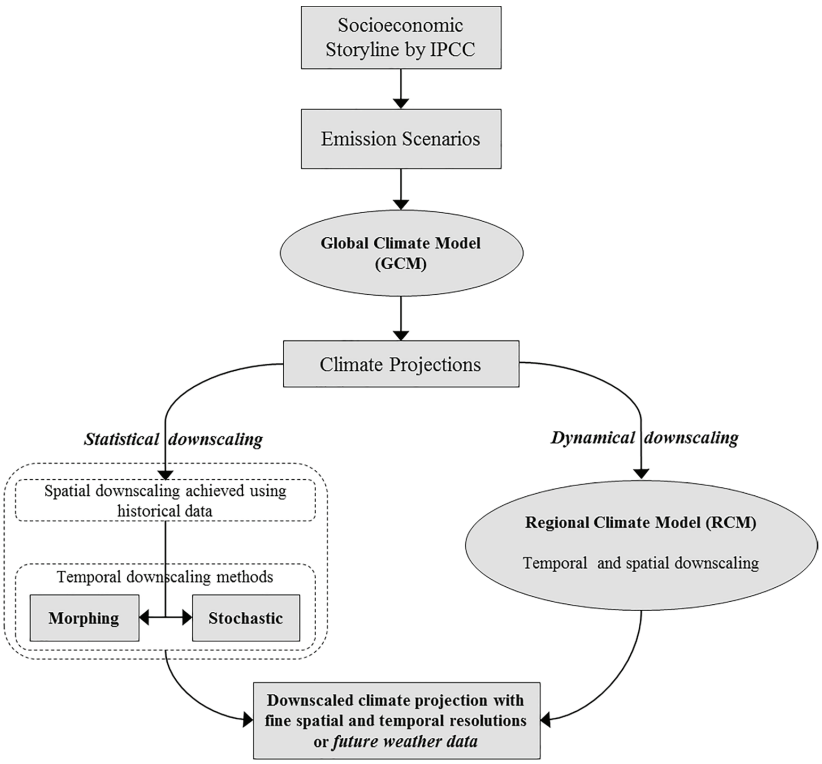

Fig. 2. Flowchart of different approaches for preparing climate projection data with fine spatial and temporal resolution suitable to generate future weather files for BPS.

2.1.2. Statistical downscaling

Statistical downscaling derives estimation of regional or local climate variables from larger-scale climate data using deterministic or stochastic approaches. The difference between the approaches depends on whether an additional noise term for random variability is explicitly included [45]. Until now, the complexity of the dynamical downscaling method and the high level of expertise that is required to interpret the results of the climate simulations have pushed BPS users to favor statistical downscaling. This approach is simpler than dynamical downscaling, however, due to the higher availability of hourly data, which can be directly extracted from RCMs, it is expected that the number of applications for locations worldwide that use dynamical downscaling will increase [46]. The next two sections briefly look into two available approaches (and their assumptions) for statistical downscaling of GCMs.

2.1.2.1. Morphing. The *morphing* downscaling method was proposed by Belcher et al. [47] and applies three transformation algorithms to the hourly values of given weather variables. The algorithms apply changes based on monthly trends and variations of GCM or RCM outputs for a given location. These three algorithms are called *Shift*, *Stretch* and *Combination of shift and stretch*.

(1) Shift is an additive formulation and adds a predicted absolute monthly mean change (Δxm) derived from a GCM or RCM to the hourly values of a weather variable in the weather file (x0) for the month m:

$$x|_m = x_0 + \Delta x_m \quad (1)$$

(2) *Stretch* has a multiplicative formulation and scales the hourly values of a variable in the weather file (x_0) by a predicted relative monthly mean change (α_m) for the month *m*.

$$x|_m = \alpha_m \cdot x_0 \quad (2)$$

(3) The *Combination of shifting and stretching* is a linear combination of the two previous transforming functions. The hourly values of a weather variable in the weather file are both shifted by adding the predicted absolute monthly mean change (Δx_m) and stretched by a predicted relative monthly mean change (α_m) for the month *m*.

$$x|_m = x_0 + \Delta x_m + \alpha_m (x_0 - x_{0,m}) \quad (3)$$

where $x_{0,m}$ is the variable x_0 averaged over month m for all the considered averaging years of future data provided by climate models.

$$x_{0,m} = \frac{1}{24 \times d_m \times N} \sum_{Nyears} \sum_{monthm} x_0$$

where N is the number of years in the averaging period, d_m is the number of days in month m, and 24 h of a day.

One of the three algorithms is applied, which depending on the weather variable. For example, the first algorithm is used for adjusting atmospheric pressure, the second is used for wind speed, and the third for temperature. A guideline on using the above algorithms for the variables in a weather file is given in [47]. CCWorldWeatherGen and WeatherShift are two available tools. They use the morphing method to create climate change weather files starting from EnergyPlus weather files (EPW). Moazami et al. [48] critically compared the output of the two tools to identify the possible consequences of applying these to BPS. The two tools have differences in some of their calculation assumptions, which are discussed in more detail in Sections 3.1.1 and 3.1.2.

2.1.2.2. Stochastic generation. Stochastic weather models are based on a statistical analysis of recorded climate data. The models can derive all other weather variables [49] using the inputs of just a few independent weather variables (e.g. solar radiation). For example, Meteonorm software is a weather generator that uses the interpolation of the principal weather variables to provide weather data for any site in the world [50]. It provides weather variables such as global irradiance on a horizontal plane at the ground level, dry-bulb temperature, dew-point temperature and wind speed. Values are delivered as monthly and yearly long-term means and data time series at the hourly and minute time resolution are generated stochastically and correspond to typical years. The model can generate hourly weather data that can be used as input for BPS. All noteworthy Meteonorm details are given in Section 3.1.3.

2.1.3. Hybrid downscaling

A hybrid approach can, in some cases, be used to reduce the computational resources and storage space required in dynamical downscaling. It is commonly called hybrid downscaling, the outputs of an RCM being stored at a coarse spatial and temporal resolution and further downscaled using the statistical methods. For example, the climate projections for the UK (UKCP09) provide future weather data on a monthly basis at a spatial resolution of 25 km^2. This data is then statistically downscaled to the hourly and/or daily temporal resolution at a 5 km^2 spatial resolution [28]. Another example is the Integrated Multi-scale Environmental Urban Model (IMEUM) in which climate variables estimated at the city scale by RCM data at a 25 km^2 resolution

Table 1
Advantages and disadvantages of downscaling methods.

Downscaling method	Advantages	Disadvantages
Dynamical downscaling using RCM	• Physically consistent data sets across different weather variables [20] • Not constrained by historical data [20]	• Large data sets [20] • Powerful computational resources and expertise required [20]
Statistical downscaling using morphing	• Flexible because it can be applied to the large number of weather files that are available worldwide [54] • Captures localized weather conditions [47,54,7] • The method is simple [47] • Low amount of computational power is required [55]	• Largely analogous to the present-day with lack of details about potential future changes in diurnal weather patterns [54] • Lack of future extreme weather conditions [54] • Potential difference in the reference timeframe of the GCM data and a chosen 'present day' typical weather file causing under- or overestimation of climate change impacts [55] • Lack of physical consistency between climate variables due to the independent 'morphing' of climate variables. It creates a different relationship between the variables to that currently observed at the site [56]
Statistical downscaling using stochastic methods	• Is possible to simulate extreme weather conditions that have not yet been observed, while being statistically representative for the location [7] • Is possible to simulate a wide range of feasible climate conditions [7]	• Relies on statistics derived from historical observations of climate [57] • There is an inherent assumption that future weather patterns will be the same as those observed historically [7] • This method has difficulties in modeling with accuracy some of the climatic variables [58]

are statistically downscaled first to the spatial resolution of 1 km^2 and then to the 100 m^2 resolution [51].

There have been several studies on relative performance of statistical and dynamical or hybrid downscaling methods in climate change impact assessments. Fowler et al. [52] provided a comprehensive insight to the choice of downscaling method when examining the impacts of climate change on hydrological systems. Wilby et al. [53] compared the relative performance of future rainfall projections generated by the range of available downscaling methods. The topic has been also discussed in BPS literature and Table 1 lists and summarizes the main advantages and disadvantages of downscaling methods given in the literature. But there is a lack of work on the effect of using different downscaling methods for generating future weather files on the energy performance of buildings.

All the above mentioned methods are capable of providing high resolution weather data for several years into the future. Weather data in a BPS readable format (e.g., EPW format) is required. Experts achieve this by following the principles used for creating Typical Meteorological Year (TMY) [21]. This method selects twelve typical meteorological months from the basis years to create TMY. The conventional period for the basis years is 30 years, as defined by the World Meteorological Organization (WMO) [59]. In the following section, the approaches that follow the above methods plus some approaches for generating extreme weather years are introduced briefly. All of these approaches are used in this study.

2.2. Generating future weather files ready to use in BPS

2.2.1. Typical future weather data sets

Hall et al. [21] in 1978 developed a method for creating TMY, which is one the most commonly used methods for creating typical weather years. The method selects the most representative month from several years of observed data for a location, for each of the twelve months of a year, based on Finkelstein–Schafer (FS) statistics. It then combines these into one year that is called TMY. It relies on statistical measures of the similarity of the distributions of daily indices such as minimum, mean, and maximum for four climate variables: dry-bulb temperature, dew-point temperature, wind speed and solar radiation [33].

As mentioned before, it is common to use the TMY method to create future typical weather data sets from many years of GCM or RCM generated data. The advantage of using TMY is a decrease in the calculation load (one year represents 30 years) whilst the most representative conditions are taken into account. However, the main disadvantage is neglecting (or underestimating) extreme weather conditions because of the averaging nature of the process [46]. The increasing recognition of climate change, that not only includes changes in average conditions, but also weather extremes [60], also means events such as hurricanes, heat waves and cold snaps will be more frequent and stronger. This phenomena has been studied at several locations around globe including Australia [61], Russia [62], UK [63] and south-east Europe [64]. Existing and new buildings will therefore face more extreme conditions more frequently and at higher intensities than those used to inform their design. As a result, designers should be equipped with methods that allow them to test their design even under extreme conditions.

2.2.2. Future weather data sets taking account of extreme conditions

As previously discussed, buildings should be assessed for more frequent and stronger future extreme weather conditions [65]. It is therefore important to take into consideration these extremes, even from the early design stage. The averaging process in creating TMY files based on 20–30 years of historical data or of future generated weather data, results in a mild year that usually excludes extreme values. Several researchers have suggested using extreme weather data sets rather than just one typical set in building simulations, to ensure that extremes and the probable impacts of climate change are not underestimated. For example, Crawley et al. [3] propose the use of more than one weather file in building simulation. They began, in their study, with four combinations of extremes to create Extreme Meteorological Year (XMY): daily maximum, daily minimum, hourly maximum, hourly minimum for an initial set of variables of dry-bulb temperature, dew-point temperature, solar insolation, precipitation, relative humidity, and wind speed. They used two approaches to select the extreme months. Firstly they looked at the daily maximum and minimum values for each day of the month and selected the month with the highest daily maximum value and the lowest daily minimum. Secondly they looked at the average hourly value for the month and selected the months with the highest hourly and lowest hourly average value. Using prototype building models, they concluded that XMY based on hourly maximum and minimum dry-bulb temperature best captured the range of energy use for the XMY. They suggest that BPS users should use three weather files, one TMY and two XMYs based on hourly maximum and minimum dry-bulb temperature to induce a range of building energy performance.

Another method for generating future weather files that can represent typical and extreme weather conditions was proposed by Nik [46]. The method is based on synthesizing one typical and two extreme (cold and warm) data sets: Typical Downscaled Year (TDY), Extreme Cold Year (ECY) and Extreme Warm Year (EWY). The process for creating a TDY starts by following the method for creating a TMY file, except that just one climate variable (dry-bulb temperature) is considered in the selection of typical months instead of four. There are different reasons for this, which includes the difficulties and uncertainties in weighting the climatic variables, as climate change does not equally affect all climate variables (refer to [46] for additional details). A similar procedure is used to create ECY and EWY data sets. However, instead of looking for the least absolute difference, the years with the maximum (for ECY) and minimum (for EWY) absolute difference are selected as the years representing the extreme temperatures for each month. Nik showed that by using the three data sets and considering TDY, ECY and EWY together (which is called Triple), it is possible to achieve a probability distribution of future conditions which is very similar to the full set of 30 years RCM data.

It was mentioned in Section 2.1.1 that it is necessary to consider several climate scenarios instead of just one scenario in the impact assessment on buildings, due to significant uncertainties in climate modeling. The method developed by Nik [46] was also used to overcome the challenge of climate uncertainties, the method synthesizing one set of representative weather files that takes into consideration several climate scenarios (e.g. in [46], five climate scenarios were considered – i.e. 5 × 30 years of data for a 30-year time span – and TDY, ECY and EWY were synthesized). This allows an impact assessment to be performed under both typical and extreme conditions with a minimum number of required simulation runs and in which climate uncertainty is taken into account.

3. Methodology

A set of 74 weather files were generated to compare the different approaches used in future climate projection. These combine all the available approaches drafted in Fig. 2 for three different future time ranges, as described in detail in Section 3.1.5. The city of Geneva, Switzerland was used in this study as a reference location to generate and compare different future weather data sets using these methods. All data were formatted into the EPW weather file format.

16 reference commercial building models, as proposed by the ASHRAE standard 90.1 [66], were simulated using EnergyPlus [67] to assess the impacts of the typology of future weather data sets on building energy simulations. The buildings cover a wide range of types, from small office buildings to large energy intensive buildings such as hospitals, building models being described in Section 3.2.1. The 16

building models were furthermore used to build a virtual neighborhood in the city of Geneva, to observe the impact at the neighborhood scale. The neighborhood contains the same building typology split as the canton of Geneva (see Section 3.2.2).

3.1. Future weather data for Geneva

The weather data sets that are used in this work were generated using three future weather generator tools (CCWorldWeatherGen, WeatherShift™, and Meteonorm) and one RCM (RCA4, the 4th generation of the Rossby Centre Regional Atmospheric Climate Model [68]). RCA4 data, downscaling four different GCMs, was used in this work.

3.1.1. The CCWorldWeatherGen tool

Jentsch et al. [55] in 2013 provided a methodology for generating future weather data for different locations around the world. They chose the output data of the HadCM3 [69], forced with IPCC A2 emission scenario and applied the morphing method to generate EPW files. The HadCM3 A2 data provided by the IPCC data distribution center (DDC) [70] simulated monthly values of relative changes in climate between the 1961–1990 baseline climate and three future time slices, the 2020s, 2050s and 2080s. They developed a Microsoft® Excel based tool called the *'Climate Change World Weather Generator'*, commonly referred to as CCWorldWeatherGen. This tool superimposes relative change on the weather variables stored in an EPW file and is freely available. It allows the user to generate future weather files for worldwide locations within three time slices: 2011–2040 (referred as '2020s'), 2041–2070 (referred as '2050s') and 2071–2100 (referred as '2080s'). It transforms an original EPW typical weather file into future weather data, formatted in the EPW format and so ready for use in BPS tools. Jentsch describes in detail the potential source of inaccuracy in the outputs of the tool due to the possible difference in the reference timeframe between HadCM3 and the EPW data [55]. For example, in this study the original TMY file is an IWEC (International Weather for Energy Calculations) data file for Geneva, derived from observations collected in the period 1982–1999. As mentioned before, the HadCM3 A2 data are relative changes in relation to the 1961–1990 baseline climate. Applying CCWorldWeatherGen to the IWEC weather file will superimpose the relative changes from the 1961–1990 baseline on to the data from 1982 to 1999. The latter period has higher temperature levels than the 1961–1990 baseline. An overestimation of results in the morphed data set is therefore expected. More details on the generation of climate variables for future weather data are available in [54,47].

3.1.2. WeatherShift™ tool

Arup and Argos Analytics consulting firms developed a tool named *WeatherShift*™ [71,72] based on the RCP4.5 and RCP8.5 emission scenarios of the IPCC Fifth Assessment Report (AR5). This applies the morphing method on to the outcomes of 14 GCMs (out of approximately 40 models) available under AR5 [19]. The tool provides future projection weather data for three time periods: 2026–2045 (referred as '2035s'), 2056–2075 (referred as '2065s'), 2081–2100 (referred as '2090s'). These are relative to the baseline climate of 1976–2005 and under the two emission scenarios. WeatherShift™ moreover provides a cumulative distribution function (CDF) that is constructed for each variable using linear interpolation between the model values [71]. This method was introduced earlier from the UK Climate Impact Programme (UKCIP) for the UK Climate Projections [73]. The CDF enables users to assign a probability to the projections, a sort of 'warming percentile'. For the purpose of this study, the 50th percentile and the RCP 8.5 emission scenario were chosen for setting the tool to generate future weather data sets base on the IWEC weather file of Geneva for the three available time periods.

3.1.3. Meteonorm

This tool is a combination of climate database, spatial interpolation tool and a stochastic weather generator. Meteonorm can calculate typical years with hourly resolution for any site and can also be used for climate change studies. This tool uses the GCMs under the IPCC fourth assessment report (AR4) rather than climate data stored in typical weather files. It can generate future weather files in different formats and according to different IPCC emission scenarios (B1, A1B and A2) for 10-year bins between 2010 and 2100 [57]. The Meteonorm version 7.2 was used in this study to generate a typical weather file and three future weather files for the A2 emission scenario and for the years 2020, 2050 and 2080 for the city of Geneva.

3.1.4. TDY, ECY and EWY out of RCA4

Part of the data from Nik's work [46] is used in this study and transformed into EPW format. The Rossby Centre Regional Atmospheric Climate Model (RCA4) [68] is used to dynamically downscale weather data from four GCMs (Table 2) to the spatial resolution of 12.5 km^2 and the hourly temporal resolution.

The adopted greenhouse gas concentration trajectories are RCP8.5 and RCP4.5 for CNRM and ICHEC, and RCP8.5 for IPSLm and MPIM. This gives an ensemble of six GCM-RCM combinations. RCA4 outputs were used to synthesize TDY, ECY and EWY for three future time periods, 2010–2039, 2040–2069 and 2070–2099. This generated six sets of representative weather data sets (each containing TDY, ECY and EWY) for each time period, resulting in a total of 54 weather files. One group of representative weather data (containing typical and extreme cold and warm) was, furthermore, synthesized by considering all the six climate scenarios at each time period (resulting in a total of nine weather files for three time periods). These files are henceforth called "Multi-Scenario" weather files (referring to the consideration of multiple climate scenarios). The three representative files in this group are named $TDY_{Multiple}$, $ECY_{Multiple}$ and $EWY_{Multiple.}$ For more details, refer to [46].

3.1.5. Generated future weather data sets

Each of the aforementioned methods provide future weather files for slightly different time slices. In the interests of harmonization, three future projected periods namely near-term (NT), medium-term (MT) and long-term (LT) were adopted. The expressions 'Near-Term' and 'Long-Term' are used in chapters 11 [74] and 12 [75] of IPCC AR5 to refer to the time periods 2016–2035 and 2081–2100 respectively. The term 'Medium-Term' is introduced in this work and follows the same logic. Table 3 shows the alignment of the original output periods of the files to the three identified time slices.

Weather files were grouped into two categories to distinguish between different generated future weather data. These were: *typical*

Table 2
The Global Climate Models (GCMs) used in the downscaling process by the Rossby Centre regional atmospheric climate model (RCA4).

Full name	Short name	Originating group	Model version
Centre National de Recherches Météorologiques	CNRM	CNRM/CERFACS, Toulouse, France	cnrm-cm5
Irish Centre for High-End Computing	ICHEC	EC-Earth Consortium, Europe	ec-earth
Institut Pierre Simon Laplace	IPSLm	IPSL, Paris, France	ipsl-cm5a-mr
Max Planck Institute for Meteorology	MPIM	MPIM, Hamburg, Germany	mpi-esm-lr

Table 3
Adopted terms for the variety of time slices used by the different methods or tools.

Adopted Term	CCWorldWeatherGen	WeatherShift™	Meteonorm	RCA4
Near-term	2011–2040	2026–2045	2011–2030	2010–2039
Medium-term	2041–2070	2056–2075	2046–2065	2040–2069
Long-term	2071–2100	2081–2100	2080–2099	2070–2099

weather data sets and *extreme weather data sets*. They include weather files from statistical and dynamical data groups as shown in Fig. 3.

The data sets are grouped into three data groups:

- TMY data group: includes two weather files, the IWEC typical meteorological year (TMY) and a TMY generated by Meteonorm,
- Statistical data group: six weather files generated using the morphing method through CCWorldWeatherGen and WeatherShift, and three weather files generated using the stochastic method through Meteonorm,
- Dynamical data group: 21 weather files generated using dynamical downscaling that represent typical conditions and 42 weather files generated using dynamical downscaling that represent extreme conditions.

Typical weather data sets refer to the files that are generated through statistical downscaling or dynamical downscaling (TDY series). Extreme weather data sets refer to ECY and EWY files that represent extreme cold and warm years (using the RCM dynamically downscaled data). All the above methods provide 72 future weather files for the city of Geneva as shown in Table 4. A total of 74 files were used in this study, including two TMY weather files.

A2, RCP8.5 and RCP4.5 are the three future emission scenarios present in the above list of weather files. According to IPCC fifth assessment synthesis report [76]: RCP8.5 scenario is broadly comparable to A2 scenario and both describe very high GHG emissions, and RCP4.5 is an intermediate scenario. The report further describes: "*Relative to 1850–1900, global surface temperature change for the end of the 21st century (2081–2100) is projected to likely exceed 1.5 °C for RCP4.5 and RCP8.5 (high confidence). Warming is likely to exceed 2 °C for RCP8.5 (high confidence), more likely than not to exceed 2 °C for RCP4.5 (medium confidence)*". The above weather data sets allow considering the uncertainty of climate projections into energy calculations. The span of values resulted from simulations under these weather files, shows the uncertainty of buildings energy performances in future following IPCC emission scenarios, and hence offer the opportunity to test a building under the wide-expected range of climate uncertainty.

3.2. Simulation test bench

3.2.1. Building models

The ASHRAE standard 90.1 suite of commercial reference building models was chosen to be used in this study [77] to assess the impact of climate change on the energy performance of buildings. The commercial reference building models were developed by Pacific Northwest National Laboratory (PNNL), under contract with the U.S. Department of Energy (DOE). These building models were originally derived from DOE's Commercial Reference Building Models with modifications from the ASHRAE 90.1 committee, Advanced Energy Design Guide series, and other building industry expert input. Detailed descriptions of the reference model development and modeling strategies can be found in PNNL's reports [78,79]. The building models used in this study are complying with ASHRAE 90.1-2013 standard. The suite is a collection of standardized building models with realistic building characteristics and includes 16 buildings of different types and dimensions (Fig. 4). The suite provides a simulation bench test to compare the relative impact of using the generated weather files (in Section 3.1) on energy performance of various building types. Technical descriptions of the selected building envelope components, used in building models, are given in Table 5.

ASHRAE 90.1 [66] defines U-factor (U-value) as: "*heat transmission in unit time through unit area of material or construction induced by a unit temperature difference between the environments on each side.*" and defines solar heat gain coefficient (SHGC) as: "*The ratio of the solar heat gain entering the space through the fenestration area to the incident solar radiation.*"U-value and SHGC of glazing in Table 5 are independent of frame material. Roof U-value of the prototype buildings varies between 0.15 and 0.20 W/(m^2 K) depending on the roof type. Wall U-value varies from 0.30 to 0.59 W/(m^2 K) depending on the wall type. For more details, please refer to PNNL's technical report [80].

3.2.2. Virtual neighborhood of Geneva

A combination of the 16 buildings was used to virtually model a neighborhood. We looked at the neighborhood of Champel in Geneva to get an idea of the scale of such a neighborhood, which has a total building area of 328 105 m^2 [81]. The distribution of the areas occupied by the buildings in the canton of Geneva was used to distribute the 16 buildings based on type. In the canton, 64% of buildings are residential and 36% are non-residential and mixed-use buildings [82]. The above assumptions gave the virtual neighborhood created for this study, which had a total energy reference area of 414 341 m^2, 64.3% residential buildings and 35.7% non-residential buildings. The composition of the virtual neighborhood is presented in Table 6. This composition was used only to assess the magnitude of impacts at the neighborhood scale. The spatial attributes of a neighborhood (organization of the buildings and infrastructure between) are not within the scope of this paper.

3.2.3. Simulation workflow

A simulation workflow was implemented in the multidisciplinary design optimization platform modeFRONTIER [84] coupled with MATLAB for post-processing of the output data. This was used to simulate the full set of 16 building models under the 74 generated future weather files, giving a total of 1 184 simulation runs. modeFRONTIER used the algorithm presented in Fig. 5 to perform the simulations.

The dynamic energy simulations of the building models were

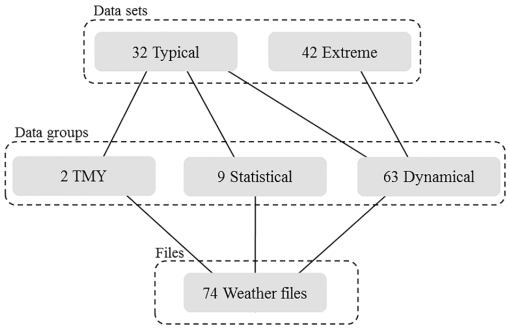

Fig. 3. Weather files are grouped into two categories: typical weather data sets and extreme weather data sets, which include weather files from statistical and dynamical data groups.

Table 4
Weather files generated for the city of Geneva and used in this study.

Method	Tool/GCM/RCM	Emission scenario	Number of weather files	Adopted term
Statistical	CCWorldWeatherGen	A2	3*	CCW_a2
	WeatherShift	RCP 8.5	3	WSH_rcp85
	Meteonorm	A2	3	MTN_a2
Dynamical-typical	MPIM-RCA4	RCP 8.5	3	MPIM_TDY_rcp85
	IPSLm-RCA4	RCP 8.5	3	IPSLm_TDY_rcp85
	ICHEC-RCA4	RCP 8.5, RCP 4.5	3 × 2	ICHEC_TDY_rcp85 ICHEC_TDY_rcp45
	CNRM-RCA4	RCP 8.5, RCP 4.5	3 × 2	CNRM_TDY_rcp85 CNRM_TDY_rcp45
	Multi GCMs-RCA4	RCP 8.5 + RCP 4.5	3	$TDY_{Multiple}$
Dynamical-extreme	MPIM_RCA4	RCP 8.5	3 × 2	MPIM_ECY_rcp85 MPIM_EWY_rcp85
	IPSLm_RCA4	RCP 8.5	3 × 2	IPSLm_ECY_rcp85 IPSLm_EWY_rcp85
	CNRM_RCA4	RCP 8.5, RCP 4.5	3 × 4	CNRM_ECY_rcp85 CNRM_EWY_rcp85 CNRM_ECY_rcp45 CNRM_EWY_rcp45
	ICHEC_RCA4	RCP 8.5, RCP 4.5	3 × 4	ICHEC_ECY_rcp85 ICHEC_EWY_rcp85 ICHEC_ECY_rcp45 ICHEC_EWY_rcp45
	Multi GCMs_RCA4	RCP 8.5 + RCP 4.5	3 × 2	$ECY_{Multiple}$ $EWY_{Multiple}$

* Refers to three time periods; one weather file for each period.

performed using the software EnergyPlus [67] version 8.5.0. Each released version of EnergyPlus undergoes two major types of validation tests [85]: analytical tests according to ASHRAE Research Projects 865 and 1052, and comparative tests according to ANSI/ASHRAE 140 [86] and IEA SHC Task34/Annex43 BESTest method. Heat conduction through the opaque envelope was calculated via the conduction transfer functions (CTF) with a 15-min time step. The natural convection heat exchange near internal and external surfaces was calculated using the thermal analysis research program (TARP) algorithm [87]. The initialization period of simulation was set to the maximum option, which is 25 days [88].

The output parameters that were obtained from EnergyPlus were

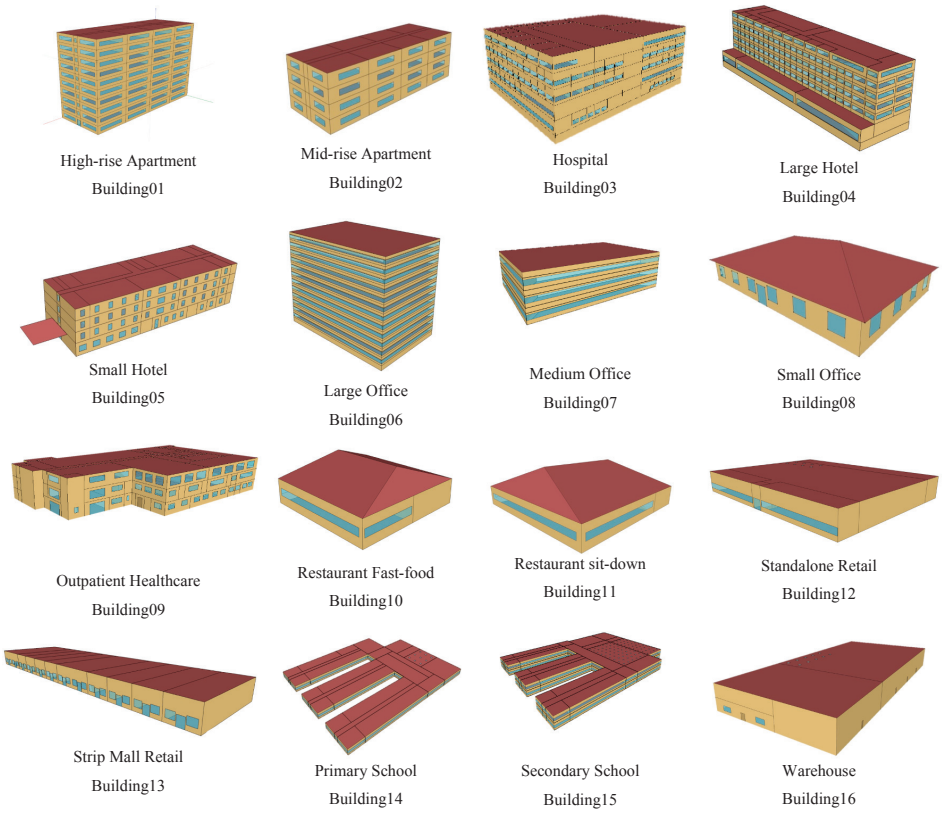

Fig. 4. Reference building models from the ASHRAE Standard 90.1. The total area of these building models and the number of their conditioned zones are presented in Table 6.

Table 5
Technical description of building envelope components of reference building models.

Building Type		U-value (W/(m^2 K))									SHGC	
		Roof			External Wall				Glazing		Glazing	
		I	II	III	I	II	III	IV	Windows	Skylight	Windows	Skylight
Apartment	High-rise	0.18	–	–	0.36	–	–	–	0.42	–	0.40	–
	Mid-rise	0.18	–	–	0.36	–	–	–	0.42	–	0.40	–
Hotel	Large	0.18	–	–	–	0.51	0.59	–	0.42	–	0.40	–
	Small	0.18	–	–	0.36	–	–	–	0.42	–	0.40	–
Office	Large	0.18	–	–	–	–	0.59	–	0.42	–	0.40	–
	Medium	0.18	–	–	0.36	–	–	–	0.42	–	0.40	–
	Small	–	0.15	–	0.36	–	–	–	0.42	–	0.40	–
Health	Hospital	0.18	–	–	–	0.51	0.59	–	0.42	–	0.40	–
	Outpatient	0.18	–	–	0.36	–	–	–	0.42	–	0.40	–
Restaurant	Fast-food	–	0.15	–	0.36	–	–	–	0.42	–	0.40	–
	sit-down	–	0.15	–	0.36	–	–	–	0.42	–	0.40	–
Retail	Standalone	0.18	–	–	–	–	0.59	–	0.42	0.75	0.40	0.6
	Strip Mall	0.18	–	–	0.36	–	–	–	0.42	–	0.40	–
School	Primary	0.18	–	–	0.36	–	–	–	0.42	0.75	0.40	0.6
	Secondary	0.18	–	–	0.36	–	–	–	0.42	0.75	0.40	0.6
Warehouse	Warehouse	–	–	0.20	–	–	–	0.30	0.42	0.75	0.40	0.6

delivered energy for space heating and cooling, and delivered energy for total electricity including electricity for heating, cooling, lighting, fans, domestic hot water and appliances. Delivered energy is defined in the ISO 52000-1:2017 standard [83] as: “energy, expressed per energy carrier, supplied to the technical building systems through the system boundary, to satisfy the uses taken into account (heating, cooling, ventilation, domestic hot water, lighting, appliances, etc.) or to produce electricity”.

In the next step, delivered energy is converted to primary energy which is defined by the standard [83] as: “energy that has not been subjected to any conversion or transformation process”.

Using primary energy allows comparisons of the energy performance of several building types that use different technical building systems supplied by different energy carriers. The primary energy conversion factors stipulated in Swiss norm SIA 380/1:2009 [89] were used. According to this standard, the factor for converting electricity to primary energy is 2.97 kWh_{PE}/kWh_{el} and for converting natural gas to primary energy is 1.15 kWh_{PE}/kWh_{gas}.

4. Results and discussion

The analysis uses graphical comparisons and statistical metrics to characterize the differences between the future weather projections generated using statistical and dynamical downscaling methods. For the sake of harmonization, all the graphs in this section use the color black for the TMY data group, green for the statistical data group, blue for typical weather files (TDY series) and red for extreme weather files (ECY and EWY series) of the dynamical data group. This section firstly presents the distributions of values for hourly dry-bulb temperature in all the weather files. Then the impacts of future weather data type on the energy simulation of buildings are assessed using just typical weather data sets. The final part of the results focuses on the importance of considering extreme conditions in designing buildings and energy systems for buildings.

4.1. Comparison of generated weather files

Each EPW weather file contains the hourly values for an entire year for a number of weather variables, e.g. dry-bulb temperature, dew-point temperature, direct and diffuse solar radiation, wind speed, and wind direction. All the generated files that were used in this study contained information on the effect of climate change on at least the following climate variables:

- Dry Bulb Temperature
- Dew Point Temperature
- Relative Humidity
- Direct Normal Radiation
- Diffuse Horizontal Radiation
- Global Horizontal Radiation
- Wind Speed

All the above items are used directly in the EnergyPlus program, which means that the results reported in this study are already affected by changes to all these variables. Boxplots of the outdoor dry-bulb air temperature, which are one of the key variables in energy simulation [3], are plotted in Fig. 6. The effect of climate change on different climate variables and the uncertainty of estimating these variables by climate models are discussed in previous works of the authors [14,32,46,90]. See Appendix B for boxplots of three other climate variables, global horizontal radiation, relative humidity and wind speed. There are boxplots for all the 74 weather files, all showing values for near-term (NT), medium-term (MT) and long-term (LT) periods. The distributions of the outdoor dry-bulb air temperature are compared with the distribution of maximum and minimum daily values for observed data for the period 1955–2017. These are used as a reference or control sample. Observed data are based on weather data from the Genève-Cointrin weather station obtained from National Centers for Environmental Information (NCEI) [91]. The brown dashed lines project lower and upper whiskers of daily minimum and daily maximum distributions of temperature and the brown horizontal dotted line marks the average daily temperature for the period of observed data.

Fig. 6 shows a pattern of continuous increase in the average dry-bulb temperature from NT to MT and LT, and for all future weather files. The slope of increase is greater for weather files with A2 and RCP 8.5 emission scenarios than for RCP 4.5, which is in agreement with the GCM projections for these scenarios. An increasing trend exists for all generated weather files. However, the maximum values of typical future weather files only get close to the historical observed value of maximum temperature under LT. This reveals the weakness of typical weather files in representing extreme conditions, as is discussed in Section 2.2.2. For extreme weather data sets, the distribution of EWY series for the RCP8.5 scenario is close to the observed maximum daily temperatures and the ECY series of RCP4.5 is close to the distribution of observed minimum daily temperatures. Using Multi-Scenario files therefore improves the coverage of both maximum and minimum borders of the distributions for dry-bulb temperature. These files

Table 6
Composition of the 16 ASHRAE standard 90.1 reference buildings in the virtual neighborhood for city of Geneva.

Building number	Name	floor Area of Thermally conditioned space[1] (m^2)	Number of floors	Number of thermal zones[2]	Windows-to-wall ratio[3]	Number of building type in the neighborhood[4]	Percentage of floor area in the whole neighborhood[5]
Building01	High-rise apartment	7 059.9	10	80	30%	20	37.8%
Building02	Mid-rise apartment	2 824.0	4	32	20%	35	26.5%
Building03	Hospital	22 436.2	5	162	16%	1	5.4%
Building04	Large hotel	10 736.3	6	195	30.2%	1	2.6%
Building05	Small hotel	3 725.1	4	54	10.9%	2	1.9%
Building06	Large office	46 320.4	12	74	37.5%	1	11.2%
Building07	Medium office	4 982.2	3	18	33%	3	3.6%
Building08	Small office	511.0	1	6	20.1%	5	0.6%
Building09	Outpatient healthcare	3 804.0	3	118	20%	1	0.9%
Building10	Restaurant fast-food	232.3	1	2	14%	8	0.4%
Building11	Restaurant sit-down	511.2	1	2	17.1%	3	0.4%
Building12	Standalone retail	2 294.0	1	5	7.1%	1	0.6%
Building13	Strip mall retail	2 090.3	1	10	10.5%	1	0.5%
Building14	Primary school	6 871.0	1	25	35%	1	1.7%
Building15	Secondary school	19 592.0	2	46	33%	1	4.7%
Building16	Warehouse	4 835.1	1	3	0.7%	1	1.2%

(1) Defined by ISO 52000-1:2017 [83] as: heated and/or cooled space.
(2) Number of thermal zones in the energy model.
(3) Defined by ASHRAE 90.1 [66] as: The ratio of vertical fenestration areas to the gross above-grade wall area.
(4) Number of each building type in the virtual neighborhood.
(5) Percentage of each building type in the total floor area of the neighborhood.

approximately cover the distributions of all other dynamical data group files. This means that it is possible to reduce the number of simulations by using Multi-Scenario weather files instead of several weather files (six in this case) with different climate scenarios, as was shown in [46] and [90].

Climate change affects climate variables and their long-term and short-term variations. Statistical data group weather files are only able to capture information on the long-term changes that are provided by the original GCM outputs (with monthly time resolution). These types of files are generated under the assumption that short-term future weather patterns will follow the same pattern and climate variability as historical weather data. They therefore cannot represent probable future extreme conditions due to climate change. Conversely, the weather files of the dynamical data group are not constrained by historical data. To better illustrate the difference between the two types of weather data, the hourly outdoor dry-bulb temperature for one day (1st February as an example) is plotted in Fig. 7 for statistical data group weather files and one dynamical data group weather file under NT, and compared with TMY IWEC.

As expected, the hourly temperature profiles of the CCW_a2, WSH_rcp85 and MTN_a2 future weather files in Fig. 7, the statistically downscaled type, have a very similar pattern to the TMY IWEC file with a higher average temperature. The MPIm_rcp85 dynamical group file does not, however, match the other profiles. This again points to the fact that weather files generated using statistical methods cannot represent short-term variations of climate conditions induced by climate change.

The annual and seasonal averages for dry-bulb temperature and their monthly variations are compared in Table 7 for 14 cases to investigate the long-term changes of average values and variations of climate variables. The 14 cases are: 30 years of observed data (1961–1990), 12 typical weather files (TMY data group, the statistical data group and TDY series of the dynamical data group) and "$Triple_{Multiple}$" which is the average of values for $TDY_{Multiple}$, $ECY_{Multiple}$ and $EWY_{Multiple}$, all under LT. The meteorological seasons were defined by Palatine Meteorological Society (1780) as periods of three months: winter starting on 1st December, spring on 1st March, summer 1st June and autumn on 1st September [92]. The absolute difference between weather files and the observed data is shown in Table 7 under "Absolute change to the baseline period 1961–1990", to help us better understand the differences between the weather files and the observed data.

The annual average temperature shows an increase for all future weather files under LT of between 0.2 and 5.2 °C in relation to the 1960–1991 baseline period. It can be highlighted that values of TMY IWEC also show an increase in annual average temperature. This can be the reason for relatively higher values of CCWorldWeatherGen and WeatherShift outputs, as discussed in Section 3.1.1. The range of values for different scenarios highlights the importance of considering several scenarios for climate change impact assessment, as emphasized by IPCC [93] and other studies (e.g., [94]).

It is also interesting to see the seasonal variations in the weather files. Table 7 shows that the highest increase of temperature in relation to the baseline for weather files and with A2 and RCP8.5 emission scenarios is in summer (except for CNRM_rcp85). Interestingly, the highest increase for weather files with RCP4.5 scenarios occurs in winter. Another notable result for RCP4.5 weather files is the decrease in temperature during spring.

$TDY_{Multiple}$ is generated to represent all the six climate scenarios in the dynamical data group. The values of annual and seasonal averages for this file are close to the mean of the other 6 scenarios. Comparing $TDY_{Multiple}$ with $Triple_{Multiple}$ shows that considering $TDY_{Multiple}$, $ECY_{Multiple}$ and $EWY_{Multiple}$ together ($Triple_{Multiple}$) results in higher values of annual and seasonal averages rather when considering $TDY_{Multiple}$ alone. Furthermore, these values show that the $Triple_{Multiple}$ is more extreme, with warmer summers and colder winters than the $TDY_{Multiple}$.

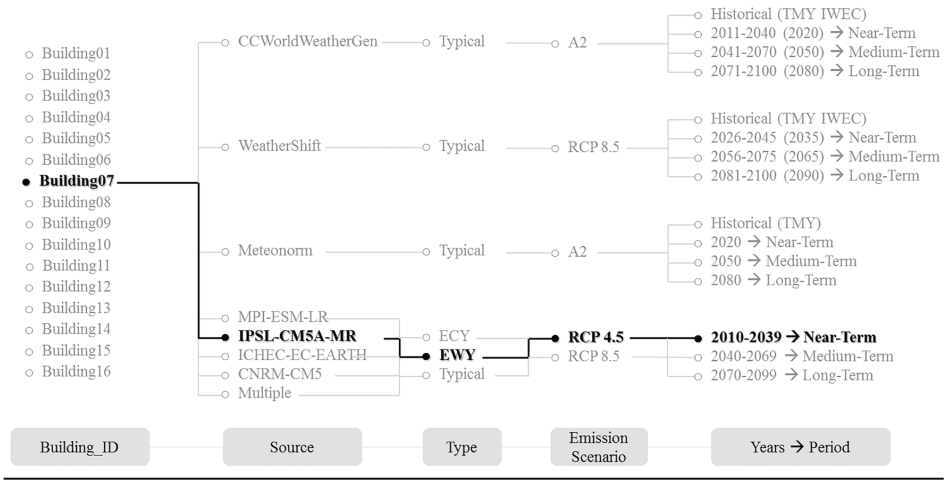

Fig. 5. Configuration of simulation runs of 16 reference buildings under the generated future weather files. Simulation of building number 07, Medium Office, using weather file 'IPSL_EWY_rcp45_NT.epw' is highlighted as an example.

4.2. Climate change impact assessment using only typical weather files

In this section, the hourly primary energy for space heating and cooling (defined in Section 3.2.3) requirements per square meter for the 16 reference buildings are calculated for one year under typical weather data sets. Fig. 8 shows the distribution of calculated values for all the buildings.

The boxplots in Fig. 8 for both statistical and dynamical under all

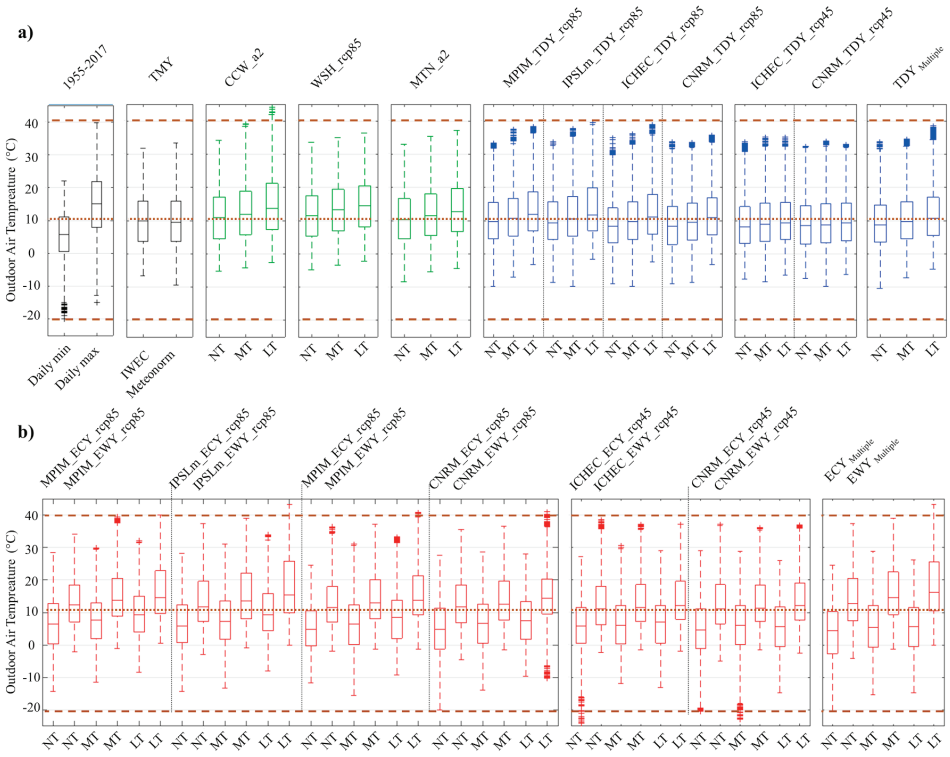

Fig. 6. Boxplots of the outdoor dry-bulb air temperature for the weather files generated by three software tools–CCWorldWeatherGen, WeatherShiftTM, Meteonorm –and six combinations of GCM-RCMs with different emission scenarios. The dashed lines show the lower w whiskers for minimum daily temperature and the upper whiskers of the maximum daily temperature and the horizontal dotted brown lines show the average according to recorded data from 1955 to 2017 of Genève-Cointrin weather station. (a) Historical observed data and typical weather data sets, (b) extreme weather data sets.

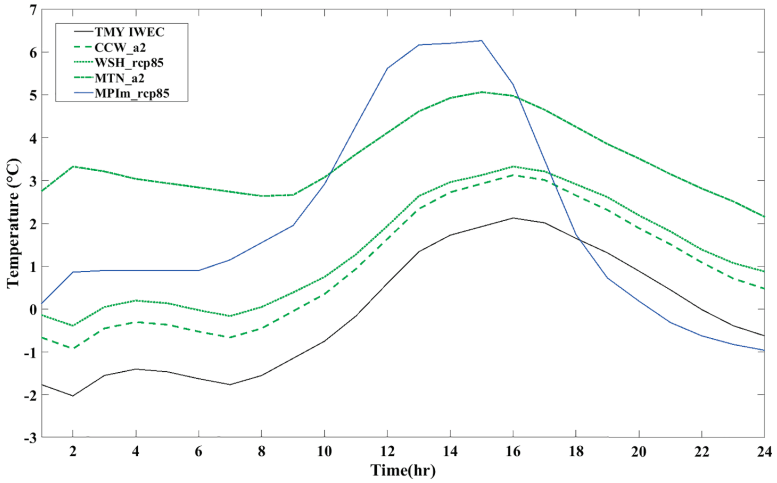

Fig. 7. Hourly outdoor dry-bulb temperature for one day (1st February as an example) are plotted for three weather files of statistical group (in green) and one weather file of the dynamical group (in blue) under NT and compared to TMY IWEC (in black).

NT, MT and LT of each building shows that the fast food restaurant has the largest range of primary energy. The range of values for this building is approximately 280–610 kWh/m^2/a for space heating and 30–160 kWh/m^2/a for space cooling. The reason for this can be the high ventilation rate of restaurant buildings compared to other buildings. The hospital has a relatively small range for primary energy for space heating (~85–130 kWh/m^2/a) and space cooling (~40–90 kWh/m^2/a). This is probably due to equipment energy use and other energy end-uses than heating, cooling and ventilation predominating in this building.

Overall, the shifting impact on primary cooling energy and primary heating energy is present for all buildings except building number 16 (warehouse). This might show that climate conditions are not the dominant force driving the energy performance of this building. A similar conclusion was proved for swimming facilities [95]. For some buildings, a heating-load dominated building under NT furthermore becomes a cooling-load dominated building under MT or LT. Examples of this are buildings number 14 and 15 (primary and secondary schools) as discussed by Pagliano et al. [96]. This reveals that both methods are able to provide enough information to show a shift in the energy use of the buildings.

The cumulative distribution of primary energy for heating and cooling for each building was calculated to show the impacts of weather data typology on energy calculations, for both hourly and annual values. As an example, Fig. 9 presents these values for building number 7 (medium office) under NT, MT and LT periods.

Fig. 9 shows that the overall primary energy for cooling for building07 (medium office) increases over time while the primary energy for heating tends to decrease moving from NT to LT. Furthermore, the uncertainty associated with calculating the building's primary energy using different weather files spreads consistently for space cooling but remains quite constant for space heating. The shape and variation of hourly values for cooling primary energy and heating primary energy are very similar for the statistical data group and the TMY IWEC file. This limitation of using the statistically downscaled method for discussing short-term variations has been previously discussed in the first part of the results, Fig. 7 demonstrating that the hourly outdoor temperature profiles of the statistical group have the same pattern as the TMY IWEC file.

The extent of uncertainty for calculating primary energy presented

Table 7
Annual and seasonal averages of outdoor temperature (°C) under LT for typical weather data sets and TripleMultiple (the average of values for TDYMultiple, ECYMultiple and EWYMultiple) and their absolute difference to the values of baseline observed period (1961–1990).

		Mean of monthly values (°C)					Absolute change to the baseline period 1961–1990 (°C)				
		Annual	Seasonal				Annual	Seasonal			
Period	Type		Spring	Summer	Autumn	Winter		Spring	Summer	Autumn	Winter
1961–1990	Observed data	9.6	9.0	17.9	10.1	1.5	0.0	0.0	0.0	0.0	0.0
1982–1999	TMY IWEC	10.4	9.8	18.9	10.3	2.4	0.7	0.8	1.1	0.2	0.9
1961–1990	TMY Meteonorm	9.8	9.1	18.2	10.2	1.8	0.2	0.1	0.4	0.1	0.3
2071–2100 (LT)	CCW_a2	14.9	13.3	25.2	15.1	5.8	5.2	4.3	7.4	5.0	4.3
2081–2100 (LT)	WSH_rcp85	14.8	14.1	23.5	15.2	6.6	5.2	5.1	5.6	5.1	5.1
2080–2099 (LT)	MTN_a2	13.3	11.9	22.7	13.8	4.6	3.6	2.9	4.8	3.7	3.2
2070–2099 (LT)	MPI _rcp85	13.0	11.0	22.5	13.0	5.5	3.4	2.0	4.6	2.9	4.0
	IPSL _rcp85	13.6	10.4	23.3	14.6	5.9	3.9	1.4	5.5	4.5	4.4
	ICHEC _rcp85	12.2	9.8	21.7	12.7	4.5	2.6	0.8	3.9	2.6	3.0
	CNRM _rcp85	11.6	9.5	20.2	12.1	4.5	1.9	0.4	2.3	2.0	3.0
	ICHEC _rcp45	10.2	8.5	18.8	10.6	2.8	0.5	−0.5	0.9	0.5	1.4
	CNRM _rcp45	9.8	7.9	18.3	10.3	3.0	0.2	−1.2	0.4	0.2	1.5
	$TDY_{Multiple}$	11.6	9.5	20.7	12.0	4.3	2.0	0.5	2.9	1.9	2.8
	$Triple_{Multiple}$	11.7	9.9	21.7	12.2	3.1	2.1	0.8	3.8	2.1	1.6

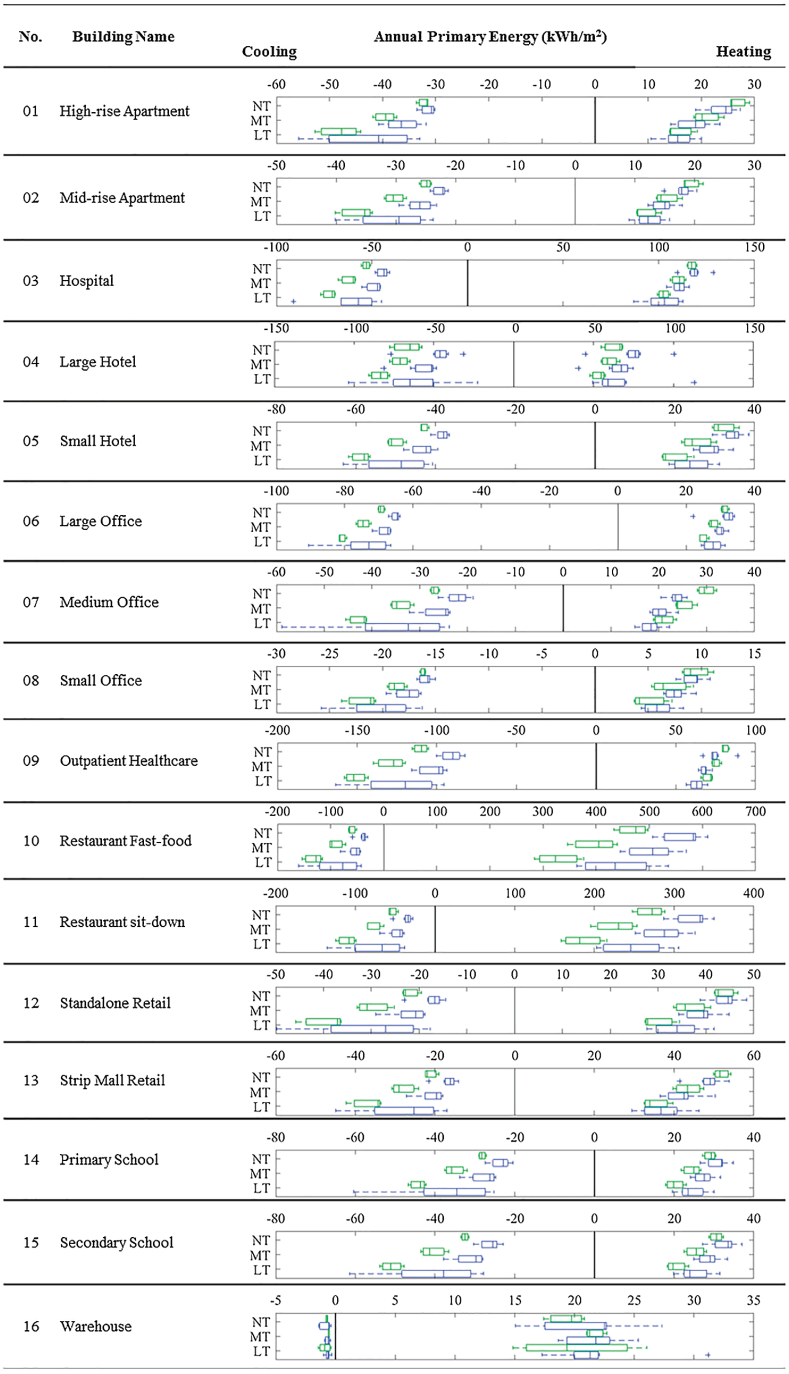

Fig. 8. The boxplots present the distribution of values for the calculated annual primary cooling energy (negative values) and primary heating energy (positive values) under typical weather data sets for all 16 reference buildings. Values of the dynamical data group are presented in blue and the statistical data group in green.

in Figs. 8 and 9 substantiate previous proposals in the literature to prefer the probabilistic approaches for predicting building performance in the future [97] rather than the deterministic ones.

Total primary energy for space air conditioning, which is the sum of both the primary energy for cooling and heating, was calculated for all buildings under future typical weather data sets. Table 8 provides the

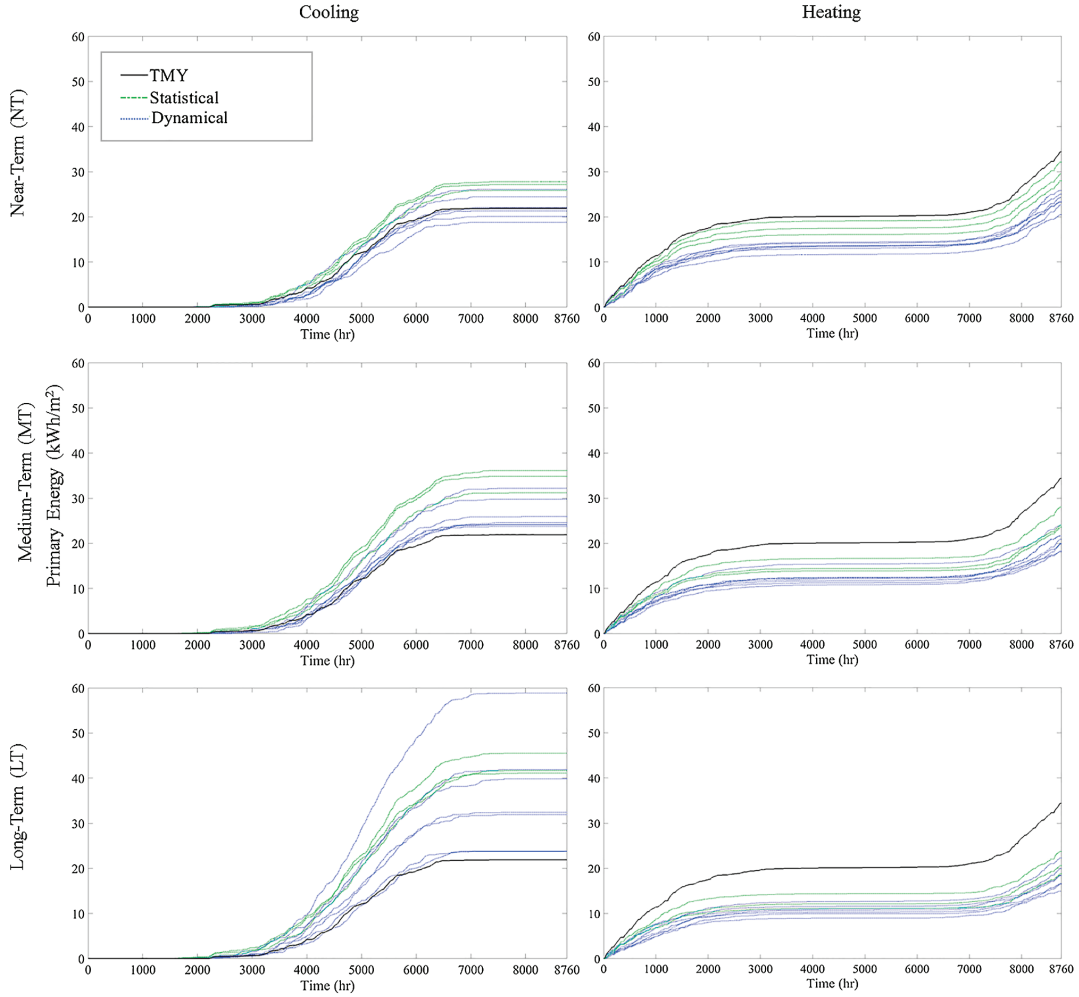

Fig. 9. Cumulative distributions of primary cooling energy (on the left) and primary heating energy (on the right) for building07 (medium office) under typical weather data sets. Results of the dynamical data group are presented in blue color and the statistical data group in green.

mean, median, minimum (min), maximum (max), range, and standard deviation (StDev) values for total annual primary energy and compares these values for the statistical and the dynamical data group.

Table 8 shows that the ranges of calculated annual primary energy demand for the dynamical group are significantly higher than corresponding values for the statistical data group. This can be due to the use of both low emission scenarios RCP4.5 and high emission scenario RCP8.5 in the dynamical data group. Sit-down and fast-food restaurants have, according to StDev values of primary energy in Table 8, the highest variation, which can and as mentioned before are probably due to the high ventilation rate for these buildings. Small office has the lowest variation, which can be due to a constant air volume ventilation system type for this building.

4.3. Climate change impact assessment using both typical and extreme weather files

It was mentioned in Section 2.2.2 that, due to the averaging nature of the process for generating typical years, that this method is unable to provide information on extreme weather conditions. This problem can be illustrated by referring to the heat wave that hit Europe in the summer of 2003. The heat wave caused the death of thousands of elderly and vulnerable people, caused power cuts and many other damage [29]. Several studies have shown daily mortality during heat waves is highly correlated to maximum daily temperature and night temperature (e.g. in France [98,99] and in Switzerland [27]). The Swiss Federal Office of Meteorology and Climatology (MeteoSwiss) provides climate indicators that characterize the climate, indicators such as hot days, frost days and tropical nights. These are also used to communicate how climate is changing. Hot days are defined as “days in which the temperature rises above 30 °C”, frost days are defined as “days on which the temperature dips below 0 °C”, and tropical nights are defined as “days on which the temperature does not dip below 20 °C”. Table 9 shows the numbers of hot days and tropical nights during 92 days of summer in 2003 (1st June-31st August) for the city of Geneva. These values were compared to calculated values for the same period for two TMY weather files (IWEC and Meteonorm), two typical weather files under NT from statistical and dynamical groups (CCW_a2 and

Table 8
Descriptive statistics of the total annual primary energy for heating and cooling of all 16 reference buildings calculated under typical weather data sets for the statistical data group (9 weather files) and the dynamical data group (21 weather files).

No.	Building name	Downscaling method	Total annual primary energy for space conditioning (kWh/m^2)					
			Mean	Median	Min	Max	Range = Max-Min	StDev
01	High-rise Apartment	Statistical	61.2	60.6	57.4	67.0	9.6	3.65
		Dynamical	56.2	55.3	51.2	69.4	18.2	4.477
02	Mid-rise Apartment	Statistical	46.0	45.5	43.2	50.5	7.3	2.522
		Dynamical	41.5	41.1	38.7	51.5	12.8	2.943
03	Hospital	Statistical	172.5	171.6	169.9	176.8	6.9	2.593
		Dynamical	161.8	160.5	155.2	178.2	23	5.65
04	Large Hotel	Statistical	132.1	131.4	125.5	140.6	15.1	5.7
		Dynamical	129.0	125.1	117.3	158.5	41.2	11.09
05	Small Hotel	Statistical	76.5	75.6	73.1	81.3	8.2	2.812
		Dynamical	73.4	72.8	70.1	85.7	15.6	3.273
06	Large Office	Statistical	102.9	102.2	100.3	106.1	5.8	2.279
		Dynamical	99.2	98.0	88.2	116.2	28	4.87
07	Medium Office	Statistical	59.9	59.2	55.1	64.8	9.7	3.26
		Dynamical	48.9	47.1	42.7	75.5	32.8	7.27
08	Small Office	Statistical	26.1	26.0	24.2	28.4	4.2	1.641
		Dynamical	25.6	25.3	23.9	31.4	7.5	1.537
09	Outpatient Healthcare	Statistical	205.3	199.7	188.7	229.9	41.2	14.47
		Dynamical	174.6	167.3	155.6	220.1	64.5	16.24
10	Restaurant Fast-food	Statistical	492.5	499.6	411.4	549.3	137.9	43.4
		Dynamical	563.9	560.1	467.8	645.5	177.7	47.9
11	Restaurant sit-down	Statistical	307.7	314.9	266.3	334.4	68.1	21.88
		Dynamical	339.4	334.8	291.4	382.5	91.1	25.57
12	Standalone Retail	Statistical	67.2	66.2	64.2	73.5	9.3	3.2
		Dynamical	62.2	61.0	57.0	81.7	24.7	5.3
13	Strip Mall Retail	Statistical	72.2	73.3	66.8	76.2	9.4	2.907
		Dynamical	64.5	63.5	57.8	79.8	22	4.88
14	Primary School	Statistical	60.4	59.3	56.2	66.6	10.4	3.59
		Dynamical	57.3	55.2	52.5	83.9	31.4	6.82
15	Secondary School	Statistical	66.8	66.0	62.2	73.6	11.4	3.91
		Dynamical	61.8	59.8	57.4	85.4	28	6.42
16	Warehouse	Statistical	21.1	21.5	16.3	26.4	10.1	2.876
		Dynamical	22.2	22.3	16.2	31.5	15.3	3.327

Table 9
Comparison of the number of hot days (Tmax ≥ 30 °C) and tropical nights (Tmin ≥ 20 °C) for the extremely hot summer of 2003 in Geneva calculated from different weather data sets.

		Number of hot days	Number of tropical nights
Observed data	Summer 2003*	51	4
TMY	IWEC	8	1
	Meteonorm	4	3
Near-Term (NT) future	CCW_a2	26	4
	$TDY_{Multiple}$	10	0
	$EWY_{Multiple}$	54	13

* Based on meteorological data from Genève-Cointrin weather station provided by National Centers for Environmental Information (NCEI) [91].

$TDY_{Multiple}$) and one extreme warm weather file ($EWY_{Multiple}$).

It can be highlighted from Table 9 that only the $EWY_{Multiple}$ weather file value is comparable with the number of hot days that occurred during the summer of 2003 in Geneva. The TMY file and future typical weather file values are far from observed values. The above example reveals how the averaging process can result in missing extreme values and therefore shows how systems designed taking into consideration only typical conditions could quickly become a costly mistake (due to under-dimensioning). The 16 buildings models were simulated in this section under both typical and extreme weather data sets for the dynamical data group, to assess the impact of extreme conditions on the energy performance of buildings. Three sets of weather data were considered for the purpose of this analysis; $TDY_{Multiple}$, $ECY_{Multiple}$ and $EWY_{Multiple}$. These represent all six climate scenarios in the dynamical data group. Fig. 10 represents the distribution of hourly energy demands taking into consideration (i) only $TDY_{Multiple}$ (8760 values), and (ii) all the three sets together, which is referred to as $Triple_{Multiple}$ (3 × 8760 values). Boxplots of hourly energy demand for cooling and heating are presented for the buildings and three time periods. This technique allows us to investigate the impact of taking into consideration extreme conditions on the distribution of heating and cooling demands for each building.

The most remarkable result to emerge from Fig. 10 is the impact of taking into consideration extreme values on the distribution of cooling demand, specifically peak values. Almost all the peak cooling demand values of all buildings are considerably higher for the $Triple_{Multiple}$ case than for the $TDY_{Multiple}$ case. This means that designing energy systems based on peak values for typical weather conditions is not the most reliable approach for future climatic conditions of stronger extreme events. The 'triple' approach allows the assessment of building performance not only under typical conditions, but also considering extreme weather conditions. Actual energy demand in commercial buildings is frequently demonstrated to be much greater than the expected energy demand obtained from the energy modeling of the buildings. This difference, often referred to as the energy performance gap, means that actual energy demand can be two to three times the modeled energy demand [100]. Much of the focus in reducing the energy performance gap is on post-construction elements such post-occupancy evaluation and continuous commissioning. Improvements in the energy simulation, such as the consideration of extreme weather conditions, however play a key role for new builds and energy-focused refurbishments.

Table 10 presents the peak loads of the cooling demand with the date and time of occurrence for each of the 16 buildings, typical and extreme warm conditions taken into consideration. The magnitude of the peaks and the time in which they occur are different for each building. This is obviously due to the variance in the type of buildings, their characteristics and their operation schedules. The peak values for

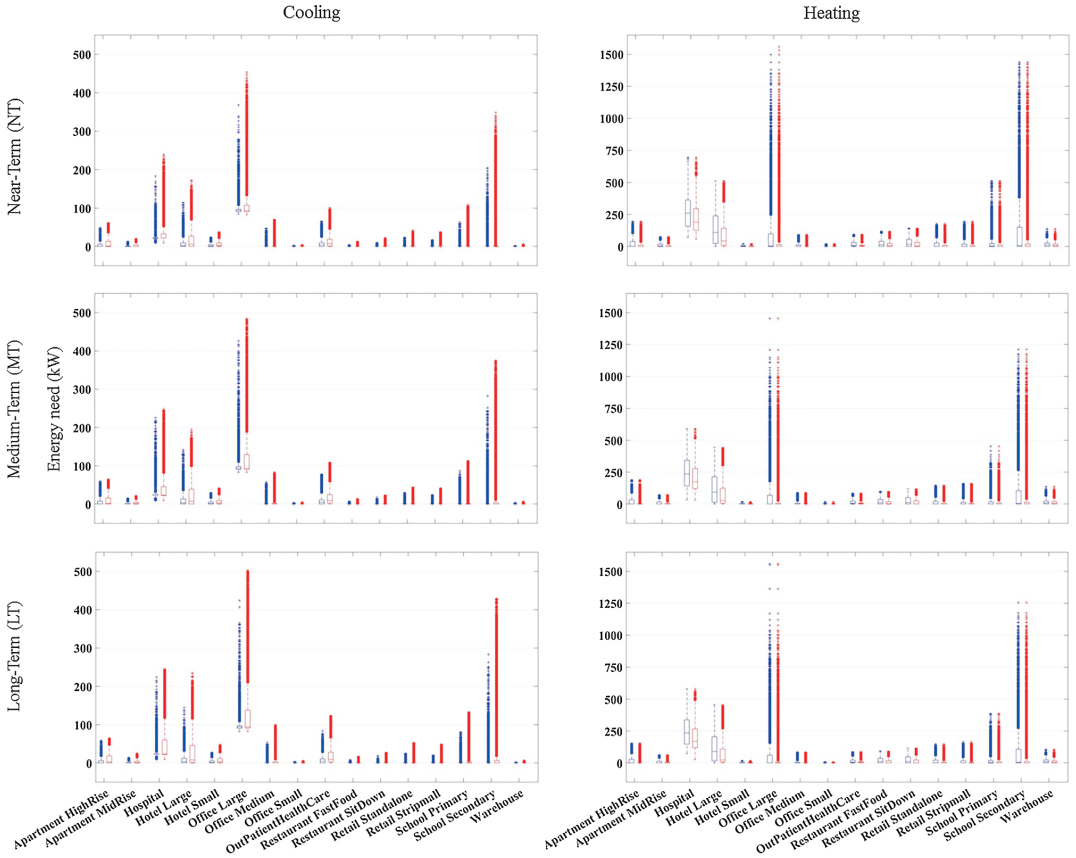

Fig. 10. Boxplot of hourly cooling demand and heating demand for all 16 reference buildings under Typical weather year (TDYMultiple) scenario in compare to demand under TDY, ECY and EWY all together ($Triple_{Multiple}$) scenario. Blue is used for $TDY_{Multiple}$ and red color is for $Triple_{Multiple}$ weather file.

$EWY_{Multiple}$ compared to $TDY_{Multiple}$ ranges from a 2% increase for the hospital to a 28.5% increase for the sit-down restaurant. The findings from Fig. 10 and Table 10 illustrate the importance of considering extreme conditions and the usefulness of the suggested approach in ensuring a robust design of buildings and energy systems for the future.

In the second part of our analysis on the impact of extreme

Table 10
Value of Peak cooling demand and the date-time of occurrence under NT for all buildings and the virtual neighborhood, values for dynamical-typical and dynamical-extreme are presented and compared.

Building name	Dynamical-typical $TDY_{Multiple}$		Dynamical-extreme $EWY_{Multiple}$		Peak cooling load relative change $EWY_{Multiple}$ to $TDY_{Multiple}$ (%)
	Peak load for cooling (kW)	Date-Time	Peak load for cooling (kW)	Date-Time	
High-rise Apartment	59.97	19 Jul-17:00	62.27	24 Jul-19:00	3.8%
Mid-rise Apartment	18.76	19 Jul-15:00	21.22	27 Jul-15:00	13.1%
Hospital	235.01	20 Jun-15:00	239.67	24 Jul-15:00	2.0%
Large Hotel	147.61	28 Jul-19:00	172.21	19 Jul-16:00	16.7%
Small Hotel	34.71	19 Jul-16:00	38.06	27 Jul-16:00	9.6%
Large Office	430.21	20 Jun-17:00	453.95	24 Jul-15:00	5.5%
Medium Office	63.03	19 Jul-15:00	70.55	27 Jul-16:00	11.9%
Small Office	5.00	19 Jul-16:00	5.47	27 Jul-16:00	9.5%
Outpatient Healthcare	93.32	20 Jun-15:00	100.82	7 Jul-16:00	8.0%
Restaurant Fast-food	11.30	19 Jul-13:00	14.16	3 Jul-18:00	25.4%
Restaurant sit-down	17.96	19 Jul-12:00	23.08	3 Jul-18:00	28.5%
Standalone Retail	34.69	19 Jul-15:00	42.29	27 Jul-15:00	21.9%
Strip Mall Retail	30.57	19 Jul-15:00	38.64	27 Jul-15:00	26.4%
Primary School	97.27	20 Jun-15:00	109.06	13 Jun-15:00	12.1%
Secondary School	316.51	20 Jun-15:00	348.09	13 Jun-15:00	10.0%
Warehouse	5.54	19 Jul-16:00	6.78	27 Jul-17:00	22.5%
Neighborhood	3457.14	19 Jul-16:00	3753.82	27 Jul-16:00	8.6%

conditions, we assess the impacts on high peak energy demand loads on the virtual neighborhood defined in Section 3.2.2. The last row of Table 10 presents the peak cooling demand load and the date and time of occurrence for the entire neighborhood. The relative change of peak load in extreme conditions compared to typical conditions is an increase of 8.6%.

As shown in Table 10, the need for air conditioning increases dramatically during extreme hot conditions. This high demand can last for days to weeks. Additionally, as mentioned before, the production capacity of power plants can be affected during this period. For example, as described by Ke et al. [101], heat waves are usually accompanied by stationary high pressure zones, resulting in light winds at the surface and therefore reduced wind generation. Increased air temperature also causes a reduction in capacity and the efficiency of gas-turbines. Even electricity transmission line loss is affected by high ambient temperature. These chains of events and high demands for a period of time implies high stress on the grid, which can lead to the failure of the system, as in the 2006 heat wave in New York City [102]. Electrical power demand of the virtual neighborhood under typical and extreme conditions was calculated to illustrate such risks at the urban scale. Fig. 11 shows the power demand for the neighborhood during the week of the peak loads for $EWY_{Multiple}$ compared to TMY and $TDY_{Multiple}$ under NT. Electric power demand was calculated by adding up for each hour the delivered energy for total electricity (defined in Section 3.2.3) for all the buildings in the neighborhood.

The minimum level of electricity demand required over a period of 24 h is referred as 'base load'. For the virtual neighbourhood based on Fig. 11, under TMY IWEC this value is around 4.5 MW. This increased throughout the five-day workweek, passing 9 MW and during the weekend remaining below 9 MW at peak. Base load is the minimum power generation requirement and is usually covered by dedicated base-load power plants [103]. The criticality is during the peak load hours, which are from 2 pm to 6 pm on weekdays and 4 pm to 9 pm during the weekend, in the case of the virtual neighborhood. The so-called peak-load power plants are usually used to cater for the demand peaks. They have a relatively high fuel cost compared with base-load power plants and they are started up whenever there is a spike in demand and stopped when the demand recedes. For the neighborhood, the peak value for TMY occurs on Friday 18 August at 5 pm, the value being 10.23 MW. This value for $TDY_{Multiple}$ is slightly higher than TMY and is 10.29 MW on Tuesday 20 June at 4 pm. The peak values for the extreme case $EWY_{Multiple}$ is above 10.28 MW for 4 days, the highest value being 10.64 MW on Thursday 27 July at 4 pm. The hourly electricity demand during the days of extreme conditions furthermore stays above values of typical conditions for almost the whole week. The peak electricity demand values for the neighborhood for $EWY_{Multiple}$ under MT and LT are 11.01 MW and 11.95 MW respectively. This means that the value of peak electricity demand can increase by 4.0%, 7.6% and 16.8% for extreme conditions under NT, MT and LT in relation to the TMY IWEC value. Power plants can, as described before, suffer reductions in efficiency during extreme conditions (heat waves), with a consequential reduction in the capacity of the energy system to cover peaks. Taking into account these issues and looking into the increase in electricity demand for the virtual neighborhood under extreme conditions, it might become a challenge for the energy system of this neighborhood to cover the margin, especially in the likely event of a reduction in generation capacity. The simulation test bench used in this study is developed based on 2013 version of ASHRAE 90.1 standard, which means the models are compliant with a recent energy code. Therefore, the above impacts can be magnified considerably if considering presence of older buildings with envelopes that have lower thermal performance; hence their energy performance is more sensitive to climate conditions. The single most marked observation that emerges from data comparison is the importance of considering extreme conditions to assure the robustness of the designed buildings or energy systems.

5. Conclusions

In this work, the dynamical and statistical methods for downscaling the outputs of GCMs were discussed and two approaches for preparing future weather data for building energy simulations were investigated, one based on using only typical weather conditions and the other based on using typical and extreme conditions. 74 weather files for the city of Geneva, Switzerland were generated using the methods and approaches considered. These were used to understand and compare the assumptions, limitations and advantages of the methods and approaches in predicting the future energy conditions of buildings. According to the results, weather files of the statistical data group are able to present the long-term impacts of climate change on averages (e.g. a gradual increase in the average dry-bulb temperature for Geneva). However, these files are not suitable for investigating the short-term changes that induce extreme weather conditions.

The ASHRAE standard 90.1 suite for commercial buildings was used to study the impacts of the future weather data type on the energy

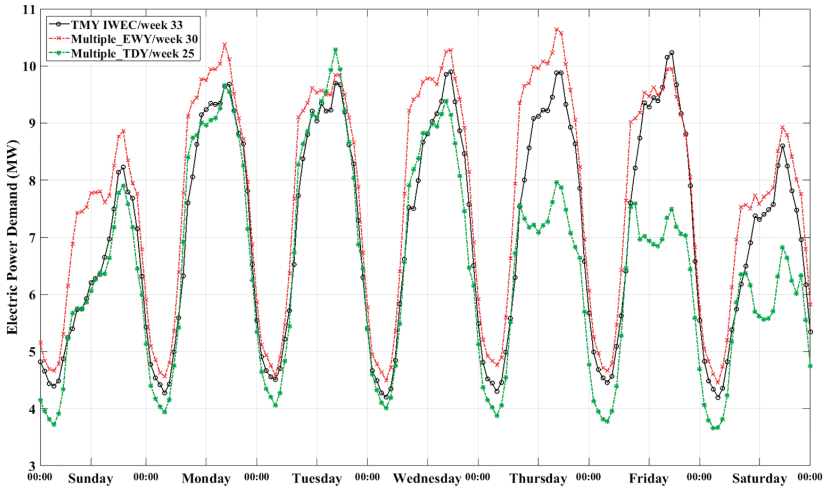

Fig. 11. The electrical load profile of virtual neighborhood for a peak summer week in Geneva, considering historical typical weather year (TMY), future typical weather year (TDYMultiple) and future extreme warm weather year (EWYMultiple) under NT.

simulation of buildings. This suite of models allows reasonably realistic building characteristics for small office buildings to large energy-intensive buildings such as hospitals, and mid to high-rise residential buildings. According to the results, all the considered types of typical weather data sets provide enough information to study the log-term shift in energy use of the buildings and using the weather files generated by statistical methods can be sufficient. Moreover, typical weather files generated from dynamically downscaled data would also reveal the shifting of energy.

This worked investigated the importance of considering extreme conditions and the possible consequences of neglecting such conditions in designing buildings at building level and neighborhood scale. The approach proposed by Nik [46] was used to generate representative weather files. This approach is based on synthesizing three weather data sets for each 30-year period: typical downscaled year (TDY), extreme cold year (ECY) and extreme warm year (EWY). Firstly, the number of hot days and tropical nights were calculated for different types of weather files according to the definitions of MeteoSwiss. These values were compared to the values observed during the extreme heat wave of the summer of 2003. The results showed only the value derived from the extreme weather file is comparable with the number of hot days that occurred during the summer of 2003 in Geneva. This number is considerably small for the cases where only typical weather data sets (TMY and TDY) are considered. Furthermore, a group of representative weather data sets based on multiple climate scenarios ($TDY_{Multiple}$, $ECY_{Multiple}$ and $EWY_{Multiple}$) were considered to evaluate the impacts of extreme conditions on the energy performance of all 16 buildings and a virtual neighborhood. According to the results, for the near-term future, the range of relative change of peak load for cooling demand under extreme conditions shows an increase of 2–28.5%, compared to typical conditions depending on the building type. Furthermore, the analysis of the virtual neighborhood revealed that the peak electric power demand for the neighborhood can increase by 4.0%, 7.6% and 16.8% under near-term, medium-term and long-term future for extreme conditions in relation to the value calculated using the TMY file. These results underline the importance of considering extreme conditions in studying the impacts of climate change on larger spatial scales (e.g. urban and city scales) and preparing urban energy systems for future conditions.

The focus of this paper was on the impacts of long-term patterns of climate change and extreme weather conditions on the energy performance of buildings. Future work should be undertaken using different methods of generating future weather files to study the thermal stress upon building occupants. It might, furthermore, be necessary to consider the effects of urban/micro climate (depending on the case), as the effects of climate change might be amplified or diminished at the urban scale, especially for extreme conditions.

In conclusion, our work provided further evidence that proper weather data sets based on high resolution data from climate models and several climate scenarios, including extreme conditions, are required to empower building engineers and architects to test their design solutions under future climate uncertainties. As discussed before, a large part of literature with focus on the impacts of future climate conditions on the performance of buildings are from the UK, where such weather files are readily accessible for several locations. It shows that the availability of such files is crucial and requires efforts at national levels. Only this type of approach will involve more experts into the discussion of finding solutions that guarantee a more robust and climate resilient built environment in the future.

Acknowledgements

This work has been written within the Research Centre on Zero Emission Neighborhoods in Smart Cities (FME ZEN). The authors gratefully acknowledge the support of the ZEN partners and the Research Council of Norway. This work has partly benefited from the support of the Swedish Research Council for Environment, Agricultural Sciences and Spatial Planning (Formas) which is gratefully acknowledged.

Appendix A

No.	Title	Year	Country
1	Climate change impacts on the thermal performance of Portuguese buildings. Results of the SIAM study	2002	Portugal
2	Climate change impacts on building heating and cooling energy demand in Switzerland	2005	Switzerland
3	The impact of climate change uncertainties on the performance of energy efficiency measures applied to dwellings	2005	UK
4	Climate change, thermal comfort and energy: Meeting the design challenges of the 21st century	2007	UK
5	Creating weather files for climate change and urbanization impacts analysis	2007	US
6	Embodied and operational carbon dioxide emissions from housing: a case study on the effects of thermal mass and climate change	2008	UK
7	Estimating the impacts of climate change and urbanization on building performance	2008	US
8	Beyond TMY: climate data for specific applications.	2008	Australia
9	Uncertainties in predicting the impact of climate change on thermal performance of domestic buildings in the UK	2008	UK
10	Climate change future proofing of buildings-Generation and assessment of building simulation weather files	2008	UK
11	Evaluating the potential impact of global warming on the UAE residential buildings - A contribution to reduce the CO2 emissions	2009	United Arab Emirates
12	Will future low-carbon schools in the UK have an overheating problem?	2009	UK
13	Resilience of naturally ventilated buildings to climate change: advanced natural ventilation and hospital wards	2009	UK
14	Identification of key factors for uncertainty in the prediction of the thermal performance of an office building under climate change	2009	UK
15	Assessment of climate change impact on residential building heating and cooling energy requirement in Australia	2010	Australia
16	The effects of future climate change on heating and cooling demands in office buildings in the UK	2010	UK
17	Predicting the performance of an office under climate change: a study of metrics, sensitivity and zonal resolution	2010	UK
18	Comparison of multi-year and reference year building simulations	2010	UK
19	Predicted changes in energy demands for heating and cooling of passive house due to climate change in Slovenia	2010	Slovenia
20	The role of adaptive thermal comfort in the prediction of the thermal performance of a modern mixed-mode office building in the UK under climate change	2010	UK
21	Translating probabilistic climate predictions for use in building simulation	2010	UK
22	Climate change adaptation pathways for Australian residential buildings	2011	Australia
23	Developing future hourly weather files for studying the impact of climate change on building energy performance in Hong Kong.	2011	Hong Kong
24	A probabilistic analysis of the future potential of evaporative cooling systems in a temperate climate	2011	UK
25	The impact of the projected changes in temperature on heating and cooling requirements in Dhaka, Bangladesh	2011	Bangladesh
26	Longitudinal prediction of the operational energy use of buildings	2011	UK
27	Climate change, building design, and thermal performance	2011	Austria
28	Assessing the risk of climate change for buildings: A comparison between multi-year and probabilistic reference year simulations	2011	UK
29	Designing net-zero energy buildings for the future climate, not for the past	2012	Canada
30	Future energy demand for buildings in the context of climate change for Burkina Faso	2012	Burkina Faso
31	Generating design reference years from the UKCP09 projections and their application to future air-conditioning loads	2012	UK

32	The natural ventilation performance of buildings under alternative future weather projections	2012	UK
33	Thermal mass in new build UK housing: a comparison of structural systems in a future weather scenario	2012	UK
34	Ranking of interventions to reduce dwelling overheating during heat waves.	2012	UK
35	Climate change influence on building lifecycle greenhouse gas emissions: case study of UK mixed-use development	2012	UK
36	Energy use, indoor temperature and possible adaptation strategies for air-conditioned office buildings in face of global warming	2012	Australia
37	Using UK climate change projections to adapt existing English homes for a warming climate	2012	UK
38	A proposed method to assess the damage risk of future climate change to museum objects in historic buildings	2012	Netherlands and Belgium
39	Thermal comfort standards, measured internal temperatures and thermal resilience to climate change of free-running buildings: a case-study of hospital wards	2012	UK
40	Assessment of hygrothermal performance and mould growth risk in ventilated attics in respect to possible climate changes in Sweden	2012	Sweden
41	Building characteristics as determinants of propensity to high indoor summer temperatures in London dwellings	2012	UK
42	A comparison of structural and behavioural adaptations to future proofing buildings against higher temperatures	2012	UK
43	Management of thermal performance risks in buildings subject to climate change	2012	UK
44	Simulating urban heat island effects with climate change on a Manchester house	2012	UK
45	Impact of climate change on thermal comfort and energy performance in offices - A parametric study	2012	Greece
46	Impact of climate change on comfort and energy performance in offices	2012	Greece
47	A comparative analysis of current and newly proposed overheating criteria for UK schools: A climate change aspect	2012	UK
48	Simulation of the impact of climate change on the current building's residential envelope thermal transfer value (ETTV) regulation in Singapore	2012	Singapore
49	Summertime impact of climate change on multi-occupancy British dwellings	2012	UK
50	Climate data and climate change - Analysis of the influence on energy demand, performance requirement and thermal comfort of buildings [Klimadaten und Klimawandel - Untersuchungen zum Einfluss auf den Energiebedarf, den Leistungsbedarf und den thermischen Komfort von Gebäuden]	2012	Germany
51	Comparison of untypical meteorological years (UMY) and their influence on building energy performance simulations	2013	Poland
52	Energy simulation of sustainable air-cooled chiller system for commercial buildings under climate change	2013	Honk Kong
53	The effectiveness of retrofitting existing public buildings in face of future climate change in the hot summer cold winter region of China	2013	China
54	Modelling to predict future energy performance of solar thermal cooling systems for building applications in the North East of England	2013	UK
55	An investigation into future performance and overheating risks in Passivhaus dwellings	2013	UK
56	Transforming existing weather data for worldwide locations to enable energy and building performance simulation under future climates	2013	UK
57	Building envelope design for climate change mitigation: a case study of hotels in Greece	2014	Greece
58	Impacts of urban location and climate change upon energy demand of office buildings in Vienna, Austria	2014	Austria
59	Impact of climate change heating and cooling energy use in buildings in the United States	2014	US
60	An outdoor-indoor coupled simulation framework for Climate Change-conscious Urban Neighborhood Design	2014	Egypt
61	Risks of summertime extreme thermal conditions in buildings as a result of climate change and exacerbation of urban heat islands	2014	US
62	Effects of future climate change scenarios on overheating risk and primary energy use for Swedish residential buildings	2014	Sweden
63	Climate change simulation for intelligent green building adaptation design	2014	UK
64	Microclimate change outdoor and indoor coupled simulation for passive building adaptation design	2014	UK
65	Sampling-based sensitivity analysis of thermal performance in domestic buildings under climate change	2014	UK
66	Environmental benefits of sustainable chiller system under climate change	2014	Hong Kong
67	Double-skin façades in the context of climate change [Doppelfassaden im Zeichen des Klimawandels]	2014	Germany
68	Impacts of climate change upon cooling and heating energy demand of office buildings in Vienna, Austria	2014	Austria
69	Analysis of performance of night ventilation for residential buildings in hot-humid climates [Sicak-nemli iklimlerdeki konut binalarinda gece havalandirmasi performansinin analizi]	2014	Turkey
70	Impact of building design and occupancy on office comfort and energy performance in different climates	2014	Creece, Germany, Australia
71	Developing a probabilistic tool for assessing the risk of overheating in buildings for future climates	2014	UK
72	Near Future Weather Data for Building Energy Simulation in Summer/Winter Seasons in Tokyo Developed by Dynamical Downscaling Method	2014	Japan
73	Generating near-extreme Summer Reference Years for building performance simulation.	2015	UK
74	Climate for Culture: assessing the impact of climate change on the future indoor climate in historic buildings using simulations	2015	Whole Europe
75	Energy demand for the heating and cooling of residential houses in Finland in a changing climate	2015	Finland
76	Impacts of climate change on energy consumption and peak demand in buildings: A detailed regional approach	2015	US
77	Preparing for climate change with computation and resiliency	2015	US
78	Study on the future weather data considering the global and local climate change for building energy simulation	2015	Japan
79	The potential of phase change materials to reduce domestic cooling energy loads for current and future UK climates	2015	UK
80	Future moisture loads for building facades in Sweden: Climate change and wind-driven rain	2015	Sweden
81	Vulnerability to climate change impacts of present renewable energy systems designed for achieving net-zero energy buildings	2016	US
82	Effect of climate change on building cooling loads in Tokyo in the summers of the 2030s using dynamically downscaled GCM data	2016	Japan
83	Future trends of residential building cooling energy and passive adaptation measures to counteract climate change: The case of Taiwan.	2016	Taiwan
84	Integrating climate change and energy mix scenarios in LCA of buildings and districts	2016	France
85	Modeling the long-term effect of climate change on building heat demand: Case study on a district level	2016	Portugal
86	Climate change future proofing of buildings—Generation and assessment of building simulation weather files.	2016	Italy
87	Future probabilistic hot summer years for overheating risk assessments.	2016	UK
88	Optimization of annual energy demand in office buildings under the influence of climate change in Chile	2016	Chile
89	Impact of climate change on heating and cooling energy demand in houses in Brazil	2016	Brazil
90	Residential buildings' thermal performance and comfort for the elderly under climate changes context in the city of Sao Paulo, Brazil	2016	Brazil
91	Analysis of the predicted effect of passive climate adaptation measures on energy demand for cooling and heating in a residential building	2016	Netherlands
92	The impact of regulations on overheating risk in dwellings	2016	UK
93	Impact of future climates on the durability of typical residential wall assemblies retrofitted to the PassiveHaus for the Eastern Canada region	2016	Canada
94	Impacts of climate change on U.S. building energy use by using downscaled hourly future weather data	2017	US
95	Prediction of the impacts of climate change on energy consumption for a medium-size office building with two climate models. Energy and Buildings	2017	US
96	Climate Change Adaptation Pathways for Residential Buildings in Southern China.	2017	China
97	Influence of climate change on summer cooling costs and heat stress in urban office buildings	2017	Belgium
98	Making energy simulation easier for future climate – Synthesizing typical and extreme weather data sets out of regional climate models (RCMs)	2017	Sweden
99	Application of adaptive comfort behaviors in Chilean social housing standards under the influence of climate change	2017	Chile
100	Cooling Energy Implications of Occupant Factor in Buildings under Climate Change	2017	South korea and Hong kong

101	Assessment of climate change impact on the required cooling load of the hospital buildings	2017	Malaysia
102	Adapting the design of a new care home development for a changing climate	2017	UK
103	The impact of climate change on the overheating risk in dwellings—A Dutch case study	2017	Netherlands
104	Energy Consumption Performance Considering Climate Change in Office Building	2017	China
105	Performance evaluation of well-insulated versions of contemporary wall systems-a case study of London for a warmer climate	2017	UK
106	Robustness of residential houses in Ecuador in the face of global warming: Prototyping and simulation studies in the Amazon, coastal and Andes macroclimatic regions	2017	Ecuador
107	Effectiveness of passive measures against climate change: Case studies in Central Italy	2017	Italy
108	Energy efficiency and resilience against increasing temperatures in summer: The use of PCM and cool materials in buildings	2017	Italy
109	Should we consider climate change for Brazilian social housing? Assessment of energy efficiency adaptation measures	2018	Brazil
110	A dynamic modelling approach for simulating climate change impact on energy and hygrothermal performances of wood buildings	2018	Finland
111	Cooling and heating energy performance of a building with a variety of roof designs; the effects of future weather data in a cold climate	2018	Canada

Appendix B

Boxplots of the global horizontal radiation, relative humidity and wind speed as some of the key variables for energy simulation, are plotted in Figs. A1, A2 and A3 respectively.

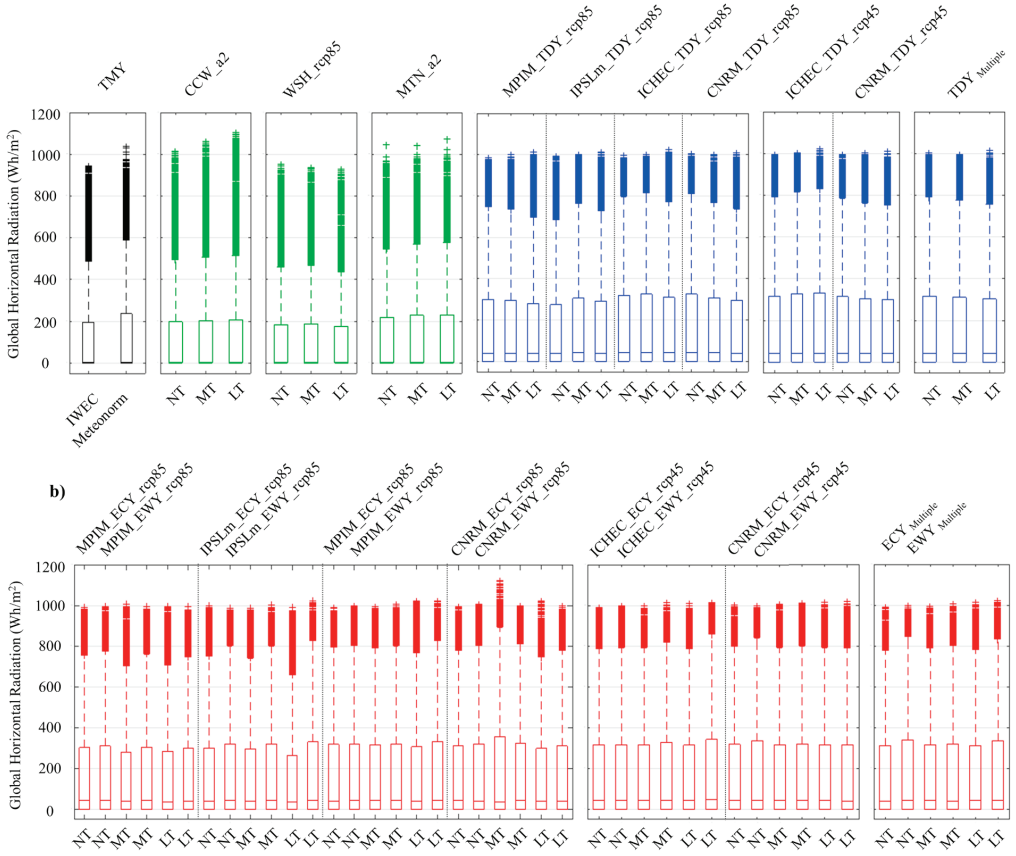

Fig. B1. Boxplots of global horizontal radiation for the weather files generated by three software tools–CCWorldWeatherGen, WeatherShiftTM, Meteonorm –and six combinations of GCM-RCMs with different emission scenarios.

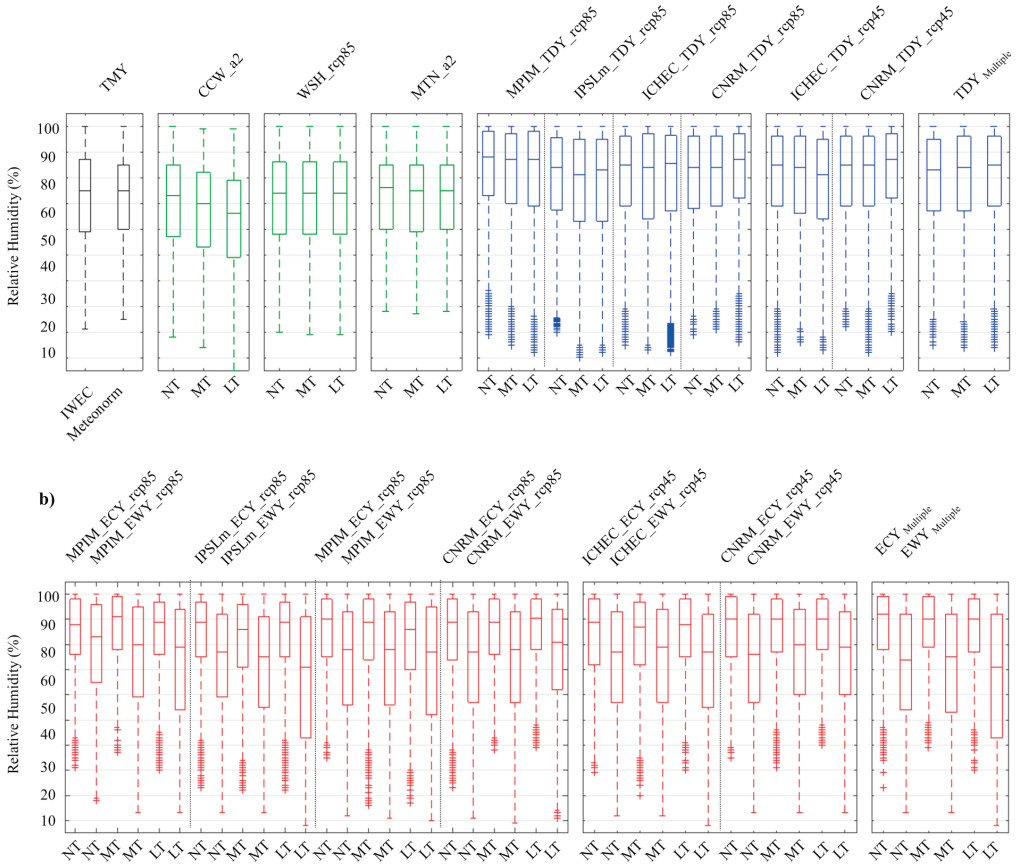

Fig. B2. Boxplots of relative humidity for the weather files generated by three software tools–CCWorldWeatherGen, WeatherShiftTM, Meteonorm –and six combinations of GCM-RCMs with different emission scenarios.

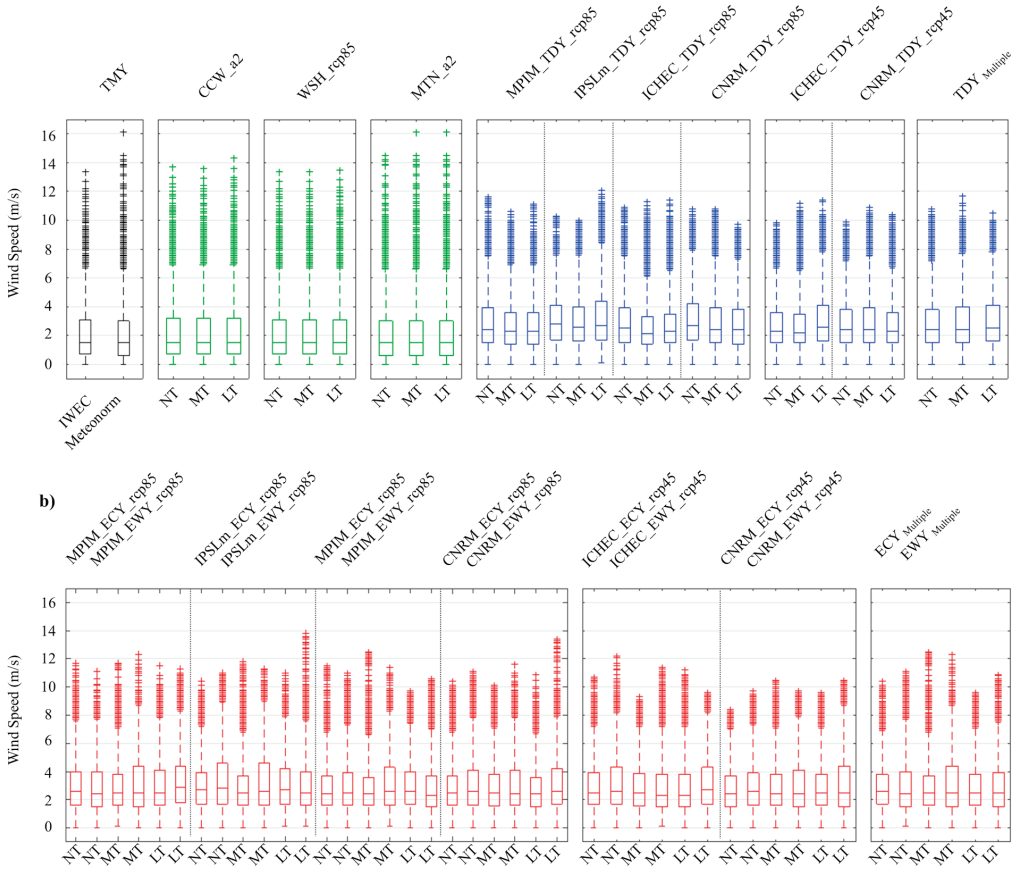

Fig. B3. Boxplots of wind speed for the weather files generated by three software tools–CCWorldWeatherGen, WeatherShiftTM, Meteonorm –and six combinations of GCM-RCMs with different emission scenarios.

References

[1] NCDC. Test Reference Year (TRY), Tape Reference Manual. TD-9706. Asheville, North Carolina: National Climatic Data Center, U.S. Department of Commerce; 1976.

[2] Crawley DB. Which weather data should you use for energy simulations of commercial buildings? In: ASHRAE, editor. ASHRAE Transactions. Atlanta; 1998. p. 498–515.

[3] Crawley DB, Lawrie LK. Rethinking the TMY: is the 'typical'meteorological year best for building performance simulation? 14th conference of international building performance simulation association. Hyderabad, India. 2015.

[4] Erba S, Causone F, Armani R. The effect of weather datasets on building energy simulation outputs. Energy Proc 2017;134:545–54.

[5] Cui Y, Yan D, Hong T, Xiao C, Luo X, Zhang Q. Comparison of typical year and multiyear building simulations using a 55-year actual weather data set from China. Appl Energy 2017;195:890–904.

[6] Nik VM, Coccolo S, Kämpf J, Scartezzini J-L. Investigating the importance of future climate typology on estimating the energy performance of buildings in the EPFL campus. Energy Proc 2017;122:1087–92.

[7] Herrera M, Natarajan S, Coley DA, Kershaw T, Ramallo-González AP, Eames M, et al. A review of current and future weather data for building simulation. Build Serv Eng Res Technol 2017;38:602–27.

[8] Yau YH, Hasbi S. A review of climate change impacts on commercial buildings and their technical services in the tropics. Renew Sustain Energy Rev 2013;18:430–41.

[9] Berger T, Amann C, Formayer H, Korjenic A, Pospischal B, Neururer C, et al. Impacts of climate change upon cooling and heating energy demand of office buildings in Vienna, Austria. Energy Build 2014;80:517–30.

[10] Moazami A, Carlucci S, Causone F, Pagliano L. Energy retrofit of a day care center for current and future weather scenarios. Proc Eng 2016;145:1330–7.

[11] Jiang A, Zhu Y, Elsafty A, Tumeo M. Effects of global climate change on building energy consumption and its implications in Florida. Int J Constr Educat Res 2018;14:22–45.

[12] Wan K, Li D, Pan W, Lam J. Impact of climate change on building energy use in different climate zones and mitigation and adaptation implications. Appl Energy 2012;97:274–82.

[13] de Wilde P, Coley D. The implications of a changing climate for buildings. Build Environ 2012;55:1–7.

[14] Nik VM. Hygrothermal simulations of buildings concerning uncertainties of the future climate PhD thesis Sweden: Chalmers University of Technology; 2012

[15] Nik VM, Mundt-Petersen SO, Kalagasidis AS, De Wilde P. Future moisture loads for building facades in Sweden: climate change and wind-driven rain. Build Environ 2015;93:362–75.

[16] Nik VM, Kalagasidis AS. Impact study of the climate change on the energy performance of the building stock in Stockholm considering four climate uncertainties. Build Environ 2013;60:291–304.

[17] Nakicenovic N, Alcamo J, Grubler A, Riahi K, Roehrl R, Rogner H-H. Special report on emissions scenarios (SRES), a special report of Working Group III of the intergovernmental panel on climate change. Cambridge University Press; 2000.

[18] Carter T. General guidelines on the use of scenario data for climate impact and adaptation assessment. In: (TGICA) TGoDaSSflaCA, editor. Intergovernmental Panel on Climate Change; 2007.

[19] Pachauri R, Meyer L. Climate change 2014: Synthesis Report. Contribution of Working Groups I, II and III to Fifth Assessment Report of the Intergovernmental Panel on Climate Change. Geneva, Switzerland: IPCC; 2014.

[20] Trzaska S, Schnarr E. A review of downscaling methods for climate change projections. African and Latin American Resilience to Climate Change (ARCC). United States: United States Agency for International Development by Tetra Tech ARD; 2014. p. 1–42.

[21] Hall IJ, Prairie R, Anderson H, Boes E. Generation of a typical meteorological year. Analysis for solar heating and cooling. San Diego (CA, USA), Albuquerque, NM (USA): Sandia Labs.; 1978.

[22] GISTEMP Team. GISS Surface Temperature Analysis (GISTEMP). NASA Goddard Institute for Space Studies. Dataset accessed 2018-04-08. https://data.giss.nasa.gov/gistemp/.
[23] Sévellec F, Drijfhout SS. A novel probabilistic forecast system predicting anomalously warm 2018–2022 reinforcing the long-term global warming trend. Nat Commun 2018;9:3024.
[24] Field CB, Barros V, Stocker TF, Dahe Q. Managing the risks of extreme events and disasters to advance climate change adaptation: special report of the intergovernmental panel on climate change. Cambridge University Press; 2012.
[25] The Global Risks Report 2016. World Economic Forum, https://www.weforum.org/reports/the-global-risks-report-2016/ [accessed June 11, 2018].
[26] Robine J-M, Cheung SLK, Le Roy S, Van Oyen H, Griffiths C, Michel J-P, et al. Death toll exceeded 70,000 in Europe during the summer of 2003. CR Biol 2008;331:171–8.
[27] Grize L, Huss A, Thommen O, Schindler C, Braun-Fahrlander C. Heat wave 2003 and mortality in Switzerland. Swiss Medical Weekly 2005;135:200–5.
[28] Mylona A. The use of UKCP09 to produce weather files for building simulation. Build Serv Eng Res Technol 2012;33:51–62.
[29] De Bono A, Peduzzi P, Kluser S, Giuliani G. Impacts of summer 2003 heat wave in Europe. United Nations Environment Programme; . 2004. Retrieved from https://wwwunisdrorg/files/1145_ewheatwaveenpdf.
[30] Flato G, Marotzke J, Abiodun B, Braconnot P, Chou SC, Collins W, et al. Evaluation of climate models. In: Stocker TF, Qin D, Plattner G-.K, Tignor M, Allen SK, Boschung J, editors. Climate change 2013: the physical science basis contribution of working group i to the fifth assessment report of the intergovernmental panel on climate change. Cambridge, United Kingdom and New York, NY, USA: Cambridge University Press; 2013. p. 741–866.
[31] Uppala SM, Kållberg P, Simmons A, Andrae U, Bechtold VDC, Fiorino M, et al. The ERA-40 re-analysis. Q J R Meteorolog Soc 2005;131:2961–3012.
[32] Nik VM. Climate simulation of an attic using future weather data sets-statistical methods for data processing and analysis. Licentiate thesis. Chalmers University of Technology, Sweden; 2010.
[33] Hensen JL, Lamberts R. Building performance simulation for design and operation. Routledge; 2012.
[34] Burke M, Davis WM, Diffenbaugh NS. Large potential reduction in economic damages under UN mitigation targets. Nature 2018;557:549.
[35] Nik V, Sasic A. Influence of the uncertainties in future climate scenarios on the hygro-thermal simulation of an attic. In: International conference on building envelope systems and technologies, Vancouver, Canada; 2010. p. 149e57.
[36] Randall DA, Wood RA, Bony S, Colman R, Fichefet T, Fyfe J, et al., 2007. Climate models and their evaluation. In: Climate Change 2007: The Physical Science Basis Contribution of Working Group I to the Fourth Assessment Report of the Intergovernmental Panel on Climate Change. Cambridge, United Kingdom and New York, NY, USA: Cambridge University Press; 2007.
[37] Regional climate model. American Meteorological Society, glossary of meteorology; 2013.
[38] Rummukainen M. State-of-the-art with regional climate models. Wiley Interdiscip Rev Clim Change 2010;1:82–96.
[39] Seaby LP, Refsgaard JC, Sonnenborg TO, Stisen S, Christensen JH, Jensen KH. Assessment of robustness and significance of climate change signals for an ensemble of distribution-based scaled climate projections. J Hydrol 2013;486:479–93.
[40] Van der Linden P, Mitchell J, editors. ENSEMBLES: Climate change and its impacts-Summary of research and results from the ENSEMBLES project. FitzRoy Road, Exeter EX1 3PB, UK: Met Office Hadley Centre; 2009.
[41] Jacob D, Petersen J, Eggert B, Alias A, Christensen OB, Bouwer LM, et al. EURO-CORDEX: new high-resolution climate change projections for European impact research. Reg Environ Change 2014;14:563–78.
[42] Kershaw T, Eames M, Coley D. Assessing the risk of climate change for buildings: a comparison between multi-year and probabilistic reference year simulations. Build Environ 2011;46:1303–8.
[43] Dee DP, Uppala SM, Simmons AJ, Berrisford P, Poli P, Kobayashi S, et al. The ERA-Interim reanalysis: configuration and performance of the data assimilation system. Q J R Meteorolog Soc 2011;137:553–97.
[44] Strandberg G, Bärring L, Hansson U, Jansson C, Jones C, Kjellström E, et al. CORDEX scenarios for Europe from the Rossby Centre regional climate model RCA4: SMHI; 2015.
[45] Jacobeit J, Hertig E, Seubert S, Lutz K. Statistical downscaling for climate change projections in the Mediterranean region: methods and results. Reg Environ Change 2014;14:1891–906.
[46] Nik VM. Making energy simulation easier for future climate – synthesizing typical and extreme weather data sets out of regional climate models (RCMs). Appl Energy 2016;177:204–26.
[47] Belcher SE, Hacker JN, Powell DS. Constructing design weather data for future climates. Build Serv Eng Res Technol 2005;26:49–61.
[48] Moazami A, Carlucci S, Geving S. Critical analysis of software tools aimed at generating future weather files with a view to their use in building performance simulation. Energy Proc 2017;132:640–5.
[49] Paassen AHV, Luo QX. Weather data generator to study climate change on buildings. Building Services Eng Res Technol 2002;23:251–8.
[50] Remund J, Kunz S. METEONORM: Global meteorological database for solar energy and applied climatology. Fabrikstrasse 14, CH-3012 Bern (Switzerland): Meteotest; 1997.
[51] Lim TK, Ignatius M, Miguel M, Wong NH, Juang H-MH. Multi-scale urban system modeling for sustainable planning and design. Energy Build 2017;157:78–91.
[52] Fowler HJ, Blenkinsop S, Tebaldi C. Linking climate change modelling to impacts studies: recent advances in downscaling techniques for hydrological modelling. Int J Climatol 2007;27:1547–78.
[53] Wilby RL, Wigley TML. Downscaling general circulation model output: a review of methods and limitations. Progr Phys Geogr: Earth Environ 1997;21:530–48.
[54] Jentsch MF, Bahaj AS, James PAB. Climate change future proofing of buildings-generation and assessment of building simulation weather files. Energy Build 2008;40:2148–68.
[55] Jentsch MF, James PAB, Bourikas L, Bahaj AS. Transforming existing weather data for worldwide locations to enable energy and building performance simulation under future climates. Renew Energy 2013;55:514–24.
[56] Jake Hacker RC, Mylona Anastasia. Chartered institution of building services engineers. Use of climate change scenarios for building simulation: the CIBSE future weather years. London: CIBSE; 2009.
[57] Remund J. SCM. The use of Meteonorm weather generator for climate change studies; 2010.
[58] Guan L. Preparation of future weather data to study the impact of climate change on buildings. Build Environ 2009;44:793–800.
[59] Arguez A, Vose RS. The definition of the standard WMO climate normal: The key to deriving alternative climate normals. Bull Am Meteorol Soc 2011;92:699–704.
[60] Fischer EM, Knutti R. Anthropogenic contribution to global occurrence of heavy-precipitation and high-temperature extremes. Nature Clim Change 2015;5:560.
[61] Lewis SC, Karoly DJ. Anthropogenic contributions to Australia's record summer temperatures of 2013. Geophys Res Lett 2013;40:3705–9.
[62] Otto FE, Massey N, Oldenborgh G, Jones R, Allen M. Reconciling two approaches to attribution of the 2010 Russian heat wave. Geophys Res Lett 2012;39.
[63] Pall P, Aina T, Stone DA, Stott PA, Nozawa T, Hilberts AG, et al. Anthropogenic greenhouse gas contribution to flood risk in England and Wales in autumn 2000. Nature 2011;470:382–5.
[64] Sippel S, Otto FE. Beyond climatological extremes-assessing how the odds of hydrometeorological extreme events in South-East Europe change in a warming climate. Clim Change 2014;125:381–98.
[65] Christensen JH, Krishna Kumar K, Aldrian E, An S-I, Cavalcanti IFA, de Castro M, et al. Climate phenomena and their relevance for future regional climate change. In: Stocker TF, Qin D, Plattner G-.K, Tignor M, Allen SK, Boschung J, editors. Climate change 2013: the physical science basis contribution of working group I to the fifth assessment report of the intergovernmental panel on climate change. Cambridge, United Kingdom and New York, NY, USA: Cambridge University Press; 2013. p. 1217–308.
[66] ASHRAE AS. Standard 90.1-2004, Energy standard for buildings except low rise residential buildings. American Society of Heating, Refrigerating and Air-Conditioning Engineers, Inc; 2004.
[67] Crawley DB, Lawrie LK, Winkelmann FC, Buhl WF, Huang YJ, Pedersen CO, et al. EnergyPlus: creating a new-generation building energy simulation program. Energy Build 2001;33:319–31.
[68] Samuelsson P, Gollvik S, Kupiainen M, Kourzeneva E, van de Berg WJ. The surface processes of the Rossby Centre regional atmospheric climate model (RCA4). Meteorology 157. Norrköping, Sweden: Swedish Meteorological and Hydrological Institute, (SMHI); 2015.
[69] Met Office FR. Met Office Hadley Centre for Climate Science and Services, Met Off. ; 2010. http://www.metoffice.gov.uk/climate-guide/science/science-behind-climate-change/hadley [accessed October 29, 2015].
[70] IPCC Data distribution centre (DDC).
[71] Robert Dickinson BB. Generating future weather files for resilience. In: Pablo La Roche MS, editor. International conference on passive and low energy architecture, PLEA 2016 - cities, buildings, people: towards regenerative environments. Los Angeles; 2016.
[72] Luke Troup DF. Morphing climate data to simulate building energy consumption. The ASHRAE and IBPSA-USA SimBuild 2016: Building Performance Modeling Conference. Salt Lake City, Utah; 2016.
[73] Phil Jones CK, Harpham Colin, Glenis Vassilis, Burton Aidan. UK Climate Projections science report: projections of future daily climate for the UK from the Weather Generator. University of Newcastle, UK; 2009.
[74] Kirtman B, Power SB, Adedoyin JA, Boer GJ, Bojariu R, Camilloni I, et al. Near-term climate change: projections and predictability. In: Stocker TF, Qin D, Plattner G-.K, Tignor M, Allen SK, Boschung J, editors. Climate change 2013: the physical science basis contribution of working group I to the fifth assessment report of the intergovernmental panel on climate change. Cambridge, United Kingdom and New York, NY, USA: Cambridge University Press; 2013. p. 953–1028.
[75] Collins M, Knutti R, Arblaster J, Dufresne J-L, Fichefet T, Friedlingstein P, et al. Long-term climate change: projections, commitments and irreversibility. In: Stocker TF, Qin D, Plattner G-.K, Tignor M, Allen SK, Boschung J, editors. Climate change 2013: the physical science basis contribution of working group I to the fifth assessment report of the intergovernmental panel on climate change. Cambridge, United Kingdom and New York, NY, USA: Cambridge University Press; 2013. p. 1029–136.
[76] Allen MR, Barros VR, Broome J, Cramer W, Christ R, Church JA, et al. IPCC fifth assessment synthesis report-climate change 2014 synthesis report; 2014.
[77] Deru M, Field K, Studer D, Benne K, Griffith B, Torcellini P, et al. US Department of Energy commercial reference building models of the national building stock. 1617 Cole Boulevard Golden, Colorado: National Renewable Energy Laboratory; 2011.
[78] Halverson MA, Rosenberg MI, Hart PR, Richman EE, Athalye RA, Winiarski DW. ANSI/ASHRAE/IES Standard 90.1-2013 Determination of Energy Savings: Qualitative Analysis. United States, Washington: Pacific Northwest National Laboratory (PNNL); 2014.
[79] Zhang J, Athalye RA, Hart PR, Rosenberg MI, Xie Y, Goel S, et al. Energy and energy cost savings analysis of the IECC for commercial buildings. United States,

Washington: Pacific Northwest National Laboratory (PNNL); 2013.
[80] Winiarski DW, Cooke A, Halverson M, Bandyopadhyay G, Butzbaugh J, Elliott DB. Analysis for Building Envelopes and Mechanical Systems Using 2012 CBECS Data. Pacific Northwest National Lab.(PNNL), Richland, WA (United States); 2018.
[81] Mohajeri N, Gudmundsson A, Scartezzini J-L. Statistical-thermodynamics modelling of the built environment in relation to urban ecology. Ecol Model 2015;307:32–47.
[82] Khoury J. Assessment of Geneva multi-family building stock: main characteristics and regression models for energy reference area determination. SCCER Future Energy Efficient Buildings & Districts (http://www.sccer-feebd.ch/); 2016.
[83] ISO C. ISO 52000-1:2017. Energy performance of Buildings—Overarching EPB assessment–Part 1: General framework and procedures.
[84] Esteco S. ModeFRONTIER 2014 User's Manual. 2014.
[85] US-DoE. Testing and Validation. In: Energy USDo, editor. EnergyPlus Energy Simulation Software; 2012.
[86] ANSI/ASHRAE 140. Standard Method of Test for the Evaluation of Building Energy Analysis Computer Programs. Atlanta (GA), USA: American Society of Heating, Refrigerating and Air-Conditioning Engineers; 2011. p. 272.
[87] Walton GN. Thermal analysis research program reference manual. Washington, United States: National Bureau of Standards; 1983.
[88] DoE U. EnergyPlus Input output reference. US Department of Energy; 2010.
[89] SIA. 380/1 (2009): Thermische Energie im Hochbau. Zürich: Schweizerischer Ingenieur und Architektenverein; 2009.
[90] Nik VM. Application of typical and extreme weather data sets in the hygrothermal simulation of building components for future climate – A case study for a wooden frame wall. Energy Build 2017;154:30–45.
[91] NOAA. National Centers for Environmental Information; 2018.
[92] Feldman TS. The history of meteorology, 1750–1800: a study in the quantification of experimental physics. Berkeley: University of California; 1983.
[93] Bernstein L, Bosch P, Canziani O, Chen Z, Christ R, Riahi K. climate change 2007: synthesis report. IPCC; 2008.
[94] Kjellström E, Nikulin G, Hansson U, Strandberg G, Ullerstig A. 21st century changes in the European climate: uncertainties derived from an ensemble of regional climate model simulations. Tellus A: Dynamic Meteorol Oceanogr 2011;63:24–40.
[95] Kampel W, Carlucci S, Aas B, Bruland A. A proposal of energy performance indicators for a reliable benchmark of swimming facilities. Energy Build 2016;129:186–98.
[96] Pagliano L, Carlucci S, Causone F, Moazami A, Cattarin G. Energy retrofit for a climate resilient child care centre. Energy Build 2016;127:1117–32.
[97] Tian W, de Wilde P. Uncertainty and sensitivity analysis of building performance using probabilistic climate projections: a UK case study. Autom Constr 2011;20:1096–109.
[98] Hémon D, Jougla E. Estimation de la surmortalité et principales caractéristiques épidémiologiques. Surmortalité liée à la canicule d'août 2003 : rapport d'étape. Institut national de la santé et de la recherche médicale(INSERM); 2003. p. 58 pages, tableaux, graphiques, cartes, 13 références bibliographiques.
[99] Vandentorren S, Suzan F, Medina S, Pascal M, Maulpoix A, Cohen J-C, et al. Mortality in 13 French Cities During the August 2003 Heat Wave. Am J Public Health 2004;94:1518–20.
[100] Pritchard R, Kelly S. Realising operational energy performance in non-domestic buildings: lessons learnt from initiatives applied in Cambridge. Sustainability 2017;9:1345.
[101] Ke X, Wu D, Rice J, Kintner-Meyer M, Lu N. Quantifying impacts of heat waves on power grid operation. Appl Energy 2016;183:504–12.
[102] Luber G, McGeehin M. Climate change and extreme heat events. Am J Prev Med 2008;35:429–35.
[103] Masters GM. Renewable and efficient electric power systems. John Wiley & Sons; 2013.

Is not included due to copyright restrictions

Paper V

Paper VI

Towards climate robust buildings: an innovative method for designing buildings with robust energy performance under climate change

Amin Moazami[1,*], Salvatore Carlucci[1], Vahid M. Nik[2, 3, 4], Stig Geving[1]

[1] *NTNU Norwegian University of Science and Technology, Department of Civil and Environmental Engineering, 7491, Trondheim, Norway*

(amin.moazami@ntnu.no; salvatore.carlucci@ntnu.no; stig.geving@ntnu.no)

[2]*Division of Building Physics, Department of Building and Environmental Technology, Lund University, 223 63, Lund, Sweden (vahid.nik@byggtek.lth.se, Tel: +46 (0) 46 222 6268)*

[3]*Division of Building Technology, Department of Civil and Environmental Engineering, Chalmers University of Technology, 412 58, Gothenburg, Sweden (vahid.nik@chalmers.se)*

[4]*Institute for Future Environments, Queensland University of Technology, Garden Point Campus, 2 George Street, Brisbane, QLD, 4000, Australia (vahid.nik@qut.edu.au)*

[*] *Corresponding author. Tel.: +47 40 476 475. E-mail address: amin.moazami@ntnu.no*

Keywords

Robust design optimization; robust design; climate change; building performance simulation; primary energy; climate uncertainty

Nomenclature and acronyms

AR	Augmented Reality
BIM	Building Information Modelling
BPS	Building Performance Simulation
CDD	Cooling Degree Days
ECY	Extreme Cold Year
EWY	Extreme Warm Year
GCM	General Circulation Model
HDD	Heating Degree Days
MOGA-II	Multi-Objective Genetic Algorithm
MSD	Mean Squared Deviation
NSGA-II	Fast Non-dominated Sorting Genetic Algorithm
PE	Primary Energy
RCM	Regional Climate Model
RDO	Robust Design Optimization
TMY	Typical Meteorological Year
ZEB	Zero Energy Balance

Abstract

Neglecting extremes and designing buildings for the past or most likely weather conditions is not the best approach for the future, while robust design techniques can be a viable option to tackle the future challenges. Concept of robust design was first introduced by Taguchi in 1940s and result of the design process is a product that is insensitive to the effect of given sources of variability, even though the sources themselves were not eliminated. In this paper, for the first time a robust design optimization (RDO) method is proposed for supporting architects and engineers to design buildings with robust energy performance under climate change and extreme conditions. To test the effectiveness of the method, the primary energy use of an obtained optimum solution is calculated for 74 different climate scenarios including typical and extreme conditions. According to the results, the performance of the optimum solution not only has 81.5% lower variation (less sensitivity to climate uncertainty) but at the same time 14.4% lower mean value of energy use in comparison to a solution that is compliant with a recent construction standard (ASHRAE 90.1-2016). Less sensitivity to climate uncertainty means better robustness against climate change and simultaneously keeping a high performance.

1 Introduction

In the design of buildings in recent years, the focus of building designers, architects and engineers, has been pointed toward minimizing the energy use in buildings or achieving a net zero energy balance (ZEB) at the building or neighborhood scale. Building performance simulation (BPS) has helped reaching more optimized solutions with better energy-efficiency. However, studies have shown that more optimal solutions can be achieved using automated optimization techniques [1]. Nguyen et al. [2] reviewed simulation-based optimization methods and concluded that a further reduction of 20- 30% can be achieved in the energy consumption of buildings using automated optimization. With the advancements in computational science and the desire for achieving higher levels of energy optimality, the use of simulation-based optimization techniques in building sector is on the rise [3]. Such techniques allow designers to systematically explore a wider design space for better solutions. This is possible by coupling an automated mathematical optimization tool with a BPS program. During the building simulation process, many different design options are evaluated to obtain the optimum for a set of objectives (e.g. zero energy balance) [4]. While these promising technologies help to achieve designs with high performance solutions, the buildings that are constructed based on these design solutions are usually very sensitive to the changes in their operational conditions. Such a performance gap between the expected level of performance and the actual performance has been discussed and demonstrated in the literature [5-7]. There are several factors influencing the discrepancy of performance of the buildings between the designed and constructed. In general, the sources of this discrepancy can be categorized in three types: epistemic uncertainties, aleatory uncertainties and errors. Epistemic uncertainty is defined as "*a potential deficiency that is due to a lack of knowledge*." [8]. Examples of epistemic uncertainties can be simplifications and numerical approximations of physical processes that are considered in numerical models of BPS tools [9]. An error is defined as "*the discrepancy between a computed, observed or measured value or condition and the trues, specified or theoretically correct value or condition*" [10]. Examples for source of errors can be the discrepancy between constructed and simulated due to human errors during the construction and also poorer quality of construction materials than designed [11]. The third type are aleatory uncertainties which is the "*uncertainty that is said to arise due to the inherently random or variable nature of a quantity, or the (usually unknown) system underlying it.*" [9]. Examples of discrepancy due to aleatory uncertainties are the influence of occupants' behavior and/or climate

conditions on the performance of buildings. While the first two sources of discrepancy, epistemic uncertainty and errors, are reducible, the aleatory uncertainty is irreducible and cannot be eliminated due to its inherent randomness and natural variability [12]. *Epistemic uncertainties* in building modelling can be reduced by improvement of numerical models, calibration using additional experimental observations, and providing better information [13]. E*rrors* can be minimized by the use of technological advancements such as Building Information Modelling (BIM) [14] and Augmented Reality (AR) [15], and offsite or prefabricated construction technologies [16]. Aleatory uncertainties cannot be eliminated and the common approach to deal with this type of uncertainty in BPS is to consider a most likely scenario. For example, occupants are normally simulated with a fixed schedule [17] as the most probable occupancy scenario. Using typical meteorological year (TMY) weather files is another example of counting for the most likely conditions [18]. This approach causes the final solution to be sensitive to the variations from the most likely conditions, which may results in malfunctioning during adverse conditions in real life. Kalkman [19] showed in identically constructed buildings the energy use can be up to17 times bigger due to the influence of occupants.. Rastogi [9] thoroughly studied the sensitivity of buildings performance to climate. The best way to deal with these uncertainties is to evaluate and design buildings under presence of them. Designing under presence of aleatory uncertainties is not a new concept and has been in discussion in other fields of industry for a long time, but not yet been applied in buildings design. The idea of this concept is that instead of eliminating the source of uncertainty, this source is presented as noise during the design phase and the goal is to achieve a design solution which has its performance least sensitive to the presence of noise. This process is called “robust design” and was introduced first by Taguchi in the 1940s [20].

The aim of this work is to use the power of simulation-based optimization technology in discovering new areas of design space, and couple it with the experience of robust design from other industrial fields, in order to achieve building designs with robust energy performance against climate uncertainties. A robust design problem can also be formulated as an optimization problem. The concept of adding robust design to conventional optimization is called robust design optimization (RDO), where the idea is to achieve minimum performance variability under the presence of uncertainty. These concepts have been widely practiced and developed in various design areas from car manufacturing [21] and electronics [22] to medicine [23] and chemical productions [24]. In this study, for the first time an RDO technique for design of buildings with robust energy performance under typical and extreme condition conditions is proposed. The main focus is to introduce a process that is relatively simple and can be used by architects and engineers from the early stage of design. The outcome of this process is a design that its energy performance is least sensitive to climate variations while its energy use is also minimum, i.e. it is energy-robust and energy-efficient under climate change.

With the occurrence of climate change, it is no more possible to design buildings only based on TMYs [25]. Climate conditions have changed and are going to change with more frequent and intense extreme conditions in near future [26]. A system that has been designed to meet required performance under typical or most likely conditions can be challenged up to its failing point under atypical or extreme conditions [27]. Examples are black outs or regional grid failures during heatwaves. One of the main reasons is the high sensitivity of buildings to the perturbation of external conditions, which causes their performance to vary significantly if the conditions fall out of typical range. For example, when the electricity demand soars during heatwaves, it is of consequence to buildings that are not designed for such conditions. Energy system failure may leave thousands of houses with no means of cooling that puts

vulnerable people at risk of death in overheated buildings, as it happened during the 1995 Chicago heatwave [28], 2003 Europe heatwave [29] and 2006 heatwave in New York City [30]. Heatwaves are good examples of how underestimation during design can easily become very costly. Buildings of today need to be designed to not only perform optimal under typical conditions, but also show minimum variation under atypical conditions. One of the main challenges on achieving this target is to consider climate uncertainty in the optimization process. The climate uncertainty and challenges in considering them in simulation-based optimization process are discussed in section 2.2. Before that, the concept of robust design and its implication in built environment is described briefly in the following section. In section 3, the proposed RDO methodology for robust energy performance under climate change is described in detail. An approach to test the effectiveness of the method is presented in Section 4, where the solutions provided by the RDO method are tested under 74 climate scenarios. The results and conclusions are provided in section 5 and 6 accordingly.

2 Background and concepts

2.1 Concept of robust design optimization and its implication in built environment

Since the introduction of robust design, this discipline has been adopted in a wide range of industries. Taguchi defined robustness as "*the state where the technology, product, or process performance is minimally sensitive to factors causing variability (either in the manufacturing or user's environment) and aging at the lowest unit manufacturing cost*" [31]. In other words, "*a product or process is said to be robust when it is insensitive to the effect of source of variability, even though the sources themselves have not been eliminated*" [32]. Further definitions for robustness from system engineering and product design are: insensitivity to anticipated risks [33], a measure of variation in performance [34], insensitivity to unforeseeable changes in the operating environment [35], insensitivity to both expected and unexpected variations [36], the ability of a system to continue to operate correctly across a wide range of operational conditions [37], the ability of a system to absorb change [38], the potential for system success under varying future circumstances or scenarios [39], and the ability of a system – as built/designed – to do its basic job in uncertain or changing environments [40].

Robust design of a product involves factors that are defined as follow [41]:

- *Control factors (or Design variables),* are variables that have to be specified by the designer;
- *Noise factors,* are uncertain parameters that designer cannot control (only the statistical characteristics of noise factors that are expected in production or in actual use of the product can be known or specified);
- *Target value (Signal factor),* is set by regulations or user of the product to express the desired value for the response of the product;
- *Response* is the output of the product with the presence of noise.

One application of robust design is in car manufacturing and specifically in car packaging design, where the target is achieving high spatial and ergonomic efficiency for the cars. For example in a study [21] for an ergonomic robust design of car packaging, the *seat cushion angle, steering-wheel-to-BOF (ball of foot) distance,* etc. were considered as control factors, the *anthropometric variability* was considered as noise factor and the response was *comfort loss* of the occupants. The aim of a robust design is to set optimal control factors in which the variation of response from the target value to be minimum under presence of

noise factors. To explain the procedure of the robust design, a block diagram representation of a product [41] is shown in Figure 1.

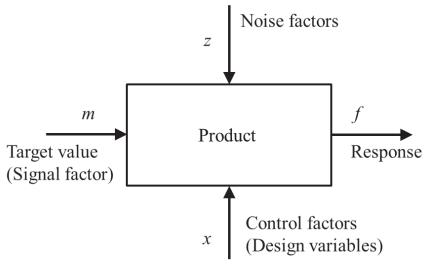

Figure 1 Block diagram of a product: P diagram

A robust design problem is a multi-objective optimization problem. The objectives are to reduce variation of the response while the mean is shifted to a target value (Figure 2).

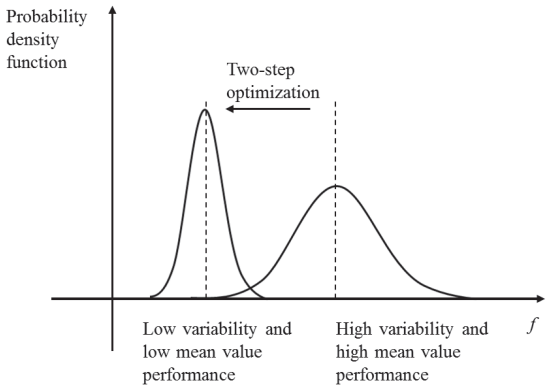

Figure 2: Robust design applied to buildings performance where the smaller mean and variation of response f is desired.

Based on this process, Taguchi developed the signal-to-noise ratio (S/N) that is a key metric used to perform the first step of the optimization process. During this step, the S/N gets maximized that is equivalent to minimizing the sensitivity of the response to the noise factors [32].

$$S/N = 10log_{10}\left[{\mu^2}/{\sigma^2}\right] \quad (1)$$

S/N is proportional to the base 10 logarithm of the ratio between the squared of the signal factors (μ) and the squared of the noise factors (σ). Adding logarithm to the metric was proposed by Taguchi and puts the S/N ratio into *decibels* units (*dB*) [32]. Taguchi described that a metric for robust design should have four properties [32]:

1. *The metric should reflect the variability in the response.*
2. *The metric should be independent of adjustment of the mean.*
3. *The metric should measure relative quality.*
4. *The metric should not induce unnecessary complications, such as control factors interactions.*

A good S/N metric has all the above properties. Later on, in section 3.4, these properties are further discussed for the specific S/N metric that is developed for the purpose of this study.

Robust design is a general concept applicable to all design procedures when uncertainty is taken into account. The aim is minimizing the sensitivity of product's performance to the presence of uncertainties in real world conditions. This concept can be transferred from industrial product to buildings simply by considering the target value as any desired performance indicator (e.g., the indoor thermal comfort condition, the indoor daylight performance or the maximum delivered energy) and noise factor as any variable that cause deviations in the performance of a building during its operation. The concept of robustness has been discussed in the building engineering literature while taking into account variety of uncertainty sources. For example [42], [43] considered energy robustness of an office building against energy related occupant behavior. They conceptualized robustness as minimum variation in energy use despite of variable occupants' behavior. Leyten and Kurvers [44] studied the indoor climate robustness of an office building. According to them, robustness is "*the measure by which the indoor environment of a building lives up to its design purpose when it is used by occupants in a real life situation*". Palme et al. [45], [46] proposed a concept for robustness of energy performance in buildings and related it to the ability of the building to mitigate the unpredictable variations induced by occupants or by external factors; Chinazzo et al. [47] assessed robustness of energy performance to the uncertainties in weather files; Hoes et al. [48] considered sensitivity of several performance indicators to the effect of user behavior. They investigated several design cases to find the most robust (the least sensitive) case to user behavior. O'Brien [49] investigated the robustness of energy use for lighting under presence of occupant behavior uncertainty. Kotireddy et al. [50] developed a methodology based on scenario analysis to assess performance robustness of low-energy buildings. The mentioned studies demonstrate that the concept of robustness in buildings has different interpretations and has not been converged with a concise approach in this field of research.

A non-exhaustive list of the built environment's terms classified according to the factors represented in the P diagram is given in *Table 1*.

Table 1: Built environment's examples classified according to the factors of the P diagram

Product	**Noise factors**	**Control factors (Design variables)**	**Responses**
Building scale: • components • systems • units/apartments Urban scale: • Building /Facility • Neighborhood • City • Region	Climate conditions: • Changes in long-term and short-term patterns of climate Occupant behavior: • Operation of appliances • Manipulation of building control settings • Windows operation • Door operation • Vent operation • Use of domestic hot water	Envelope Thermal properties: • Insulation thickness • U-value of glazing • G-value of glazing Building Geometry: • Air volume • Window-to-wall ratio • Net floor area Control settings: • Maximum solar irradiance to draw down solar shading devices • Set point temperature to open windows for enabling natural ventilation • Heating set point temperature • Cooling set point temperature	• Energy use • Thermal discomfort • CO_2 concentration • Visual discomfort (glare) • Noise level

Robust design process originally was formulated in a way that the process can be performed with minimum cost and resources. This was due to high costs of experimental tests and also limited computational powers for running simulations. Taguchi used *orthogonal array* that is a method for setting experiments with only fraction of the full combinations [32]. But with the availability of better numerical models and high computational power, this concept was later introduced in simulation-based optimization process, and is referred to as robust design optimization (RDO) [51]. In other words, RDO is when the concept of robust design is added to the conventional optimization [52, 53]. In conventional optimization, the deterministic approach does not consider the impact of unavoidable uncertainties (noise factors) associated with the input design variables in real engineering environment. This results in optimum solutions that their performance measure is sensitive and can vary significantly due to distribution of noise factors. The design problems of buildings engineering also can be formulated as RDO problems, where the objective is to achieve a performance measure (e.g. energy) with minimum sensitivity to a noise factor (e.g. climate).

For this study, a number of design variables for an office building are optimized to achieve a minimum variation of its energy performance under the disturbance of mutable climate variables. In this case, the noise factor is climate change and the objectives of RDO scheme are to minimize mean energy performance while minimizing energy performance variability under climate change. Inspired by the work of Taguchi, two metrics (two objective functions) were developed for an optimization process that results in solutions with minimum variation in energy performance of a building under presence of climate uncertainty. The first objective is a S/N ratio metric customize for the purpose of this study that fulfill the four properties described earlier. The second objective focuses on minimizing the energy use. These metrics are introduced in section 3.4.

The first challenge in the intended RDO process is introducing climate change as noise factor into the optimization problem. The following section is dedicated to climate uncertainty and challenges to consider it in simulation-based optimization.

2.2 Climate uncertainty and simulation-based optimization

Detailed weather data with daily or hourly resolution are required to properly describe, through simulation, the dynamic energy behavior of a building [54]. Weather data defines the external boundary conditions for BPS. Current practice in BPS is using a typical meteorological year (TMY) weather files which represent the most likely climate conditions based on historical recorded data [18]. TMYs are one-year weather files representing typical conditions of a 30-year period of measured data for a given location. One of the main disadvantages of this method is its averaging nature: the generation of a typical weather year neglects the extreme weather conditions. Apart from historical data, with today's technology, climate models' data: General Circulation Models (GCMs) and Regional Climate Models (RCMs), can provide information on possible future climate conditions. These models are able to generate years of future climate data based on different climate scenarios [55] for most locations on the earth. Future climate data are then required to be transformed to suitable format for use in BPS. Moazami et al. [56] investigated available techniques to transform these data to suitable resolutions for BPS and design purposes. Theoretically, in order to take into account climate uncertainty, it is possible today to run a design under 100 of years of consistent climate data representing past recorded data and future possible climate scenarios. The availability of these data makes it possible to study the sensitivity of a design or to look for design alternative that demonstrate minimum sensitivity to climate conditions. However, this

means that at each step of optimization, hundreds of simulation runs should be performed to be able to calculate the RDO objectives. The optimization scheme may therefore become infeasible due to high computational cost. The following example helps to grasp a feeling of the time and the computation resources that are required to consider all possible scenarios and minimize mean and variation of energy performance under these scenarios. Let's consider 30 years of future climate data with an ensemble of 4 scenarios (two GCM-RCMs and two emission scenario) are generated while 30 years of historical data are also available. These provide 150 years of climate data. In the case of running the optimization process, each optimization step will contain 150 annual simulations. In other words, for an optimization process of 1000 evaluations, 150000 simulation runs are required. Considering that each simulation takes 1 minute and the possibility of four parallel simulations, the optimization process will take around 26 days. The required time-scale is not feasible in buildings design practice.

To solve both issues with high number of simulations and exclusion of extreme conditions, a work by Nik [57] proposed a method to synthesize a set of representative weather data sets, including one typical year and two extreme cold and warm years, namely Typical Downscaled Year (TDY), Extreme Cold Year (ECY) and Extreme Warm Year (EWY). This method has the advantage of decreasing the number of simulations enormously, while considering extreme conditions and future climate uncertainties into account. The method for generating TDY, ECY and EWY is explained in detail in [57]. In short, the method is based on Finkelstein–Schafer (FS) statistics [18]; picking the months with the most similar cumulative distribution temperature to the whole data sets as the typical months and constructing TDY based on them. For ECY and EWY, those months with the largest differences are picked as the extreme cold and warm. The method and its usefulness have been verified in different applications [56-58]. The method for synthesizing representative weather data sets was developed further to track all the possible extremes at each time step for any desired climate variable. To do so, the typical and extreme values of a climate variable were picked according to the hourly (instead of monthly) distribution at each time step (hour) considering all the years and climate scenarios. This results in three time-series (with the length of 8760 hours), each containing the most typical, the lowest and the highest values at each time step. These data sets are generated only for calculation purposes and they cannot be considered as weather data since they do not reflect the natural variations of the climate system (unlike TDY, ECY and EWY which are arranged based on monthly distributions and reflect natural variations). Nevertheless, each hourly value is a possible future condition that may challenge the designs.

The above approach allows applying climate change as noise factor in simulations by only using three weather files (three-year of climate data). This means, the simulation runs of the mentioned example reduce to 3000 (1000 evaluation × 3 simulation runs using TDY, ECY and EWY weather files), and as a result optimization process will require 12.5 hours.

In this study weather files generated for city of Geneva were used. Geneva was chosen due to the wealth of available data and the possibility of representing both cold winters and warm summers. The set of the representative weather files was synthesized in a previous study [56].

3 Simulation-based optimization method for design of energy-efficient buildings with robust energy performance

In this paper, we specifically refer to a multi-objective RDO that identifies a set of optimal building design solutions to achieve robust energy performance with high efficiency. The set of design solutions make the

buildings to have high energy-efficiency and low performance-variability while noise factor is present. It implies low energy use and a minimum sensitivity to disturbances. This specific robust design optimization problem can be formulated as:

$$\min_{x\in\mathbb{R}^n}\{f_1(\boldsymbol{x},\boldsymbol{u}_i), f_2(\boldsymbol{x},\boldsymbol{u}_i)\} \quad (2)$$

$$g_i(\boldsymbol{x},\boldsymbol{u}_i) \le 0 \quad \forall \boldsymbol{u}_i \in \mathcal{U}_i, \quad i = 1,\dots,r \quad (3)$$

$$x_L \le x \le x_U \quad (4)$$

where $\boldsymbol{x}$ is the vector of design variables, $f_1(\boldsymbol{x},\boldsymbol{u}_i)$ and $f_2(\boldsymbol{x},\boldsymbol{u}_i)$ are the objective functions, $g_i(\boldsymbol{x},\boldsymbol{u}_i)$ are inequality constraints subject to the uncertainty parameters that can take any arbitrary values in the *uncertainty domain* $\mathcal{U}_i \subseteq \mathbb{R}^m$. Using this formalism, the goal of this robust design optimization problem is to find a *set* $X(\mathcal{U}_i)$ (i.e. the set of the minimum-cost building variants) among all the available building variants which is feasible considering all the noises factors $\boldsymbol{u}_i \in \mathcal{U}_i$

$$X(\mathcal{U}_i) = \{x | g_i(\boldsymbol{x},\boldsymbol{u}_i) \le 0 \quad \forall \boldsymbol{u}_i \in \mathcal{U}_i, \quad i = 1,\dots,r\}. \quad (5)$$

The design effect of these two objectives , as shown in Figure 2, isa narrow distribution of primary energy with the mean value close to the target value (ideally zero). Optimizing $f_1(\boldsymbol{x},\boldsymbol{u}_i)$ will minimize the sensitivity of performance to the noise and is a measure of robustness. Optimizing $f_2(\boldsymbol{x},\boldsymbol{u}_i)$ will minimize the primary energy use and is a measure of energy-efficiency. These effects are visualized in *Figure 3*.

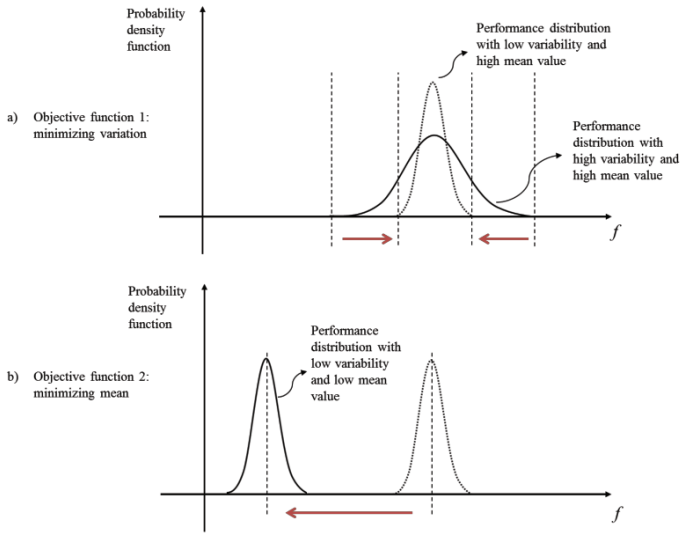

Figure 3 visualization of the designed effects of the two objective functions

3.1 Formulating the objective functions

As mentioned before, the focus of this study is to achieve robustness against climate uncertainty. In this regard, the achieved distribution of energy performance (e.g. Figure 3) is only due to variations of climate. To apply climate as a source of performance variability, as described in section 2.2, the method suggested by Nik [57] is adopted; using one typical and two extreme weather files (to be called triple method hereafter). In this method, the distribution of climate scenarios is summarized into three weather files: TDY, EWY and ECY. Reminding that the TDY file represents the most likely climate evolution and

EWY and ECY are the extreme warm and cold climate evolutions, $PE_{TDY,i}$, $PE_{ECY,i}$ and $PE_{EWY,i}$ are the primary energy use (PE) calculated for the time-step i using the TDY, EWY and ECY weather files.

To develop a custom S/N ratio for the specific task of this study, the four properties described in section 2.1 were considered as a guideline. The first property is to define a metric that *reflects the variability in the response*. Accordingly, the mean squared deviation (MSD) is calculated, which is the average squared differences between $PE_{ECY,i}$ and $PE_{EWY,i}$ values with $PE_{TDY,i}$ as reference values. Considering $PE_{TDY,i}$ as reference values, this function can be used to measure how far the values of $PE_{ECY,i}$ and $PE_{EWY,i}$ are from these reference values as measure of variability. The second property requires the metric to be *independent of adjustment of the mean*. For this reason, a second objective function was introduced. In this objective, calculated value of $PE_{TDY,i}$ is separately minimized, which makes the first objective being independent of the adjustment of $PE_{TDY,i}$. For the third property, *the metric should measure relative quality,* the S/N is calculated as relative change of $PE_{TDY,i}$ squared to MSD. At the final step, adding logarithm to the metric was proposed by Taguchi and puts the S/N ratio into *decibels* units (dB) [32]. With this transformation, the multiplicative changes in the metrics are transformed to additive changes, which helps reduce the effect of interactions between the design variables. It means the influence of each design variable is independent of the effects of the other design variables, which fulfills the fourth property. This metric is formulated as objective function n.1 and is descried below. By minimizing the first objective, the difference of energy performance under extreme and typical is minimized, which means the sensitivity of response to the changing of climate is minimized, while simultaneously the second objective minimize the annual primary energy $PE_{TDY,i}$, which is the annual total primary energy required by the building under average conditions (TDY). These objectives are formulated as below:

Objective function n.1: the purpose of $f_1(\boldsymbol{x}, \boldsymbol{u}_i)$ is to squeeze the energy performances calculated using EWY and ECY towards the one calculated using TDY. In this regard MSD is defined as:

$$MSD = \frac{1}{2p}\sum_{i=1}^{p}\left[\left(PE_{ECY_{(\boldsymbol{u}_1),i}} - PE_{TDY_{(\boldsymbol{u}_1),i}}\right)^2 + \left(PE_{EWY_{(\boldsymbol{u}_1),j}} - PE_{TDY_{(\boldsymbol{u}_1),i}}\right)^2\right] \quad (6)$$

Following Eq. (1) for S/N ratio and in order to maintain the usual convention according to which an optimization is a minimization process, S/N is negated when used as objective function. Therefore, $f_1(\boldsymbol{x}, \boldsymbol{u}_i)$ is:

$$f_1(\boldsymbol{x}, \boldsymbol{u}_i) = -10log_{10}\left[\frac{\left(PE_{TDY_{(\boldsymbol{u}_1),i}}\right)^2}{MSD}\right] \quad (7)$$

Where p is the the temporal resolution of data. For example, if one is interested in yearly energy performance and calculates it accumulating 12 monthly values, p has to be set at 12. If one is interested in the yearly energy performance calculated over hourly values, p has to be set at 8760; otherwise, for daily energy performance calculated over the 24 hours in a day, p has to be set at 24. Minimizing $f_1(\boldsymbol{x}, \boldsymbol{u}_i)$

results in minimizing the sensitivity of the response (energy use) to the variability of noise (climate conditions).

Objective function n.2: The purpose of $f_2(\boldsymbol{x}, \boldsymbol{u}_i)$ is to optimize building's energy use under the most likely climate conditions. The objective functions can be formulated as:

$$f_2(\boldsymbol{x}, \boldsymbol{u}_i) = \sum_{i=1}^{p} PE_{TDY(\boldsymbol{u}_1),i} \tag{8}$$

With the two objectives described above, it is now possible to conceptualize an RDO process in which climate uncertainty is introduced as noise factor in simulations by only using three weather files. In this process, objective function n.1 minimize the deviation between responses under extremes and average conditions. Objective function n.2 brings the primary energy with the mean value close to the target value (ideally zero). The above concept is visualized in Figure 4 for two time steps during heating period and cooling period.

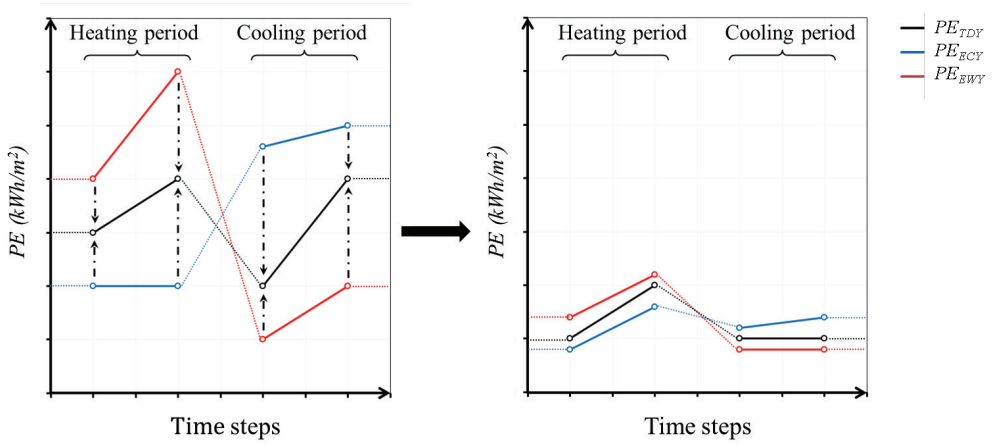

Figure 4 The concept of robust design optimization using three weather files: TDY, ECY and EWY

The above formulation allows performing robust design optimization at different temporal resolutions. This feature is required because the effect of a noise factor on the performance variability of a building system varies according to its typical response time. For example, when optimizing building envelope properties, one would need to consider the seasonal effect of climate variation, so the monthly resolution might be appropriate; otherwise, if someone want to optimize building's devices such as automated shadings, the temporal resolution of climate variation has to be finer, e.g. day or hour. For this reason, in the development of the optimization process, two set of design variables were considered: building envelope properties and control settings. Two configurations based on these two groups were designed for optimization process (see section 3.4). Before moving to the formulation of optimization process, in the following sections (section 3.2 and 3.3) the energy models and design variables that are considered for this study are described.

3.2 Building models

The commercial reference building models were developed by Pacific Northwest National Laboratory (PNNL), under contract with the U.S. Department of Energy (DOE) [59]. The package includes 16 building types model. These models are provided in three categories: "*new construction*", "*post-1980*" and "*pre-1980*" (existing buildings constructed in or after 1980 and before 1980). The *new construction* models are modified according to recent editions of ASHRAE 90.1 Standard [60]. Detailed descriptions of the reference model development and modeling strategies can be found in PNNL's reports [61] [62]. For the purpose of this study, which is testing the proposed methodology for supporting the design of buildings with robust energy performance, the small office building model is used. Two base-case were considered; one from *new construction* category complying with ASHRAE 90.1-2016 standard and one from *post-1980* category. These cases are called "2016-compliant base-case" representing a newly built building quality and "1980-compliant base-case" representing an existing building quality. It allows assessing energy robustness of models representing newly built and existing old buildings under climate uncertainty. This case-study also shows the potential improvement by "robustifying" the energy performance of buildings. The reference building models are also categorized based on ASHRAE climate zones [63]. The climate zones are classified according to calculated heating degree-day base 18°C (HDD_{18}) and cooling degree-day base 10°C (CDD_{10}). In order to find the model best suit for Geneva, 5-year average (2013 to 2017) of degree-day values were calculated for Geneve-Cointrin weather station. The calculated values are 2831 for HDD_{18} and 1460 for CDD_{10}, which is in accordance to Cold-Humid (5A) of ASHRAE climate zones. For this reason, the energy models base-case models are chosen from 5A climate zone. Summary of geometry description, thermal zones, envelope properties, and control settings of the building models are given in Figure 5, Table 2 and Table 3.

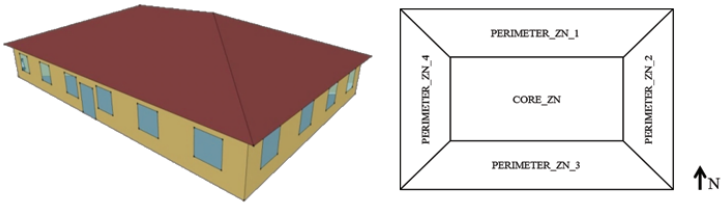

Figure 5 Reference building model geometry and zone planning

Table 2 Description of the thermal zones

Zone	Area (m^2)	Conditioned (Y/N)	Volume (m^3)	Gross wall area (m^2)	Window Glass Area	Lighting (W/m^2)	People (m^2/person)	Number of people	Appliance (W/m^2)
CORE_ZN	149.7	Yes	456.5	0.0	0.0	10.8	16.6	9	6.8
PERIMETER_ZN_1	113.5	Yes	346.1	84.5	20.6	10.8	16.6	7	6.8
PERIMETER_ZN_2	67.3	Yes	205.3	56.3	11.2	10.8	16.6	4	6.8
PERIMETER_ZN_3	113.5	Yes	346.1	84.5	16.7	10.8	16.6	7	6.8
PERIMETER_ZN_4	67.3	Yes	205.3	56.3	11.2	10.8	16.6	4	6.8
Attic	568.0	No	720.3	0.0	0.0	0.0	-	0	0.0
Total	511.3		2 279.6	281.6	59.7			31	

The dynamic energy simulations of the building models were performed using the software EnergyPlus [64] version 8.5.0. Each released version of EnergyPlus undergoes two major types of validation tests [65]: analytical tests according to ASHRAE Research Projects 865 and 1052, and comparative tests according to ANSI/ASHRAE 140 [13] and IEA SHC Task34/Annex43 BESTEST method. Heat

conduction through the opaque envelope was calculated via the conduction transfer functions (CTF) with a 15-minute time step. The natural convection heat exchange near internal and external surfaces was calculated using the thermal analysis research program (TARP) algorithm [66]. The initialization period of simulation was set to the maximum option, which is 25 days [67]. The primary energy use was calculated by converting the simulation outputs for delivered energy. The conversion factors specified in Swiss norm SIA 380/1:2009 [68] were used to convert delivered energy to primary energy, so that, the factor for converting electricity to primary energy is 2.97 kWhPE/kWhel and for converting natural gas to primary energy is 1.15 kWhPE/kWhgas.

3.3 Design variables for optimization

The considered input variables for the target building are divided into two groups: building envelope properties and control settings. Building envelope properties involves five categories: window properties, roof properties, wall properties, floor properties, and infiltration. The control settings include cooling, heating and shading setpoints. A total of 15 variables were finally determined. The considered design variables for the thermal properties of the building envelope were all assumed to be continuously uniform. The control settings were assumed to be discrete variables with integer values representing different assigned information as indicated in Table 3.

Table 3 Design variables and their ranges for optimization and the values of base-cases

Category	Description of variables	Variable names	Unit of measure	Type of variable	2016-compliant base-case value	1980-compliant base-case value	Sampling ranges
Properties of the building envelope							
Window properties	U-value	X01	W/(m^2 K)	Continuous	0.41	3.35	[0.20, 5]
	SHGC	X02	-	Continuous	0.38	0.39	[0.10, 0.90]
	Visible transmittance	X03	-	Continuous	0.49	0.80	[0.10, 0.90]
Roof properties	Solar absorptance	X04	-	Continuous	0.70	0.92	[0.10, 0.90]
	Thermal resistence	X05	(m^2 K)/W	Continuous	8.10	2.98	[0.20, 33.20]
Wall	Solar absorptance	X06	-	Continuous	0.70	0.92	[0.10, 0.90]
	Thermal resistance	X07	(m^2 K)/W	Continuous	3.07	1.34	[0.20, 33.20]
Floor	Thermal resistance	X08	(m^2 K)/W	Continuous	0.22	0.22	[0.20, 33.20]
Infiltration	Flow per Exterior Surface Area	X09	1/h	Continuous	0.37	1.72	[0.04, 1]
Daily control settings							
Cooling setpoint	Setpoint temperature	X10	°C	Discrete	24 (whole year)	24	24, 24.50, 25…,27
Heating setpoint	Setpoint temperature	X11	°C	Discrete	21 (whole year)	21	19, 19.50, 20, 20.5, 21
Shading setpoint	Solar incidence on south window	X12	W/m^2	Discrete	No shading	No shading	200, 250, 300…, 1000
	Solar incidence on north window	X13	W/m^2	Discrete	No shading	No shading	200, 250, 300…, 1000
	Solar incidence on east window	X14	W/m^2	Discrete	No shading	No shading	200, 250, 300…, 1000
	Solar incidence on west window	X15	W/m^2	Discrete	No shading	No shading	200, 250, 300…, 1000

3.4 Formulation of optimization process

As mentioned above, building systems are characterized by different response times, thus in order to identify reliable values for the input variables considering the appropriate time effect of the noise factor, a two-step optimization process was designed. First, a monthly resolution was used to account for the seasonal effect of climate variation, and yearly primary energy was used to optimize the building envelope properties. Second, an hourly resolution was used to account for short-term weather evolution, and daily primary energy was used to optimize building's control settings such as the maximum irradiance incident on a window for lowering automated solar shadings. In addition, this two-step optimization process will provide an insight whether, to design an energy robust building, it is sufficient to apply only optimal control settings without improving the building envelope or *vice versa*, or whether both strategies were important, but there might be a priority option between them. Of course, in the context of a building refurbishment, the deployment of optimum control settings requires less interventions and costs, while the renovation of the building envelope may require a large capital investment. For the mentioned reasons, two different optimization configurations were developed. To conduct the optimization tasks, the dynamic energy simulation engine EnergyPlus [64] was integrated into the modular environment for process automation and optimization in the engineering design process modeFRONTIER [69], which embeds a multi-objective optimization engine that integrates several optimization algorithms and sampling strategies. For the purpose of this work Genetic Algorithm (GA) is used for the multi-objective optimization. GA is the most common optimization strategy used in building performance analysis [2]. modeFRONTIER provides both Fast Non-dominated Sorting Genetic Algorithm (NSGA-II) algorithm [70] and Multi-Objective Genetic Algorithm (MOGA-II) [71]. MOGA-II is an improved version of MOGA [72]. To decide which optimization algorithm is best suited, in the first optimization process, both the algorithms were used with similar initial population. MOGA-II found providing better results and was chosen for the second optimization process.

The multi-objective optimization process results in a two-dimensional solution space with a Pareto frontier. Figure 6 demonstrate the strategy used in this study for post-processing and selecting the Pareto optimal. In this method, the Pareto frontier is normalized to zero-one interval ($0 \leq f_i^t(x) \leq 1$) using following transformation [73]:

$$f_i^t(x) = \frac{f_i(x) - f_i^{min}}{f_i^{max} - f_i^{min}} \tag{9}$$

With f_i^{max} and f_i^{min}, the maximum and minimum of $f_i(x)$, $x \in \mathbb{R}^s$. Then the closest point to the utopia point ($f_1 = 1$ and $f_2 = 0$) is chosen as the optimal solution. This method was used because the significance of both objective functions was considered equal and also the values of the two objective functions were expressed in different orders of magnitude.

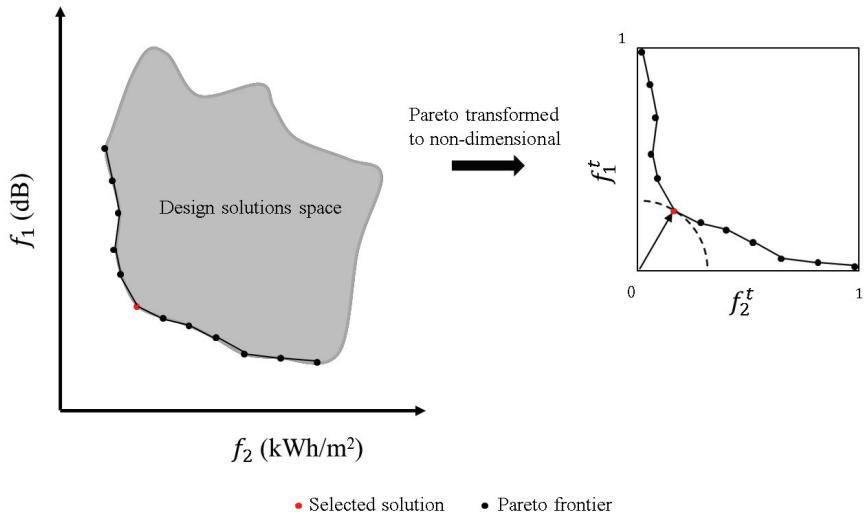

Figure 6 The approach for selection of the best solution from the Pareto

Configuration no.1: Optimization of the building envelope

In this task, only input variables related to thermal properties of the building envelope are optimized for robustness. The noise factor applied is the weather file used for running the simulation. Two different weather files were used to represent the extreme climate conditions, specifically EWY and ECY. The optimization process was performed for both NSGA-II and MOGA-II. The parameter settings of the algorithms are important for their performance. Hamdy et al. [74] recommended that the minimum required number of evaluations for optimization of building energy models is 1400-1800. The population size for population-based optimizations is recommended to be 2-4 times the number of design variables [75]. Following the recommendations, for each algorithm 1620 evaluations were considered by using population size of 27 (3×9 design variables) and number of generations equal to 60. The initial population is generated based on random sequence. For the other settings, the default values were kept unchanged. These settings are reported in Table 4. During each evaluation, three energy simulations are run (using the EWY, ECY and TDY files) to calculate the two objective functions in Eq.(7) and Eq.(8).

Table 4 Parameter settings the selected optimization algorithms

Optimization algorithm	No. of evaluations	Simulation resolution	*p*	No. of runs	population size	No. of generations	Probability of cross-over	Probability of mutation
NSGA-II	1620	Monthly	12	1	27	60	0.9	1.0
MOGA-II	1620	Monthly	12	1	27	60	0.5	0.1

A workflow to perform the above optimizations was established in modeFRONTIER as illustrated in Figure 7 with a flowchart demonstrating the flow of information.

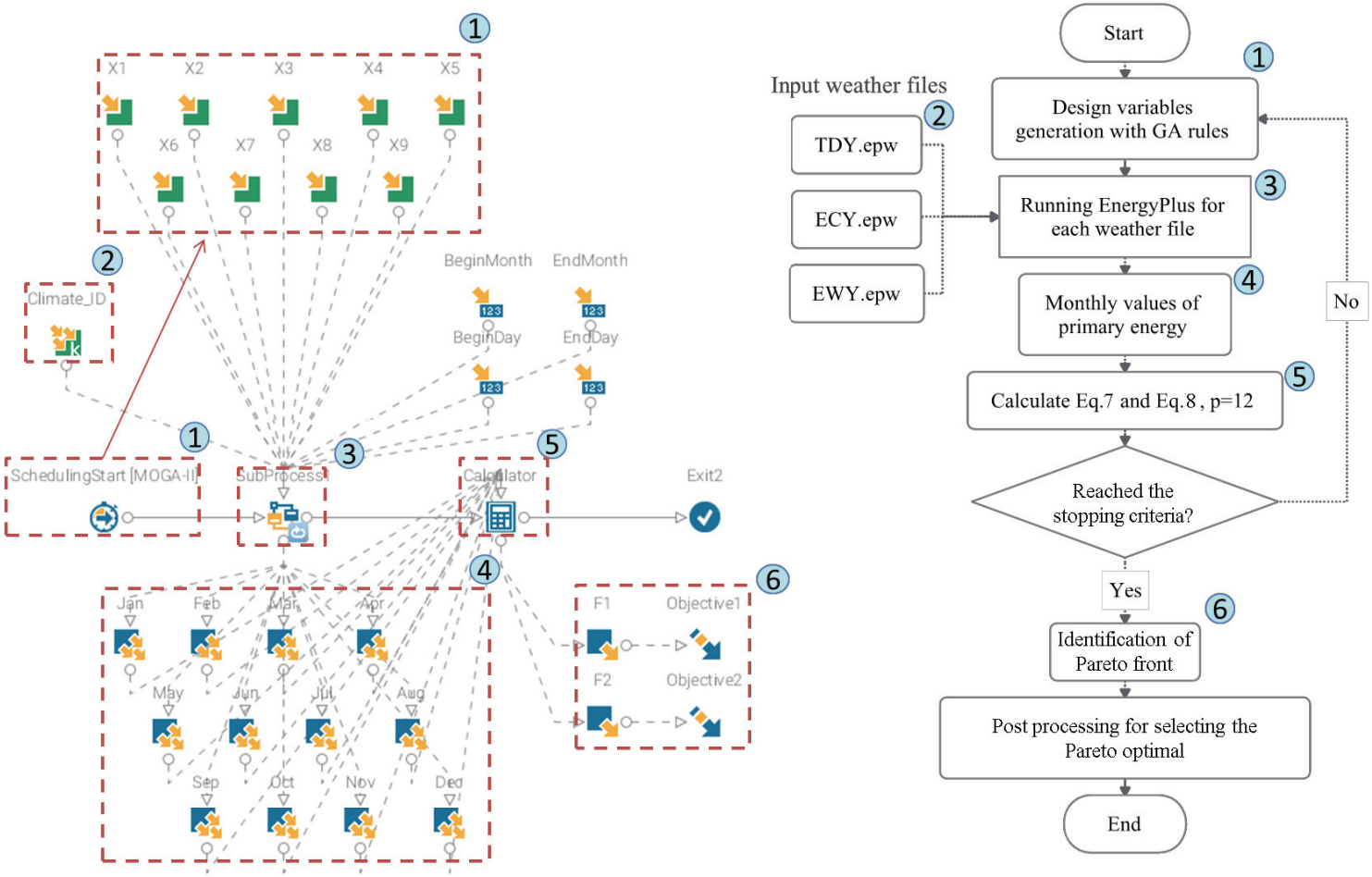

Figure 7 The implemented workflow of optimization process in modeFRONTIER for configuration no.1. The flowchart describes the flow of information during the process.

Configuration no.2: Optimization of the control settings

The second process involves optimization of daily control setting using TDY, ECY and EWY based on hourly typical and extreme values (see section 2.2). The configuration differs from the first because the input variables related to thermal properties of building envelope are excluded and only the control settings are considered in the optimization run that uses the same noise of the configuration no.1. The optimization is performed for each day of the year using MOGA_II algorithm, but the number of evaluations is now 48, while the probability of directional cross-over and the probability of mutation are kept the same. The initial population with 6 designs is generated using a random sequence and the number of generations is set to 8. These values were set using trials and errors to perform the process with an acceptable convergence level and feasible time. Figure 8 shows an optimization evolution for one day as an example. In each evaluation, 3 energy simulations were run under the three weather files. A total of 365 optimizations were performed to find optimum control settings for each day of the year, with objective functions set according to Eq.(7) (p=24) and Eq.(8). The last solution at each optimization is considered as optimum control setting for that day.

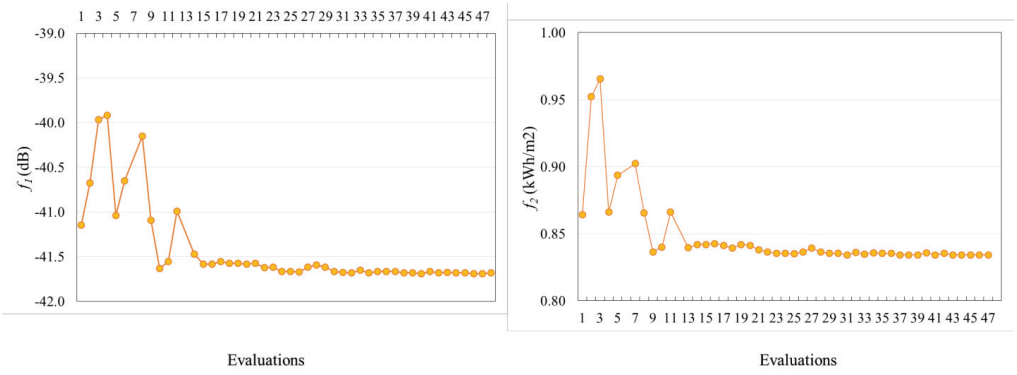

Figure 8 Evolution of objective functions. Example of optimizing control settings for a day.

Figure 9 demonstrate the flowchart of the optimization process for the above configuration.

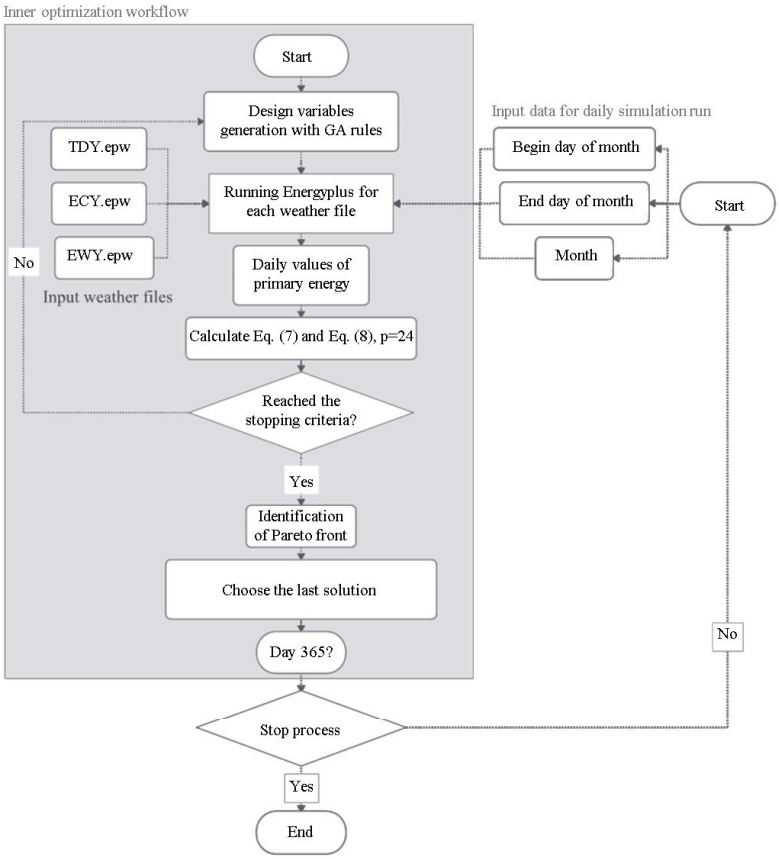

Figure 9 Flowchart of the optimization process implemented in modeFRONTIER for configuration no.2

3.5 Assessment of optimization strategies

Six cases were designed to render the impacts of each group of design variables on the energy-robustness and energy-efficiency of base-cases. First on a newly built building, the aforementioned optimization process applied to the base-case building model compliant to the 2016 requirements.

1. *2016-base*: It is the 2016-compliant base-case model with fixed values of heating and cooling setpoints and no automated solar shadings.

Three cases were developed to identify the most effective optimization strategy:

2. *2016-EnvelopeOpt:* The building envelope properties of the 2016-base model are changed to their optimum values, but the control settings are not optimized;
3. *2016-ControlOpt:* Automated solar shading is added to the 2016-base model and optimum daily *values* are used for setting the setpoint values for space heating and cooling and solar shading control;
4. *EnvelopeOpt+ControlOpt:* Both envelope properties and control settings of 2016-base are replaced with optimum values.

Afterwards, the existing building that we assumed to be compliant to 1980s quality standards considered for the purpose of optimization. It should be noted that the exclusive optimization of the building envelope without the upgrade of the HVAC systems may not be compatible with the latest legislative requirements (e.g., in Europe the Directive on energy performance of buildings), and the lifecycle of an HVAC system, in any case, is not longer than 30 years. Therefore, if we renovate a 1980-compliant base-case building by upgrading the HVAC systems to recent requirements (let's say 2016) and optimize the building envelope to maximize its energy-robustness and energy-efficiency, we obtain the previously mentioned *Envelope optimized-2015-case*. Furthermore, if we optimize both the envelope properties and the control settings, we obtain the *EnvelopeOpt+ControlOpt*. Thus, we will study the case where an existing building gets enhanced by optimizing its control settings that would require a little investment.

5. *1980-base:* The building model has the same geometry of the 2015-base, but its constructions are set according to typical 1980s quality standards.

Therefore, an additional case will be studied:

6. *1980-ControlOpt:* Automated solar shading is added to 1980-base model, and optimum daily values are used for setting the setpoint values for space heating and cooling and solar shading control.

4 Robustness evaluation

Finally, in order to test the effectiveness of the proposed method and demonstrate the most energy-robust building variant against climate change among the solutions, all of them are tested against a weather file dataset made of 74 representative weather files generated for the city of Geneva. The set of the representative weather files was synthesized in a previous study [56] in order to consider both extreme and typical climate conditions that represent a suitable test bench for investigating the energy performance of a building under a changing climate. In short the weather files are divided into three groups:

- TMY group: includes two weather files, the IWEC typical meteorological year (TMY) and a TMY generated by Meteonorm,
- Statistical group: six weather files generated using the morphing method through CCWorldWeatherGen and WeatherShift, and three weather files generated using the stochastic method through Meteonorm,
- Dynamical group: 21 weather files generated using dynamical downscaling that represent typical conditions and 42 weather files generated using dynamical downscaling that represent extreme conditions.

Typical weather files refer to the files that are generated through statistical downscaling or dynamical downscaling (TDY series). Extreme weather files refer to ECY and EWY files that represent extreme cold and warm years (using the RCM dynamically downscaled data). All the above methods provide 72 future weather files for the city of Geneva. More details are provided in [56].

This assessment methodology is applied to identify the most effective optimization strategy to render a new building with robust energy performance under against climate change and to measure the robustness potential.

5 Results

The first optimization round was performed to find optimal values for the building envelope properties (2016-EnvelopeOpt). The optimization parameters were set as described in section 3.4. Figure 10 shows the scatterplot of the simulated building variants using MOGA_II and NSGA_II algorithms, which are represented on the plan of the two objective functions. MOGA_II demonstrate a better performance by covering a larger area of the design space and providing Pareto frontier closer to the utopia point.

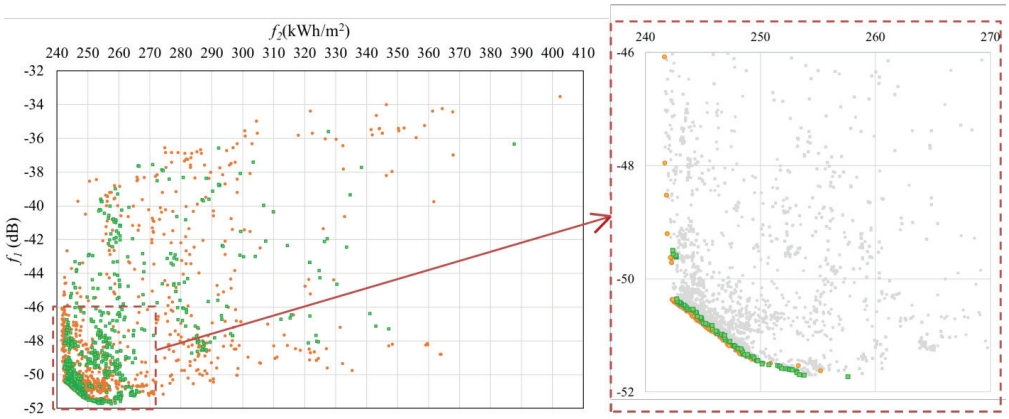

Figure 10 Scatter plot for the optimization of building envelope properties (in orange are building variants using MOGA_II algorithm and in green the ones based on NSGA_II algorithm).

The optimal solution is selected from the Pareto frontier using the approach described in section 3.4. In this approach, first the Pareto frontier is normalized to values between zero and one, and then the solution with minimum distance to ideal point is selected as optimal solution. The normalized Pareto frontier and the selected solution are shown in Figure 11.

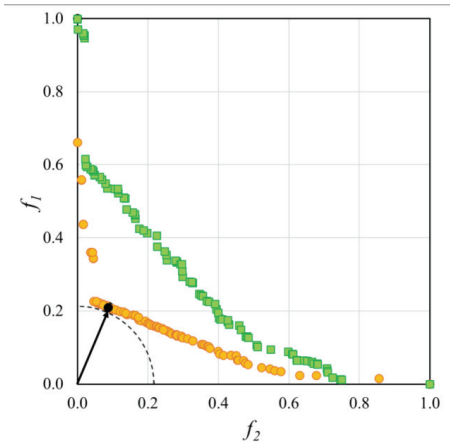

Figure 11 Normalized Pareto frontier with the selected optimal solution in black (in orange are normalized Pareto frontier using MOGA_II algorithm and in green the ones provided by NSGA_II algorithm).

After finding the solution for 2016-EnvelopeOpt, the next step is to find solutions for 2016-ControlOpt, EnvelopeOpt+ControlOpt and 1980-ControlOpt using optimization configuration no.2.

This configuration allows finding optimum daily values for heating, cooling and shading setpoints. For 2016-ControlOpt case, the optimum values are found while the envelope properties remain as 2016-base case. Same process is applied for 1980-ControlOpt case by keeping envelope properties as 1980-base case. For EnvelopeOpt+ControlOpt case, these values are found while the optimum building envelope properties are set as according to 2016-EnvelopeOpt. This step is combination of configuration no.1 and no.2. The above mentioned process provides solutions for configuration of the six cases described in section 3.5. After performing all the optimizations, the six cases are assessed considering their robustness against climate change. Each case underwent 74 annual simulations using 74 representative weather files (described in section 4).

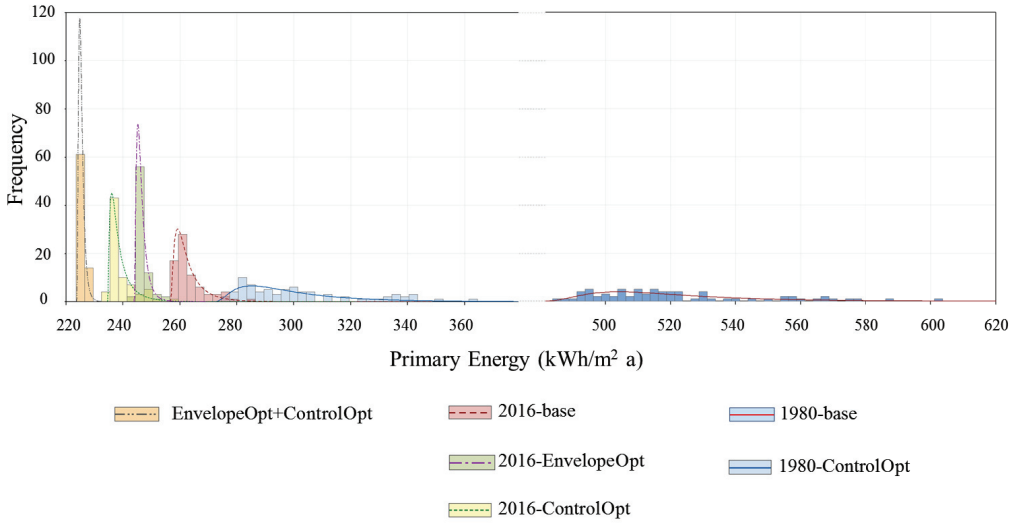

Figure 12 Qualitative distributions comparison of the six cases. For better readability, the distribution of 1980-base is separated from other cases.

Figure 12 shows the results of this assessment, which are distribution of 74 values of primary energy calculated for each case under 74 different weather files, including typical and extremes. It demonstrates the primary energy use of 1980-base case has significantly high sensitivity to the changing climate following by cases 1980-ControlOpt, 2016-base, 2016-EnvelopeOpt, 2016-ControlOpt and EnvelopeOpt+ControlOpt. The statistics calculated based on 74 values of primary energy calculated for each case are presented in Table 5. On the right side of the table the relative changes (%) of mean and standard deviation (SD) of all cases are compared to their values calculated for 1980-base and 2016-base cases.

Table 5 Descriptive statistics based on 74 calculated primary energy use for each case.

Cases	Primary energy use (kWh/m2)					Relative Change (%) to 1980-base value		Relative Change (%) to 2016-base value	
	Mean	SD	Min	Median	Max	Mean	SD	Mean	SD
1980-base	521.7	26.3	485.1	514.7	602.4	0.0%	0.0%	98.1%	354.5%
1980-ControlOpt	301.8	21.4	275.4	296.5	363.5	-42.1%	-18.7%	14.6%	269.6%
2016-base	263.4	5.8	257.1	260.7	284.0	-49.5%	-78.0%	0.0%	0.0%
2016-ControlOpt	239.4	4.6	234.9	237.5	257.1	-54.1%	-82.4%	-9.1%	-19.9%
2016-EnvelopeOpt	246.7	2.1	244.2	246.2	254.6	-52.7%	-92.1%	-6.3%	-64.0%
EnvelopeOpt+ControlOpt	225.5	1.1	223.9	225.1	228.9	-56.8%	-95.9%	-14.4%	-81.5%

Looking deeper into the results, the distribution of 2016-CotrolOpt has lower mean than 2016-EnvelopeOpt but with longer tail, that actually covers the distribution of 2016-EnvelopeOpt case. This means, although EnvelopeOpt case has higher energy demand but the demand is more predictable under extreme conditions than 2016-CotrolOpt case. Comparing 1980-base and 1980-ControlOpt, optimum control settings cause significant reduction in the mean of primary energy use, but the variation remains significantly high and unreliable during extreme climate conditions. However, the highest value of 1980-CotrolOpt case is still lower than the lowest value of 1980-base case, which means a significant improvement only by applying minimum intervention using optimum control settings. EnvelopeOpt+ControlOpt case has very narrow distribution in compare to other cases and at the same time with the lowest mean value.

Looking into statistics provided in Table 5, the calculated standard deviation of EnvelopeOpt+ControlOpt case, is around 5 times (81.5 %) smaller than 2016-base case and almost 24 times (95.9 %) smaller than 1980-base case. It points to a significant reduction of variability in the primary energy use, while having the lowest mean value of primary energy use. This makes EnvelopeOpt+ControlOpt case not only the most energy-efficient case but also the case with most robust energy performance. It demonstrates the effectiveness of the proposed method for designing buildings with robust energy performance under future climate uncertainties.

Furthermore, according to the results, shading and control settings has the highest impact on energy-efficiency. In other words, by adjusting the cooling- and heating-setpoints to optimum values as well as the solar incident setpoint for shading, it is possible to significantly reduce the primary energy use under typical conditions. While optimizing the building envelope properties effectively reduces f_1, which means the solution has lower variability in its response when exposed to extreme conditions and as a result better robustness of energy performance.

6 Conclusions

This paper has given an account of several available technologies such as: building performance simulation tools, simulation-based optimization techniques, robust design approach and climate models data and delivered a method based on combination of them that allows designing buildings which have

more robust and efficient energy performance in the face of climate change. The main goal of this study was to provide a computationally feasible and easy to understand method that can be used effectively by building designers, architects and engineers to improve the robustness of their designs against future climate uncertainties.

In summary, our work propose a robust design optimization (RDO) workflow, where the aim is to achieve an optimum solution that it's energy performance has minimum sensitivity to climate variations. The key to the feasibility of the method is considering climate variations by using only three weather files that represent, typical (TDY), extreme warm (EWY) and extreme cold (ECY) weather conditions. A multi-objective optimization process was configured with two objective functions. Minimization of the two objective functions provided in this study, ensures having a building with low energy use under most likely conditions and minimum variation when the conditions change or become extreme. In the first step, building envelope properties of the 2016 compliant model (2016-base case) were optimized and the selected optimum solution is called 2016-EnvelopeOpt (Figure 10). In the second step performed, the building envelope properties of 2016-base case kept unchanged, while shading was added, and the daily control setting of heating, cooling and shading were optimized. The solution from this step is called 2016-ControlOpt. The same process was performed on the 1980 compliant model (1980-base case), in which the envelope properties were kept unchanged and control settings were optimized and presented as 1980-ControlOpt.

Comparing these results allows:

- Understanding the impact of different interventions, from deep and costly intervention on envelope properties to less costly intervention on shadings and control settings, on the energy-robustness of the building.
- Showing the impact of such intervention on a building that is built according to a recent energy code, and a building that is built according to 1980s construction quality.

In the final step, optimization performed to find optimum control settings of heat, cooling and shading for the case with optimum envelope properties (EnvelopeOpt+ControlOpt case). This resulted as EnvelopeOpt+ControlOpt case, which both envelope properties and control settings are optimized.

The results demonstrated that by having optimum daily setpoint temperatures for cooling and heating, and solar incident setpoint for shading, it is possible to reduce significantly the primary energy use under typical conditions (2016-ControlOpt and 1980-ControlOpt cases). While optimizing the building envelope properties (2016-EnvelopeOpt) reduce significantly the variability of performance under changing climate conditions including extreme. And finally, by optimizing both the envelope properties and the control settings, the most energy-efficient solution with robust energy performance is achieved (EnvelopeOpt+ControlOpt case). This case has considerably less sensitivity to climate conditions by having low-variability performance, while requiring minimum energy use.

The simplicity and the low computational demand of the process ascertain the feasibility and applicability of this method. The approach can be used at any stage of design process and can help architects and engineers to improve robustness of their design against future climate uncertainties. The approach used in this study can be used as a guideline to develop further robust design methods for other sources of variations than climate and other target performances than energy.

7 Acknowledgement

This work has been written within the Research Centre on Zero Emission Neighborhoods in Smart Cities (FME ZEN). The authors gratefully acknowledge the support of the ZEN partners and the Research Council of Norway. This work has partly benefited from the support of the Swedish Research Council (Formas) which is gratefully acknowledged.

8 References

[1] Suh W-J, Park C-S, Kim D-W. Heuristic vs. meta-heuristic optimization for energy performance of a post office building. 12th Conference of International Building Performance Simulation Association, Sydney, Australia2011. p. 14-6.
[2] Nguyen A-T, Reiter S, Rigo P. A review on simulation-based optimization methods applied to building performance analysis. Applied Energy. 2014;113:1043-58.
[3] Evins R. A review of computational optimisation methods applied to sustainable building design. Renewable and Sustainable Energy Reviews. 2013;22:230-45.
[4] Attia S. Computational Optimisation for Zero Energy Building Design, Interviews with Twenty Eight International Experts. Architecture et climat; 2012.
[5] Menezes AC, Cripps A, Bouchlaghem D, Buswell R. Predicted vs. actual energy performance of non-domestic buildings: Using post-occupancy evaluation data to reduce the performance gap. Applied Energy. 2012;97:355-64.
[6] Bartlett K, Brown C, Chu A-M, Ebrahimi G, Gorgolewski M, Hodgson M, et al. Do our green buildings perform as intended. World Sustainable Building Conference (SBE2014)2014.
[7] Li P, Froese TM, Brager G. Post-occupancy evaluation: State-of-the-art analysis and state-of-the-practice review. Building and Environment. 2018;133:187-202.
[8] Iaccarino G. Quantification of Uncertainty in Flow Simulations Using Probabilistic Methods: Stanford University; 2008.
[9] Rastogi P. On the sensitivity of buildings to climate - the interaction of weather and building envelopes in determining future building energy consumption: EPFL; 2016.
[10] IEC. 60050-191: International electrotechnical vocabulary: Chapter 191: Dependability and quality of service. International Electrotechnical Commission, Geneva. 1990.
[11] Bordass B. Energy performance of non-domestic buildings: closing the credibility gap. in Proceedings of the 2004 Improving Energy Efficiency of Commercial Buildings Conference: Citeseer; 2004.
[12] C.J. Hopfe, Uncertainty and sensitivity analysis in building performance simulation for decision support and design optimization, Ph.D, Eindhoven University of Technology. 2009.
[13] ANSI/ASHRAE 140. Standard Method of Test for the Evaluation of Building Energy Analysis Computer Programs. Atlanta (GA), USA: American Society of Heating, Refrigerating and Air-Conditioning Engineers; 2011. p. 272.
[14] Ham Y, Golparvar-Fard M. Mapping actual thermal properties to building elements in gbXML-based BIM for reliable building energy performance modeling. Automation in Construction. 2015;49:214-24.
[15] Ham Y, Golparvar-Fard M. EPAR: Energy Performance Augmented Reality models for identification of building energy performance deviations between actual measurements and simulation results. Energy and Buildings. 2013;63:15-28.
[16] Pan W, Gibb AGF, Dainty ARJ. Strategies for Integrating the Use of Off-Site Production Technologies in House Building. Journal of Construction Engineering and Management. 2012;138:1331-40.
[17] Delzendeh E, Wu S, Lee A, Zhou Y. The impact of occupants' behaviours on building energy analysis: A research review. Renewable and Sustainable Energy Reviews. 2017;80:1061-71.
[18] Hall IJ, Prairie R, Anderson H, Boes E. Generation of a typical meteorological year. Analysis for solar heating and cooling. San Diego, CA, USA: Sandia Labs., Albuquerque, NM (USA); 1978.

[19] Kalkman A. Calculation of energy consumption in dwellings: theory and field data, presented at the one day forum of the "5th meeting of IEA Annex 53", Rotterdam, The Netherlands, 2012.
[20] Taguchi G. Introduction to quality engineering: designing quality into products and processes. 1986.
[21] Lanzotti A. Robust design of car packaging in virtual environment. International Journal on Interactive Design and Manufacturing (IJIDeM). 2008;2:39-46.
[22] Blaabjerg F, Pecht MM. Special Issue on Robust Design and Reliability of Power Electronics, IEEE Transactions on Power Electronics, May 2015. IEEE Transactions on Power Electronics. 2015;30:2373-4.
[23] Truong N, Shin S, Choi Y, Jeong S, Cho B. Robust design with time-oriented responses for regenerative medicine industry. The Third International Conference on the Development of Biomedical Engineering in Vietnam: Springer; 2010. p. 67-70.
[24] Koolen JLA. Simple and robust design of chemical plants. Computers & Chemical Engineering. 1998;22:S255-S62.
[25] Crawley DB, Lawrie LK. Rethinking the TMY: Is the 'typical'meteorological year best for building performance simulation? 14th Conference of International Building Performance Simulation Association. Hyderabad, India2015.
[26] Sévellec F, Drijfhout SS. A novel probabilistic forecast system predicting anomalously warm 2018-2022 reinforcing the long-term global warming trend. Nature communications. 2018;9:3024.
[27] Ke X, Wu D, Rice J, Kintner-Meyer M, Lu N. Quantifying impacts of heat waves on power grid operation. Applied Energy. 2016;183:504-12.
[28] Kaiser R, Le Tertre A, Schwartz J, Gotway CA, Daley WR, Rubin CH. The effect of the 1995 heat wave in Chicago on all-cause and cause-specific mortality. American journal of public health. 2007;97 Suppl 1:S158-S62.
[29] De Bono A, Peduzzi P, Kluser S, Giuliani G. Impacts of summer 2003 heat wave in Europe. United Nations Environment Programme Retrieved from https://wwwunisdrorg/files/1145_ewheatwaveenpdf. 2004.
[30] Luber G, McGeehin M. Climate Change and Extreme Heat Events. American Journal of Preventive Medicine. 2008;35:429-35.
[31] Taguchi G, Chowdhury S, Taguchi S. Robust engineering: learn how to boost quality while reducing costs & time to market: McGraw-Hill Professional Pub; 2000.
[32] Fowlkes WY, Creveling CM. Engineering Methods for Robust Product Design: Using Taguchi Methods in Technology and Product Development: Addison-Wesley Publishing Company; 1995.
[33] Floricel S, Miller R. Strategizing for anticipated risks and turbulence in large-scale engineering projects. International Journal of project management. 2001;19:445-55.
[34] Clausing DP. Total quality development. Mechanical Engineering. 1994;116:94.
[35] Olewnik A, Brauen T, Ferguson S, Lewis K. A framework for flexible systems and its implementation in multiattribute decision making. Journal of Mechanical Design. 2004;126:412-9.
[36] Bates RA, Kenett RS, Steinberg DM, Wynn HP. Achieving robust design from computer simulations. Quality Technology & Quantitative Management. 2006;3:161-77.
[37] Gribble SD. Robustness in complex systems. Hot Topics in Operating Systems, 2001 Proceedings of the Eighth Workshop on: IEEE; 2001. p. 21-6.
[38] Yassine AA. Investigating product development process reliability and robustness using simulation. Journal of Engineering Design. 2007;18:545-61.
[39] Bettis RA, Hitt MA. The new competitive landscape. Strategic management journal. 1995;16:7-19.
[40] Chalupnik MJ, Wynn DC, Clarkson PJ. Comparison of ilities for protection against uncertainty in system design. Journal of Engineering Design. 2013;24:814-29.
[41] Phadke MS. Quality engineering using robust design: Prentice Hall PTR; 1995.
[42] Buso T, Fabi V, Andersen RK, Corgnati SP. Occupant behaviour and robustness of building design. Building and Environment. 2015;94:694-703.
[43] Fabi V, Buso T, Andersen RK, Corgnati SP, Olesen BW. Robustness of building design with respect to energy related occupant behaviour. IBPSA. Chambery, France2013. p. 1999-2006.
[44] Leyten JL, Kurvers SR. Robust Indoor Climate Design. ISIAQ; 2011.

[45] Palme M, Isalgué A, Coch H, Serra R. Energy consumption and robustness of buildings. Proceedings of the CESB10 Conference2010.
[46] Palme M, Isalgué A, Coch H. Avoiding the possible impact of climate change on the built environment: The importance of the building's energy robustness. Buildings. 2013;3:191-204.
[47] Chinazzo G, Rastogi P, Andersen M. Robustness Assessment Methodology for the Evaluation of Building Performance With a View to Climate Uncertainties. Proceedings of BS 20152015.
[48] Hoes P, Hensen J, Loomans M, De Vries B, Bourgeois D. User behavior in whole building simulation. Energy and buildings. 2009;41:295-302.
[49] O'Brien W. Occupant-proof buildings: can we design buildings that are robust against occupant behaviour. 13th Conference of International Building Performance Simulation Association2013. p. 1746-54.
[50] Kotireddy R, Hoes P-J, Hensen JLM. A methodology for performance robustness assessment of low-energy buildings using scenario analysis. Applied Energy. 2018;212:428-42.
[51] Park G-J, Lee T-H, Lee KH, Hwang K-H. Robust Design: An Overview. AIAA Journal. 2006;44:181-91.
[52] Gorissen BL, Yanıkoğlu I, den Hertog D. A practical guide to robust optimization. Omega. 2015;53:124-37.
[53] Gabrel V, Murat C, Thiele A. Recent advances in robust optimization: An overview. European Journal of Operational Research. 2014;235:471-83.
[54] Hensen JL, Lamberts R. Building performance simulation for design and operation: Routledge; 2012.
[55] Trzaska S, Schnarr E. A review of downscaling methods for climate change projections. African and Latin American Resilience to Climate Change (ARCC). United States: United States Agency for International Development by Tetra Tech ARD; 2014. p. 1-42.
[56] Moazami A, Nik VM, Carlucci S, Geving S. Impacts of future weather data typology on building energy performance – Investigating long-term patterns of climate change and extreme weather conditions. Applied Energy. 2019;238:696-720.
[57] Nik VM. Making energy simulation easier for future climate – Synthesizing typical and extreme weather data sets out of regional climate models (RCMs). Applied Energy. 2016;177:204-26.
[58] Nik VM. Application of typical and extreme weather data sets in the hygrothermal simulation of building components for future climate – A case study for a wooden frame wall. Energy and Buildings. 2017;154:30-45.
[59] Deru M, Field K, Studer D, Benne K, Griffith B, Torcellini P, et al. US Department of Energy commercial reference building models of the national building stock. 1617 Cole Boulevard Golden, Colorado: National Renewable Energy Laboratory; 2011.
[60] ASHRAE AS. Standard 90.1-2004, Energy standard for buildings except low rise residential buildings. American Society of Heating, Refrigerating and Air-Conditioning Engineers, Inc; 2004.
[61] Halverson MA, Rosenberg MI, Hart PR, Richman EE, Athalye RA, Winiarski DW. ANSI/ASHRAE/IES Standard 90.1-2013 Determination of Energy Savings: Qualitative Analysis. United States, Washington: Pacific Northwest National Laboratory (PNNL); 2014.
[62] Zhang J, Athalye RA, Hart PR, Rosenberg MI, Xie Y, Goel S, et al. Energy and Energy Cost Savings Analysis of the IECC for Commercial Buildings. United States, Washington: Pacific Northwest National Laboratory (PNNL); 2013.
[63] ASHRAE. Standard 169-2013, Climate Data for Building Design Standards," 1791 Tullie Circle NE· Atlanta, GA 30329.
[64] Crawley DB, Lawrie LK, Winkelmann FC, Buhl WF, Huang YJ, Pedersen CO, et al. EnergyPlus: Creating a new-generation building energy simulation program. Energy and Buildings. 2001;33:319-31.
[65] US-DoE. Testing and Validation. In: Energy USDo, editor. EnergyPlus Energy Simulation Software2012.
[66] Walton GN. Thermal analysis research program reference manual. National Bureau of Standards. United States, Washington1983.
[67] DoE U. EnergyPlus Input output reference. US Department of Energy. 2010.

[68] SIA. 380/1 (2009): Thermische Energie im Hochbau. Zürich: Schweizerischer Ingenieur und Architektenverein; 2009.
[69] Esteco S. ModeFRONTIER 2014 User's Manual. 2014.
[70] Deb K, Agrawal S, Pratap A, Meyarivan T. A fast elitist non-dominated sorting genetic algorithm for multi-objective optimization: NSGA-II. International conference on parallel problem solving from nature: Springer; 2000. p. 849-58.
[71] Rigoni E, Poles S. NBI and MOGA-II, two complementary algorithms for Multi-Objective optimizations. Dagstuhl Seminar Proceedings: Schloss Dagstuhl-Leibniz-Zentrum für Informatik; 2005.
[72] Fonseca CM, Fleming PJ. Genetic Algorithms for Multiobjective Optimization: FormulationDiscussion and Generalization. Icga: Citeseer; 1993. p. 416-23.
[73] Augusto OB, Bennis F, Caro S. A new method for decision making in multi-objective optimization problems. Pesquisa Operacional. 2012;32:331-69.
[74] Hamdy M, Nguyen A-T, Hensen JLM. A performance comparison of multi-objective optimization algorithms for solving nearly-zero-energy-building design problems. Energy and Buildings. 2016;121:57-71.
[75] Mauro GM, Hamdy M, Vanoli GP, Bianco N, Hensen JL. A new methodology for investigating the cost-optimality of energy retrofitting a building category. Energy and Buildings. 2015;107:456-78.